HYDRAULIC MODELING OF THERMAL OUTFALL DIFFUSERS FOR THE SAN ONOFRE NUCLEAR POWER PLANT

by
Robert C. Y. Koh
Norman H. Brooks
E. John List
Eric J. Wolanski

W. M. Keck Laboratory of Hydraulics and Water Resources
Division of Engineering and Applied Science
CALIFORNIA INSTITUTE OF TECHNOLOGY
Pasadena, California

Report No. KH-R-30 January 1974

HYDRAULIC MODELING OF THERMAL OUTFALL DIFFUSERS FOR THE SAN ONOFRE NUCLEAR POWER PLANT

Final Report

to

Southern California Edison Company

by

Robert C. Y. Koh
Norman H. Brooks
E. John List
Eric J. Wolanski

Work Performed under SCE P.O. No. T2062905

W. M. Keck Laboratory of Hydraulics and Water Resources
Division of Engineering and Applied Science
California Institute of Technology
Pasadena, California

Report No. KH-R-30

January 15, 1974

ABSTRACT

Various hydraulic model tests were performed in connection with the design and performance of the offshore thermal outfalls for the San Onofre Nuclear Generating Station (jointly owned by the Southern California Edison Company and the San Diego Gas and Electric Company) near San Clemente, California. These include model investigations of: (i) the multiple port discharges for the proposed Units 2 and 3, (ii) the existing submerged single outlet discharge from Unit 1, (iii) the discharge of heated water from the Units 2 and 3 intakes during heat treatment, and (iv) hydraulic characteristics of discharge ports.

On the basis of these investigations, the diffusion structure for each of the proposed two new units was designed to be 2500 feet long aligned perpendicular to shore. The diffuser for Unit 3 will extend from 3500 to 6000 feet from shore, and that for Unit 2 from 6000 to 8500 feet from shore. Each diffuser will have 63 discharge nozzles aimed offshore (±25° from the pipe axis, 20° above horizontal). The momentum of the discharge produces an offshore drift of the diluted warm-water plume.

The maximum temperature rise on the surface caused by the discharge was found to decrease with increasing longshore current speed, and the discharge momentum from the jets was effective in preventing significant re-entrainment in the event of reversing or low currents.

Although the California thermal discharge requirements specify a maximum surface temperature increase of 4°F (beyond 1000 feet from the discharge structure), the laboratory target maximum was established at 2.5°F, to account for possible model-prototype differences and unmodeled effects. The hydraulic model studies showed that the proposed outfall design meets the laboratory target value for a variety of possible longshore current conditions; therefore, it is predicted that the prototype outfall operation will meet the California thermal discharge requirements.

TABLE OF CONTENTS

TABLE OF CONTENTS (Continued)

LIST OF FIGURES

LIST OF FIGURES (Continued)

LIST OF FIGURES (Continued)

LIST OF FIGURES (Continued)

LIST OF FIGURES (Continued)

LIST OF FIGURES (Continued)

LIST OF FIGURES (Continued)

LIST OF TABLES

CHAPTER 1

INTRODUCTION

Hydraulic laboratory studies were conducted to investigate outfall configurations for the thermal discharge from proposed Units 2 and 3 at the San Onofre Nuclear Generating Station (Figure 1.1), jointly owned by the Southern California Edison Company and San Diego Gas and Electric Company. The hydraulic design is based on a condenser flow of 1850 cfs for each of the two units with a temperature rise of 20°F; possible ultimate development of four new units at 1100 MW(e) each was briefly considered. There is one existing unit of 450 MW(e) capacity. The new California thermal standards[1] (essentially ambient $\Delta T < 4°F$) in effect preclude the use of shoreline or single outlet discharges for new units and necessitate the use of multiport diffusers.

A number of different experimental investigations were performed in the course of developing the conceptual design for the new Units 2 and 3 discharge diffusers. In addition, the thermal field was measured in a special model for the reverse-flow operation (heat treatment of the intake lines) for Units 2 and 3. The normal operation of Unit 1 was also tested and compared with field measurements of temperature. All the tests, with the exception of the final confirming tests reported herein, have been documented in a series of seven progress reports.

From the results of the preliminary tests (Progress Report No. 4) we established a preliminary design for the discharge structures for Units 2 and 3, each consisting of a diffuser of 2500 ft length containing 76 discharge nozzles with a nominal discharge velocity of 13 ft/sec. The two diffusers are aligned perpendicular to shore and extend from approximately 3500 ft to 8500 ft offshore. The discharge ports are

---

[1] State Water Resources Control Board, Sacramento, California, "Water Quality Control Plan for Control of Temperature in the Coastal and Interstate Waters and Enclosed Bays and Estuaries of California," 8 pp., May 18, 1972 (date of latest revision).

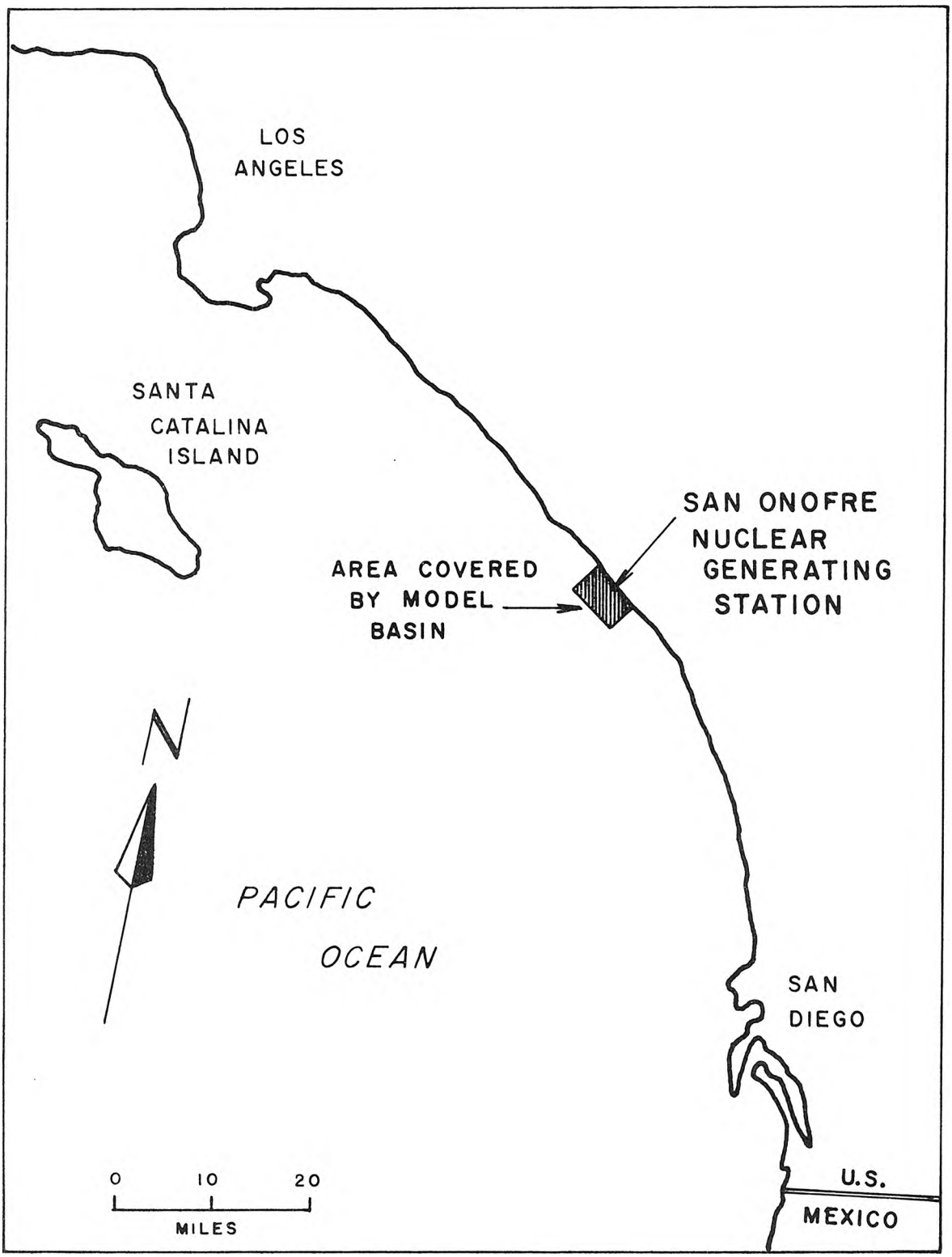

Figure 1.1 Site map of San Onofre Nuclear Generating Station. (Area covered by model basin is approximately 3 miles by 5.4 miles.)

nozzle-riser assemblies at alternate angles of $\pm$ 25° with respect to the longitudinal axis of the diffuser and 20° up from horizontal. The nozzles are positioned 6 ft from the ocean bottom.

The preliminary design was then modified somewhat by the engineers of the Southern California Edison Company (SCE) in consideration of other factors such as structural requirements, cost, construction problems, and minor changes in the final detailed bathymetry obtained at the diffuser site. The two main changes in the diffuser design were a reduction in the number of ports from 76 to 63 and revised depth profiles along the diffusers (of a few feet). Although these changes were not great, a set of confirming tests were conducted in order to provide a model evaluation of the prototype as finally designed by the Southern California Edison Company.

This report describes the results of this confirming series of tests. For completeness, salient features of all the previous tests reported in Progress Reports 1 through 7 are presented in summary form in the Appendix.

CHAPTER 2

DESIGN EVALUATION PHILOSOPHY

2.1 California Thermal Standards

The California thermal standards for coastal waters relate to three zones:

1. the shoreline,
2. the substrate,
3. the ocean surface beyond 1000 feet from any point of the diffusion structure.

For the first two, any rise of water temperature more than 4°F above natural is prohibited. For the third zone the contour for $\Delta T = 4°F$ must be completely contained within the 1000-foot limit more than 50% of any complete tidal cycle. This means that design for compliance must be based on the worst day of the year.[2]

2.2 Design Philosophy

For compliance with the California thermal standards, the following strategy has been proposed. The most efficient way to achieve $\Delta T < 4°F$ at 1000 feet from the outfall is by initial mixing of the condenser discharge with seawater by means of an outfall diffuser; it may easily be shown that the rate of surface cooling is so slow as to be negligible for purposes of meeting the requirements. At the very minimum, the dilution obtained by the diffuser must be 5, or in other words, each part of condenser discharge must be jet-mixed with at least 4 parts of seawater.

---

[1] It is interesting to note the inconsistency in the time period for compliance between the thermal requirements (1 day) and the wastewater requirements (30 days). Both sets of requirements were adopted by the California Water Resources Control Board within the past two years. If the thermal outfalls could be designed for the 50% requirement based on the most adverse month instead of day, shorter diffusers would be sufficient to meet the requirements.

However, the prediction of dilution is not precise, so that a dilution factor of 8 (or 2.5°F rise) was set for the design target in the laboratory work as discussed in Section 2.3. To obtain dilutions of this magnitude in the depths of water available under conditions of slow ambient currents requires diffusion structures of the order of two to three thousand feet long per unit.

For protection of the shoreline, it is proposed to aim the discharge jets in the offshore direction to produce a general offshore drift superimposed on the longshore current. When the tide reverses, this technique provides greater protection against re-entrainment of previously discharged water into the plume. Furthermore, this approach minimizes any contact of warm water with the shoreline. The diffusion structure itself would be some distance offshore, on the bottom; a shoreline discharge of any type is effectively prohibited by the requirements because of the supply of water needed for dilution.

For protection of the substrate it is desirable to achieve a two-layer flow after initial mixing. The diluted warm water layer can then drift away from the site as a surface layer (the thickness may be more than half the depth), and allow cool new diluting water to circulate underneath the warm layer. In this way, contact of warm water with the bottom is avoided.

The current patterns are the primary ocean variables affecting the design (other than topography). To investigate buildup and recirculation it is necessary to consider not only the frequency of different speeds, but also critical tidal sequences.

2.3 Laboratory Target Value of ΔT.

The prototype thermal standards have been stated in Section 2.1, with limits based on 4°F rise above natural background. This rise of 4°F includes any existing rise in ambient water temperature due to the operation of Unit 1.

The purpose of the model studies was to help establish what diffuser configuration will be required to guarantee meeting these requirements

with a high degree of assurance. If the prototype operation were to exceed the standard, the consequences could be very adverse for SCE and the community. Therefore, it is important to examine the accuracy of the hydraulic model prediction and to make suitable allowances for model-prototype differences.

For the basin models a target value of 2.5°F rather than 4.0°F has been established, in order to allow a margin of 1.5°F for model-prototype differences. The detailed breakdown, based on the writers' judgment, is as follows:

(1). Target value of ΔT selected as laboratory criterion — 2.5°F

(2). Model-prototype differences

a. Possible direct error in model-prototype behavior due to fluid effects which are impossible to model exactly (friction on the ocean bottom, interfacial friction between warm and cool layers, Reynolds number effect on initial jets, distortion of scales, ocean turbulence):

$\pm$ 25% x 2.5° — 0.6°

b. Effects which are not modeled. Allowance is made for only one of the following effects at any one time: — 0.6°

(i) Onshore currents (with jets aimed offshore, an onshore current resisting the offshore jetting could cause some "piling up" of warm water and reduce the initial dilution).
Estimated: 0.5°F

OR

(ii) Increase of background temperature by Unit 1 discharge, when the plume of Unit 1 is carried over Units 2 or 3.
Estimated: 0.6°F

OR

(iii) Unknown prototype current patterns which may have complex adverse effects when all spatial and temporal correlations are considered (including recirculation of warm water through the intakes, and recirculation of an old thermal field over the outfall one or more times).
Estimated: 0.5°F

Subtotal	3.7°

(3). Final margin of safety covering all other factors, (such as slight errors in prediction of condenser flows and temperature; as-built depths departing slightly from design depths for ports, and any unanticipated sources of error)

± 8% x 3.7°	0.3°
TOTAL	4.0°F

Further studies in a large model might bring about some reductions in the margin of 1.5°F, represented by items 2 and 3 above, but it cannot be eliminated; it is also possible that further studies might necessitate increasing the margin, although the above values are considered conservative.

There have been no reported model-prototype comparisons as yet for diffusers of the type proposed. We await with interest the results for the diffuser for the Fitzpatrick Plant on Lake Ontario (with jets aimed offshore), in order to assess the magnitude of errors of the type discussed in item 2 above.

The Caltech basin model is about half as big as most, but covers larger prototype areas than most because of the very large diffusers. It has a nominal horizontal scale of 800:1 compared to other models which are as large as 100:1 horizontal (for example, Northport model at MIT). For larger models, the scaling errors (Item 2a) can be expected to be less; if it is necessary to get more accurate modeling, then it is essential to build a much larger model, in a larger basin, such as the 100 x 132 foot basin in Caltech's Azusa Hydraulics Laboratory.

The effect of Unit 1 discharge cannot be properly modeled in the distorted model (4:1) required to test the Units 2 and 3 diffusers. The principal effect is expected to be an increase of ambient temperature in the diffuser area of Units 2 and 3, which will cut into the allowed rise of 4°F above natural.

In summary, a subjective assessment of how well the basin model reproduces the worst condition in the prototype leads to the conclusion that 2.5°F should be used as the laboratory target value. This number is normalized by dividing the initial $\Delta T = 20°F$, giving 12.5% as the target value of $\Delta T/\Delta T_o$.

CHAPTER 3

HYDRAULIC MODELING LAWS

Hydraulic modeling depends on proper dynamic similitude for the most important features of the flow field. For a thermal discharge from a large multiport diffuser (length L) it is convenient to distinguish three parts of the flow field: 1) near field; 2) intermediate field; and 3) far field.

3.1 Near Field

In the near field, the dominant feature is the jet discharge and entrainment of ambient fluid producing the initial dilution. The extent of this zone is only a few multiples of the depth. The individual jets are characterized by (see Figures 3.1 and 3.2):

q = port discharge
d = jet diameter = $\sqrt{C_c}D$
D = port diameter
C_c = contraction coefficient
u_j = $q/(\pi d^2/4)$
ϕ = jet inclination to horizontal
S_o = initial dilution at the surface (centerline of jet)
g' = $g\Delta\rho/\rho$
$\Delta\rho/\rho$ = relative density difference (ambient less discharge)
b = port spacing
u_c = current velocity
θ = angle of current direction to diffuser alignment
α = angle of current direction to jet direction
a = height above bottom to center of nozzle
y_o = depth over center of nozzle.

The jet dilution at the surface is

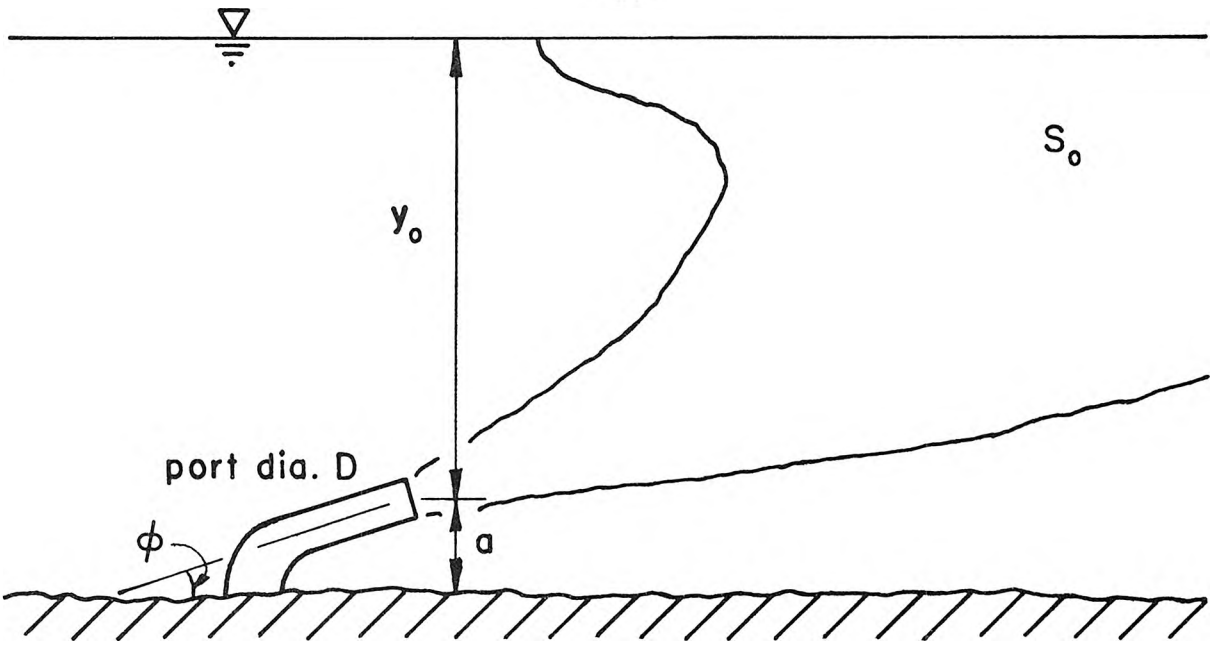

Figure 3.1 Exit port orientation and nomenclature.

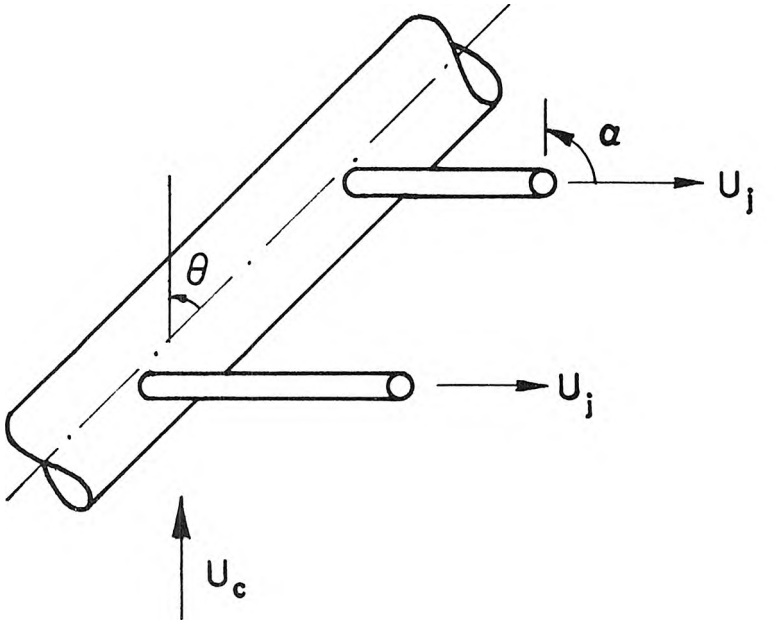

Figure 3.2 Diffuser orientation and nomenclature.

$$S_o = f(y_o/d,\ F,\ b/y_o,\ a/d,\ \phi,\ \theta,\ \alpha,\ u_j/u_c)\ , \qquad 3.1$$

where

$$F = u_j/\sqrt{g'd}\ . \qquad 3.2$$

It is presumed that the port spacing is close enough so that there is interference between adjacent jets, as desired for approximating a line source. In this situation the Reynolds number is not modeled, but it should be kept high enough to ensure turbulent flow from the model nozzles.

To model the flow in this zone it is essential to have undistorted geometry and to follow the Froude Law ($F_r = 1$). In the notation of ratios (the subscripts r, p, and m, refer to ratio, prototype and model respectively),

$$y_r = y_p/y_m = d_p/d_m\ . \qquad 3.3$$

This length ratio applies to all lengths, and angles are preserved. The Froude Law is

$$F_r = 1 = \frac{u_r}{(g'_r y_r)^{1/2}} \qquad 3.4$$

or

$$u_r = \sqrt{g'_r y_r}\ . \qquad 3.5$$

The velocity ratio applies to both the jet velocity and ambient current velocity.

Note that the Froude number is based on g', rather than g; the Froude number thus defined is called the densimetric Froude Number. Since free surface effects are unimportant there is no need to model for the ordinary Froude number, based on g. Therefore the density ratio $(\Delta\rho/\rho)_r$ or g'_r need not be unity.

The Reynolds number R of any of the jets is

$$R = \frac{u_j d}{\nu} \qquad 3.6$$

where ν = kinematic viscosity of discharge fluid. The ratio of Reynolds numbers in a Froude model is

$$R_r = \frac{u_r d_r}{\nu_r} \qquad 3.7$$

$$R_r = \frac{g'_r{}^{1/2} y_r^{3/2}}{\nu_r} . \qquad 3.8$$

Typical prototype jet Reynolds numbers will be:

$$R_p = \frac{u_j d}{\nu} , \qquad 3.9$$

$$= \frac{(13)\ (1.7)}{10^{-5}} , \qquad \nu \doteq 1.0 \times 10^{-5}\ \text{ft}^2/\text{sec} \text{ (sea water at 77° F)}$$

$$u_j \doteq 13\ \text{fps} *$$

$$= 2.2 \times 10^6 . \qquad d \doteq 1.7\ \text{ft} *$$

To obtain fully turbulent jets, the smallest tolerable model Reynolds number R_m is probably about 10^3 according to our observations in the basin. Therefore

$$R_r < \frac{2.2 \times 10^6}{10^3} = 2200 \qquad 3.10$$

and

$$\frac{g'_r{}^{1/2} y_r^{3/2}}{\nu_r} < 2200 . \qquad 3.11$$

In the laboratory typical discharge temperatures were 95° F, giving $\nu_m = 0.78 \times 10^{-5}$ ft^2/sec, and $\nu_r = 1.28$. Also typically

$$g'_r = \frac{(\Delta\rho/\rho)_p}{(\Delta\rho/\rho)_m} = \frac{.0028}{.0041} = 0.68 \qquad 3.12$$

---

* Exact values are not given because they vary slightly from one end of the diffuser to the other.

The restriction on the vertical scale ratio then becomes:

$$y_r < \left\{ \frac{(2200)\ (1.28)}{(.68)^{1/2}} \right\}^{2/3} = 226 \qquad 3.13$$

Thus if $y_r = y_p/y_m$ is larger than 226 the jet Reynolds number will be too small for adequately turbulent flow. For the confirming tests reported herein, a scale of $y_r = 200$ has been used.

3.2 Intermediate Field

Beyond the initial mixing zone, the flow becomes essentially horizontal in two layers -- an upper warm water layer (the diluted discharge) overriding the ambient seawater. Currents are induced in the ambient seawater by the entrainment of the jets. The overall patterns of these induced currents, toward and away from the diffuser, have been studied in the model basin. The distances of concern are of the order of several times the total diffuser length L, as depicted in Fig. 3.3.

The induced flow pattern at this scale is driven by the momentum and buoyancy in the diffuser discharge. Resistance to flow at this scale arises from bottom friction and interfacial friction between warm and cool layers.

To reproduce the correct buoyancy effects the Froude Law must again be followed:

$$F_r = \frac{u_r}{\sqrt{g'_r y_r}} = 1, \text{ or, } u_r = \sqrt{g'_r y_r}\ , \qquad 3.14$$

where y_r is the vertical length ratio, g'_r is the effective gravity ratio $(g\Delta\rho/\rho)_r$. This scaling also ensures the equivalence of all Richardson numbers; a typical Richardson number is defined as

$$Ri = \frac{\frac{-g}{\rho}\frac{d\rho}{dy}}{\left(\frac{du}{dy}\right)^2} \ . \qquad 3.15$$

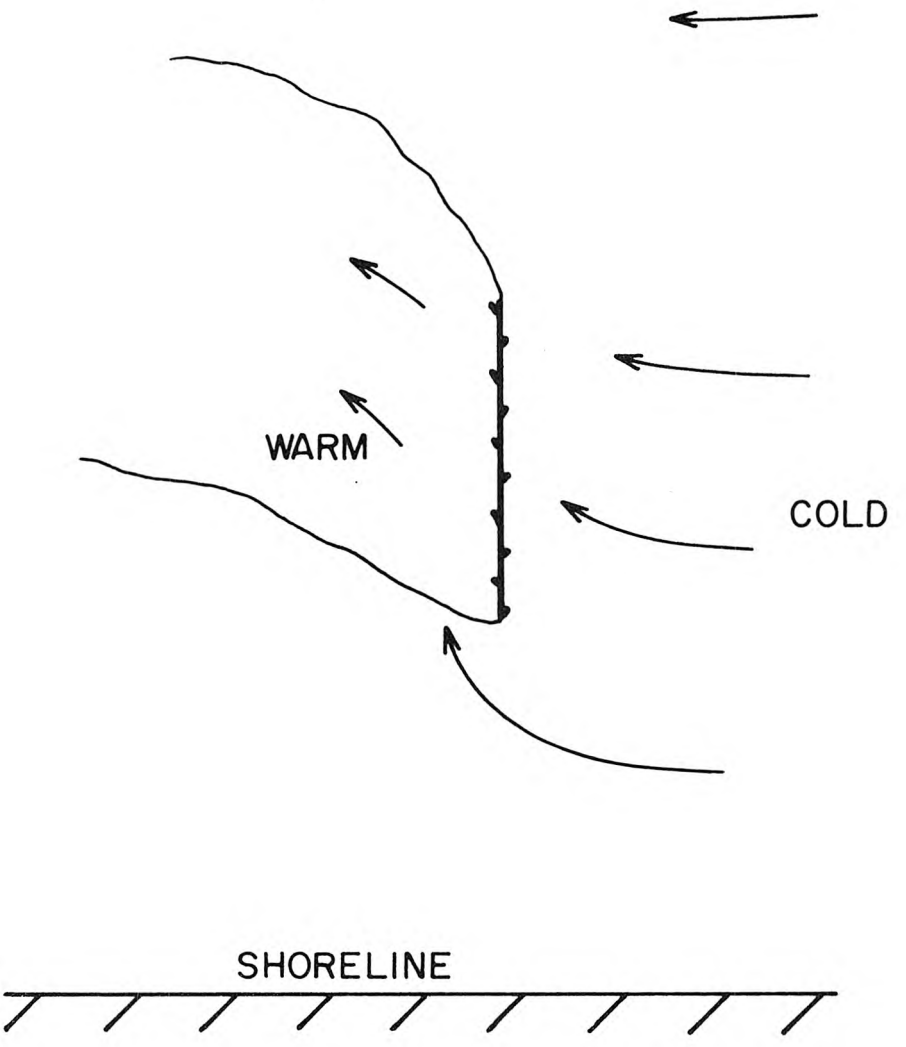

Figure 3.3 Typical flow pattern in intermediate field for diffuser perpendicular to shore with jets aimed offshore.

The ratio of Richardson numbers is

$$Ri_r = \frac{g'_r y_r}{u_r^2} = F_r^{-2} = 1 \qquad 3.16$$

The equivalence of Richardson numbers ensures that internal stratified flow phenomena such as generation and breaking of interfacial waves are correctly modeled dynamically.

The frictional effects should also be properly modeled. The bottom friction of the current depends on the friction factor f which is

$$f = f(R_c, \frac{4y_1}{k}) \ , \qquad 3.17$$

where y_1 is the total local depth, k is the bottom roughness, and R_c is the Reynolds number for the current, given as:

$$R_c = \frac{4u_c y_1}{\nu} \ . \qquad 3.18$$

Typical values for the prototype are

$$u_c = 0.1 \text{ knot} = 0.17 \text{ fps},$$

$$y_1 = 40 \text{ ft},$$

$$\nu = 1.3 \times 10^{-5} \text{ ft}^2/\text{sec (sea water at 59°F)},$$

$$R_c = \frac{4 \times 0.17 \times 40}{1.3 \times 10^{-5}} = 2.1 \times 10^6 \ . \qquad 3.19$$

The surface roughness is quite low for the sandy bottom off San Onofre and might be taken as k = 0.05 ft (equivalent to a surface roughness of 15 mm). Then $4 y_1/k = 4(40)/0.05 = 3200$, and by the Moody friction factor diagram we find, for $R_c = 2.1 \times 10^6$ and $4y_1/k = 3200$:

$$f_p = 0.015 \qquad 3.20$$

At model scales of $y_r = 200$ and $g'_r = 0.68$, $u_r = \sqrt{200 \times 0.68} = 11.7$, giving a model current $u_{cm} = 0.17/11.7 = 0.0145$ fps. The model depth is 0.2 ft and the viscosity (fresh water at 67°F) is $\nu_m = 1.1 \times 10^{-5}$ ft^2/sec. Therefore in the model, the Reynolds number for the ambient current is

$$R_{cm} = \frac{4u_{cm}u_m}{\nu_m} = \frac{4(.0145)(0.2)}{1.1 \times 10^{-5}} = 1.05 \times 10^3 \ . \qquad 3.21$$

This is still in the laminar range; the model friction factor is estimated to be $f_m = 0.061$. (Note that predictions of friction factors are somewhat uncertain at Reynolds numbers near critical.) The model friction factor would still be 0.061 even if the sand in the bed of the basin were finer, because of the low Reynolds number.

The ratio of friction factors is

$$f_r = f_p/f_m = 0.015/0.061 = 0.25 \ . \qquad 3.22$$

Thus to counteract the resulting excessive friction which would arise in an undistorted model, the horizontal dimensions (L) should be foreshortened by distortion; namely

$$f_r = \frac{y_r}{L_r} = 0.25 \ , \qquad 3.23$$

or $$L_r/y_r = \text{distortion factor (D.F.)} = 4 \ .$$

Intuitively, this result may be understood by remembering that

$$f \propto \text{friction slope} \propto \frac{\text{vertical distance}}{\text{horizontal distance}} \ .$$

For interfacial friction between warm and cold layers, a similar argument applies; the model interfacial friction is proportionately too

large, and is counteracted by reducing horizontal dimensions. Interfacial friction factors depend on both Richardson and Reynolds numbers in a complex way. A distortion factor of four may be taken as a good estimate, pending further research on the matter. We reject large distortion factors of the order of 10, but on the other hand, we believe model distortion is necessary for models of this size.

If the model is to be distorted, then the length of the diffuser must be scaled by the horizontal length, not the vertical. For n ports at spacing b,

$$L = nb \ ,$$

$$L_r = n_r b_r \ . \qquad 3.24$$

The near-field scaling necessitates taking $b_r = y_r$ to preserve the correct ratio of b/y_o; otherwise the initial mixing would be incorrectly modeled.

The number of ports must thus be scaled as

$$n_r = L_r/y_r = D.F. \qquad 3.25$$

In other words if the distortion factor is 4, the number of ports is reduced by factor of 4, as the length L is reduced by factor 4 also (from what it would be undistorted). The diffuser is <u>locally undistorted</u> in terms of ports <u>per unit length</u>, and momentum, volume, and buoyancy fluxes <u>per unit length</u>. The ocean current was similarly reproduced: momentum and volume fluxes per unit width are scaled by Froude Law, but with overall flow field widths and lengths reduced relatively by the distortion factor.

This approach is justified <u>only</u> when the ratio of model diffuser length L_m to model depth y_{1m} is still large ($\gtrsim 10$) and the number of ports in the model is still large ($n_m \gtrsim 10$).

There is still one conflict of scaling, namely the length of the initial mixing zone in front of the diffuser. This distance should really be scaled in an undistorted way, a certain number of flow depths, or by the vertical length ratio y_r. Thus if the mixing zone extends for 2 ft in the model when $y_r = 200$ and $L_r = 800$, it should be interpreted to be 400 ft rather than 1600 ft in the prototype. The initial mixing zone is thus somewhat too large in a distorted model but this is not believed to be a serious problem. To be conservative, the 1000 ft limit of the requirements is scaled according to L_r, or relatively too close to the diffuser; however, the initial mixing is accomplished within this distance anyway.

The time-scale ratio in a distorted model to produce the correct horizontal displacements in unsteady flow must be

$$t_r = L_r/u_r = \frac{L_r}{\sqrt{g'_r y_r}} \quad . \tag{3.26}$$

For example, given $L_r = 800$, $g'_r = 0.68$, $y_r = 200$, then $t_r = 68.6$, or one day in the prototype becomes 21 minutes in the model.

3.3 Far Field

The far field is the zone of drift flow far away from the diffuser, and is not represented by the hydraulic model. Most of the heat loss is in the far field. For a uni-directional flow the rate of temperature decay is

$$\frac{\Delta T}{\Delta T_s} = e^{-\frac{K}{\rho c_p h} t} \tag{3.27}$$

where h = depth of heated layer, $t = x/u$ = time of travel, ΔT = excess temperature above the equilibrium temperature, and ΔT_s is the initial value of ΔT at the end of the initial mixing zone. Typically K is of the order 100 BTU/°F ft^2 day; $\rho c_p = 61.6$ BTU/°F ft^3; and $K/\rho c_p \approx 1.6$ ft/day. If $h \sim 30$ ft, then the exponent in the equation becomes $-.053t$, for t in days. The half life is then found from $e^{-.053t} = 0.5$ or $t = 13$ days. For one day the heat loss is only of the order of 5%.

If heat loss were to be scaled in the model we would require

$$\left(\frac{K}{\rho c_p h}\, t\right)_r = \frac{K_r L_r}{(\rho c_p)_r y_r u_r} = 1 \ , \qquad 3.28$$

or taking $(\rho c_p)_r = 1$,

$$\frac{L_r}{y_r} = \text{D.F.} = \frac{\sqrt{g'_r y_r}}{K_r} \ .$$

The order of magnitude of the distortion factor would be found as follows:

$$y_r = 200 \ ,$$

$$g'_r = 0.68$$

$$K_r = 1.33$$

$$(K_{lab} \approx \tfrac{3}{4} K_{field}) \ , \qquad 3.29$$

$$\text{D.F.} = \frac{(0.68 \times 200)^{1/2}}{1.33} = 8.8$$

In other words the model loses heat so fast that a distortion of almost 9 is required to counteract it; or put another way, if the model is distorted only by a factor of 4, then the heat loss in the model will be about 2.2 times too fast. In one simulated prototype day the model would lose 11% of the heat instead of 5%. Some adjustment of the results is necessary for tests which reproduce time periods of the order of prototype days.

In summary, the hydraulic modeling is concerned with the near and intermediate fields which are dominated by hydrodynamic effects, rather than the far field which is dominated by heat loss and long-time advection.

CHAPTER 4

EXPERIMENTAL EQUIPMENT

4.1 Model Basin*

A 20 ft by 36 ft basin was constructed to house the physical model for the investigation of the three-dimensional thermal dispersion due to the discharge of cooling water from coastal nuclear power plants. The basin walls consisted of concrete blocks which were mortared onto the concrete laboratory floor. A plastic sheet shaped to fit was placed in the basin to prevent any leakage. Approximately twenty tons of sand (median diameter $\doteq$ 0.8 mm) were placed on the plastic sheet and shaped to simulate the sloping nearshore shelf. A pumped recirculation system was also installed on the model basin so that a longshore ocean current (both unidirectional and reversing) could be simulated. The recirculation system consisted of two pumps which could be used either singly or in parallel to allow the simulation of a wide range of current speeds. The intake and discharge of the recirculation system consisted of five manifolds at each end of the basin, with each manifold equipped with a throttling valve for control of the flow distribution. Immediately in front of the manifolds a cradle containing rubberized hair was used to ensure an even flow distribution. Figure 4.1 shows a schematic of the basic components. Photographs of various subcomponents are shown in Figures 4.2 through 4.5.

4.2 Diffuser Model

To simulate the discharge of cooling water through the diffusion structures, model diffusers were constructed of copper pipes with stainless steel nozzles soldered on. The model diffusers were heat insulated

---

*The development of the model basin and associated instrumentation was supported jointly by contracts from Southern California Edison Company and Bechtel Corporation (for Pacific Gas and Electric Company).

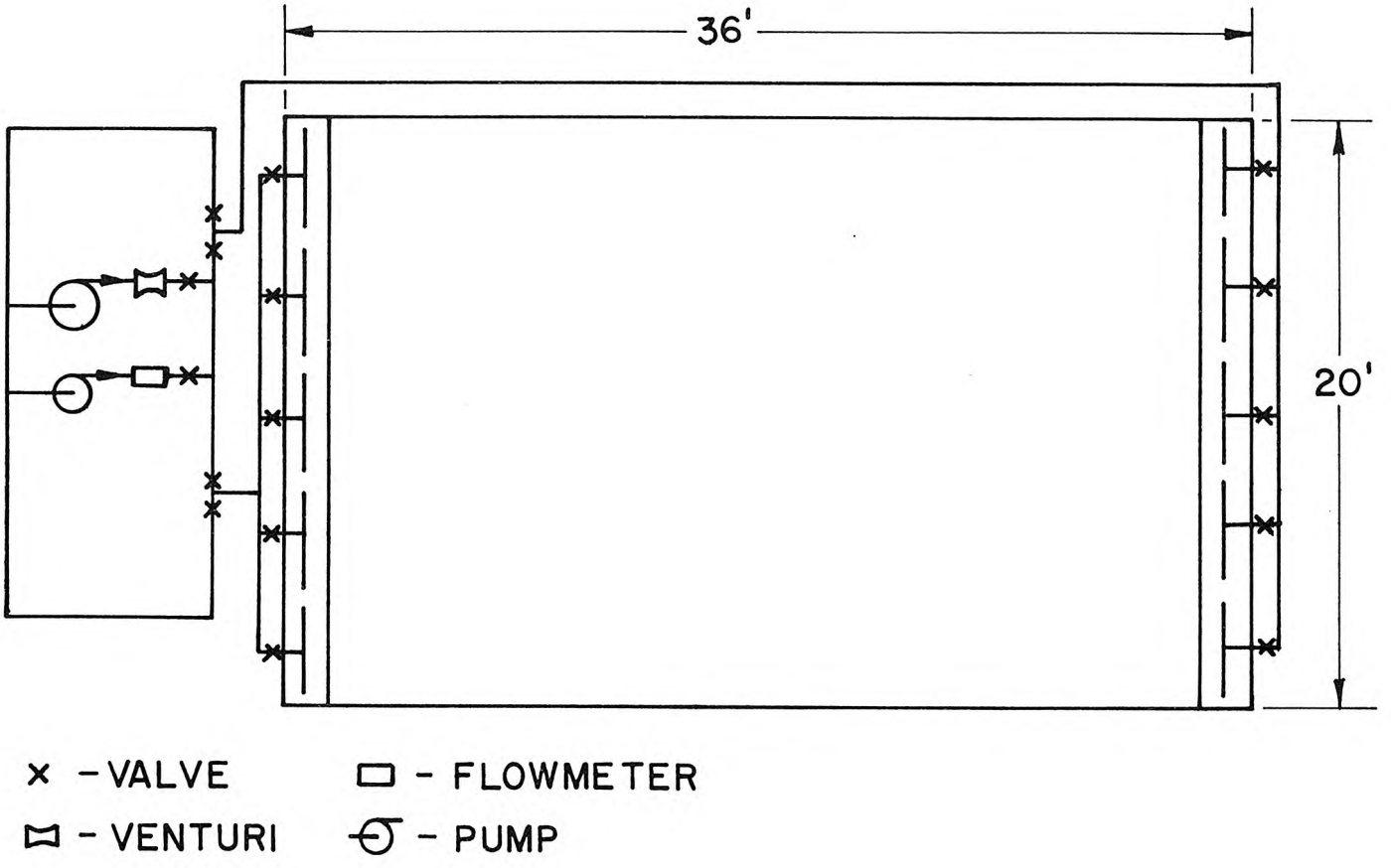

Figure 4.1. Schematic of the laboratory test tank layout.

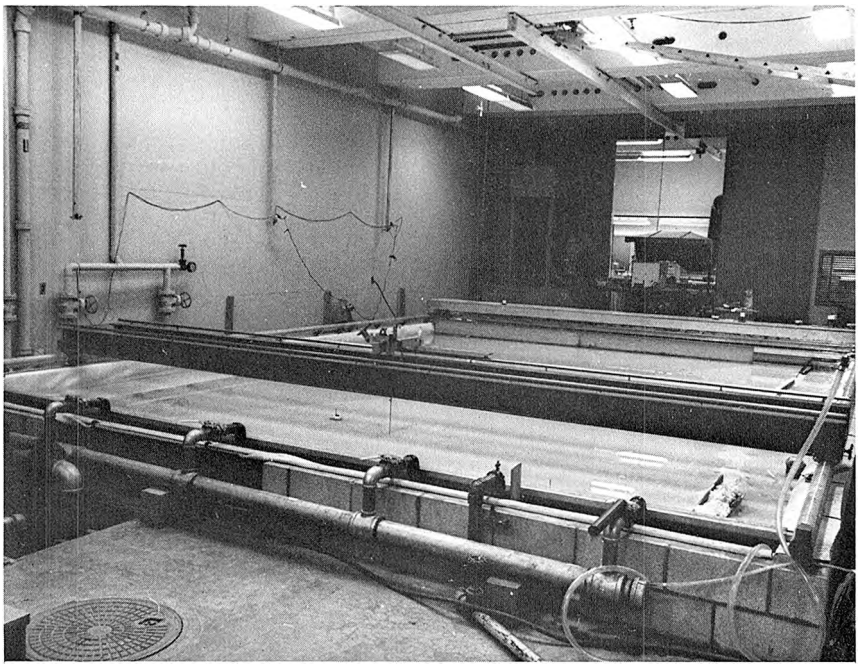

Figure 4.2. Overall view of test basin.

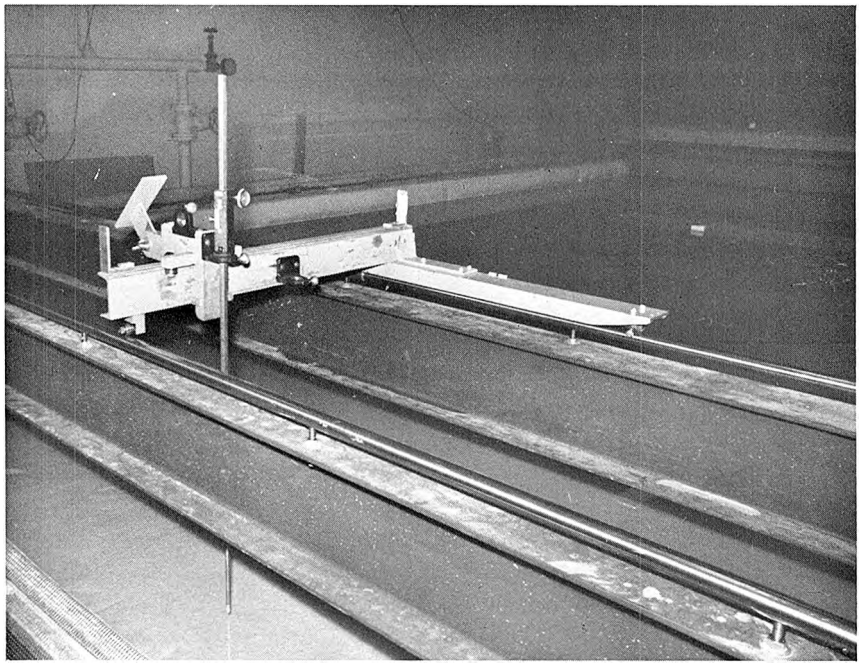

Figure 4.3. Test carriage and depth probe.

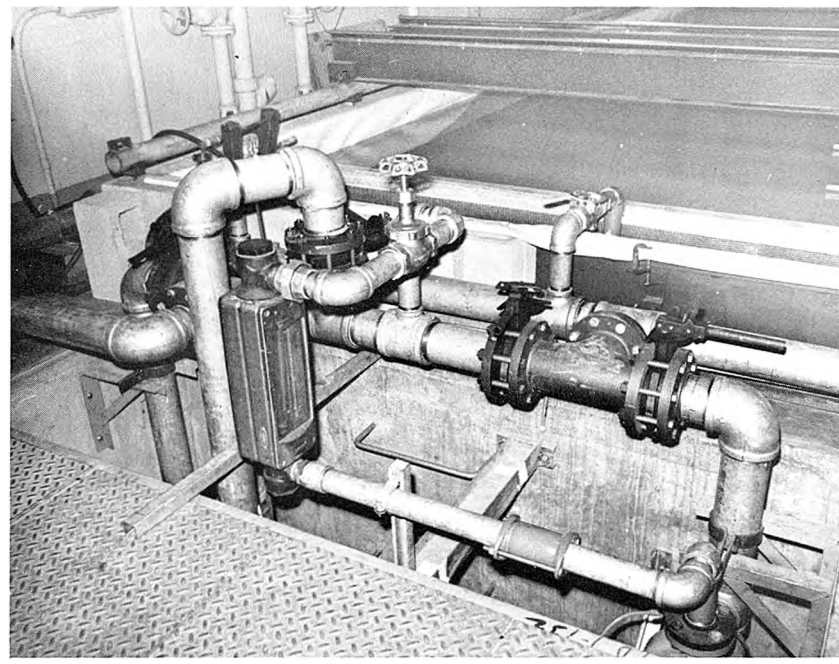

Figure 4.4. Piping and valves for controlling flow direction and rate. Pumps and venturi meter are out of sight in the pump well.

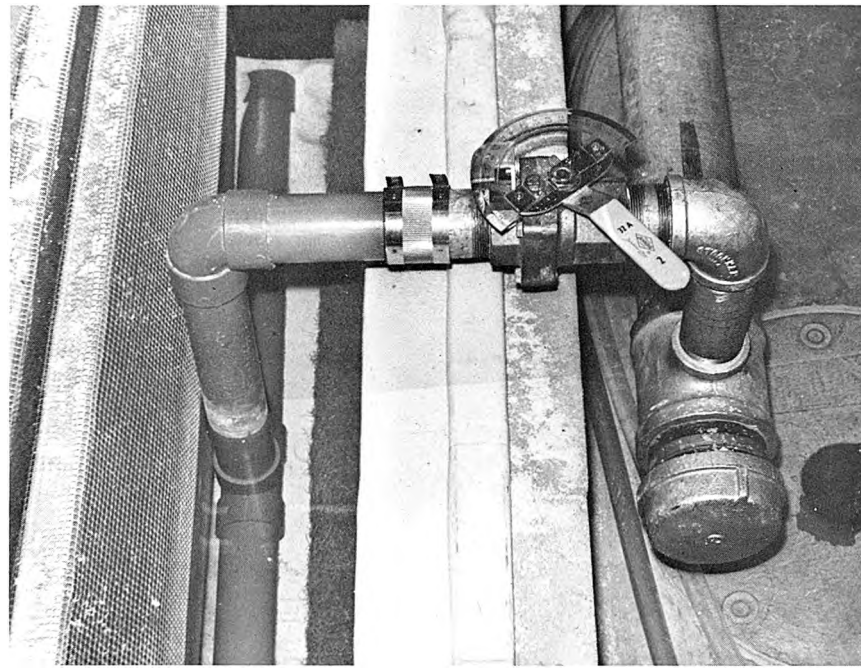

Figure 4.5. Manifold control valve and rubberized hair screen (extreme left).

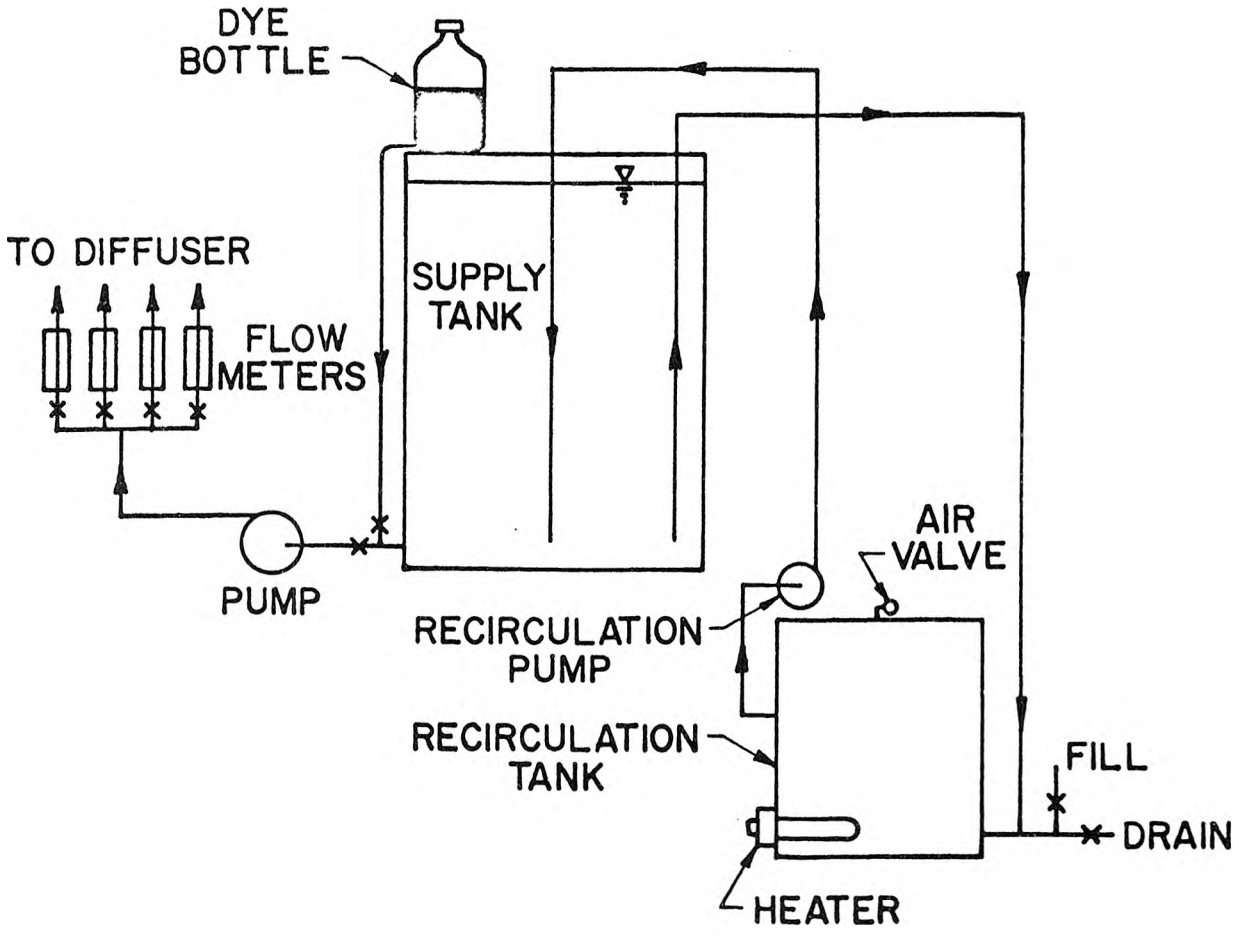

Figure 4.6. Schematic of warm water supply system.

by means of approximately 1/2 inch of foam material. A thermistor was also mounted within each diffuser to monitor the temperature of the discharge water.

Schematics of the warm water discharge system and the model diffusers and intakes are shown in Figures 4.6 through 4.8. Figures 4.9 through 4.11 show photographs of the various components of the discharge system. The model diffusers (Figures 4.7 and 4.11) were installed by burying them in the sand bed with only the nozzles showing, as in the prototype. Thus only the nozzles themselves needed to be scale modeled. The sizes were chosen to make the contracted jet diameters scale like y_r. The

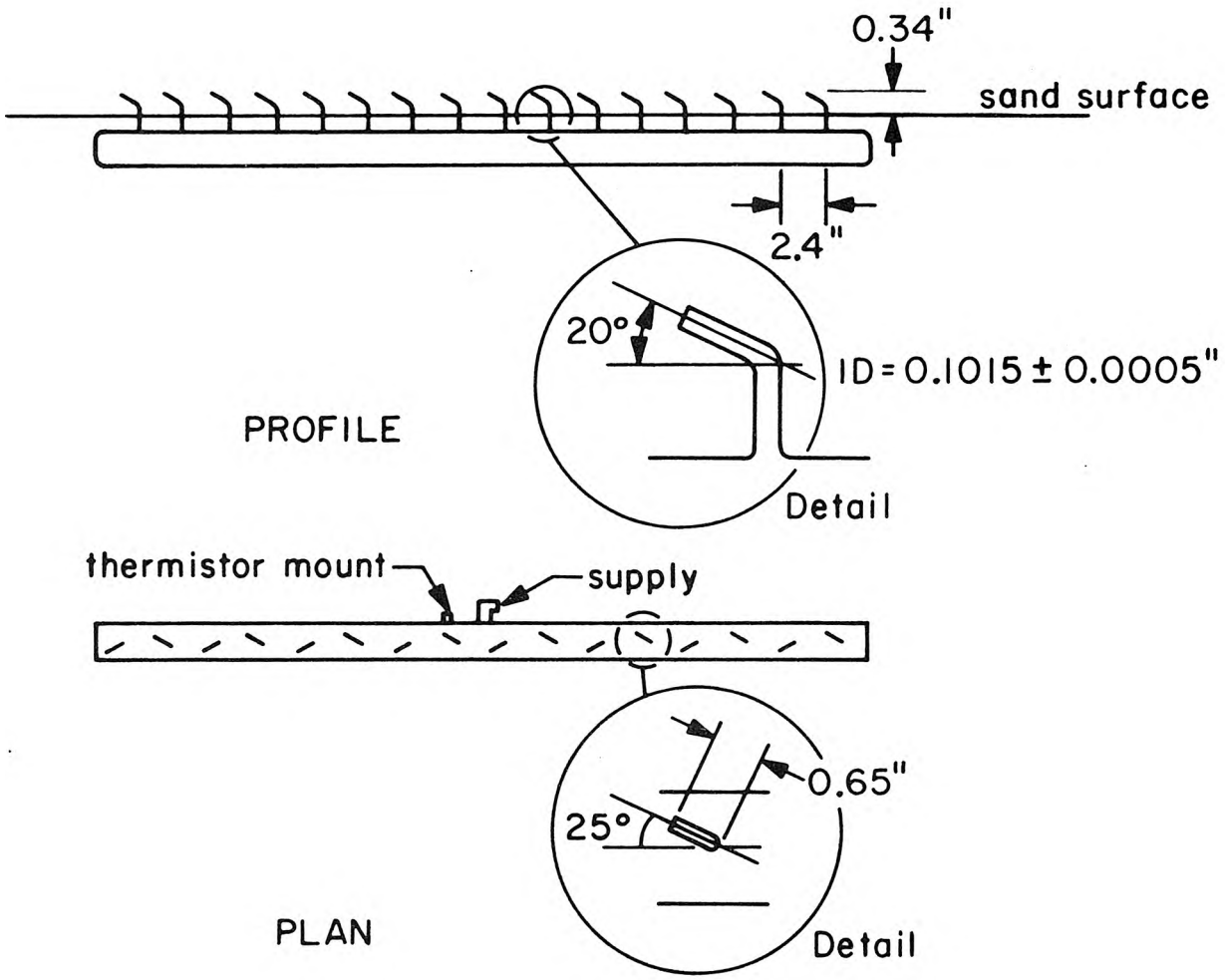

Figure 4.7 Schematic of model diffusers used in confirming tests (16 ports, L_r = 787.5, y_r = 200).

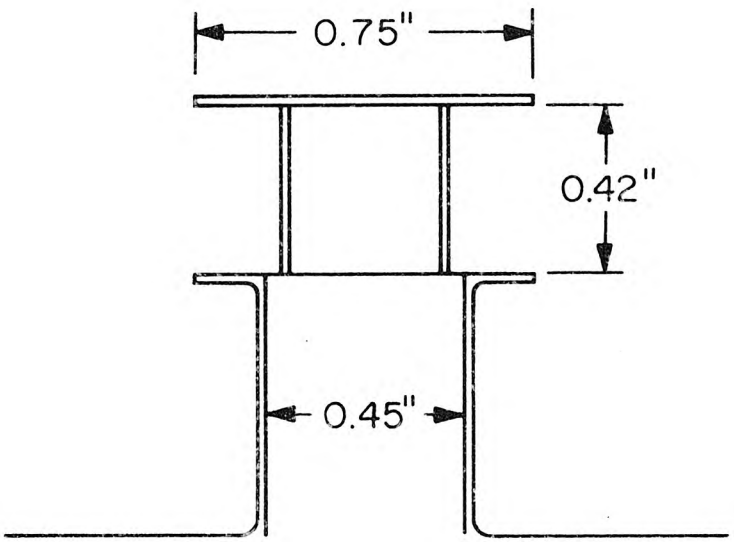

PROFILE

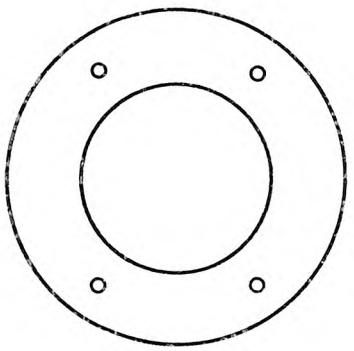

PLAN

Figure 4.8 Schematic of model intakes used in confirming tests (L_r = 787.5, y_r = 200). (See Figures 4.11 and A-14.)

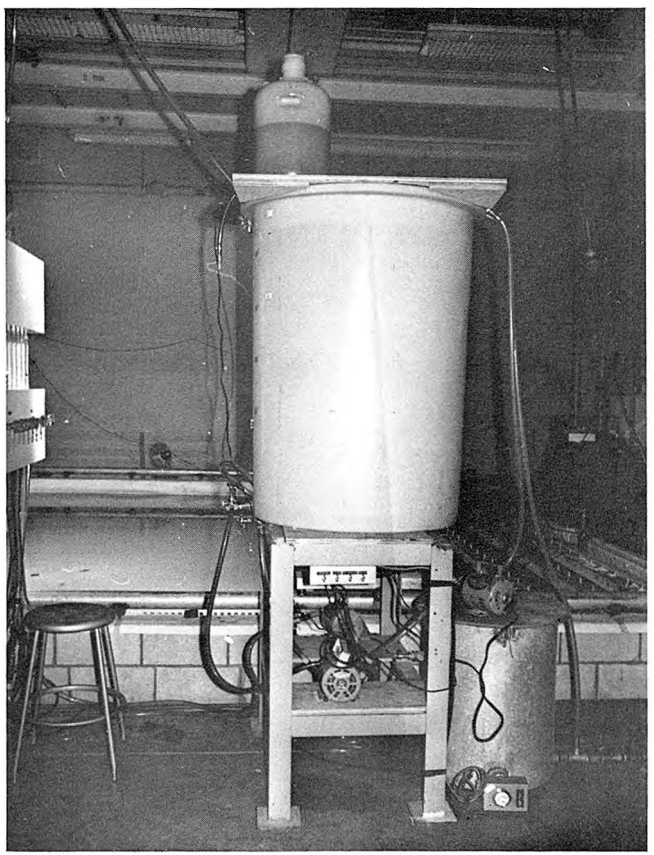

Figure 4.9. Warm water supply system.

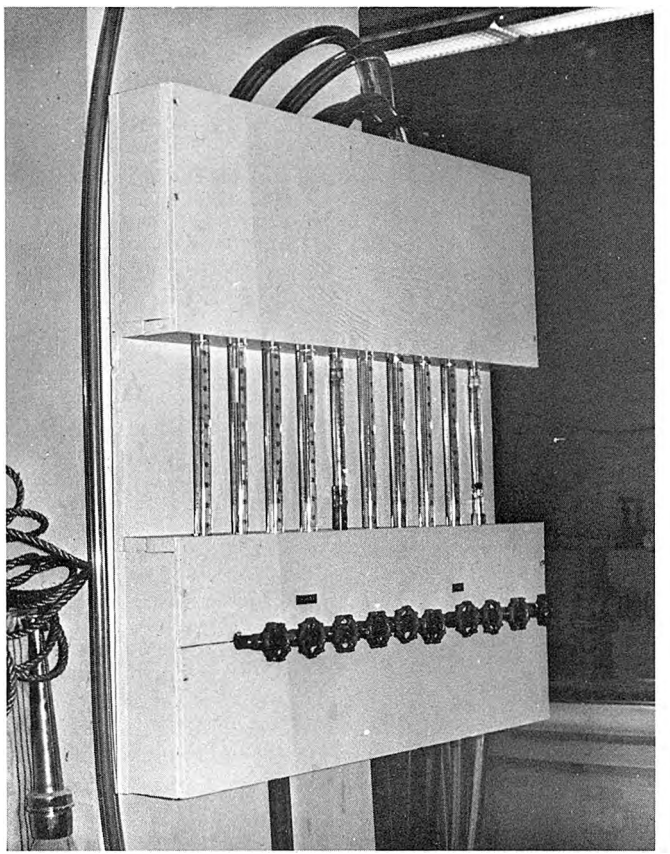

Figure 4.10. Flow measurement for outfalls and intakes.

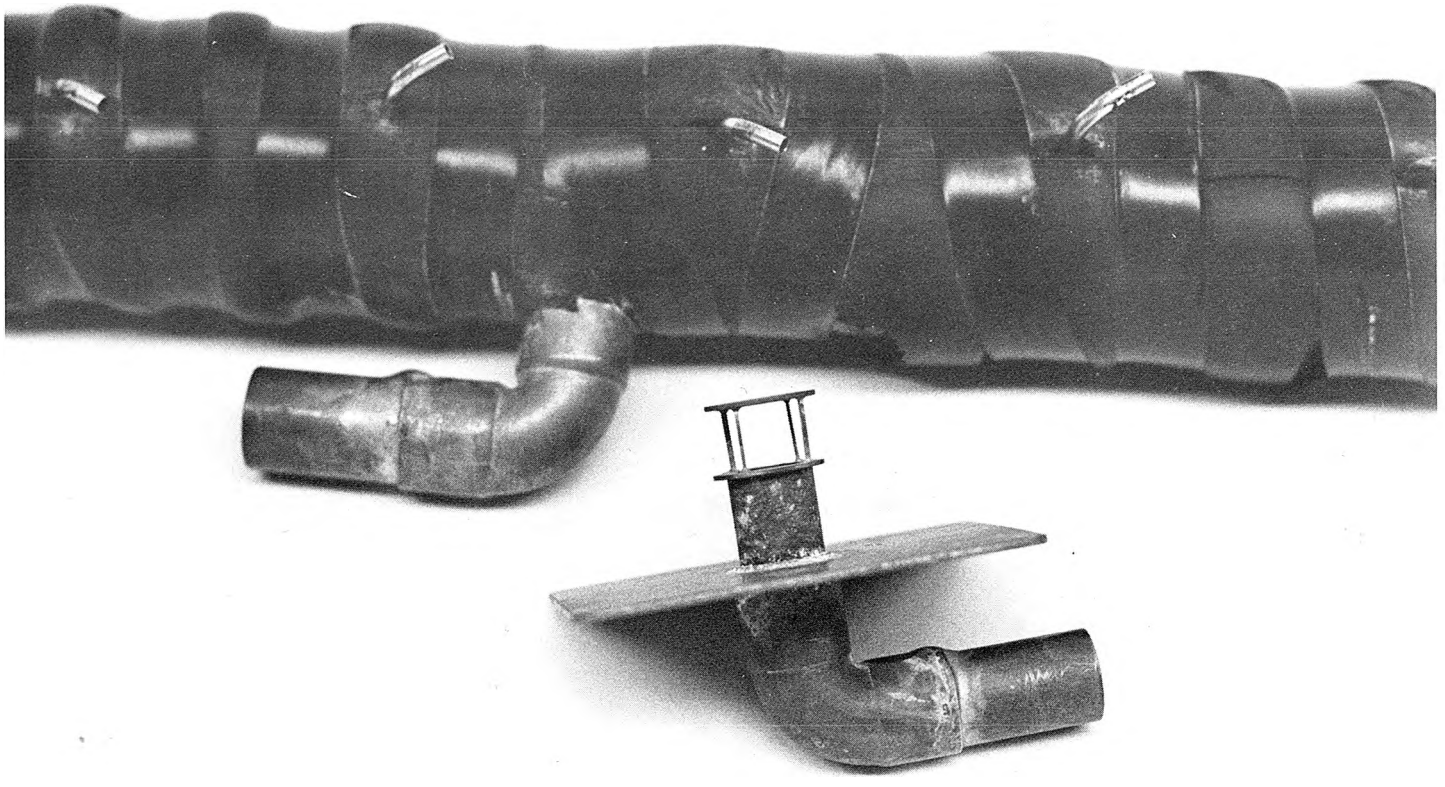

Figure 4.11. Photograph of portion of model diffuser and intake (only one of each is shown).

hoses for conveying the hot water to the diffusers were also buried in the sand. The delivery of warm water to the center of the model diffusers is only a model detail to minimize starting transients, whereas the prototype diffuser is fed from the shoreward end via the outfall pipe.

The model intakes (Figures 4.8 and 4.11) cannot be properly scaled in a distorted model, and thus the flow details near the intakes were studied in separate undistorted models of $y_r = 100$ to determine the entrainment of the Unit 1 discharge into the intakes for Units 2 and 3 and to measure the thermal field during reverse flow for heat treatment. The intakes in the distorted model mainly serve the purpose of providing sinks of appropriate strengths.

4.3 Instrumentation for Thermal Measurement

Temperature measurement in the basin was carried out with laboratory-calibrated thermistors*. A total of 112 thermistors could be located throughout the hydraulic model in such a way that the temperatures recorded could be used to plot maps of the isotherms in the vicinity of the diffusers. The voltage drops across the thermistors in appropriate bridge circuits were measured and recorded with a 7-channel analogue-to-digital signal converter and digital tape recorder; the connections were made sequentially in 16 groups of seven via a time-sequence multiplexer constructed especially for the model. With this arrangement it was possible to sample all 112 thermistors 42 times in a period of a few seconds. The temperatures so obtained were recorded on digital tape which was later processed by an IBM 370/158 computer to plot temperature contours in the model automatically. The accuracy of the system allows discrimination of temperature variations of less than 0.1°C. In addition, a thermistor rake containing 12 thermistors spaced vertically at 0.5 cm intervals was used to obtain vertical temperature profiles.

Details of the temperature measurement system are shown in Figures 4.12 through 4.15.

*Supplied by Victory Engineering Co. (Model No. 32A1).

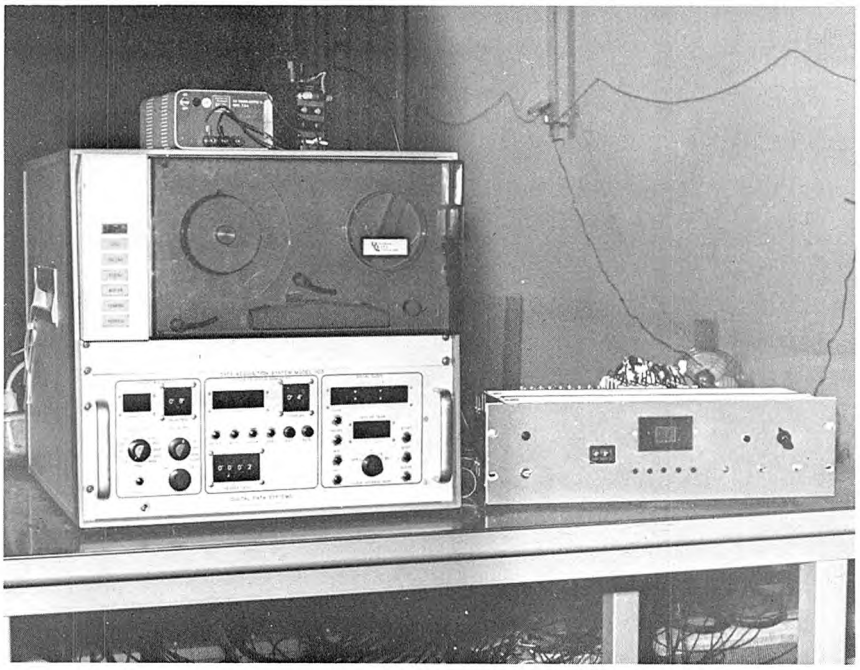

Figure 4.12. Analogue-to-digital data system and multiplexer.

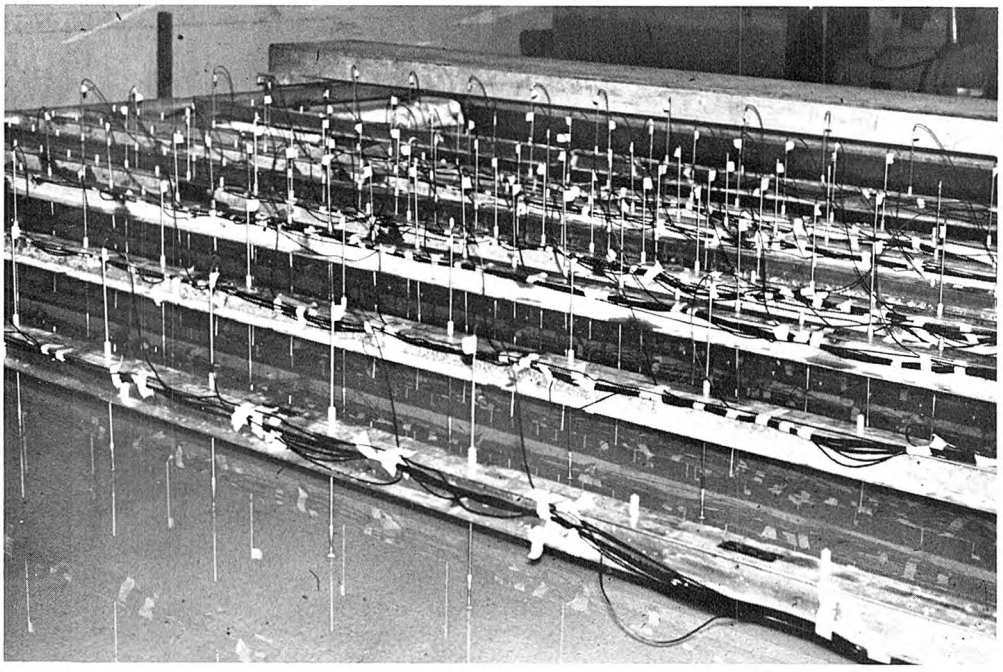

Figure 4.13. Thermistors mounted in the basin.

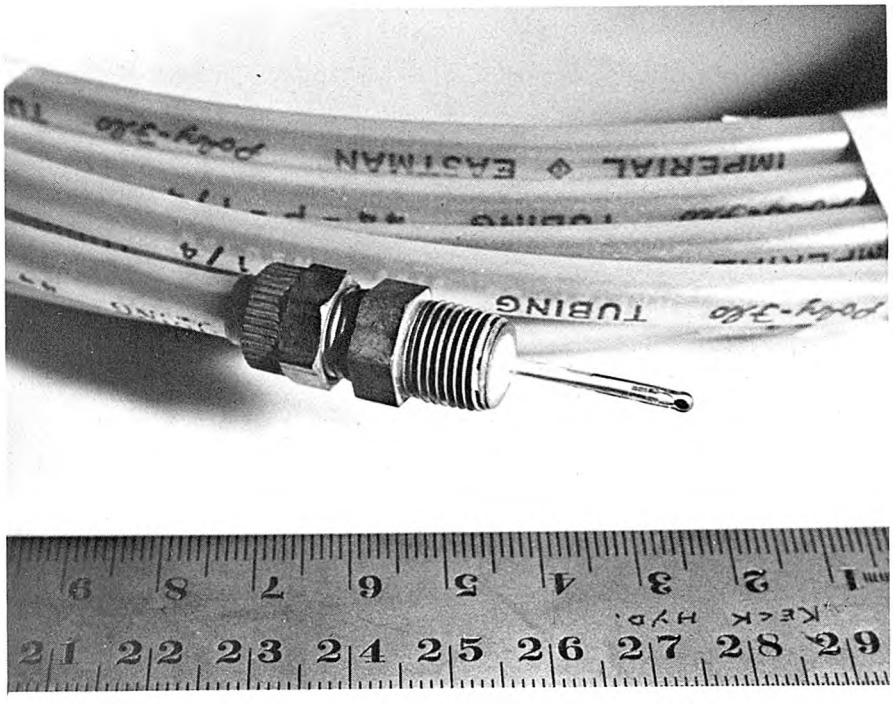

Figure 4.14. Close-up of thermistor used to monitor temperature inside diffuser pipe.

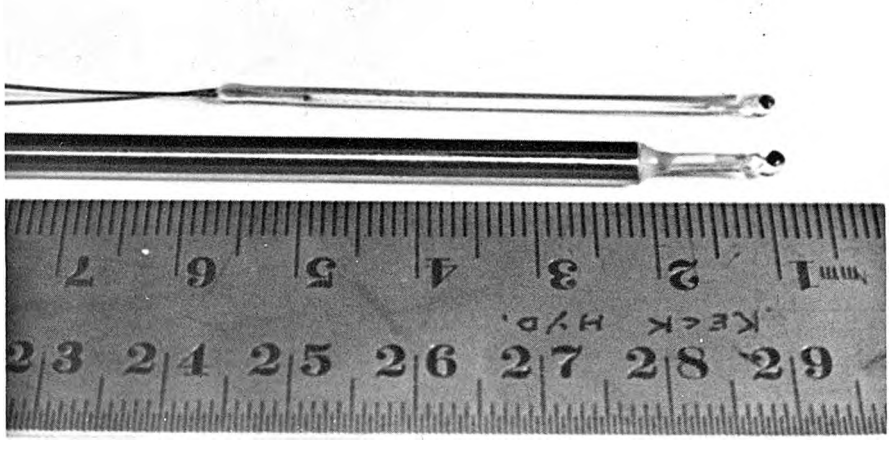

Figure 4.15. Close-up of thermistor before and after mounting for use in arrays (Figure 4.13).

4.4 Overhead Photography

A Nikon F camera equipped with a 17mm lens was used to obtain overhead photographs of the operation of the model in the basin (with the help of dye). The extreme wide angle lens was necessary in order to cover most of the basin area from the available ceiling height. The camera was equipped with a motor drive so that it could be triggered from the laboratory floor level. The basin was illuminated by 6 electronic flash units mounted on the wall and columns of the laboratory. One of the flashes was triggered by the camera and the rest by means of slave units.

CHAPTER 5

DESCRIPTION OF THE EXPERIMENTS

The primary basin experiments to measure thermal fields can be divided into three categories, performed in the following order:

1) Preliminary experiments to determine the general behavior of heat dispersion as a function of the diffuser design variables (alignment, length, depth) and the ocean current.

2) Experiments to delineate the chosen preliminary design among a set of alternatives established from (1).

3) Confirming tests based on detailed bathymetry and actual diffuser design.

Results of tests in categories 1 and 2 have been reported in Progress Reports 1, 2, and 4.* The overall project includes, in addition to the above, tests on a sectional model (at approximately 50:1 undistorted scale) to determine the near field jet behavior (Progress Report No. 5); tests on discharge of Unit 1 and reverse flow for heat treatment in Units 2 and 3 at an undistorted scale of 100:1 (Progress Reports No. 6 and 7); and hydraulic performance tests of individual discharge nozzles (Progress Report No. 3). Detailed results from previous tests already reported in Progress Reports 1 through 7 will not be included in this final report. However, the salient features of those tests are presented in summary form in the Appendix for completeness.

Three basic ocean current sequences were used in the confirming tests reported herein:

a) Steady unidirectional currents of various magnitudes (e.g., 0, 0.1, 0.25, 0.5 knots prototype).

---

*See Reference List (p.102) for complete list of progress reports.

b) Reversing currents of various amplitudes, corresponding to a period of 12 hours for one complete cycle (semi-diurnal tide).

c) Special current sequences chosen from field data collected at the San Onofre site.

The test procedure began with the preparation of the bottom profile. The twenty tons of white sand in the basin was molded to the proper bottom slopes (based on recent bathymetric survey results furnished by SCE) by scraping the sand surface with a template attached to an aluminum beam which in turn was attached to the instrument carriage. Several passes were necessary to obtain a smooth uniform surface. The bottom at San Onofre was approximated by five discrete slopes as shown in Figure 6.2. After the bottom profile was established, the model diffusers and intakes were buried to their appropriate positions. The thermistor array, when used, was then positioned over the diffuser system to allow measurement of the thermal field.

Prior to the beginning of each run, the desired ocean current was established in the basin and allowed to stabilize. At the same time, the hot water system was filled with water at the desired temperature. Immediately before the experiment, the ambient temperature was measured by means of both the thermistor array and a laboratory mercury thermometer. The experiment commenced at $t = 0$ when the hot water discharge was started. Basin water was withdrawn through the intakes at the same rate, and discharged to the wastewater sump. Thermal measurements were taken at intervals of several minutes (corresponding to several hours in the prototype) throughout the duration of the experiment (approximately 30 minutes). For simulating a reversing ocean current, the valves in the recirculating system were adjusted manually to achieve the desired flow rate and flow direction as functions of time. The ambient temperature at the discharge manifold of the recirculating pump and the water temperature inside the diffusers were also continuously monitored.

At the conclusion of each experiment, the data for the thermal field, loaded in digital form on magnetic tape, was then processed in the Caltech Computing Center. The thermal maps obtained show values of $\Delta T/\Delta T_o$ and must be multiplied by ΔT_{op} (prototype) = 20°F to get prototype predictions of ΔT. In the model basin ΔT_{om} was larger (approximately 30°F), but the scaling is nonetheless dynamically correct.

In all the experiments, both those reported herein and in the progress reports summarized in the Appendix, the water in the test basin before the run was uniform in density and temperature. In the field, there may be some thermal stratification particularly during the summer. This effect was not investigated. It can be expected, however, that any gravitationally stable thermal stratification in the prototype would decrease the apparent temperature excess on the surface. Thus the reported results would be conservative.

The results of the various tests will be presented in Chapter 6 .

CHAPTER 6

EXPERIMENTAL RESULTS

The experiments conducted during the final confirming test period can be classified into two categories:

1) Tests at a steady longshore current where vertical thermal profiles were taken using the thermistor rake and photographic coverage was made.

2) Tests at various longshore current sequences (steady, reversing, and special) where surface temperature patterns were taken using the thermistor array.

The schematic plan and profile of the basin layout are shown in Figures 6.1 and 6.2 respectively. In these experiments, only the Units 2 and 3 intake and discharge structures are incorporated. The existing Unit 1 structures and those for possible future Units 4 and 5 are excluded in the tests, the former due to the fact that it is not possible to realistically model single outlet discharges in a distorted model,* the latter because of the uncertainty in the future plans and the unknown design of the structures.

The model ratios chosen for this series of tests are 787.5:1 horizontal and 200:1 vertical making the distortion factor 3.94. This allows the proper modeling of 63 discharge ports in the prototype by 16 in the model (see Eq. 3.25). A summary of the experiments conducted is shown in Table 6.1, and the model ratios and basic data in Table 6.2.

6.1 Vertical Temperature Profiles

The first series of tests conducted (Category 1 above) consists of five runs (C-2 through C-6) where the thermistor rake was used to obtain vertical thermal profiles at various locations around the diffusion

---

*See Progress Report No. 6 and Section A5.

Table 6.1

Summary of Experiments for Confirming Tests

Run No.	Current (Prototype Knots)	Data Obtained	See Figure No.	On Page No.
C-2	0.0	Vertical ΔT profiles	6.3, 6.8	42, 47
C-6	0.05	Vertical ΔT profiles	6.4, 6.9	43, 48
C-5	0.1	Vertical ΔT profiles	6.5, 6.10	44, 49
C-4	0.25	Vertical ΔT profiles	6.6, 6.11	45, 50
C-3	0.5	Vertical ΔT profiles	6.7, 6.12	46, 51
C-11	0.0	Surface ΔT mapping	6.13, 6.14	60, 61
C-10	0.05	Surface ΔT mapping	6.15	62
C-9	0.1	Surface ΔT mapping	6.16	63
C-8	0.25	Surface ΔT mapping	6.17	64
C-7	0.5	Surface ΔT mapping	6.18	65
C-17	0.05R *	Surface ΔT mapping	6.20, 6.21	67, 68
C-16	0.15R	Surface ΔT mapping	6.22-6.24	69-71
C-18	0.40R	Surface ΔT mapping	6.25-6.28	72-75
C-12	SP1 **	Surface ΔT mapping	6.29-6.34	76-81
C-13	SP2	Surface ΔT mapping	6.35-6.36	82-83
C-14	SP3	Surface ΔT mapping	6.37-6.39	84-86
C-15	SP4	Surface ΔT mapping	6.40-6.48	87-95

* R indicates reversing current of given amplitude.

** SP indicates special current sequence (see Figures 6.29, 6.35, 6.37, 6.40 for current sequences used).

Table 6.2

Summary of Modeling Ratios for Confirming Tests

	Ratios: $\frac{\text{Prototype}}{\text{Model}}$
L_r, horizontal lengths	787.5
y_r, vertical lengths	200
$\left(\frac{\Delta\rho}{\rho}\right)_r$, density difference	0.63
u_r, velocity	11.66
n_r, number of nozzles	3.938
t_r, time	67.5
Q_r, discharge	1.84×10^6

Diffuser Characteristics

	Model	Prototype
Length (nominal)	38.4 in.	2520 ft
Number of Ports	16	63
Port Spacing	2.4 in.	40 ft
Nozzle Diameter	0.1015 in.	20.3 in. * †
Jet Velocity at the Nozzle	1.12 fps	13.1 fps * †
Jet Reynolds number at the Nozzle	1215	2.22×10^6 * †
Nozzle Angle up from horizontal	20°	20°
Nozzle Angle with axis of diffuser pipe (in horizontal plane)	±25° (alternating)	±25° (alternating)
Elevation of the center of the nozzle above the sea floor	0.34 in.	5.67 ft *

† at vena contracta

* values as scaled from model to prototype. In the actual prototype, these represent nominal values since they vary somewhat from one end of the diffuser to the other.

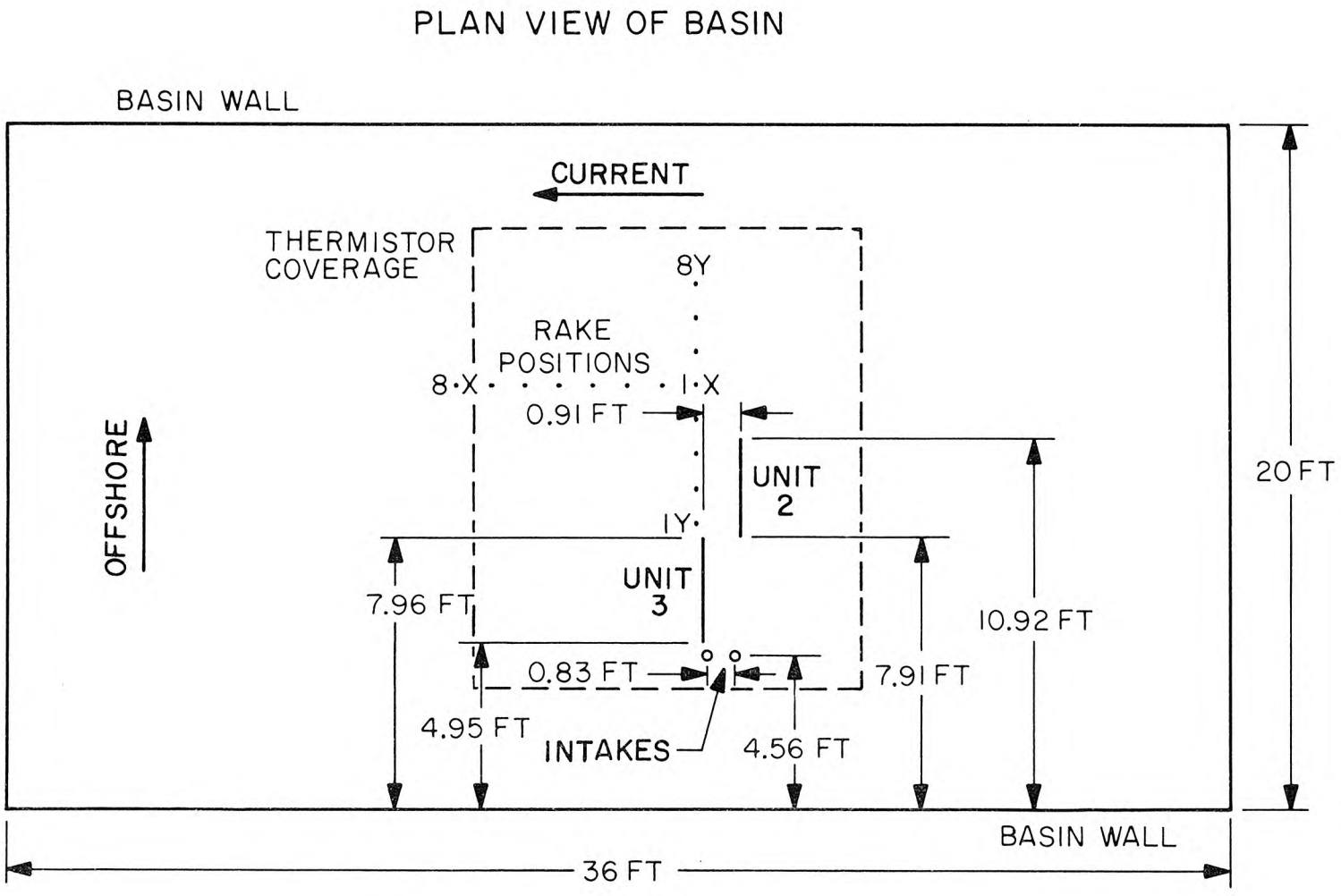

Figure 6.1 Schematic plan of basin layout used in confirming tests. (Horizontal scale is 787.5:1. Note that diffuser lengths are center to center of first and last ports; therefore model L_m = 3.21 ft (3.01 x 16/15) and prototype L_p = 2520 ft (787.5 x 3.21)). Rake positions at 1 ft intervals. Basin wall approximately at shoreline.

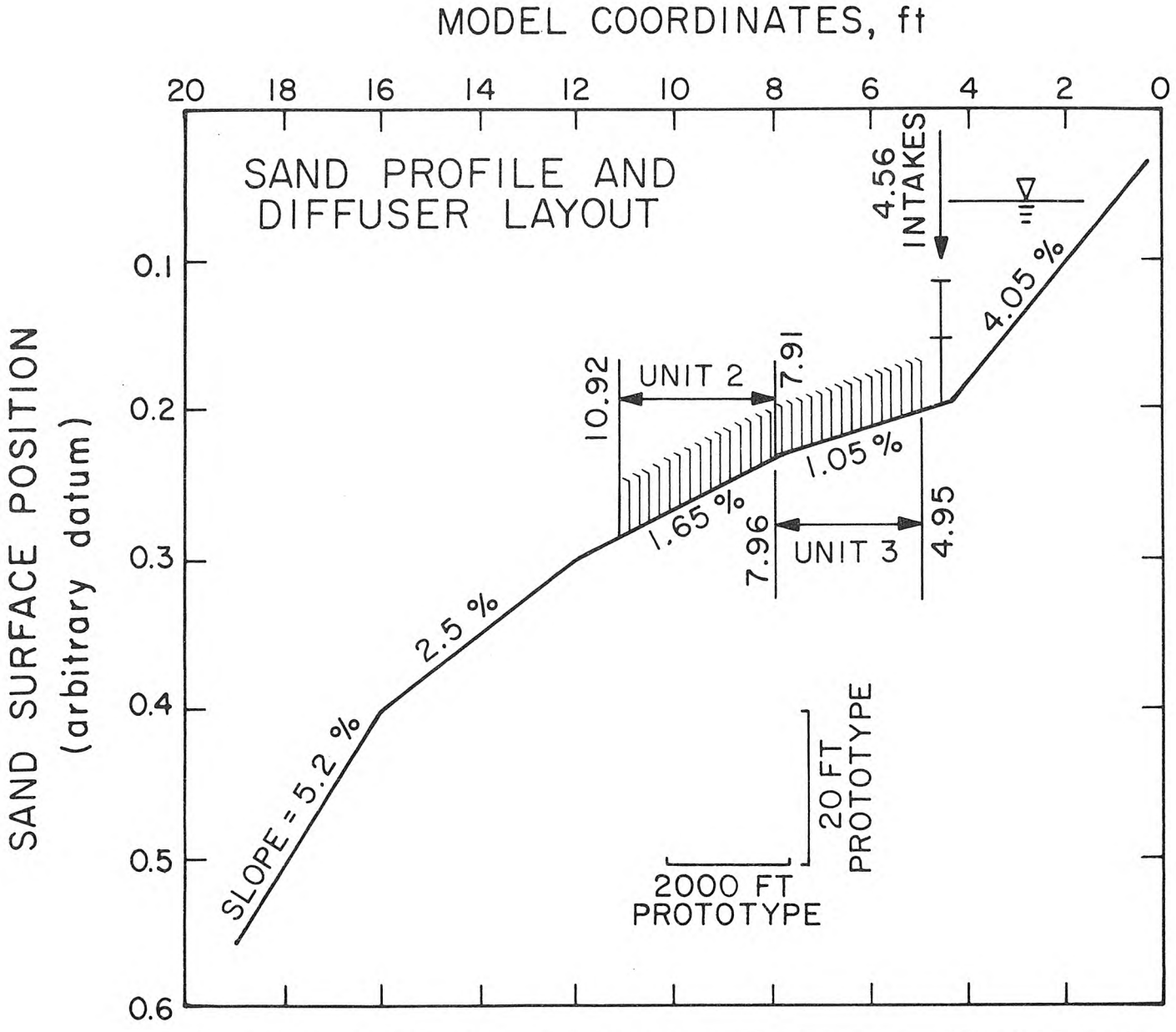

Figure 6.2 Profile of basin layout in confirming test. (Vertical scale is 200:1, model distortion is 3.94:1.)

structures. These runs were for the case when the longshore currents were steady at 0, 0.05, 0.1, 0.25, 0.5 knots. Figures 6.3 through 6.7 show photographs of the dispersion pattern and Figures 6.8 through 6.12 show the vertical profiles at selected stations for the various runs. It can be observed from the photographs that the offshore momentum in the discharge exerts a fairly strong induced circulation for the cases of low longshore current speeds. For higher current speeds, the ambient current plays a more dominant role in the dispersion. From the vertical profiles it is seen that there is no sharp dividing line between the surface warm layer and the bottom cool layer although the temperature decreases with depth. (It should be noted, however, that the thermistor rake does not extend to the full depth.)

6.2 Heat Loss Corrections

Before presenting the results of the tests with the thermistor array, it must be noted that due to the small depth in the laboratory, the effect of surface heat loss is more pronounced than in the field. The raw data obtained are, therefore, not conservative due to this effect. In order to correct for this effect, the following approximate estimate was made.

From the experimental results to be presented, a dilution of 8 (or more) is obtained in most of the runs. Assuming that the drift current created by the offshore discharge is 5000 ft wide and 30 ft thick, a drift velocity of about 0.2 fps is predicted in the field. The time it takes to traverse 10,000 ft (which is of the order of the thermistor coverage) is 800 min. or 0.56 day. In the field, the heat loss effect would have caused a decrease in temperature such that

$$\frac{\Delta T}{\Delta T_s} = e^{-\frac{K}{\rho c_p h} t}$$

where ΔT is the excess temperature at the surface after heat loss during time t

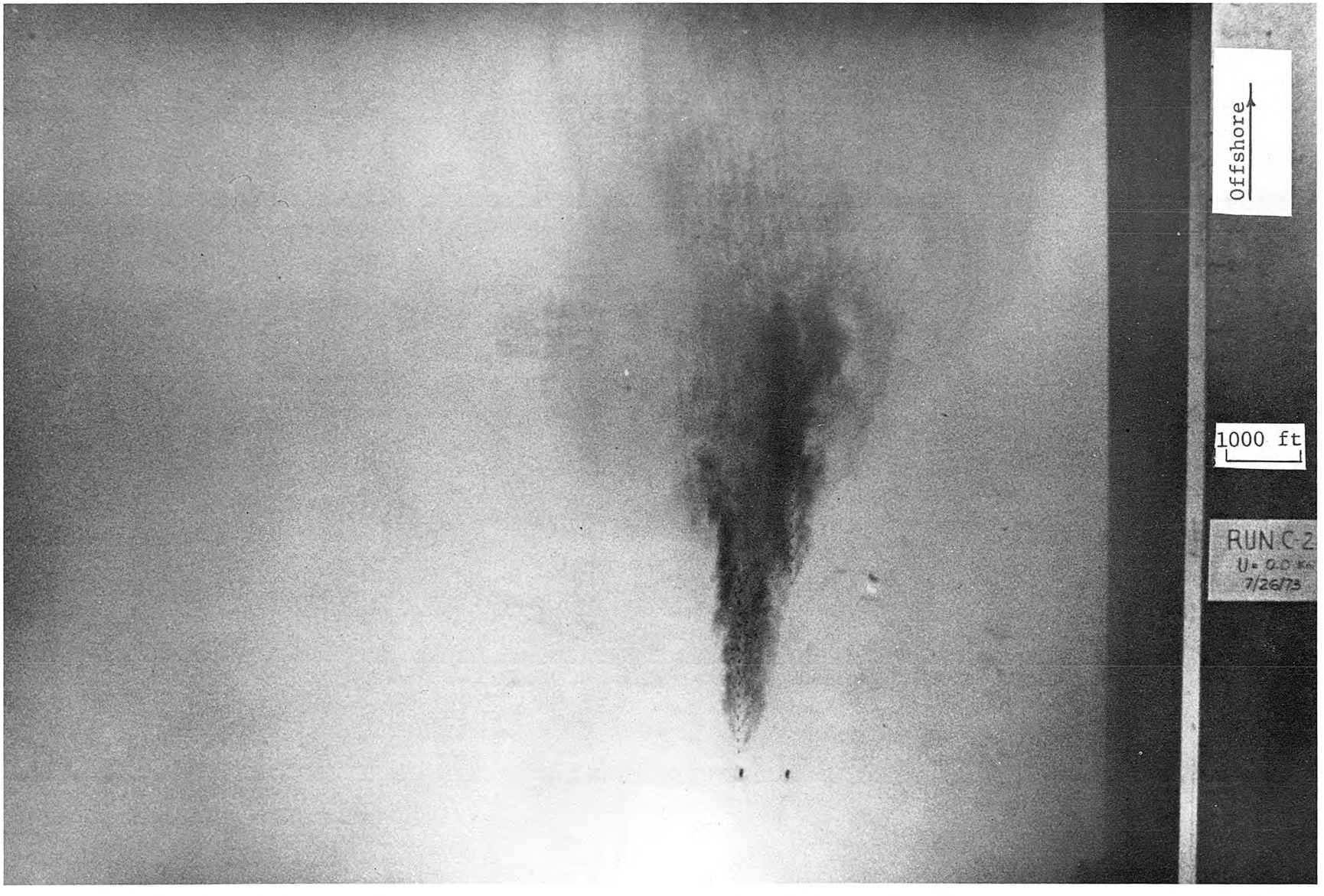

Figure 6.3 Overhead photograph of warm water dispersion for ambient along-shore current speed = 0.0 knots.

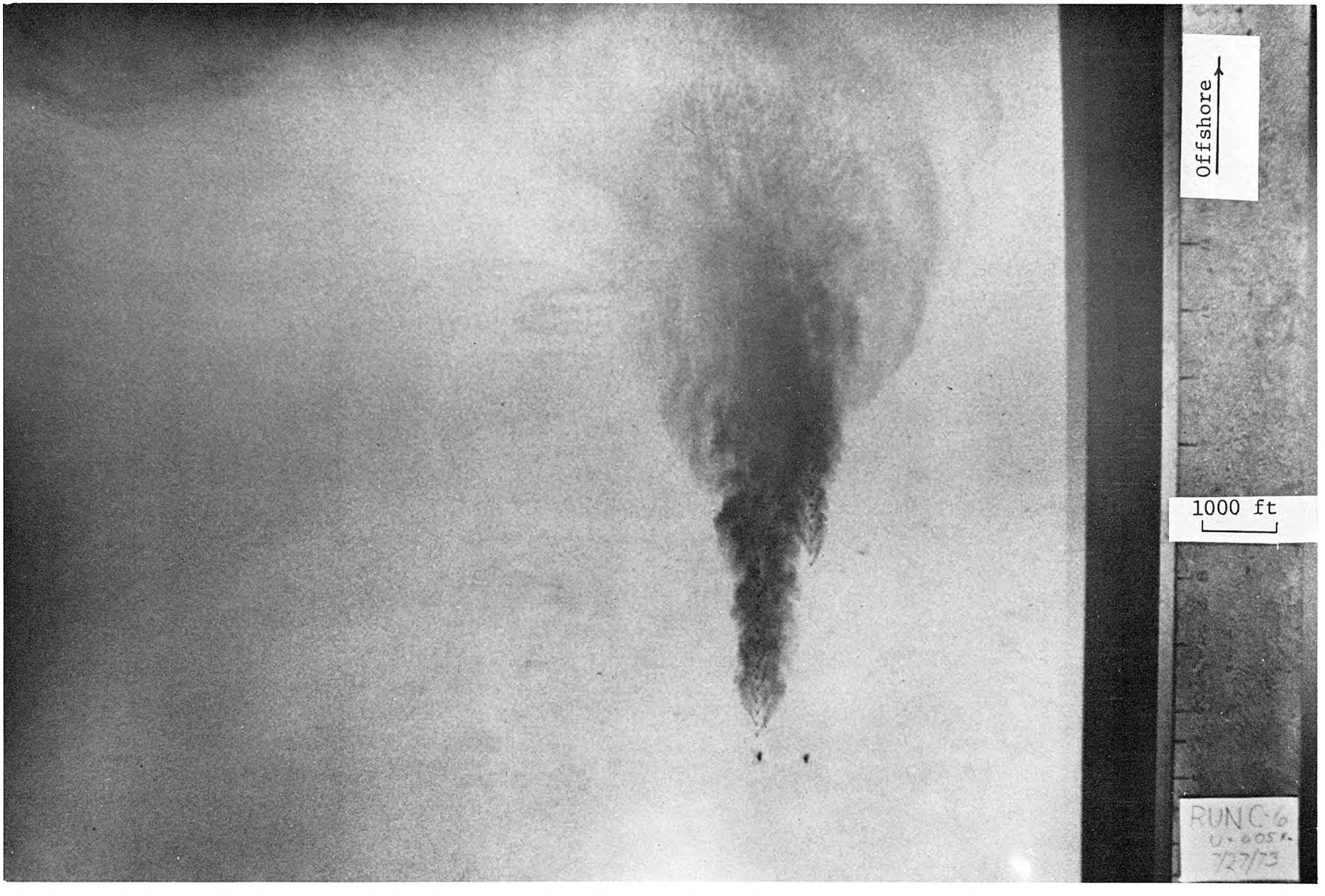

Figure 6.4 Overhead photograph of warm water dispersion for ambient along-shore current speed = 0.05 knots.

Figure 6.5 Overhead photograph of warm water dispersion for ambient along-shore current speed = 0.1 knots.

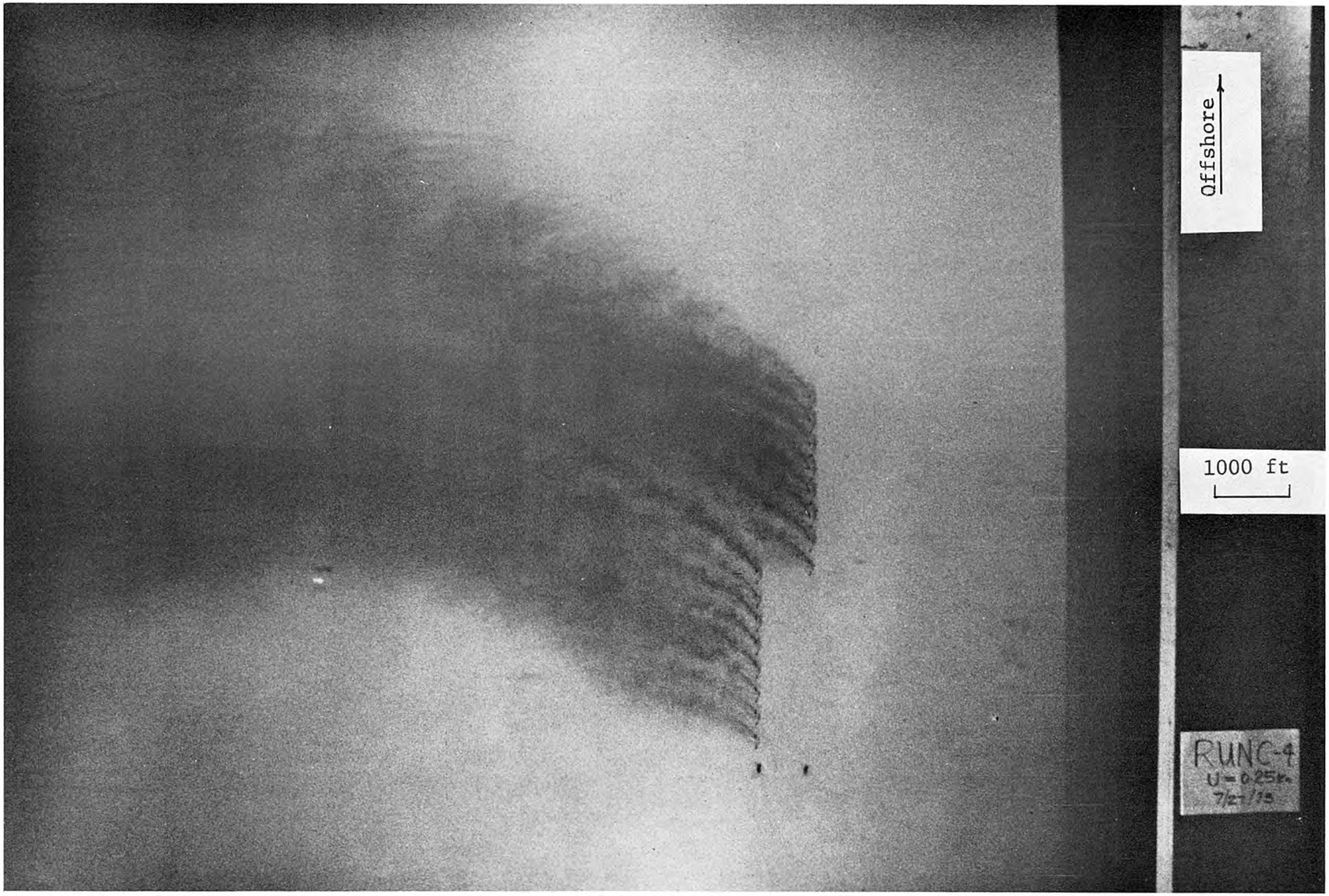

Figure 6.6 Overhead photograph of warm water dispersion for ambient along-shore current speed = 0.25 knots.

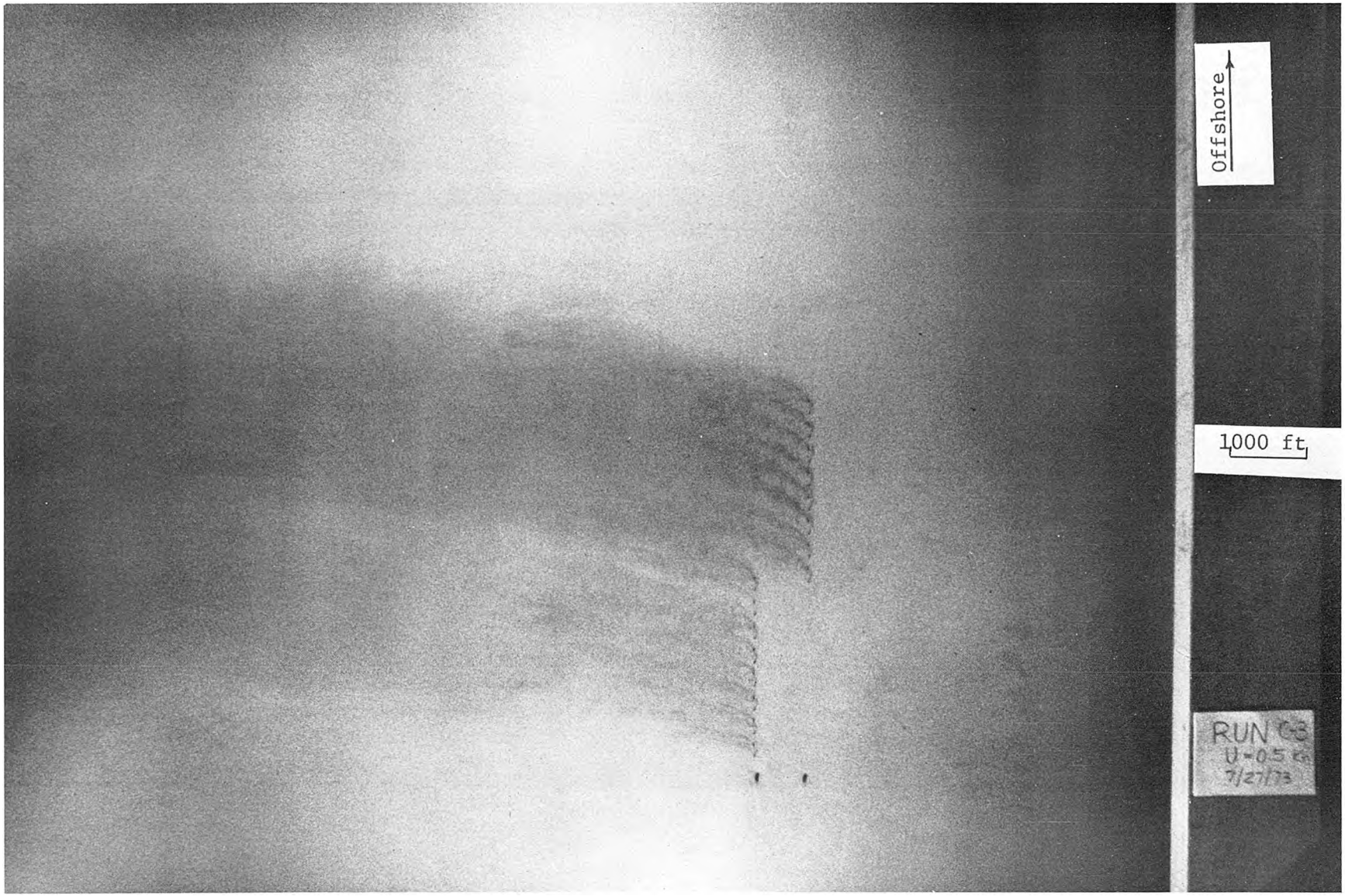

Figure 6.7 Overhead photograph of warm water dispersion for ambient along-shore current speed = 0.5 knots.

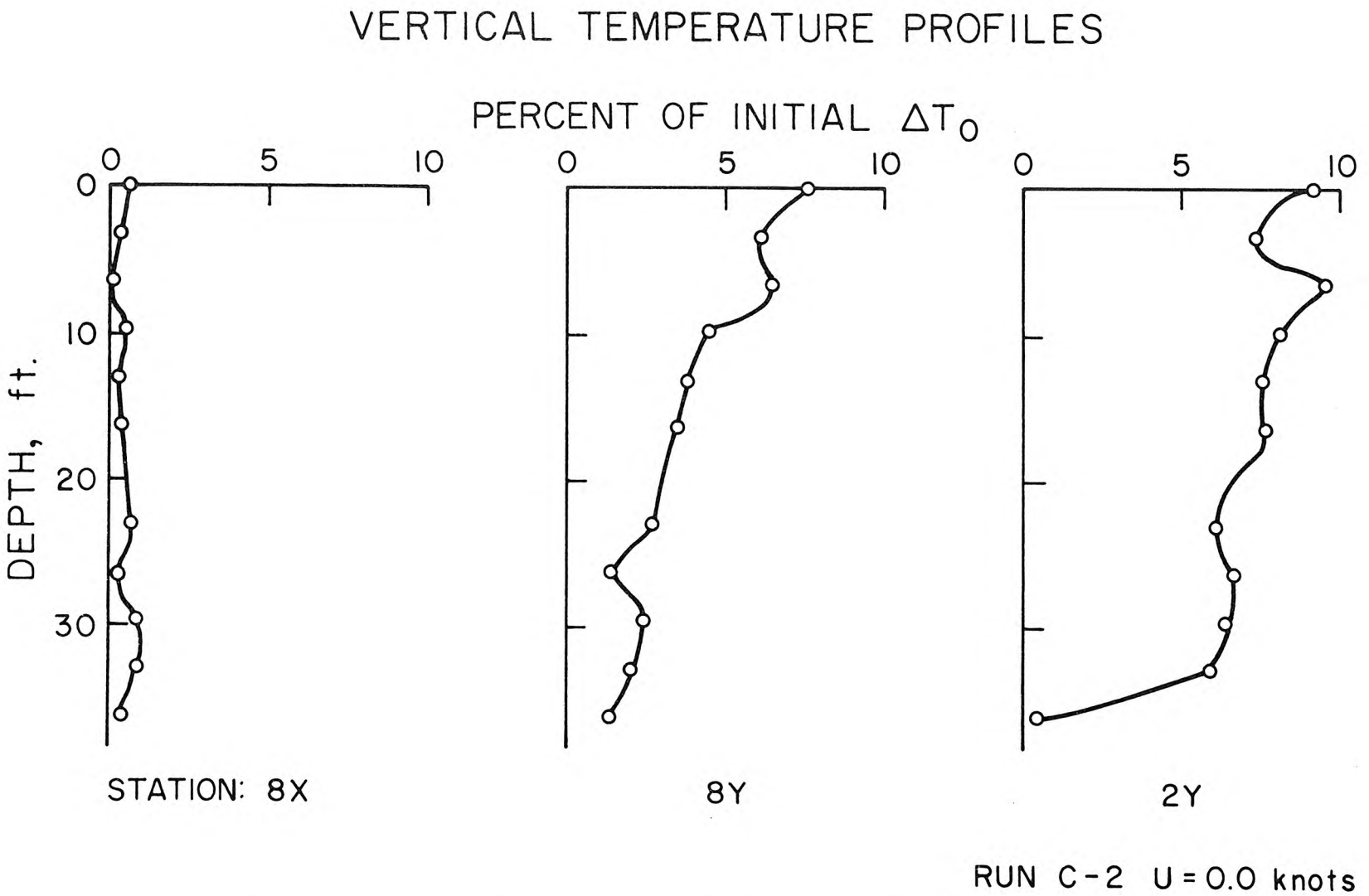

Figure 6.8 Vertical excess temperature profiles at selected stations for a steady current of 0.0 knots (data taken between 10 and 20 minutes into the experiment; see Figure 6.1 for station locations).

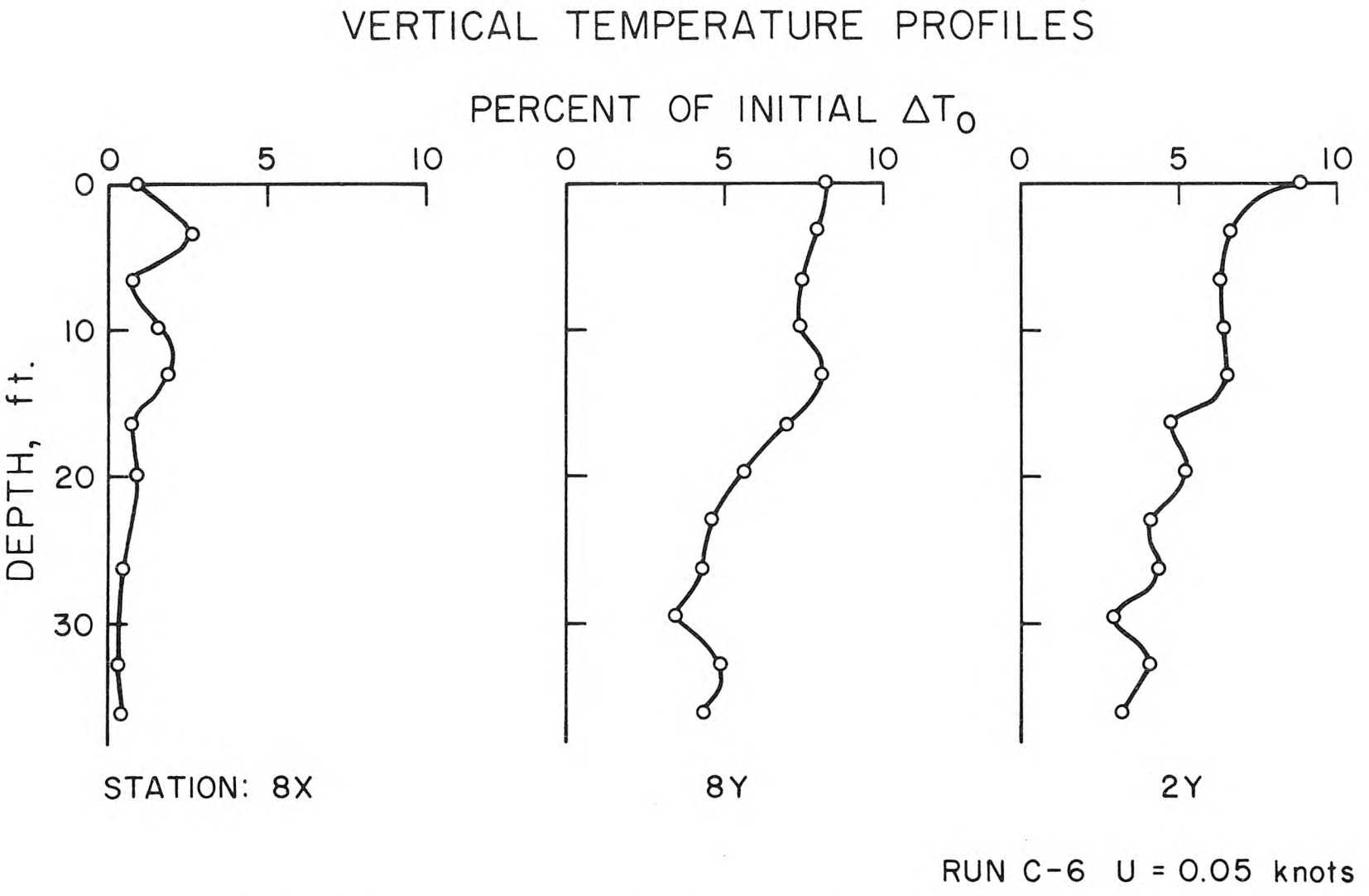

Figure 6.9 Vertical excess temperature profiles at selected stations for a steady current of 0.05 knots (data taken between 10 and 20 minutes into the experiment; see Figure 6.1 for station locations).

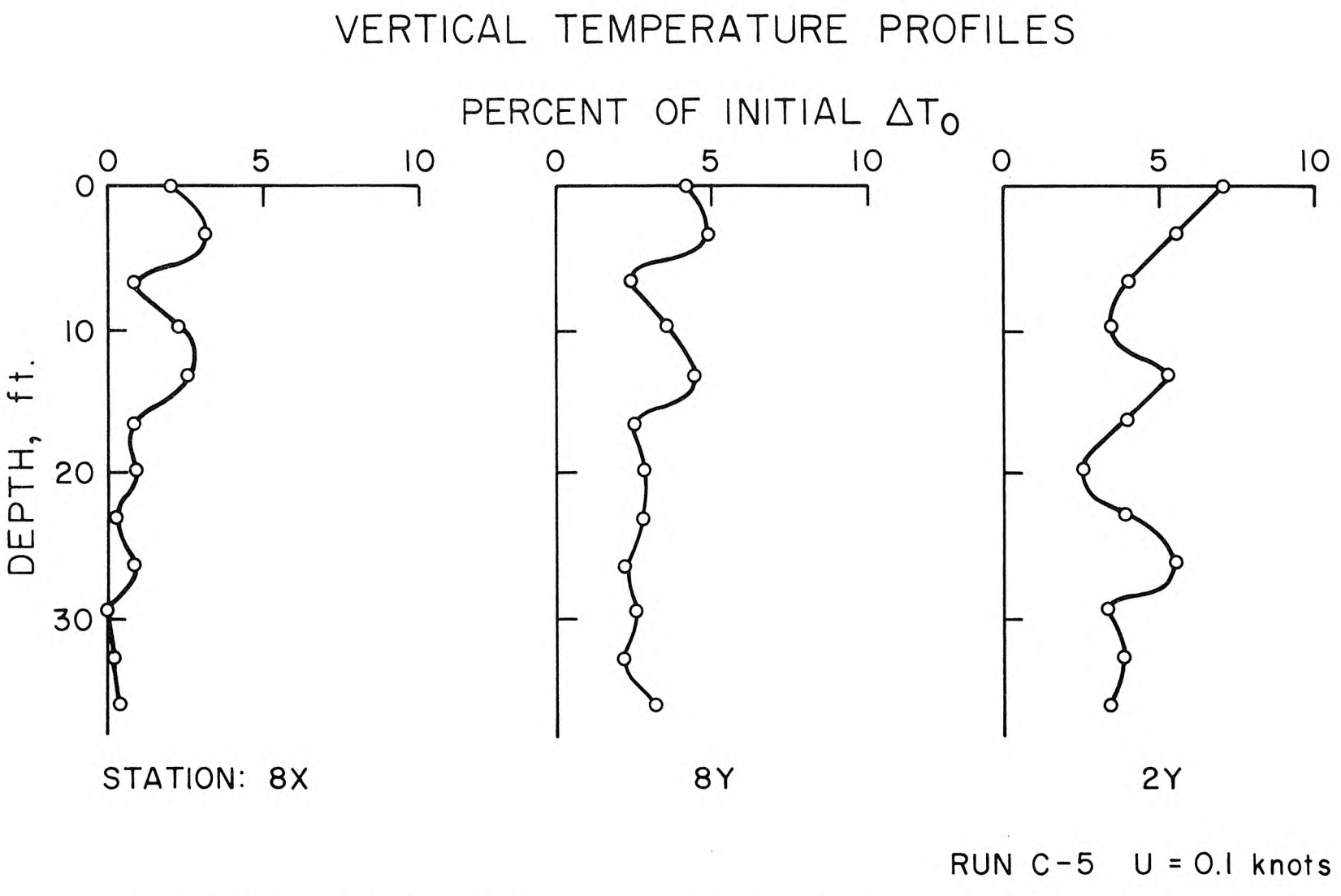

Figure 6.10 Vertical excess temperature profiles at selected stations for a steady current of 0.1 knots (data taken between 10 and 20 minutes into the experiment; see Figure 6.1 for station locations).

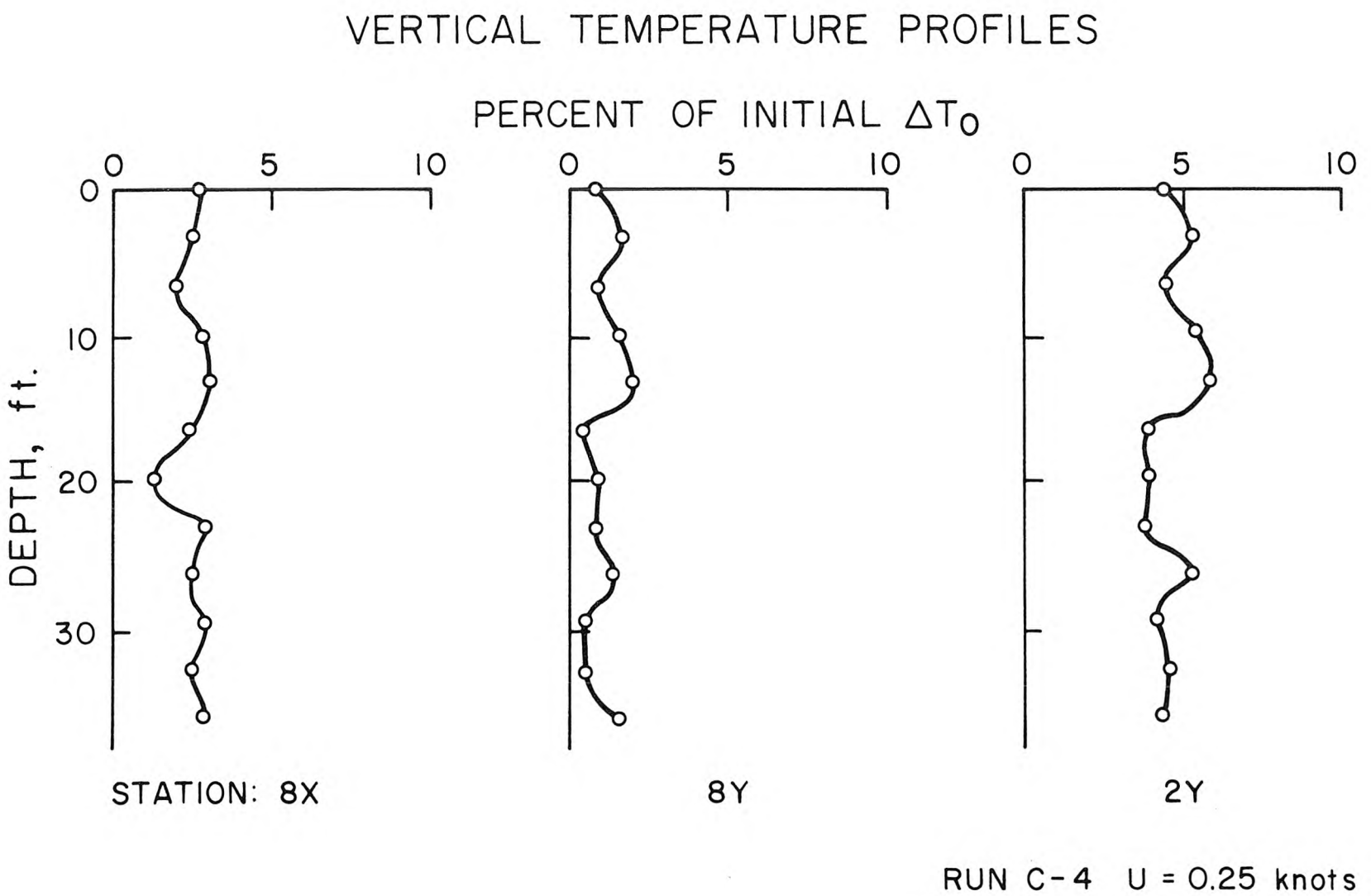

Figure 6.11 Vertical excess temperature profiles at selected stations for a steady current of 0.25 knots (data taken between 10 and 20 minutes into the experiment; see Figure 6.1 for station locations).

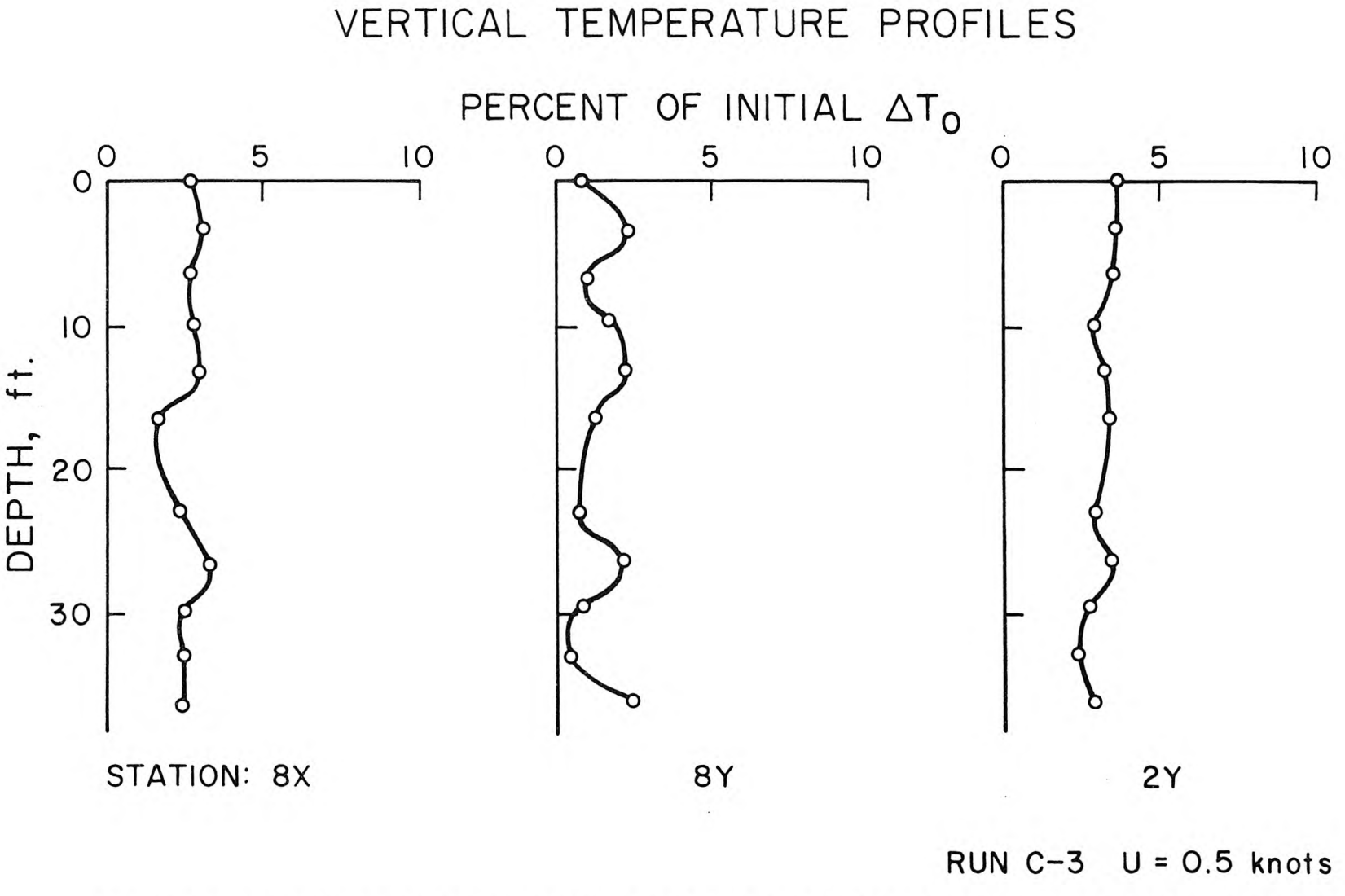

Figure 6.12 Vertical excess temperature profiles at selected stations for a steady current of 0.5 knots (data taken between 10 and 20 minutes into the experiment; see Figure 6.1 for station locations).

ΔT_s is the initial excess temperature at the surface immediately after initial jet mixing (t=0).

K is the heat loss coefficient

ρ is the density of water

c_p is the specific heat of water

h is the depth of the drift layer

and t is the time.

Using typical prototype values K = 100 BTU/ft^2 day°F, h = 30 ft, t = 0.56 day, and ρc_p = 61.6 BTU/ft^3°F

$$\frac{\Delta T}{\Delta T_s} = 0.97.$$

In other words, in the prototype heat loss would render the excess temperature 3% less than otherwise.

In the model basin, the measured heat loss coefficient* was K = 75 BTU/ft^2 day °F and the corresponding value of $\Delta T/\Delta T_s$ is thus:

$$\left(\frac{\Delta T}{\Delta T_s}\right)_m = e^{-\frac{75 \times .0083}{62.3 \times 0.15}} = .936 .$$

Hence, the heat loss effect would give rise to 6.4% less ΔT than otherwise. Expressed in terms of ΔT_o, the temperature excess of the discharge, the two values are 3% ÷ 8 and 6.4% ÷ 8 or 0.375% and 0.8% respectively. Thus all values of temperature excess expressed as percentage of source ΔT_o obtained in the experiments must be corrected by adding the difference of 0.42%. This result is approximate being dependent on the choice of many quantities of uncertain magnitude. In view of these uncertainties, a conservative additive correction of 0.5% was adopted for all the results which will be presented. It may be noted that this is only 0.1°F (prototype) and is probably smaller than other modeling errors; but since it is systematically unconservative, it was decided to make this small adjustment.

---

* Measured by Jean St. Marcoux as a project for the course Env 112c.

6.3 Surface Temperature Distributions

A summary of all the experiments in the series using the thermistor array together with experimental parameters and pertinent results (corrected for surface heat loss effect as indicated above) are included in Table 6.3. The entries in the table will be explained and discussed below.

In each experiment, temperatures at the surface were measured by calibrated thermistors at 112 locations surrounding the diffusers. Thermal maps were prepared from data obtained at intervals of several minutes (several hours in the prototype). Due to the large number of maps taken, only example cases will be presented. They are placed at the end of this chapter for ease of reference. These maps show surface isotherms in the vicinity of the diffusers, i.e. lines of constant temperature. The contour interval is 2.5% (in $\Delta T/\Delta T_o$). Local extrema in the field are delineated by letters with maxima starting at A and minima at Z. The values of the temperature at these extrema are listed on the right of each contour map. The diffusers are shown as two straight lines. The symbols on the left of each map are explained as follows using Figure 6.17 as an example.

RUN C-8	run number
U = 0.25	prototype current speed in knots
TA = 21.5	ambient temperature in °C
TH = 36.2	discharge temperature in °C
TIME = 00:18:00	model time into experiment (hours:minutes:seconds)

Figures 6.13 and 6.15 through 6.18* show the surface isotherms for steady currents of prototype magnitudes 0, 0.05, 0.1, 0.25, 0.5 knots respectively. It may be observed that

a) The maximum measured temperature excess decreases with increasing current,

b) the offshore discharge momentum exerts a strong influence on the flow even at U = 0.1 to 0.2 knots,

---

* All the remaining figures in this chapter appear as a group on pp. 60-97.

Table 6.3

Summary of Surface Temperature Maxima in Confirming Tests

The field surface temperature increments (ΔT) are expressed as percentages of the temperature rise of the discharge (ΔT_c) for all the experiments in this series. The headings are explained as follows:

Run No.	Run sequence number
U	The prototype current speed in knots (R indicates reversing current with maximum = U; SP indicates special current).
F'_{max}	$(\Delta T/\Delta T_o)_{max}$ in percent, as measured anywhere in basin.
R'_{max}	$(\Delta T/\Delta T_o)_{max}$ in percent, as measured in basin beyond the 1000 ft limit (based on 787.5 horizontal scale).
F_{max}	F'_{max} in percent corrected for (a) ambient temperature due to finite basin size, and (b) difference in heat loss effect between model and prototype.
R_{max}	R'_{max} corrected for (a) and (b) above in percent.

Note: Details of corrections in F_{max} and R_{max} are discussed on pages and 41, 52, 58, 59.

		$\Delta T/\Delta T_o$			
		Uncorrected		Corrected	
Run No.	U (knot)	F'_{max} (%) (anywhere)	R'_{max} (%) (>1000 ft)	F_{max} (%) (anywhere)	R_{max} (%) (>1000 ft)
C-7	0.5	6.5	6.1	6.8	4.5
C-8	0.25	7.9	7.1	7.5	5.9
C-9	0.1	12.4	10.3	12.9	10.8
C-10	0.05	13.9	9.8	14.4	10.3
C-11	0	13.5	11.1	14.0	11.6
C-12	SP1	11.6	9.4	12.1	9.9
C-13	SP2	13.9	10.7	14.4	11.2
C-14	SP3	11.2	11.2	11.7	11.7
C-15	SP4	13.1	10.4	13.6	10.9
C-16	0.15R	11.3	10.4	11.8	10.9
C-17	0.05R	12.8	11.5	13.3	12.0
C-18	0.4R	11.9	11.0	12.4	11.5

c) for currents of magnitude 0.1 knot or less, the peak ΔT occurs towards the offshore end of the nearshore diffuser (i.e., Unit 3).

These figures may be examined in relation to the photographs shown in Figures 6.3 through 6.7 which depict the same model conditions.

Figure 6.14 shows a summary of the maximum temperature excess measured anywhere and beyond 1000 ft from the diffusers for the Run C-11 with no ambient longshore current. It shows that a quasi-steady state is reached in a matter of less than 10 minutes for the region around the diffuser.

In addition to experiments with a steady longshore current, three runs (C-16, 17, 18) were made in which the current reverses twice in each 12-hour prototype cycle (semi-diurnal tide). The amplitudes of the reversing currents tested are 0.05, 0.15, and 0.4 knots (prototype). (The letter R indicates current reversal.) Figure 6.19 shows the current history used. Figures 6.20 and 6.21 show two contour maps for a reversing current u = 0.05R at model times of 12 and 15 minutes, i.e., when the instantaneous currents are approximately 0.025 knots (right to left on the figure) and -0.03 knots respectively. Comparison with the case of no current (Figure 6.13) reveals that the surface isotherm patterns are similar and that the dilutions are comparable.

Figures 6.22 through 6.24 show maps taken for u = 0.15R at model times of 9, 12 and 15 minutes corresponding to instantaneous currents of 0.05, 0.075, -0.1 knots respectively. While the patterns do reflect the current direction and magnitude, a noticeable widening of the thermal field (up and down coast) is seen to occur due to the current reversal, which essentially oscillates the thermal pattern causing somewhat more dispersal.

Figures 6.25 through 6.28 show the case of u = 0.4R at model times of 6:22, 12, 15, and 21 minutes corresponding to instantaneous currents at -0.25, 0.2, -0.25, and 0.35 knots respectively. The thermal patterns are seen to be different from the case of steady currents at the same speed. The oscillating current spreads the heated water over a larger

area and "hot spots" generated during low currents are swept away when the current increases. For example, the "hot spots" marked A and C in Figure 6.28 (when the current is at 0.35 knots) were generated during the previous period of low current. It is interesting to note that A and C represent the hottest spots in that map.

In examining the thermal maps for reversing currents and comparing them to those for steady currents, it should be borne in mind that at the instant when the (reversing) current is at the maximum, the thermal field may be deflected downcoast only half as far as the case if the current were steady at the same magnitude due to the difference in prior history of the currents.

Four experiments were also conducted where the longshore current is varied according to actual field data measured*. These experiments are designated SP1 through SP4.

The current sequence SP1 used is shown in Figure 6.29. Figures 6.30 through 6.33 show surface thermal maps for the case SP1 at 8, 14, 20 and 32 minutes (model time) when the instantaneous currents are approximately 0.05, 0.02, 0.2, and 0.37 knots (prototype) respectively (see Figure 6.29). Prior to the time of Figure 6.30 the current had been low. The map therefore resembles that of a steady current. The same comment may be applied to the map in Figure 6.31 except for the widening of the pattern offshore due to the current variations. The maps in Figures 6.32 and 6.33 were taken after the current had been increasing (virtually monotonically). The "hot spot" E in Figure 6.32 had been generated earlier and was swept downstream. Figure 6.34 shows the summary of maximum surface temperature excesses (anywhere and beyond the 1000 ft limit) for this run and should be compared with the current sequence (Figure 6.29) to reveal the inverse correlation of current speed with maximum surface temperature excess.

Figure 6.35 shows the current sequence used in SP2, a sequence of low current and Figure 6.36 shows a thermal pattern for the same case. Only one map is shown for this case because all the others are similar. This is because the current sequence SP2 is basically very slow and never

---

* "Current Meter Observations and Statistics Off San Onofre Nuclear Generating Station, 5 Jan. - 22 Nov. 1972", Intersea Research Corporation, January, 1973.

reverses. The same is true for SP3 (Figure 6.37) and only two maps (Figures 6.38 and 6.39) are shown for that case.

Figure 6.40 shows the current sequence used in u = SP4 and Figures 6.41 through 6.47 show the surface thermal contours for the same case at model times of 6, 8, 10, 20, 22, 24, and 28 minutes. The current sequence for this case is rather interesting. The current starts off at 0.2 knots and gradually decreases to 0 in 7 model minutes. It remains low for a period of 13 minutes and then rises to over 0.3 knots in about another 5 minutes. The maps shown in Figures 6.41 through 6.47 correspond to instantaneous current magnitudes of 0.02, 0.0, 0.06, 0.0, 0.13, 0.3 and 0.23 knots respectively. Examination of Figure 6.41 shows that the thermal pattern in no way resembles one at U = 0.02 knot steady current. This is because the current had previously been at 0.2 knot (and slightly above). Comparison of this map with that shown in Figure 6.17 (u = 0.25 knot steady) shows that the warmer zone is more concentrated around the diffusers in the SP4 case as it should be since the current is slowing down. Figure 6.42 shows the map when the current had decreased to zero. Warm spot E is developing although the pattern is still displaced to the left since the current had been flowing in that direction. Figure 6.43 shows the map after the current starts again although still at a low velocity. The patterns in Figure 6.43 and 6.44 are quite similar to the case of no current (Figure 6.13). Figures 6.45 and 6.46 show maps taken when the current is increasing from a prolonged period of low values. It may be noted that warm spots generated during the low current, are being carried away. Finally Figure 6.47 shows the case when the instantaneous current is 0.23 knots after it has reached a maximum of 0.35 knots. The summary of maximum surface temperature excesses for u = SP4 is shown in Figure 6.48. Again, comparison with the current sequence (Figure 6.40) reveals an inverse correlation of temperature excess with current speed.

Examination of these and other maps for all the runs performed revealed that the effects of the reversing current are to i) distribute the heat over a larger area near the diffuser and, ii) create relative hot spots during slack current that are convected along as the current

speed increases again. It will be shown later in Figures 6.49 and 6.50 that the maximum ΔT outside the 1000 ft limit decreases with increasing current for a steady current, while for reversing current, it is essentially independent of current amplitude.

6.4 Maximum Temperature Rise above Ambient

Of particular interest are the values of the temperature rise measured a) anywhere in the basin, and b) beyond 1000 ft horizontal distance from the discharges. These are summarized in Table 6.3, p.54, columns 3 and 4, expressed as percentages of ΔT_o the temperature excess at the source.

Since the basin is of limited extent, there is a tendency for the overall temperature in the basin to rise gradually in the course of the experiment. A special thermistor was therefore installed in the north (upstream during unidirectional current) end of the basin at the recirculating pump discharge manifold at a depth of several inches. In this manner, the gradual rise in the basin background temperature could be continuously monitored. The data from each experiment thus consists of temperature measurements of the 112 thermistors for generating the surface thermal contour maps and the background temperature in the basin as measured by the "ambient" probe described above. The former measurements could then be corrected by the ambient probe measurement. At the end of the analysis of each experiment, the maximum temperature measured in the basin, both anywhere and beyond the 1000 ft limit, and the ambient probe measurements were plotted versus time. All temperatures are expressed as percentages of the source ΔT_o. Example graphs are included here as Figures 6.14, 6.34 and 6.48 (pages 61, 81, and 95).

The correction for the gradual rise in ambient temperature in the basin is not a trivial matter. Two features of the flow should first be pointed out before discussing the method used in the correction. First, it takes a certain amount of time for a fluid particle to travel from the location of measurement of the ambient probe to that of the diffusers. Thus, for the case of a steady current, the ambient temperature correction was made with an appropriate time delay depending on the current speed.

Second, it was observed in this series of experiments (as well as in the previous tests) that for low currents the offshore drift flow generated by the diffuser discharge tended to be deflected to both sides by the offshore wall of the basin and thence, traveled both upstream and downstream along the offshore wall, then gradually circled back and was re-entrained into the drift current. This occurred most noticeably when the current was low and was eliminated only at relatively high currents (0.2 knots or more). This re-entrainment tended to increase the measured temperature in the thermal field. The same phenomenon also tended to increase the temperature measured by the ambient probe, although to a lesser degree. It is expected that if the far wall were absent, this recirculation would either not occur or would only occur at a much later time. Since the ambient probe was located deeper than the layer of warm water, it did not sense the full temperature of the re-entrained water. In Table 6.3, where the results are summarized, the ambient correction is based on using the appropriate time delay since it is conservative.

The above discussion of the correction for the ambient temperature applies only to the case of steady currents. For reversing currents, it was found that for low current amplitudes, the same phenomenon of recirculation induced by the deflection due to the far wall of the basin occurred. In Table 6.3, the results are not corrected for runs with reversing currents since this is conservative (i.e., the correction if made would tend to reduce the percentages given).

The data for the maximum relative surface temperature excess above the ambient, measured beyond 1000 ft (based on the horizontal length scale) of the discharge structures, are summarized in Figures 6.49 and 6.50 for all the runs in this series. As a comparison, the results obtained in a previous series of experiments for the N2* configuration (very nearly the same except for nozzle numbers and spacing) are also shown. It is clearly seen that the maximum temperature excess decreases for increasing steady currents, while if the current reverses, the maximum temperature excess is independent of the current amplitude. The maxima for the special current runs are shown at the right side of Figure 6.50 inasmuch as they do not have a nominal current speed.

---

* See Section A-3 of Appendix.

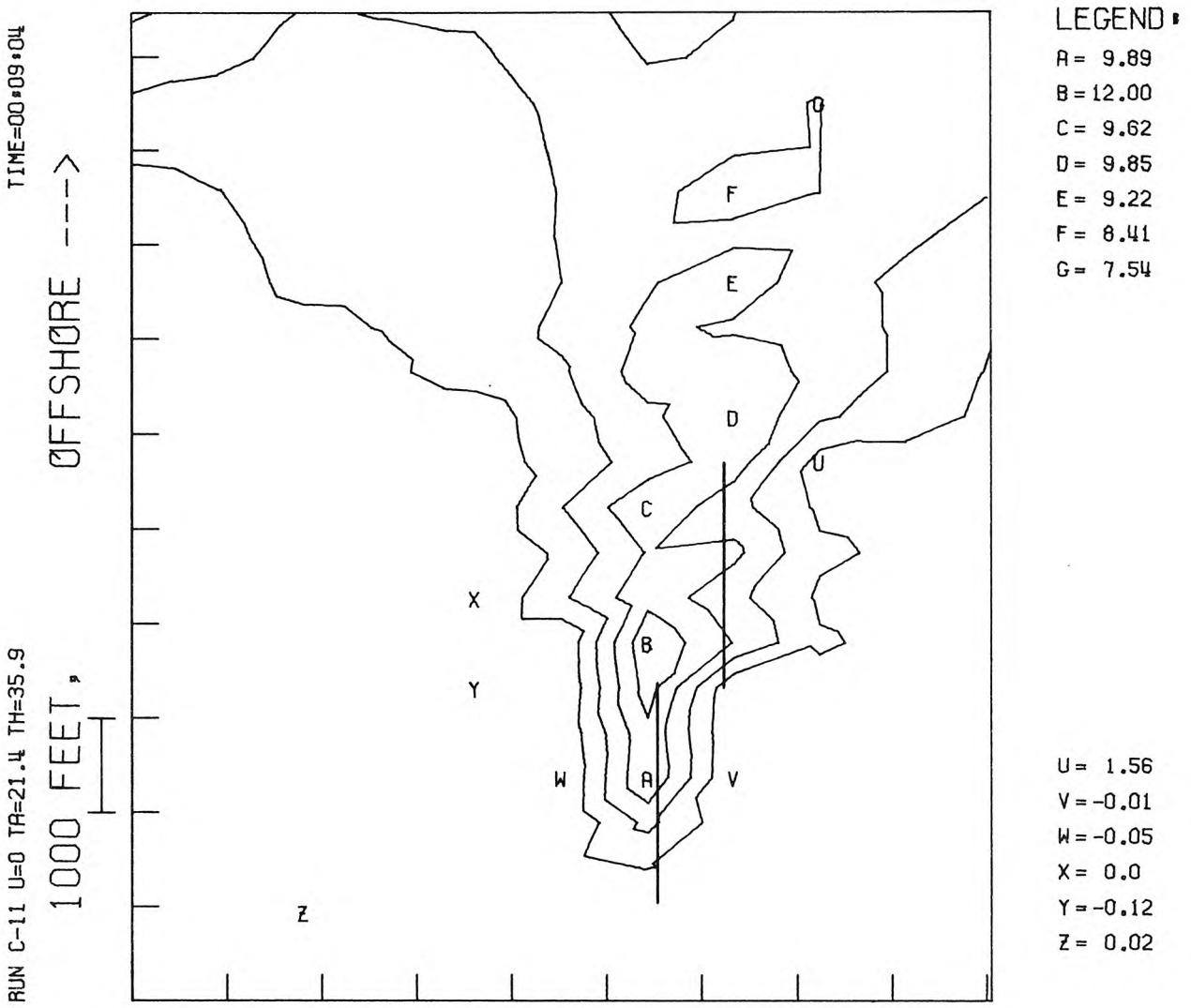

Figure 6.13 Surface isotherms (in increments of 2.5% of source ΔT_o) for steady ambient current u = 0.0 knots (diffusers shown as straight lines).

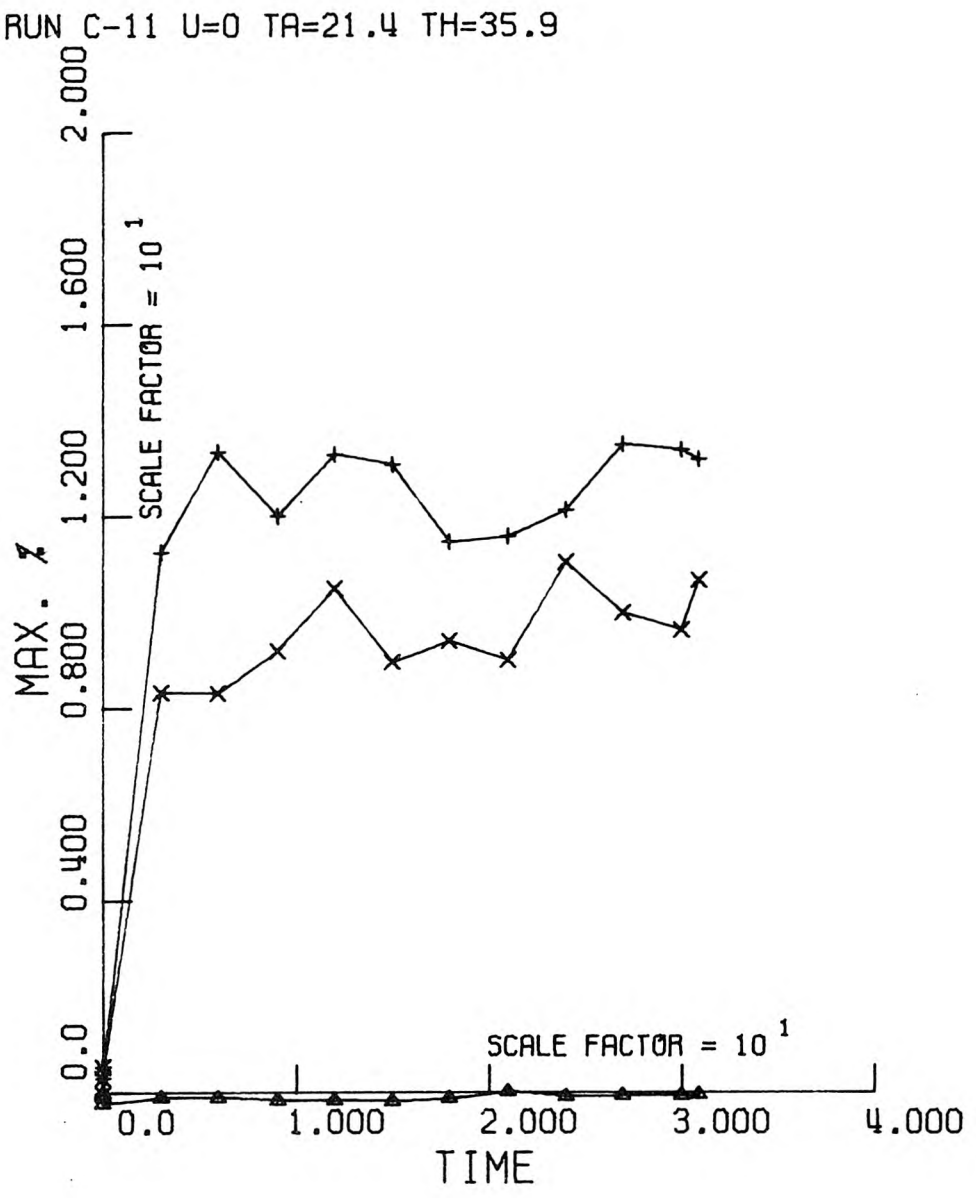

Figure 6.14 Summary of maximum temperature excesses (in % of source temperature excess) measured anywhere in basin (+), beyond 1000 ft of diffusers (x) and ambient temperature. (Run C-11, u = 0.0 knot).

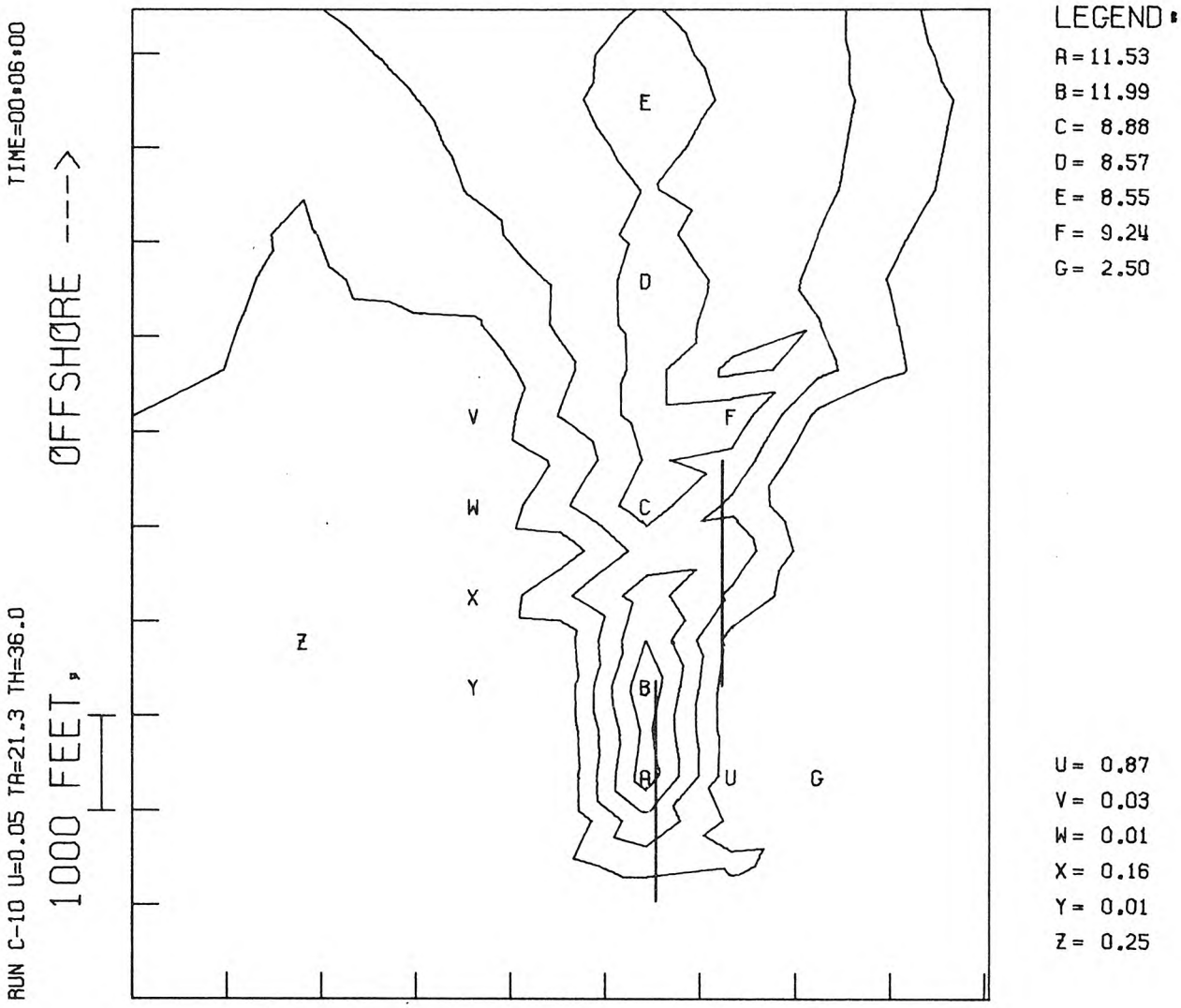

Figure 6.15 Surface isotherms (in increments of 2.5% of source ΔT_o) for steady ambient current u = 0.05 knots (diffusers shown as straight lines).

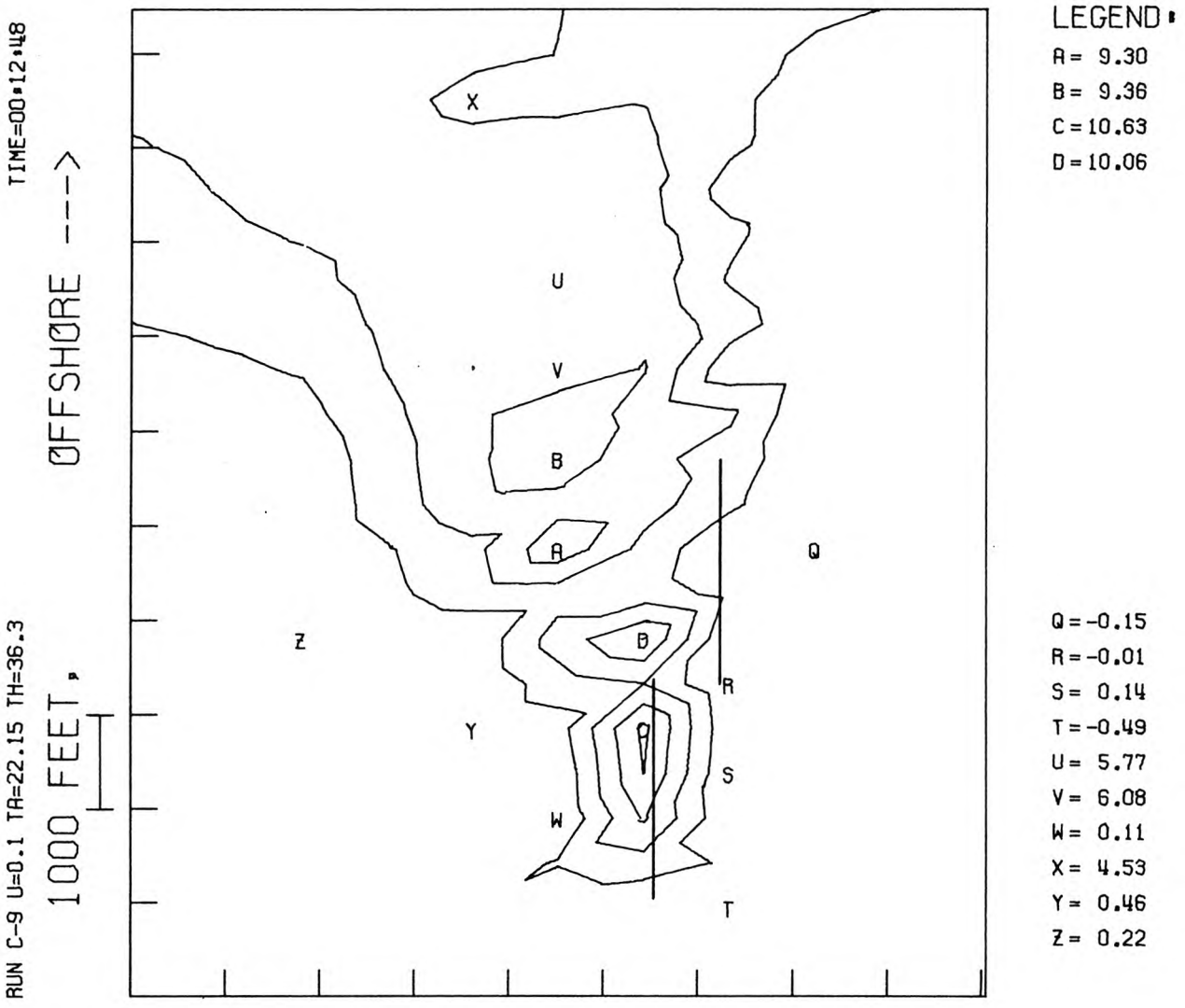

Figure 6.16 Surface isotherms (in increments of 2.5% of source ΔT_o) for steady ambient current u = 0.1 knots (diffusers shown as straight lines).

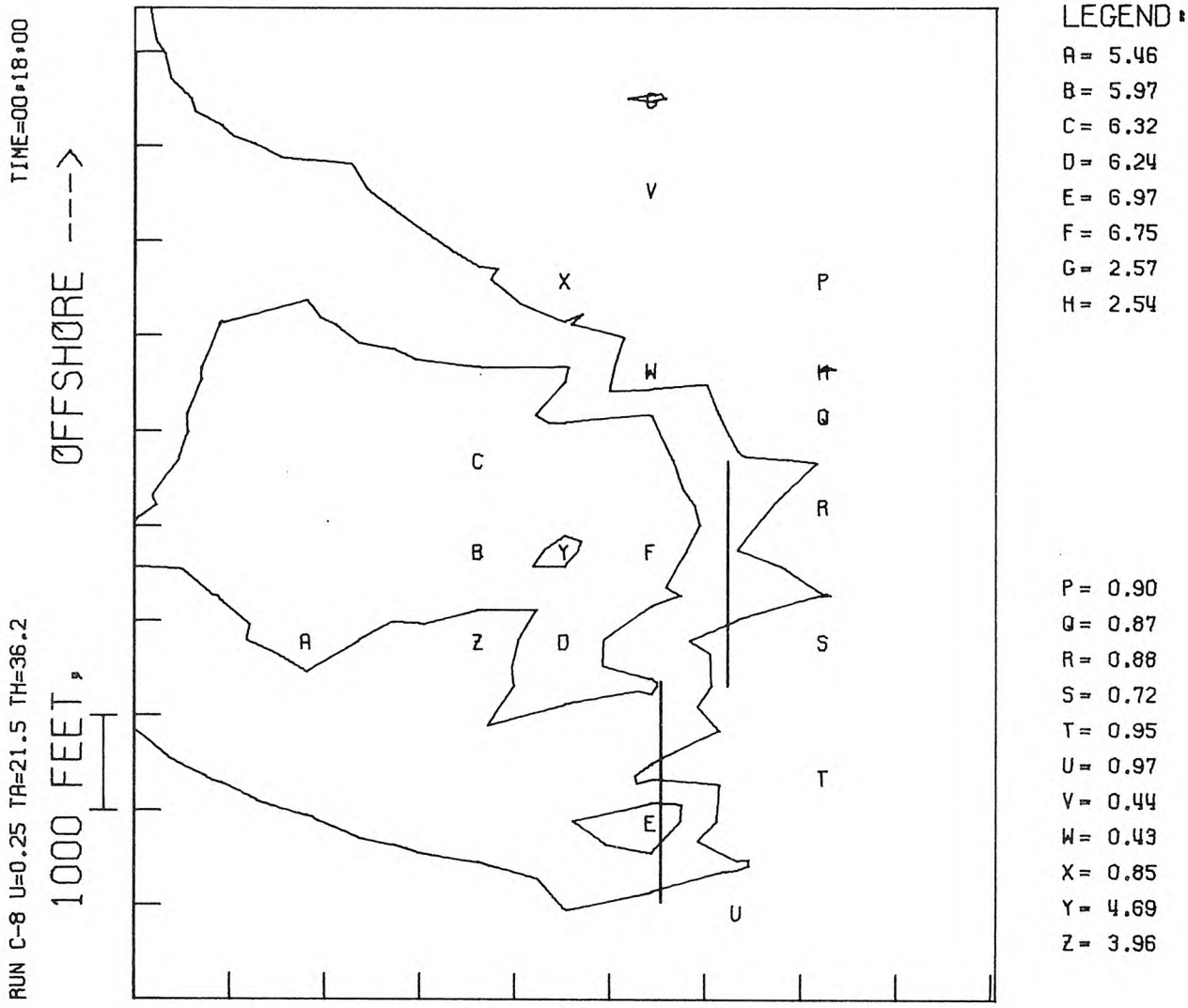

Figure 6.17 Surface isotherms (in increments of 2.5% of source ΔT_o) for steady ambient current u = 0.25 knots (diffusers shown as straight lines).

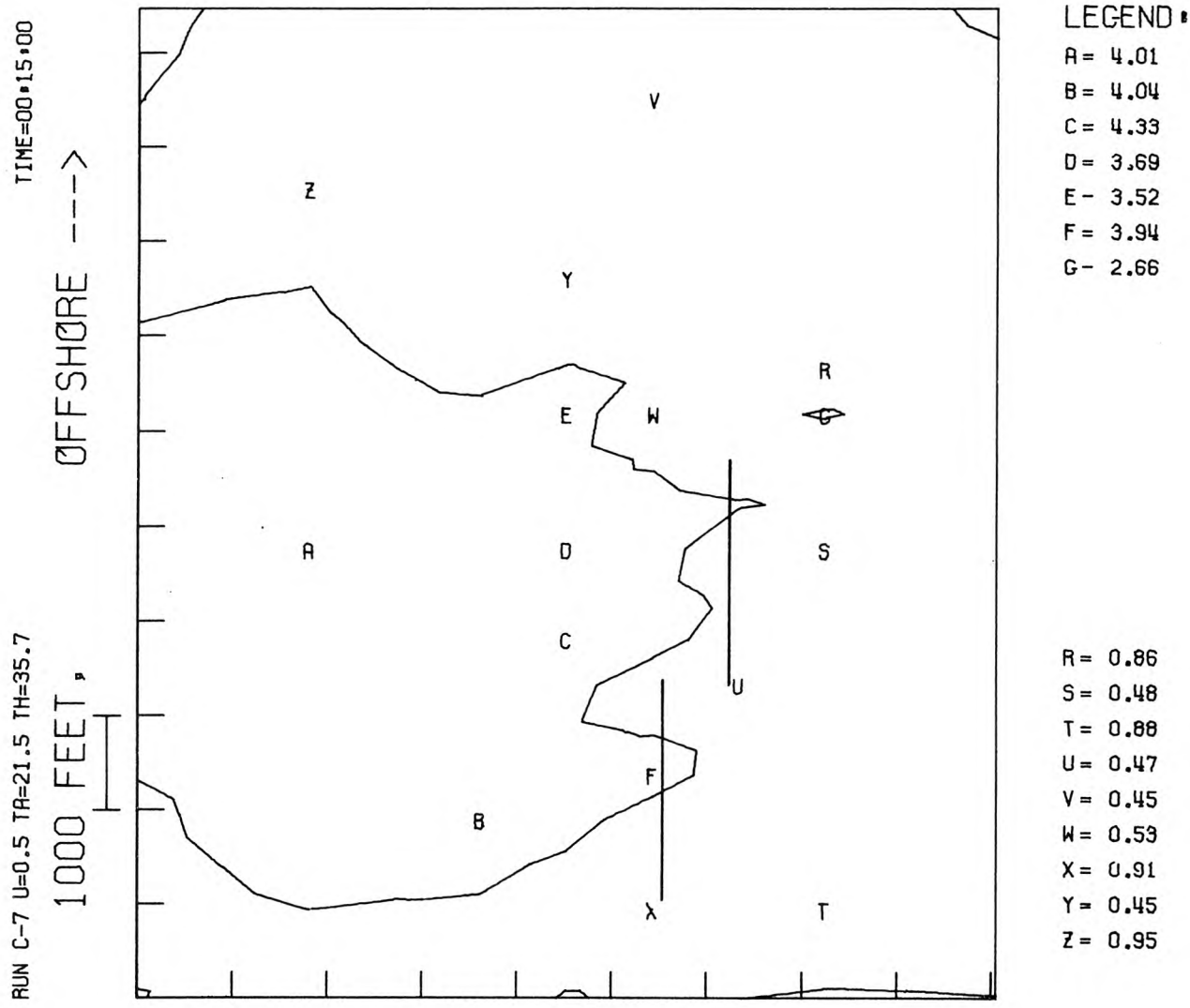

Figure 6.18 Surface isotherms (in increments of 2.5% of source ΔT_o) for steady ambient current u = 0.5 knots (diffusers shown as straight lines).

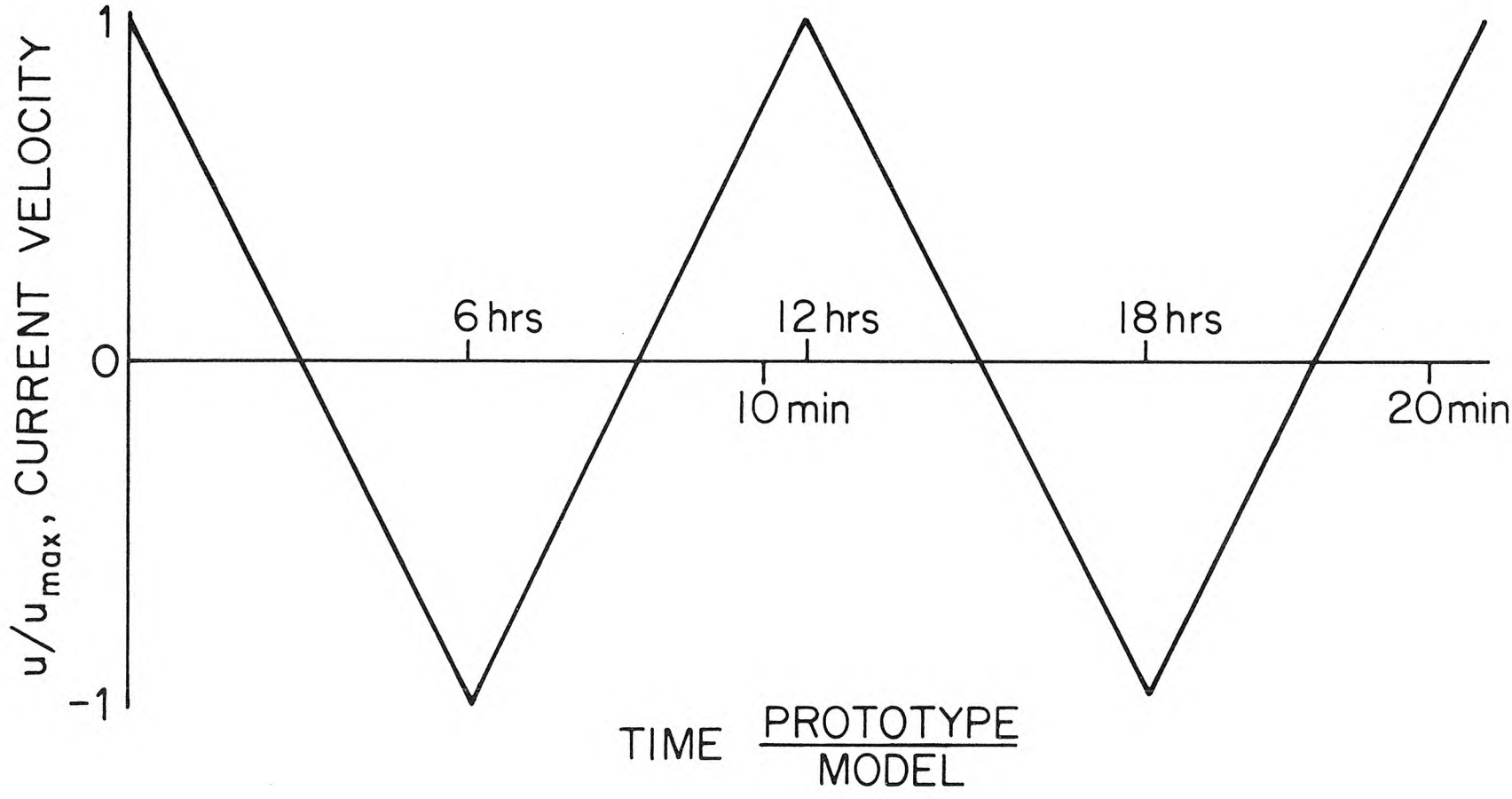

Figure 6.19 Typical reversing current sequence used in runs C-16 through C-18. (Current velocity normalized to peak values.)

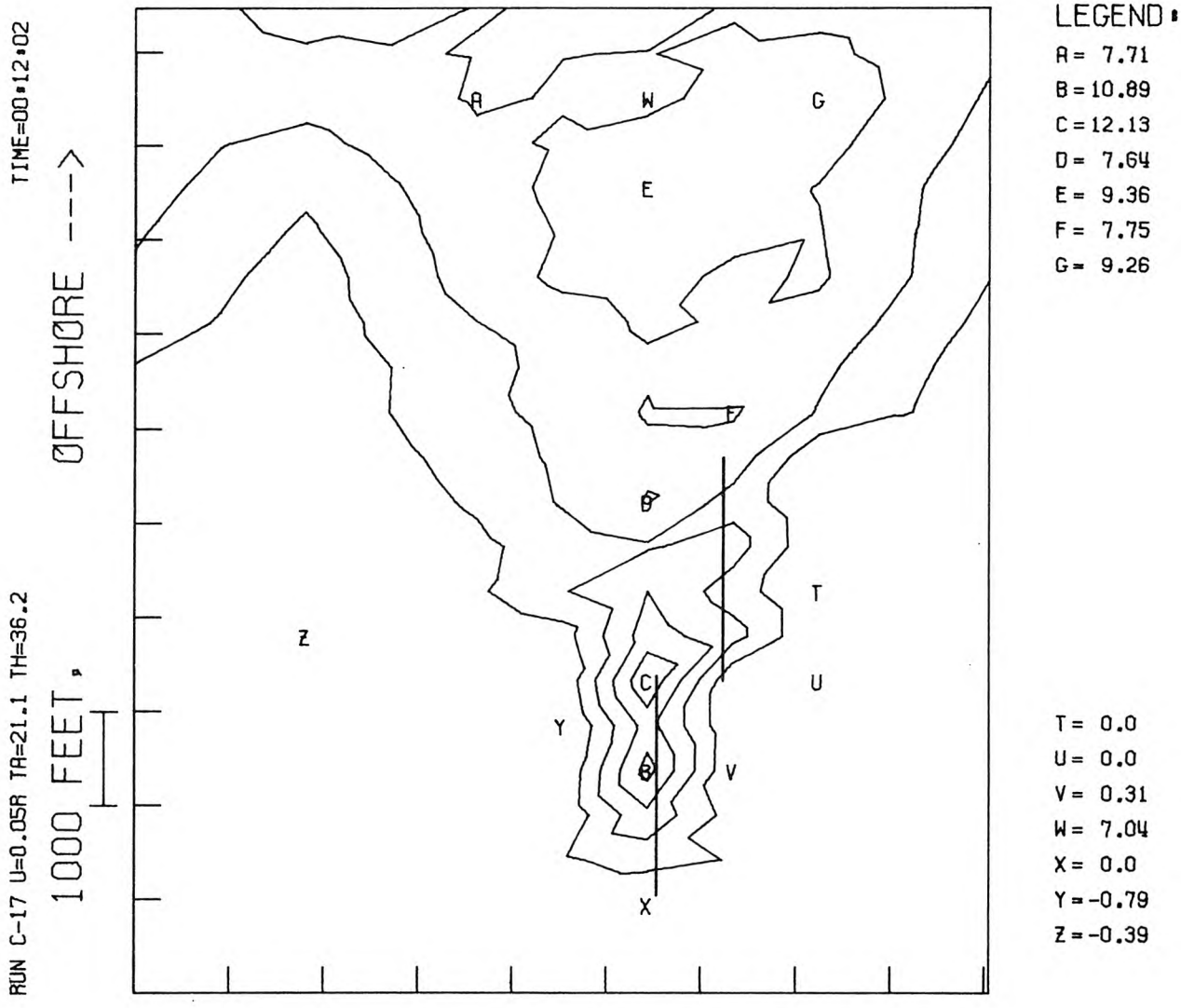

Figure 6.20 Surface isotherms (in increments of 2.5% of source ΔT_o) for reversing current of amplitude 0.05 knots. (Diffusers shown as straight lines; instantaneous current speed = 0.025 knots.)

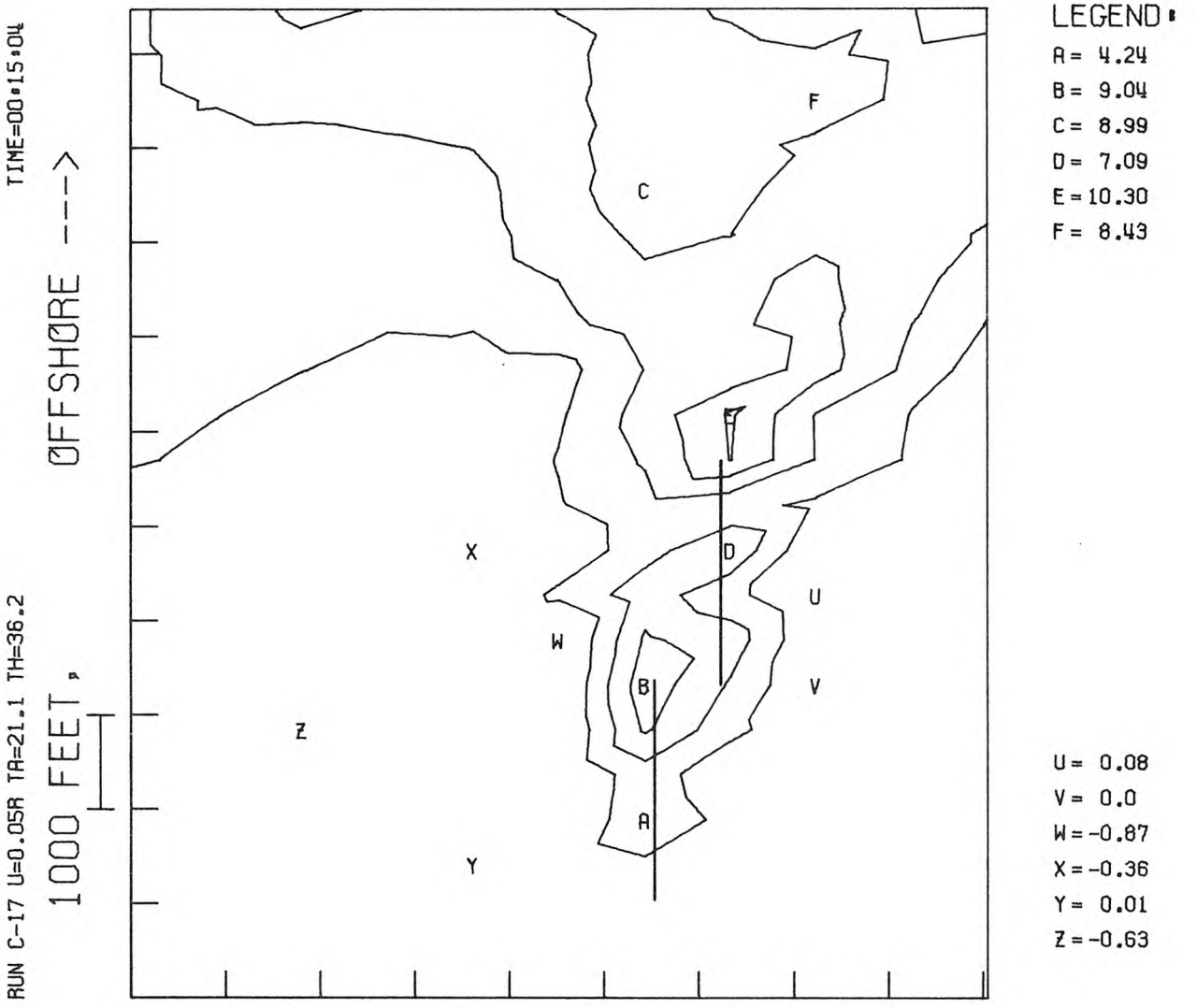

Figure 6.21 Surface isotherms (in increments of 2.5% of source ΔT_o) for reversing current of amplitude 0.05 knots. (Diffusers shown as straight lines; instantaneous current speed = -0.03 knots.)

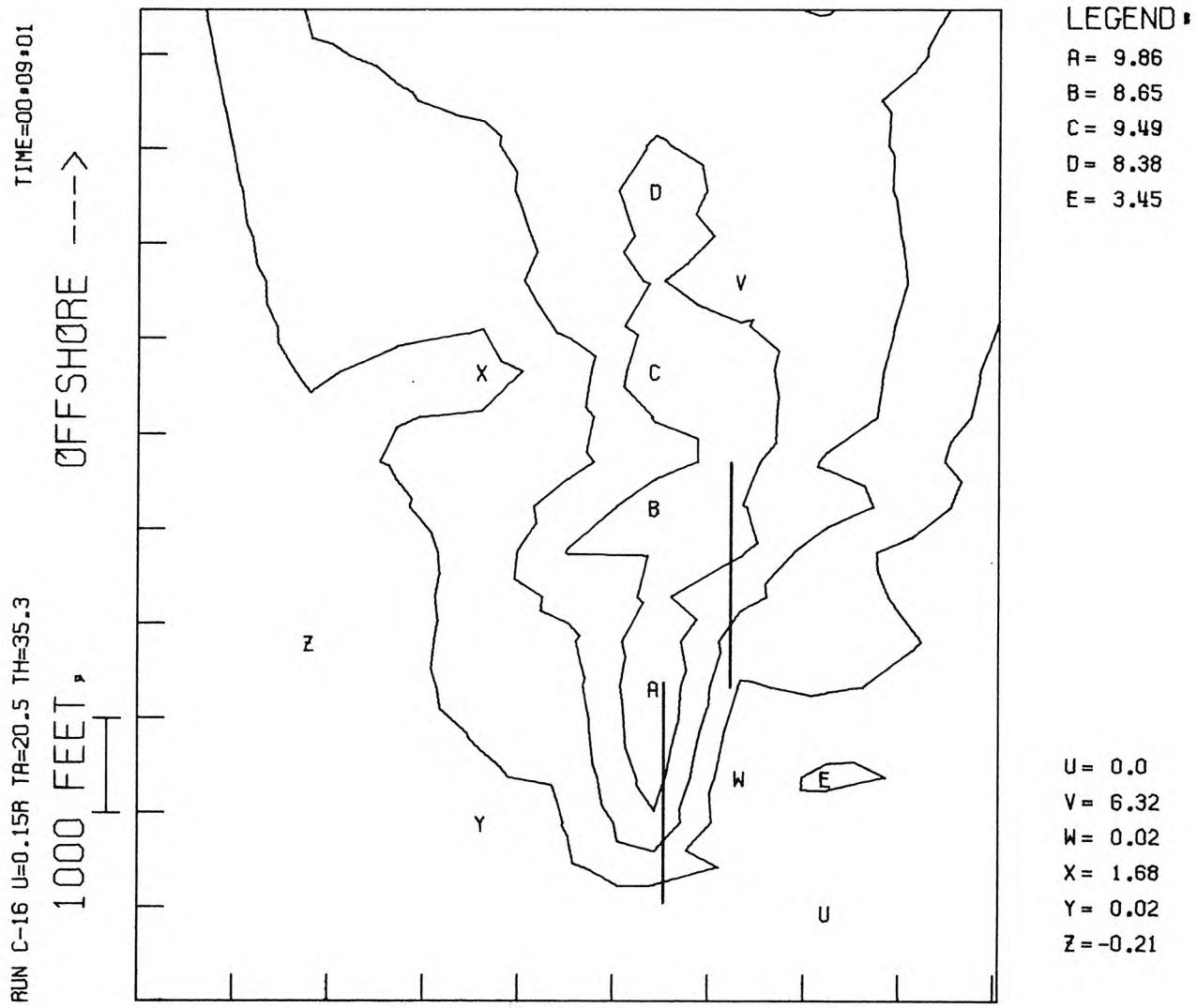

Figure 6.22 Surface isotherms (in increments of 2.5% of source ΔT_o) for reversing current of amplitude 0.15 knots. (Diffusers shown as straight lines; instantaneous current speed = 0.05 knots.)

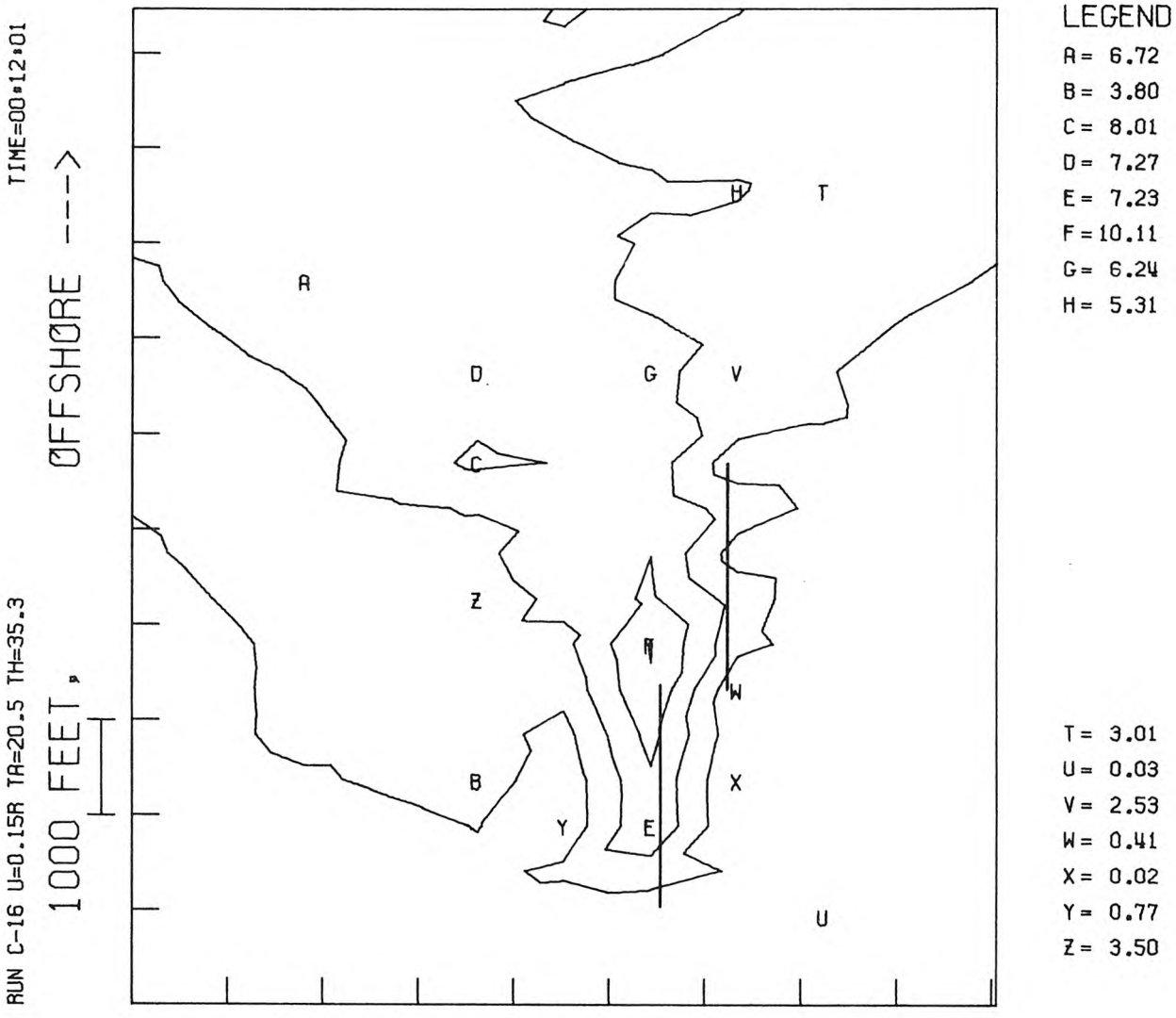

Figure 6.23 Surface isotherms (in increments of 2.5% of source ΔT_o) for reversing current of amplitude 0.15 knots. (Diffusers shown as straight lines; instantaneous current speed = 0.075 knots.)

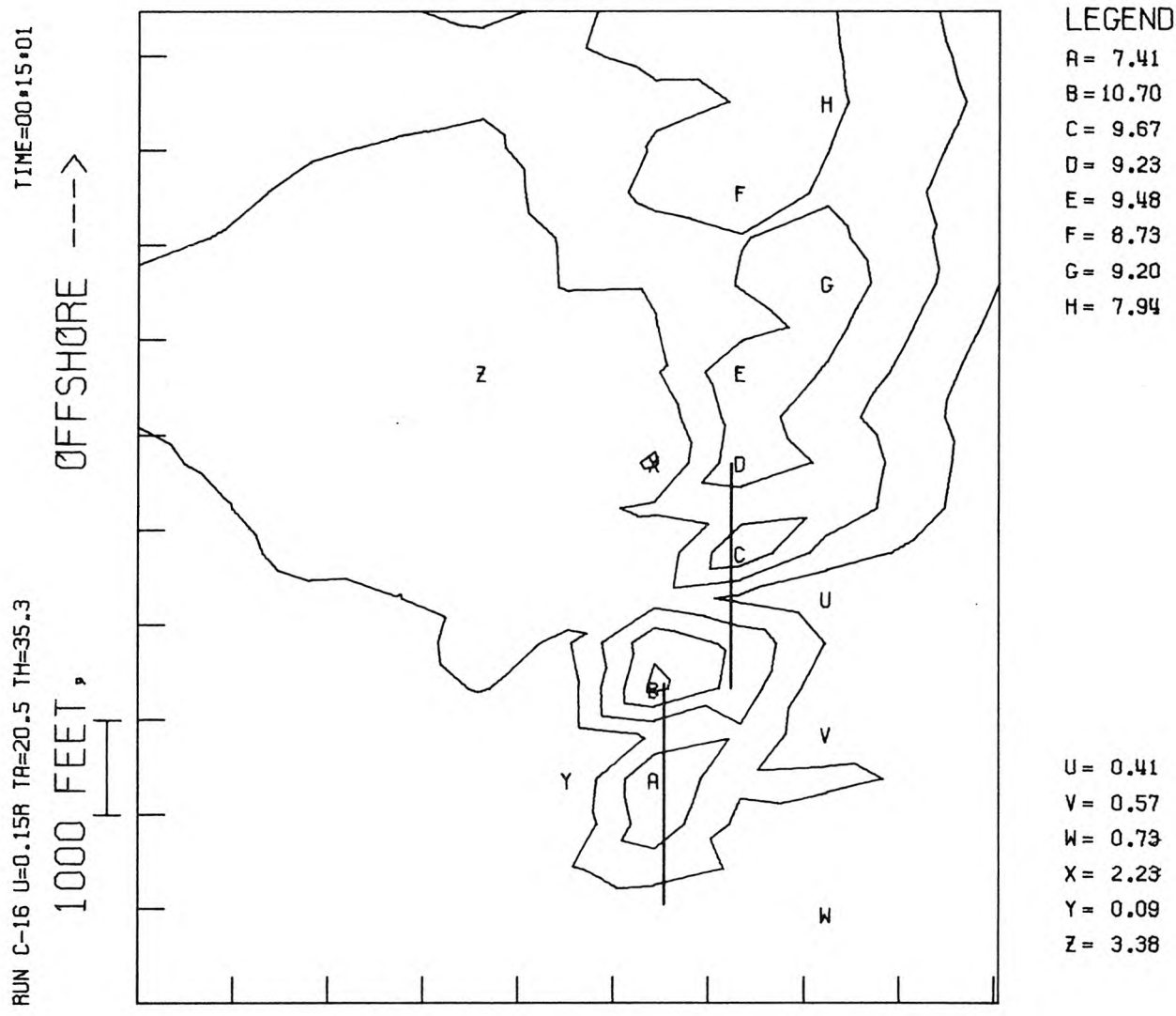

Figure 6.24 Surface isotherms (in increments of 2.5% of source ΔT_o) for reversing current of amplitude 0.15 knots. (Diffusers shown as straight lines; instantaneous current speed = -0.1 knots.)

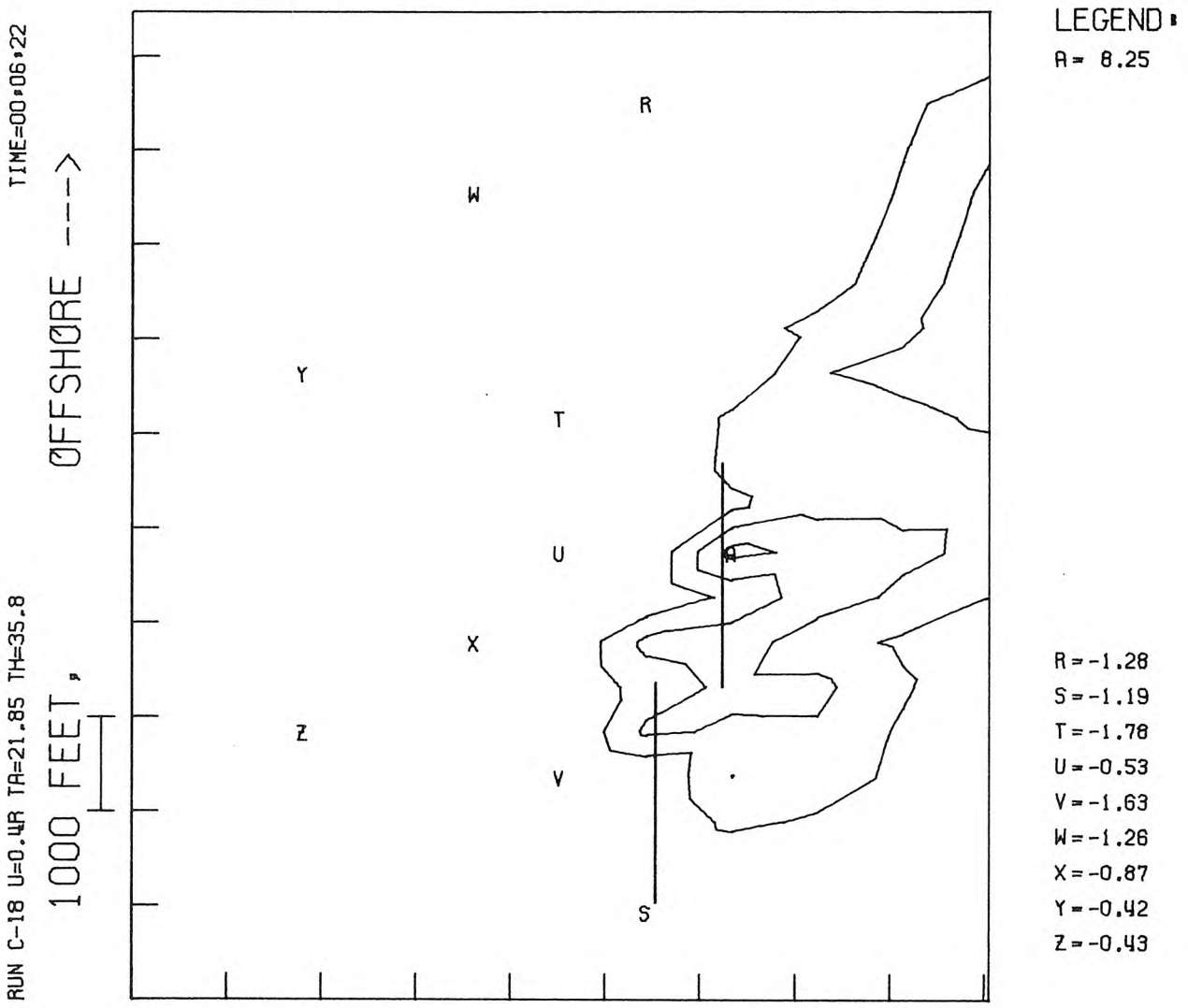

Figure 6.25 Surface isotherms (in increments of 2.5% of source ΔT_o) for reversing current of amplitude 0.4 knots. (Diffusers shown as straight lines; instantaneous current speed = -0.25 knots.)

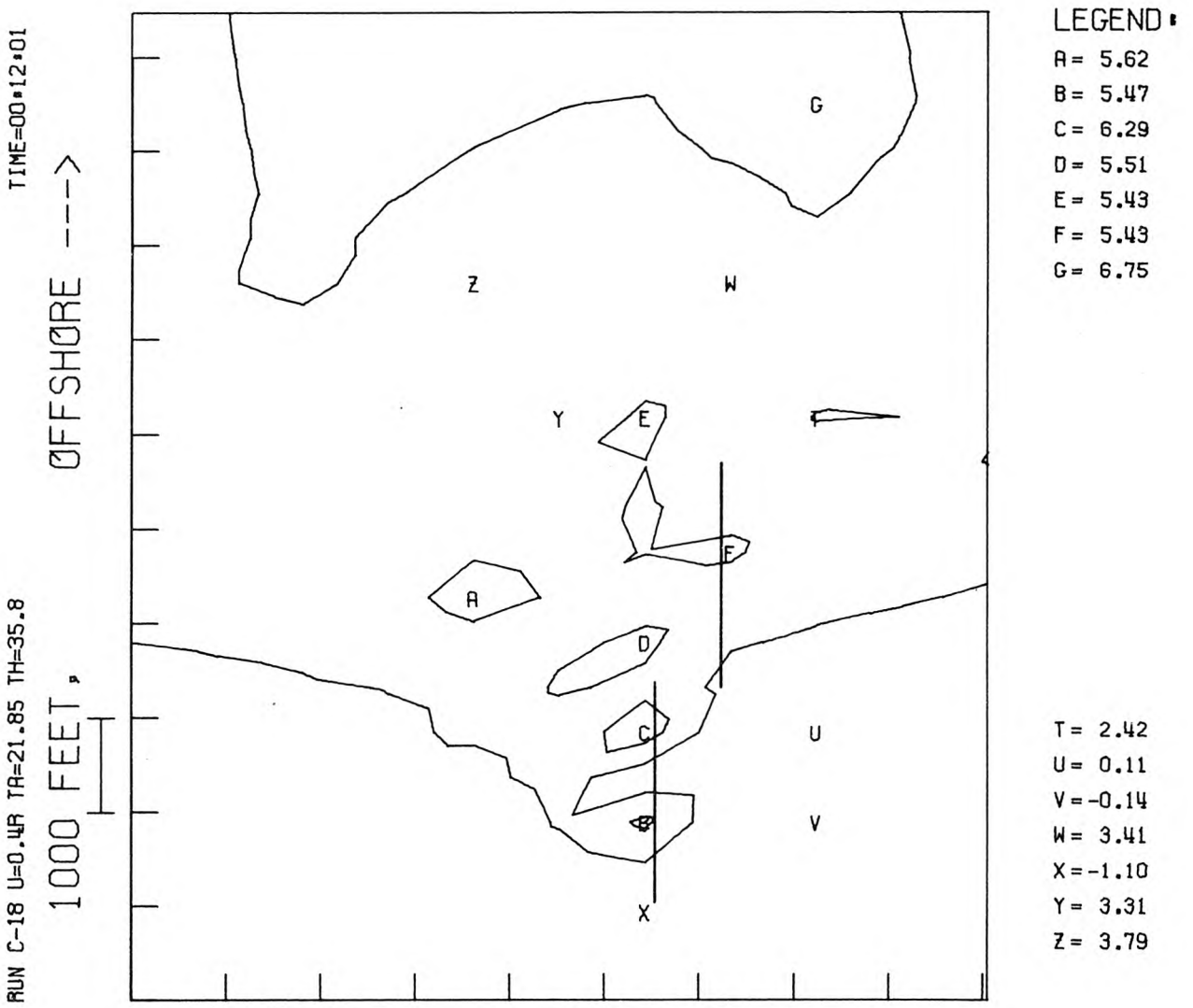

Figure 6.26 Surface isotherms (in increments of 2.5% of source ΔT_o) for reversing current of amplitude 0.4 knots. (Diffusers shown as straight lines; instantaneous current speed = 0.2 knots.)

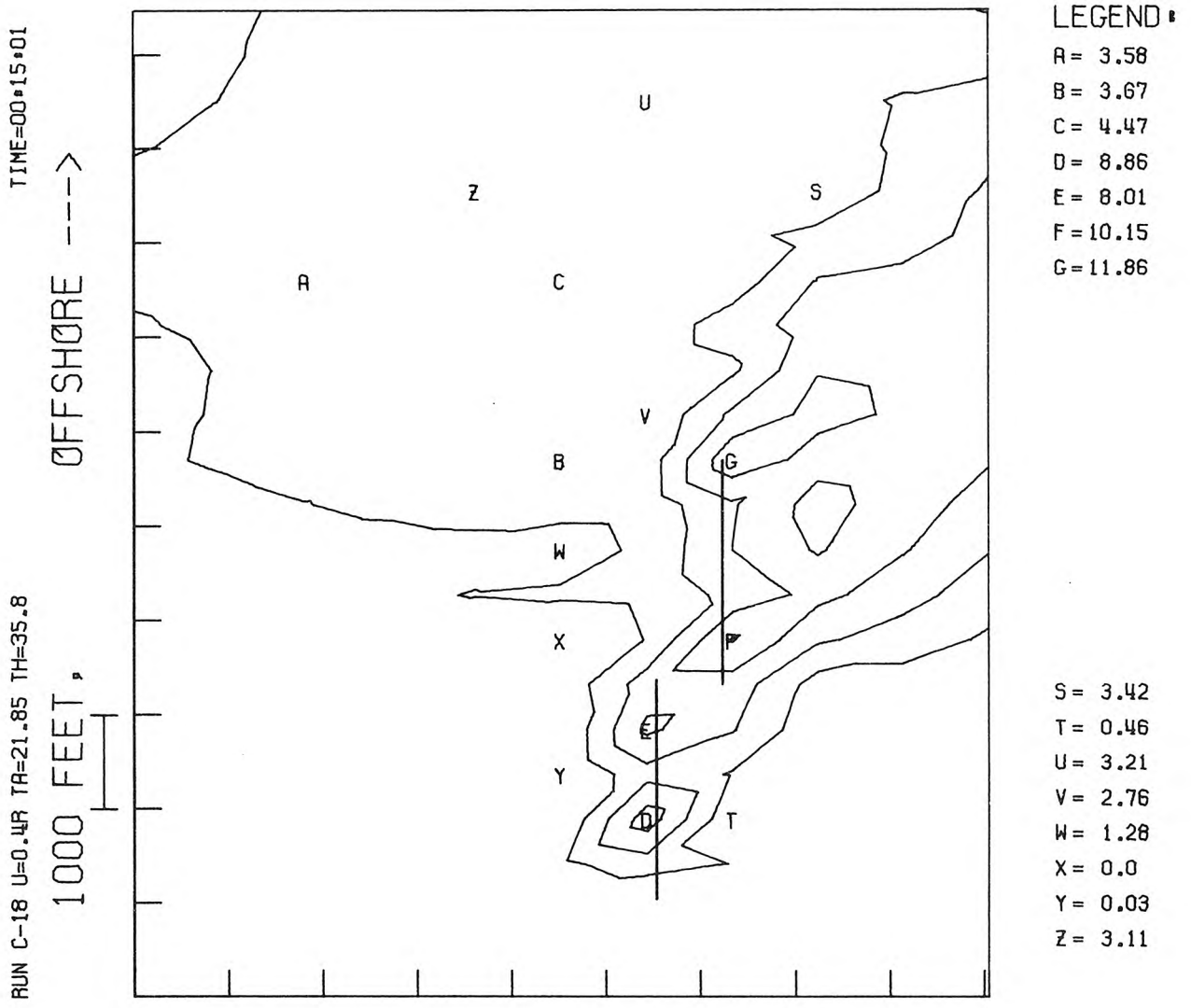

Figure 6.27 Surface isotherms (in increments of 2.5% of source ΔT_o) for reversing current of amplitude 0.4 knots. (Diffusers shown as straight lines; instantaneous current speed = -0.25 knots.)

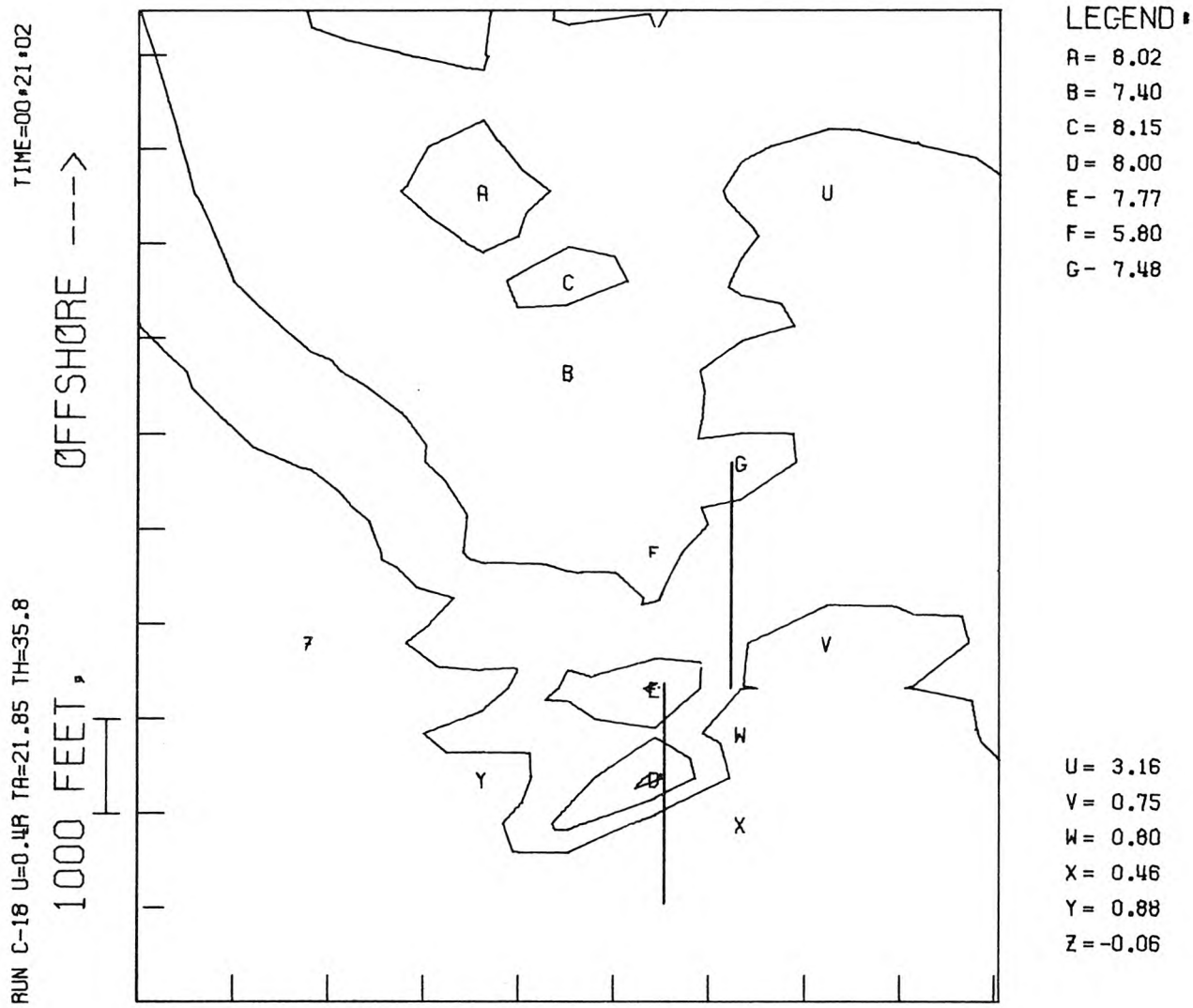

Figure 6.28 Surface isotherms (in increments of 2.5% of source ΔT_o) for reversing current of amplitude 0.4 knots. (Diffusers shown as straight lines; instantaneous current speed = 0.35 knots.)

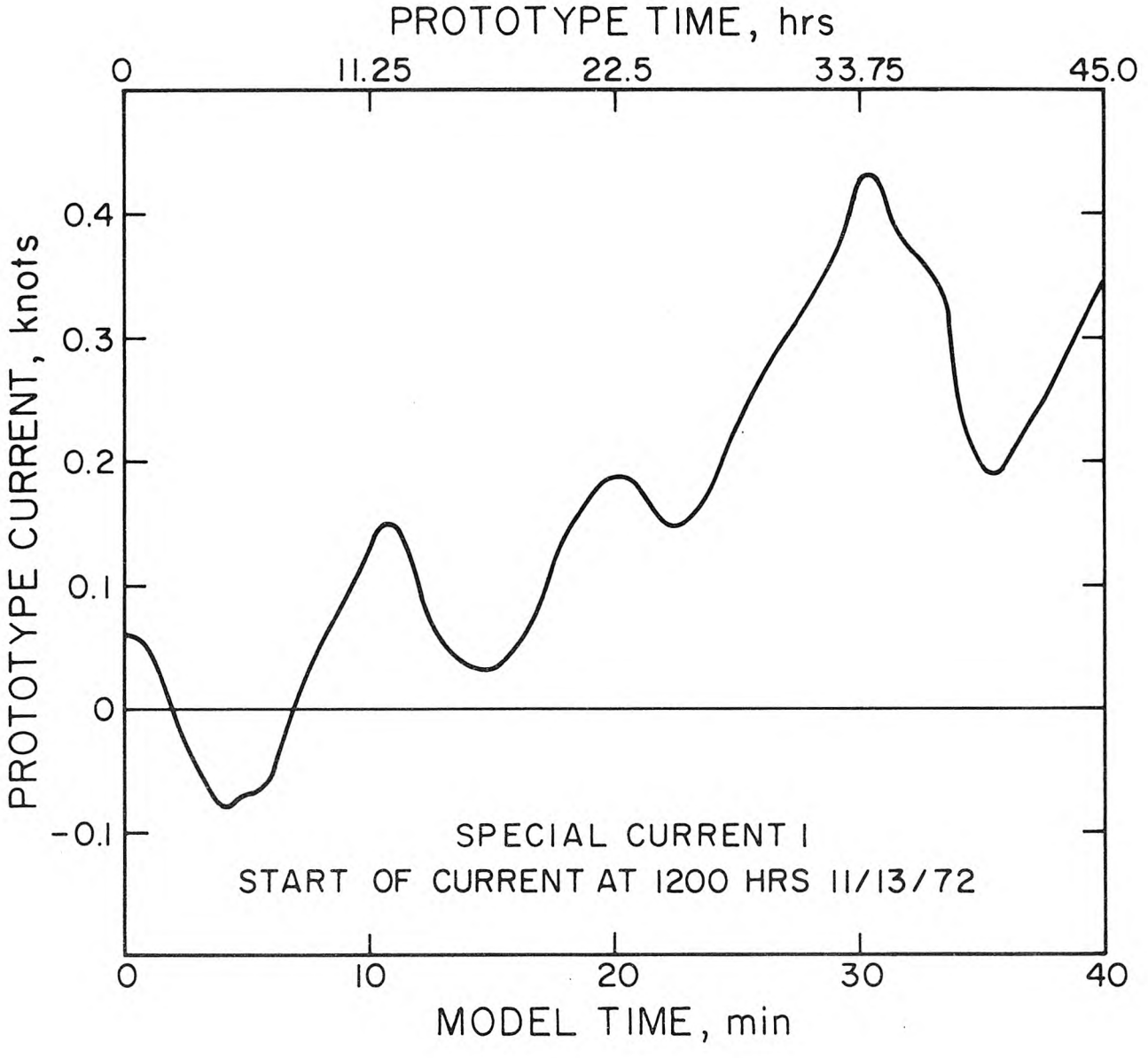

Figure 6.29 Longshore current sequence (SP1) used in Run C-12.

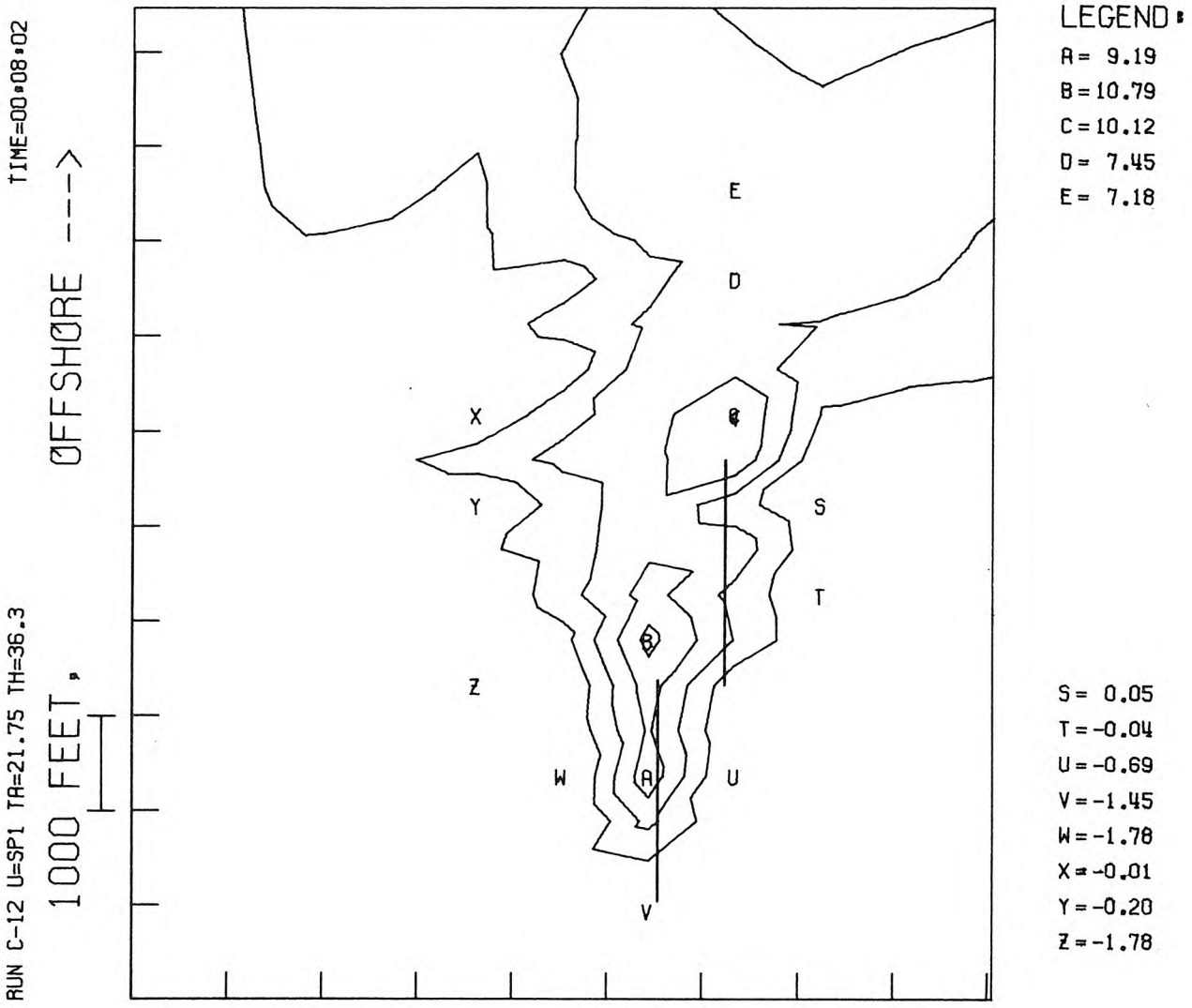

Figure 6.30 Surface isotherms (in increments of 2.5% of source ΔT_o) for special current sequence SP1 (Figure 6.29). (Diffusers shown as straight lines; instantaneous current speed = 0.05 knots.)

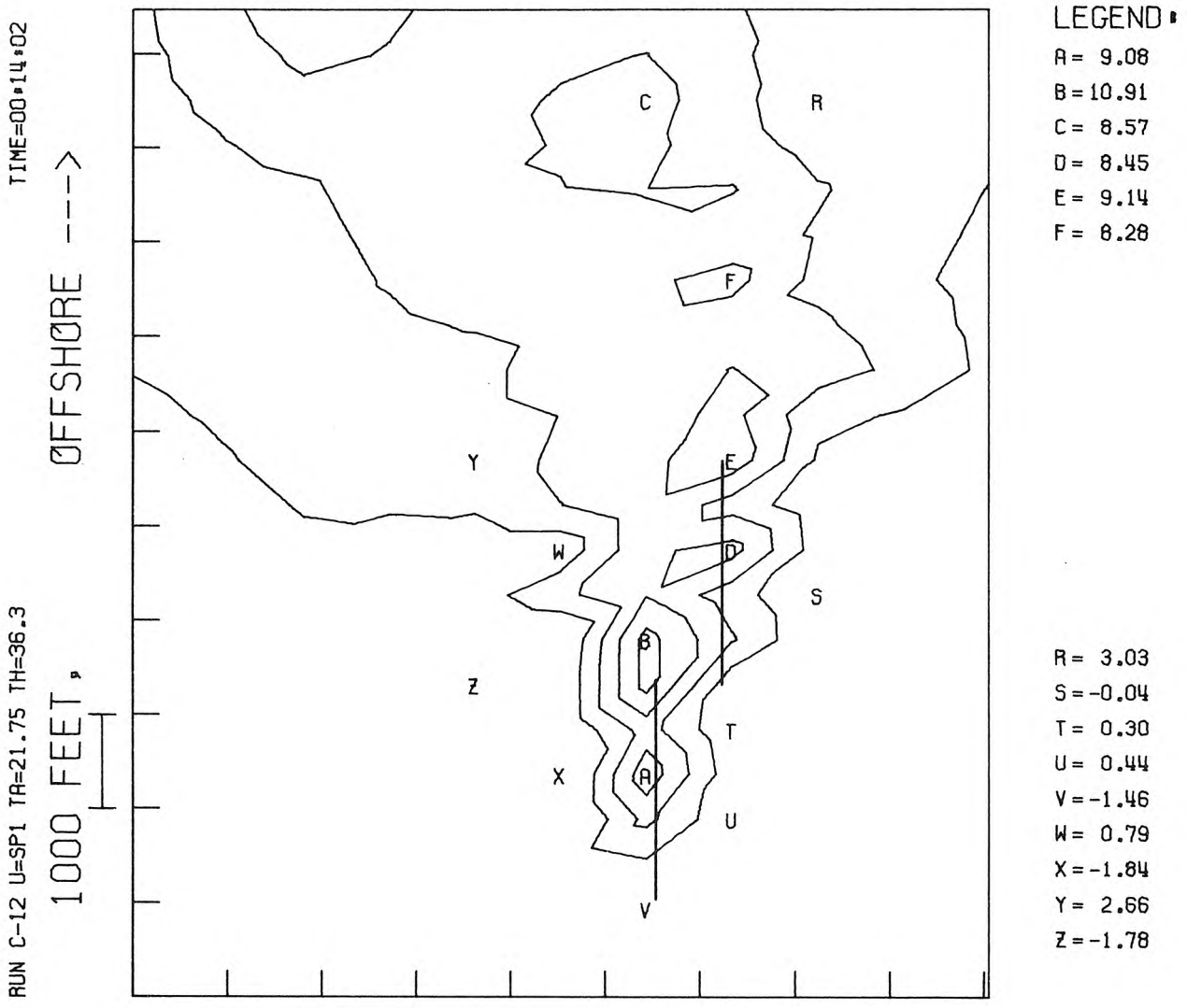

Figure 6.31 Surface isotherms (in increments of 2.5% of source ΔT_o) for special current sequence SP1 (Figure 6.29). (Diffusers shown as straight lines; instantaneous current speed = 0.02 knots.)

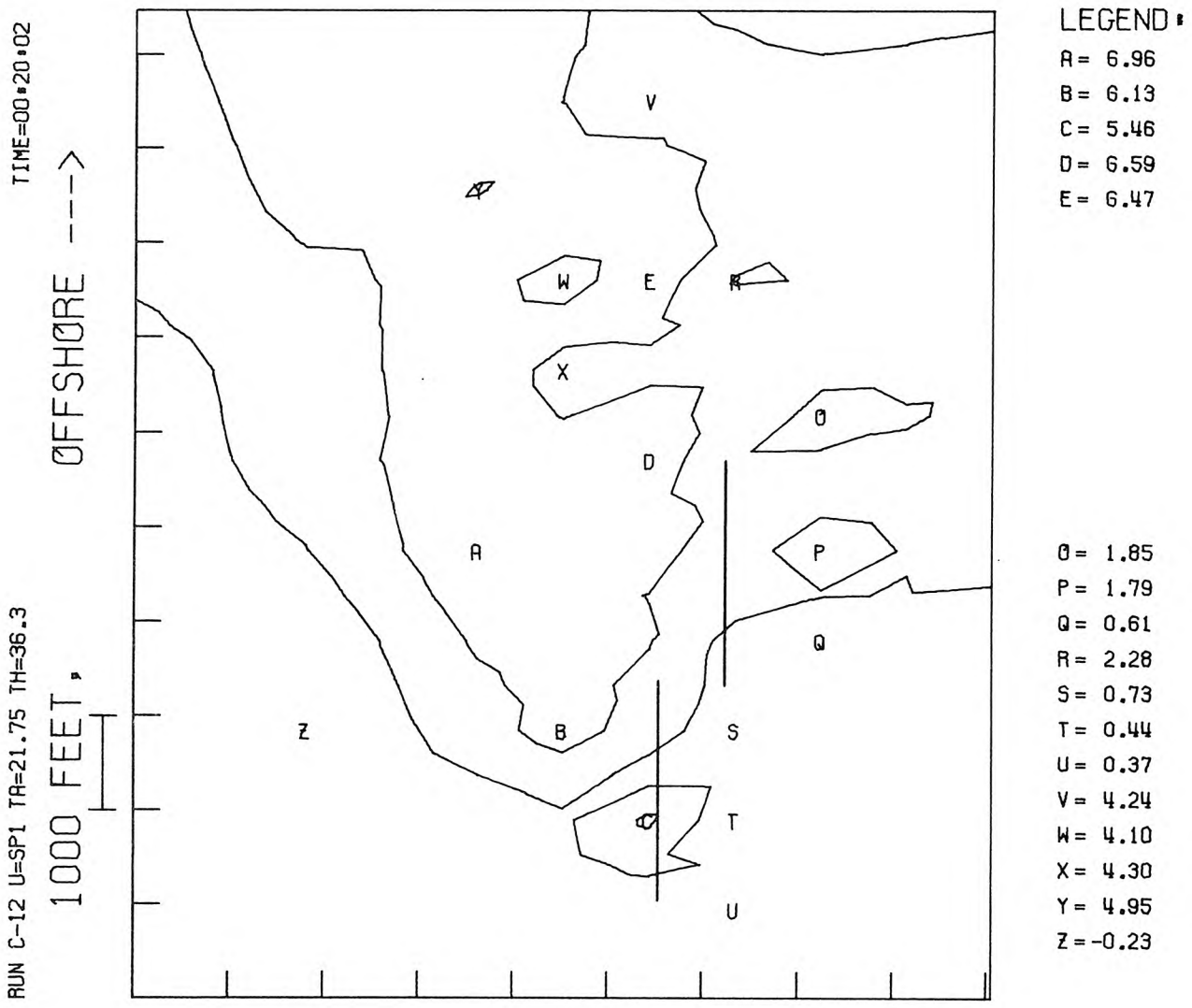

Figure 6.32 Surface isotherms (in increments of 2.5% of source ΔT_o) for special current sequence SP1 (Figure 6.29). (Diffusers shown as straight lines; instantaneous current speed = 0.2 knots.)

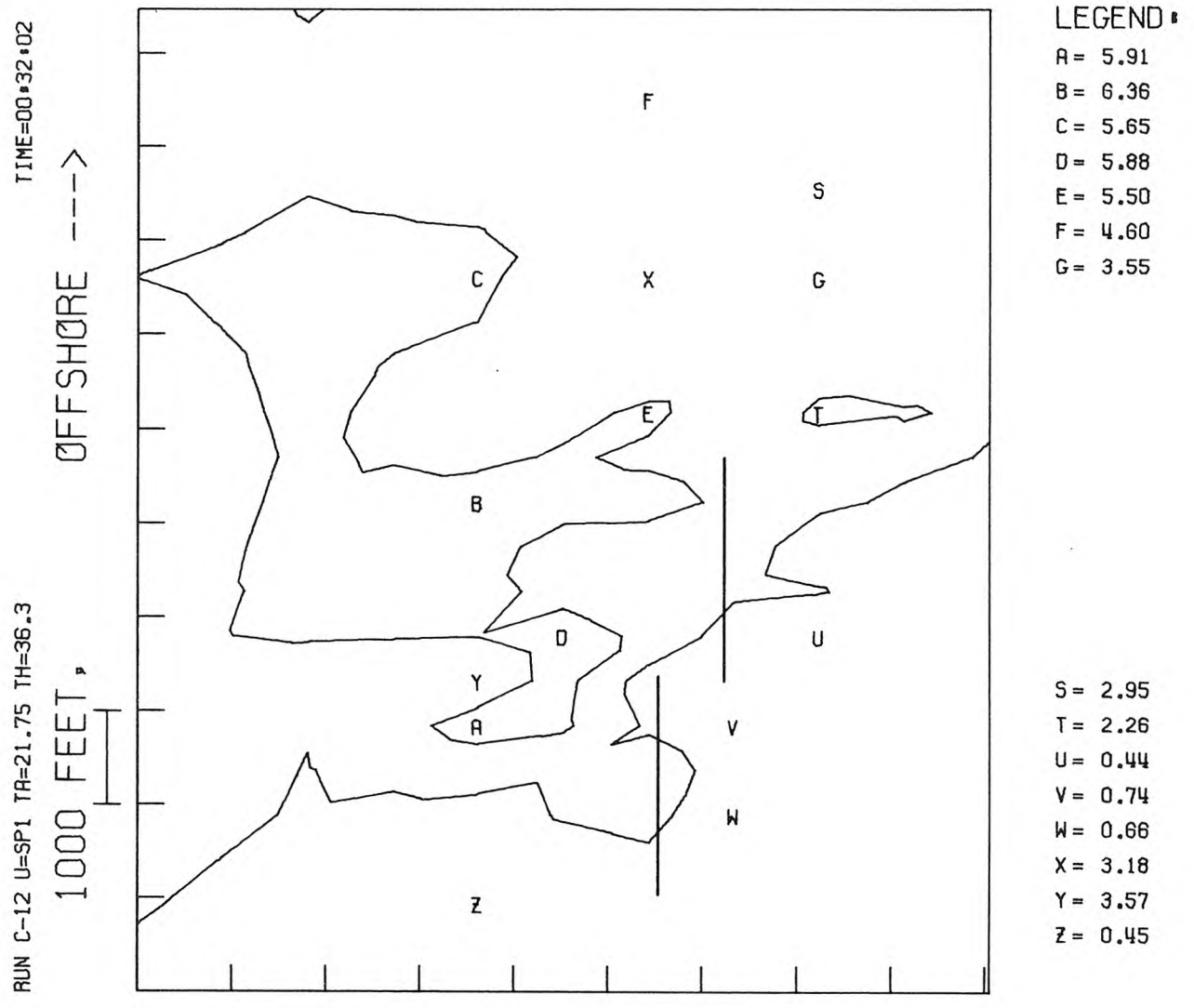

Figure 6.33 Surface isotherms (in increments of 2.5% of source ΔT_o) for special current sequence SP1 (Figure 6.29). (Diffusers shown as straight lines; instantaneous current speed = 0.37 knots.)

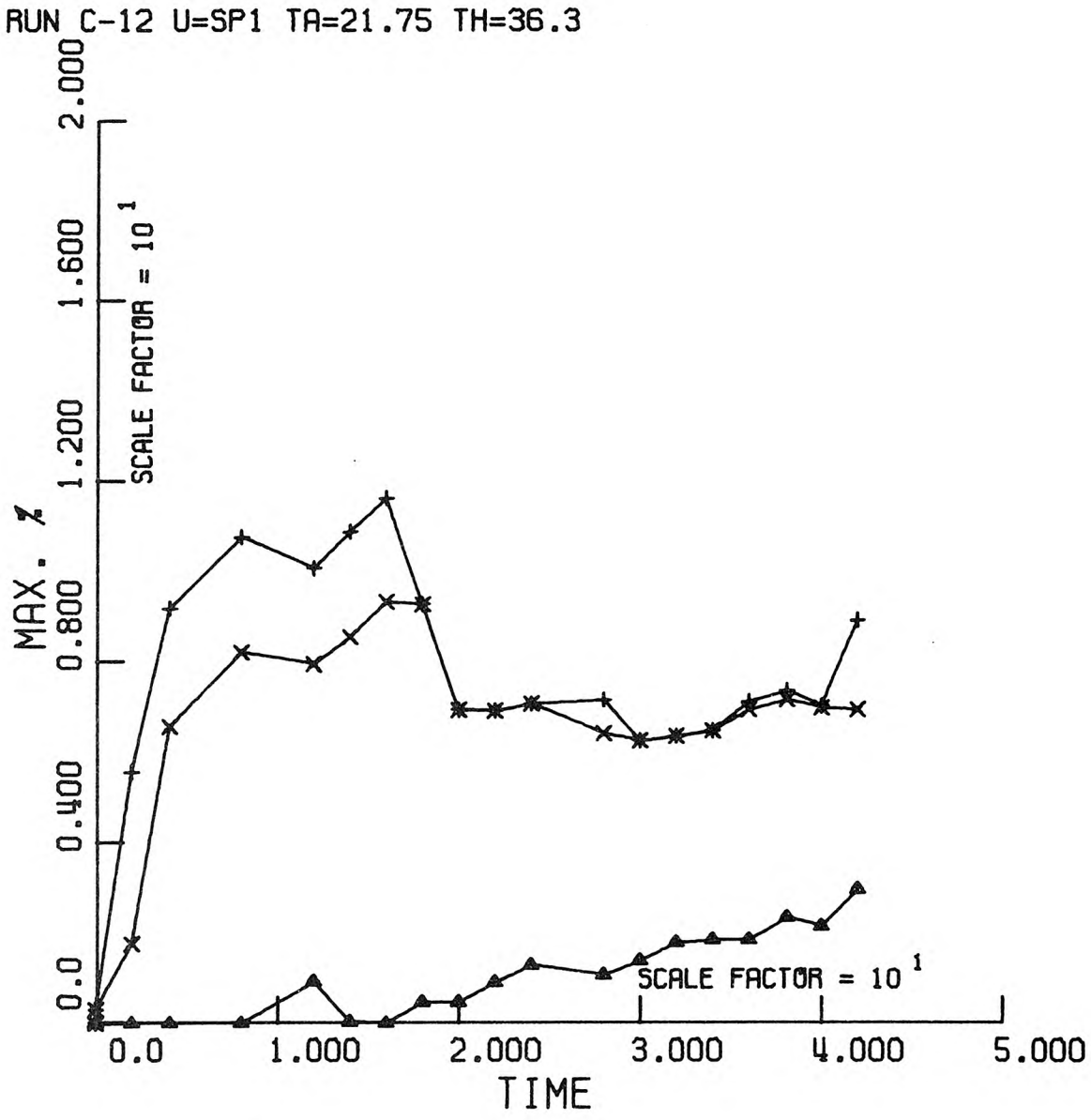

Figure 6.34 Summary of maximum temperature excesses (in % of source temperature excess) measured anywhere in basin (+), beyond 1000 ft of diffusers (x), and ambient temperature. (Run C-12, u = SP1, Figure 6.29.)

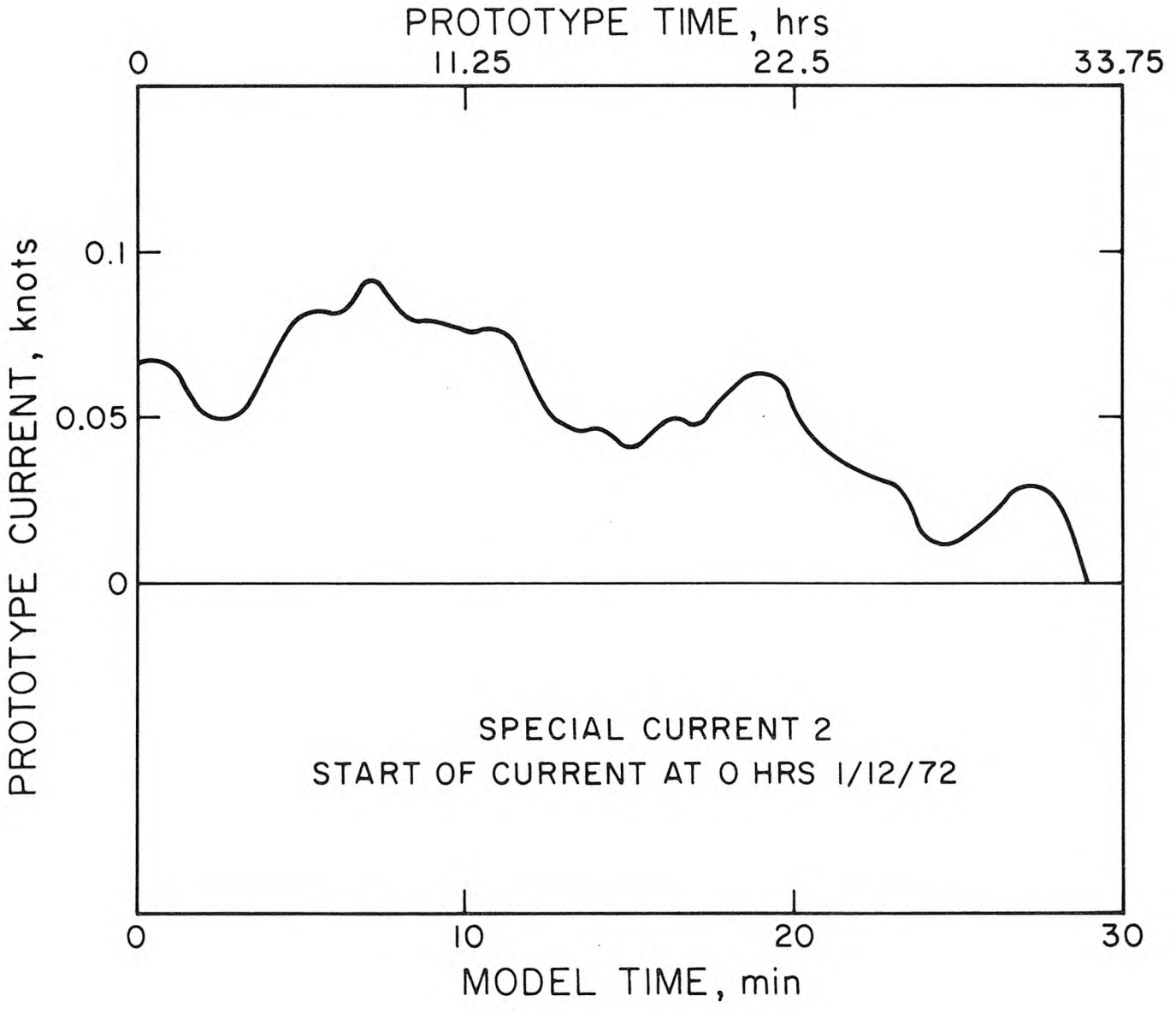

Figure 6.35 Longshore current sequence (SP2) used in Run C-13.

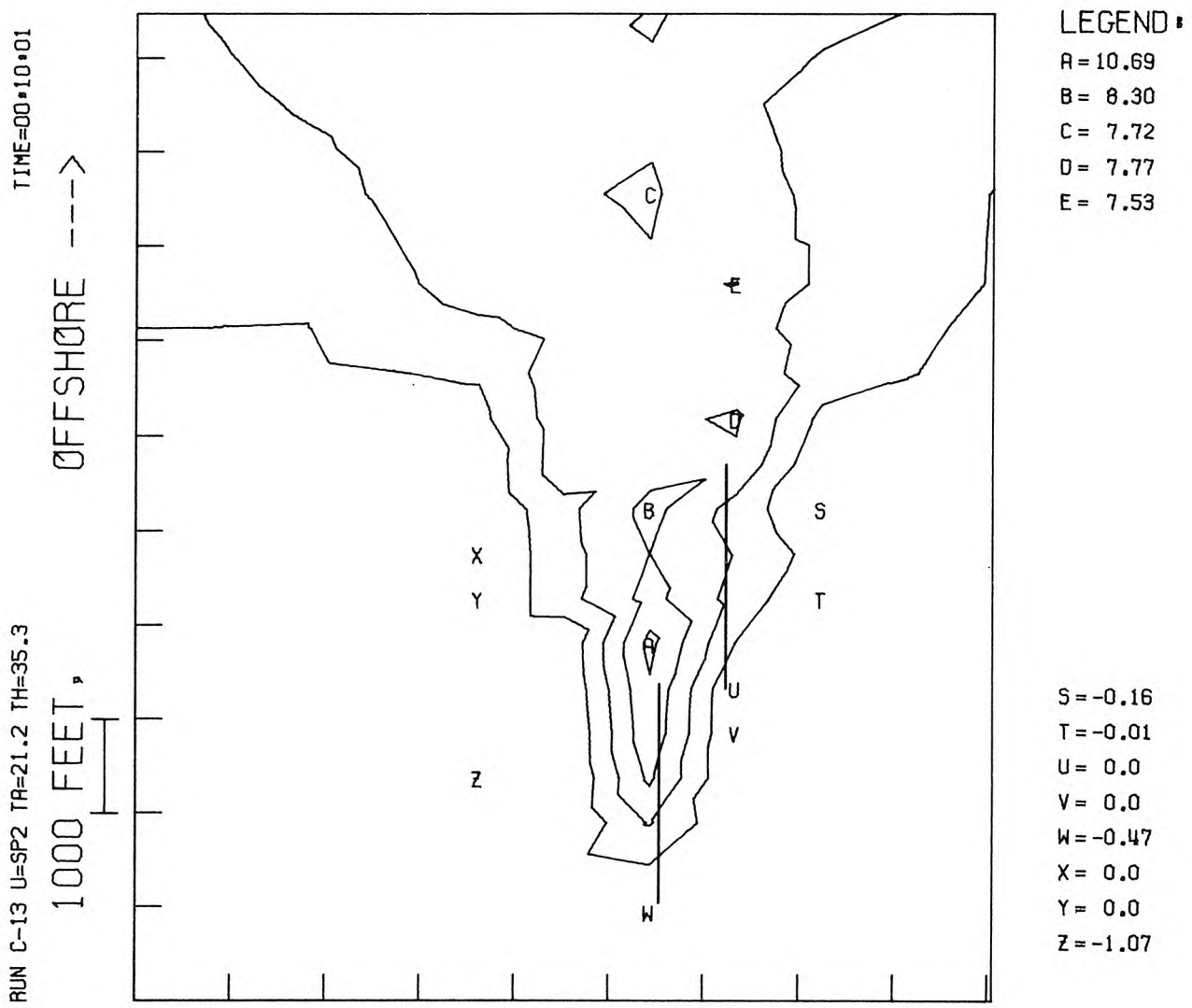

Figure 6.36 Surface isotherms (in increments of 2.5% of source ΔT_o) for special current sequence SP2 (Figure 6.35). (Diffusers shown as straight lines; instantaneous current speed = 0.075 knots.)

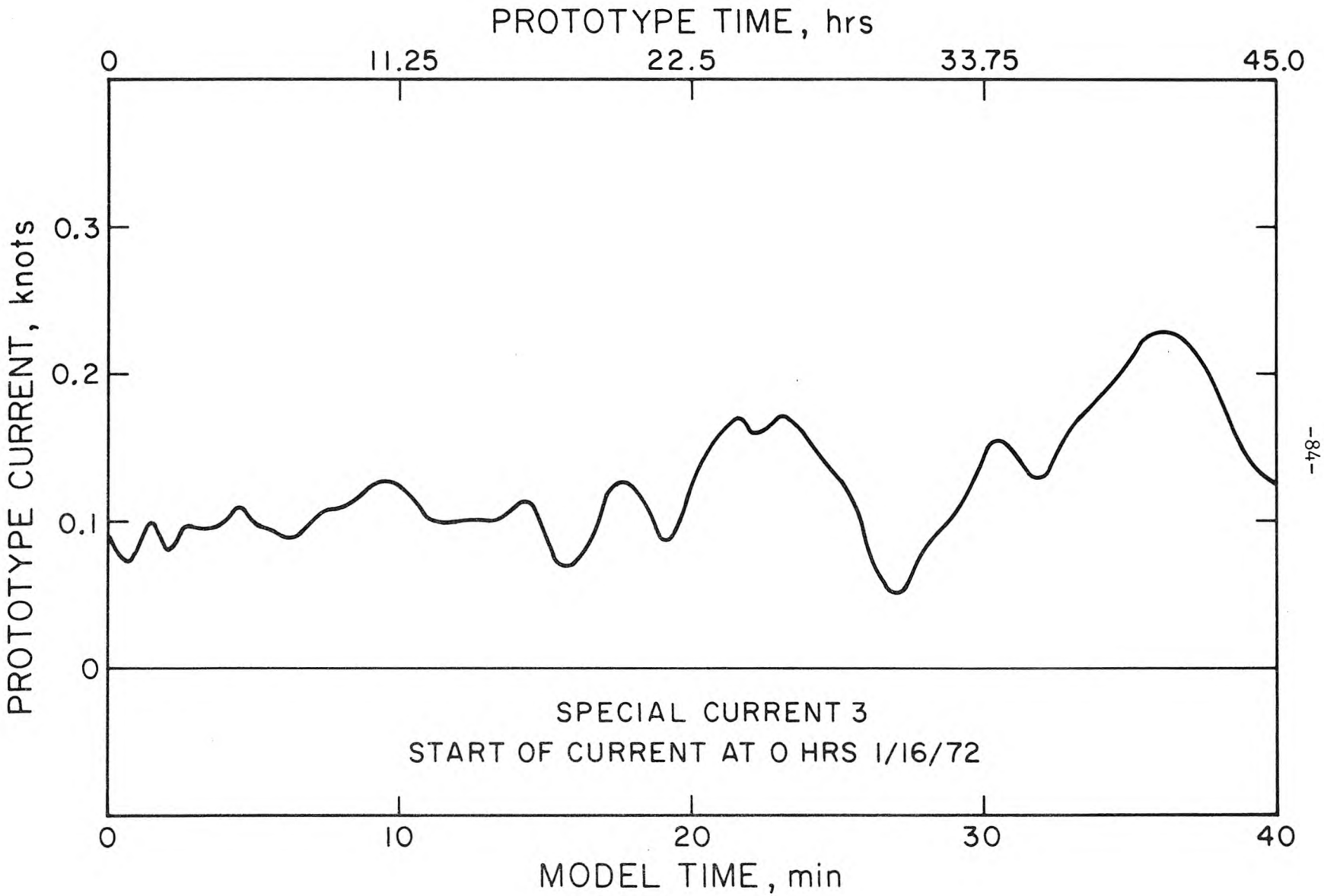

Figure 6.37 Longshore current sequence (SP3) used in Run C-14.

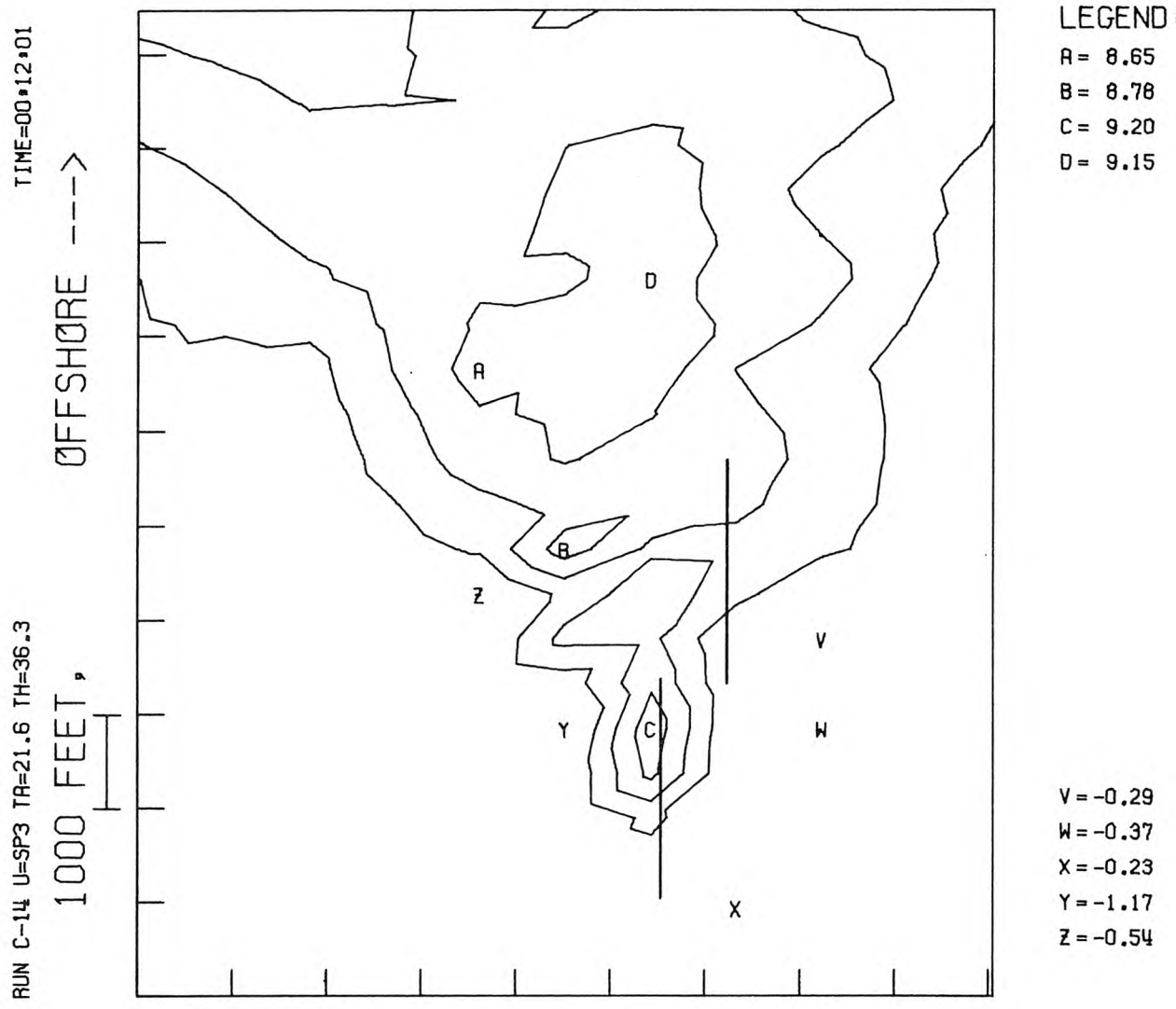

Figure 6.38 Surface isotherms (in increments of 2.5% of source ΔT_o) for special current sequence SP3 (Figure 6.37). (Diffusers shown as straight lines; instantaneous current speed = 0.1 knots.)

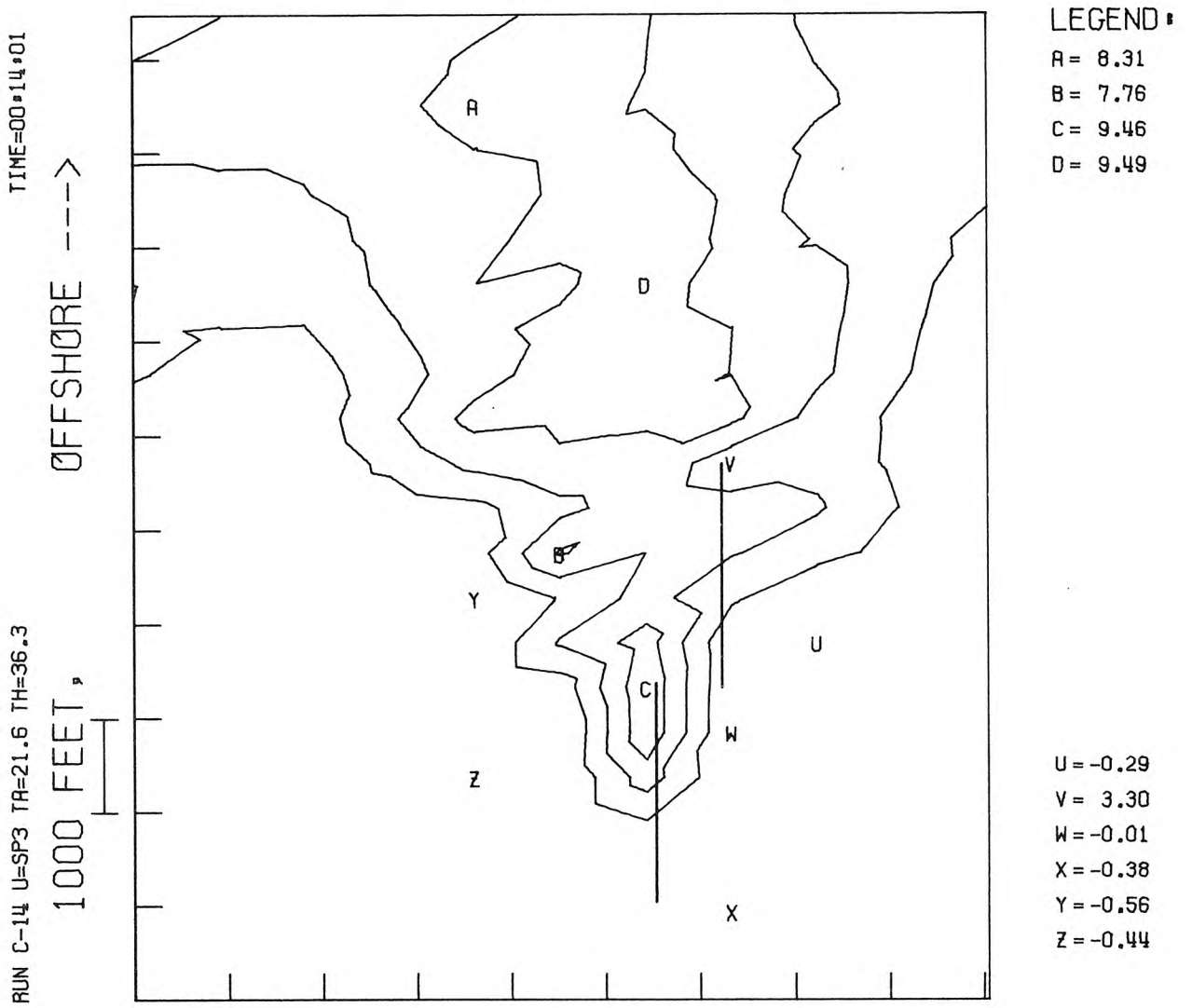

Figure 6.39 Surface isotherms (in increments of 2.5% of source ΔT_o) for special current sequence SP3 (Figure 6.37). (Diffusers shown as straight lines; instantaneous current speed = 0.1 knots.)

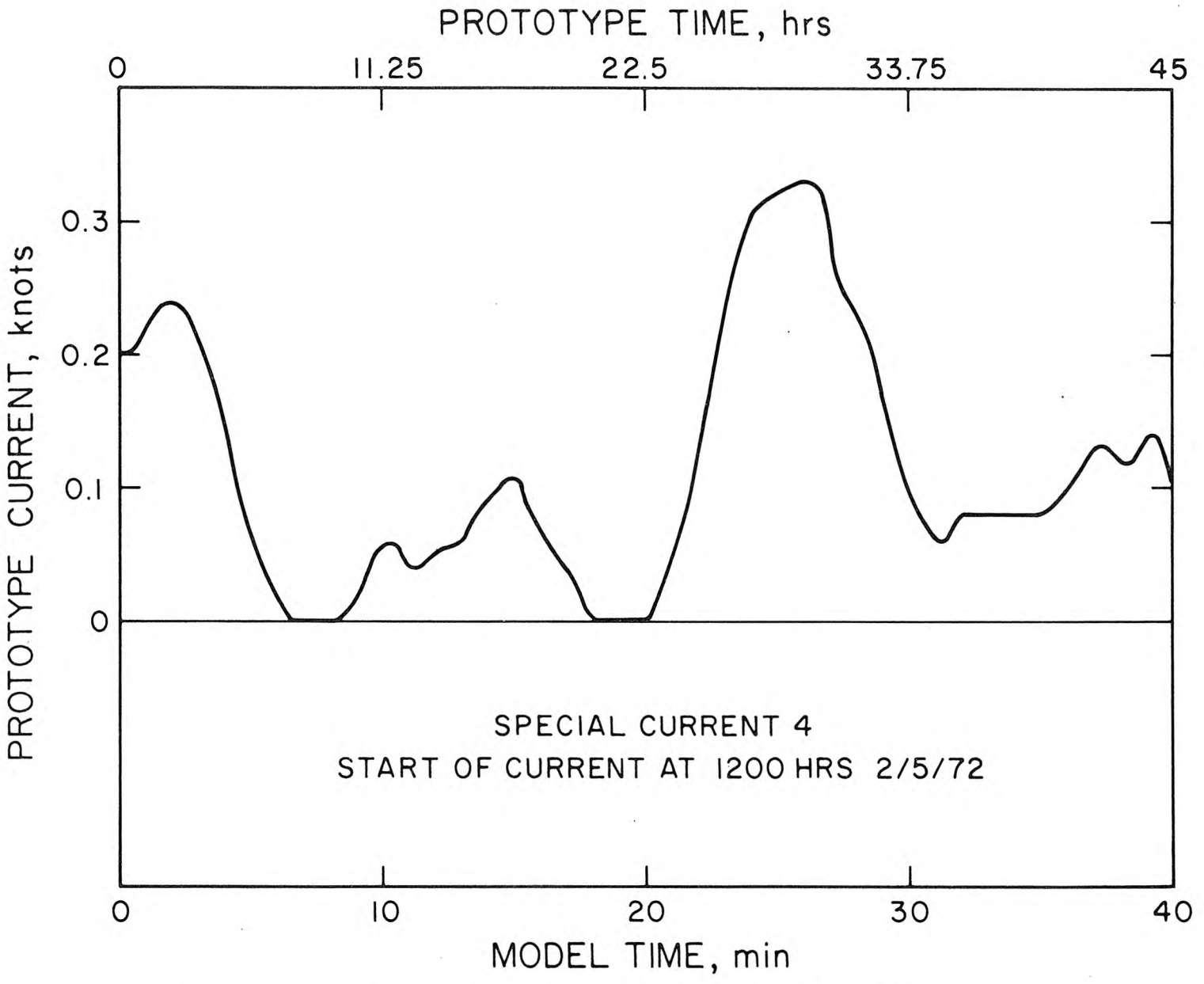

Figure 6.40 Longshore current sequence (SP4) used in Run C-15.

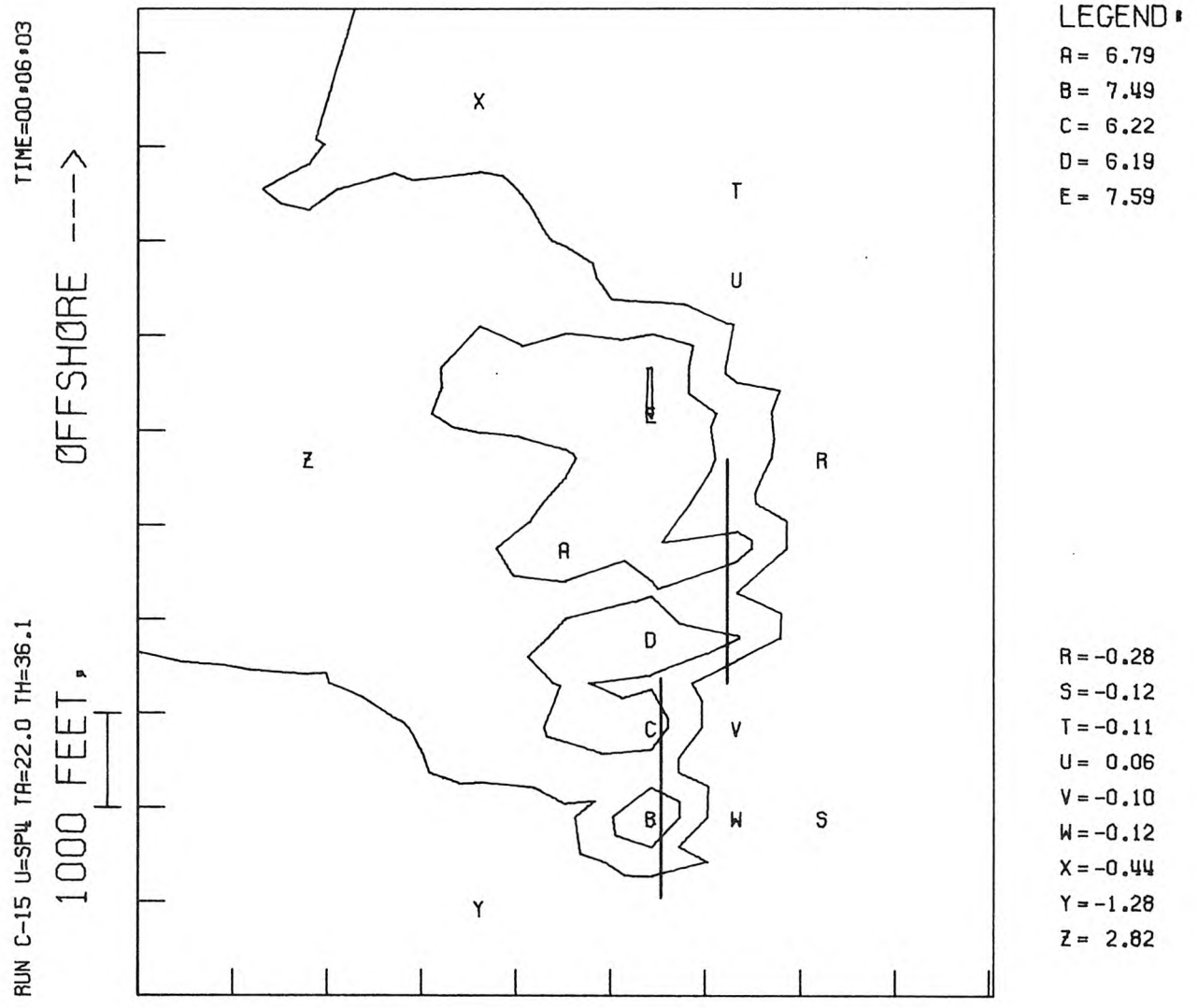

Figure 6.41 Surface isotherms (in increments of 2.5% of source ΔT_o) for special current sequence SP4 (Figure 6.40). (Diffusers shown as straight lines; instantaneous current speed = 0.02 knots.)

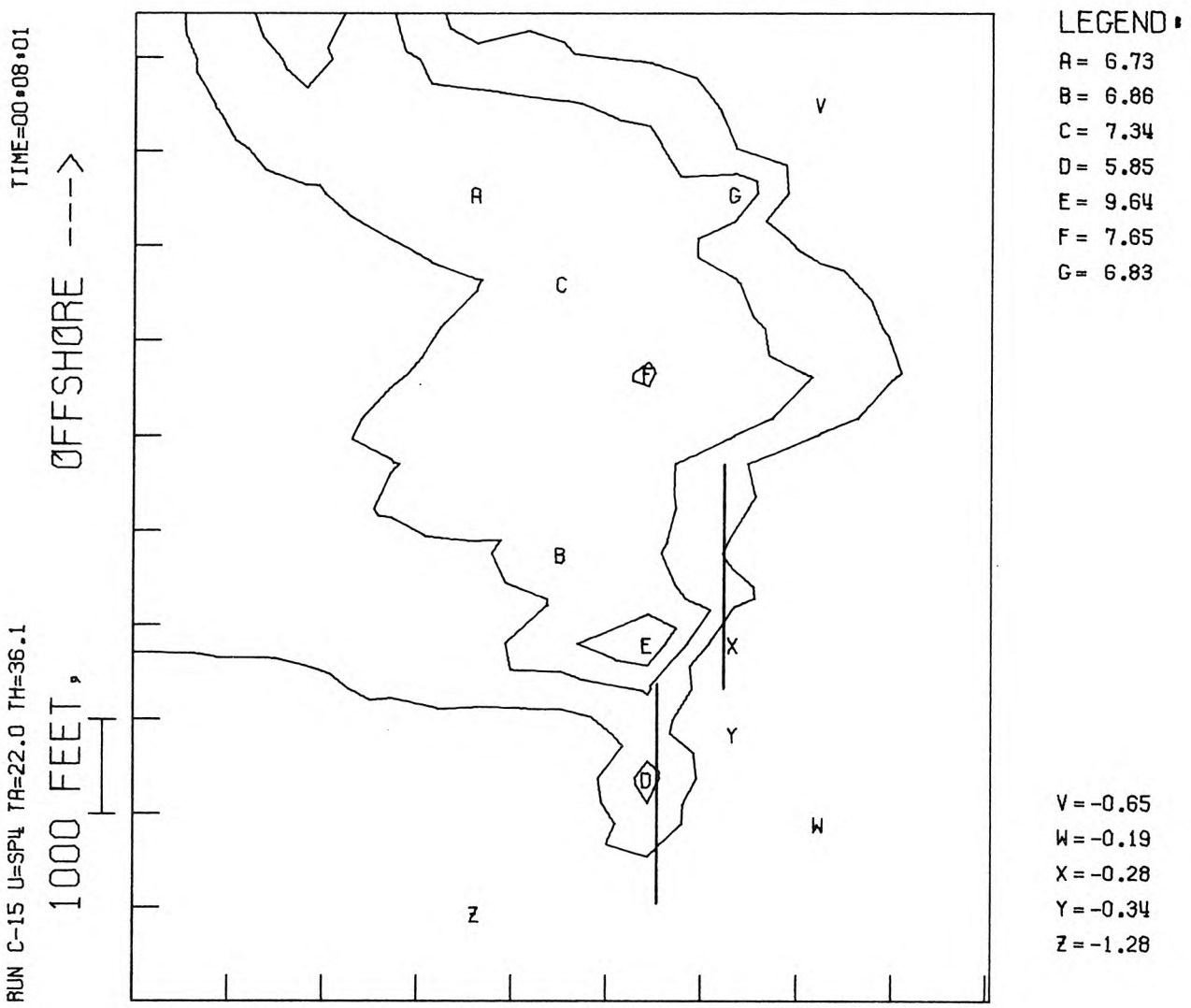

Figure 6.42 Surface isotherms (in increments of 2.5% of source ΔT_o) for special current sequence SP4 (Figure 6.40). (Diffusers shown as straight lines; instantaneous current speed = 0.0 knots.)

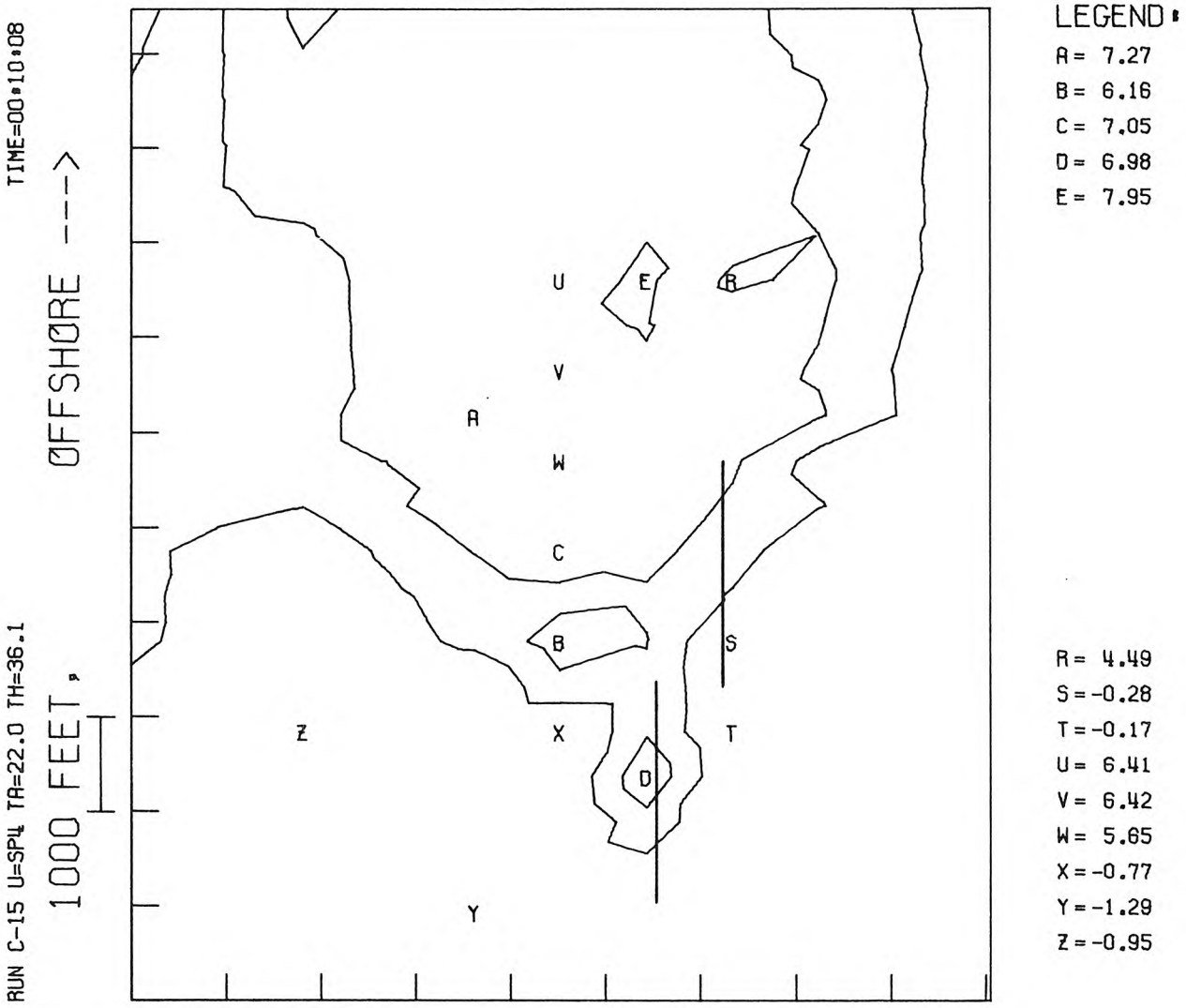

Figure 6.43 Surface isotherms (in increments of 2.5% of source ΔT_o) for special current sequence SP4 (Figure 6.40). (Diffusers shown as straight lines; instantaneous current speed = 0.06 knots.)

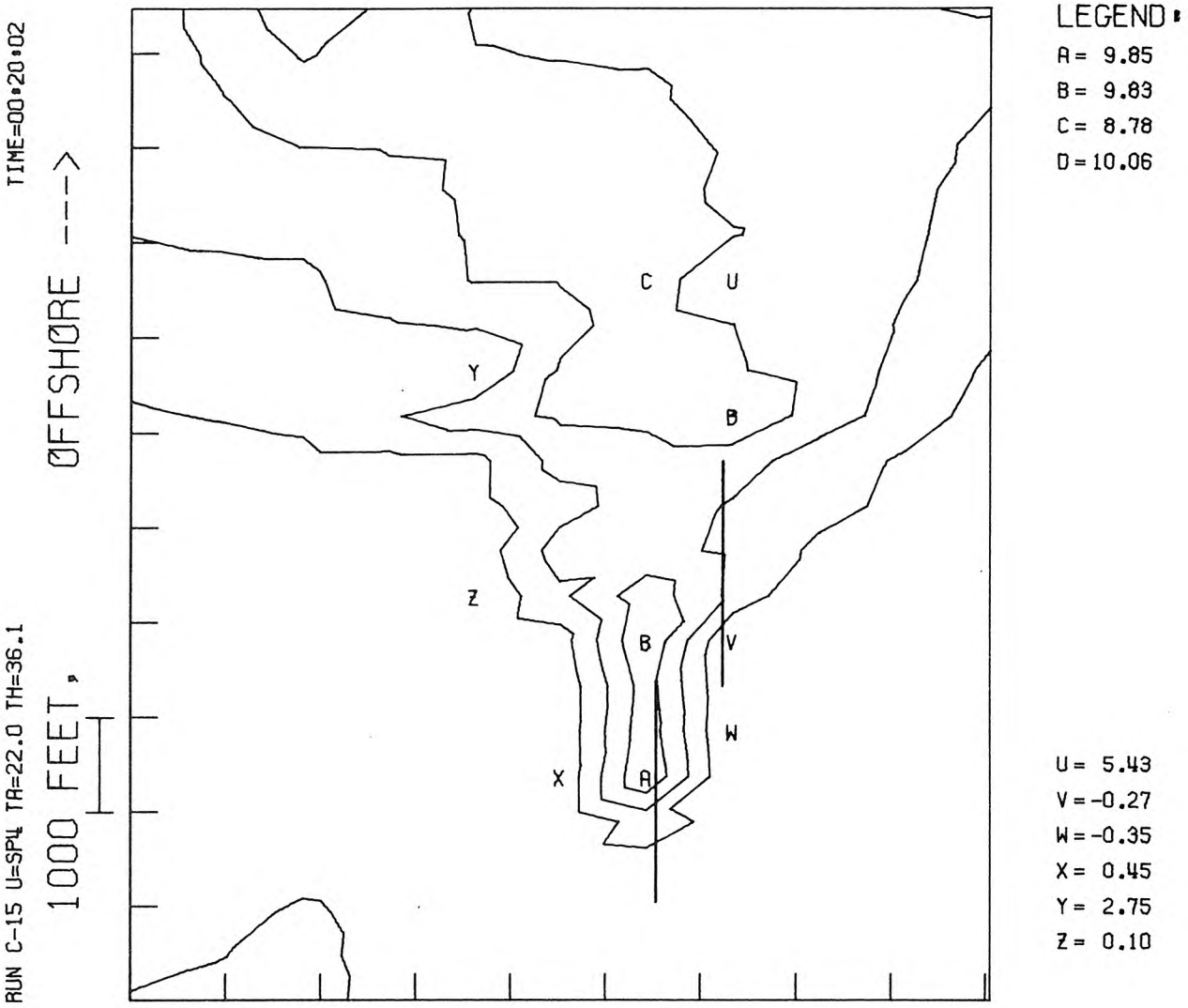

Figure 6.44 Surface isotherms (in increments of 2.5% of source ΔT_o) for special current sequence SP4 (Figure 6.40). (Diffusers shown as straight lines; instantaneous current speed = 0.0 knots.)

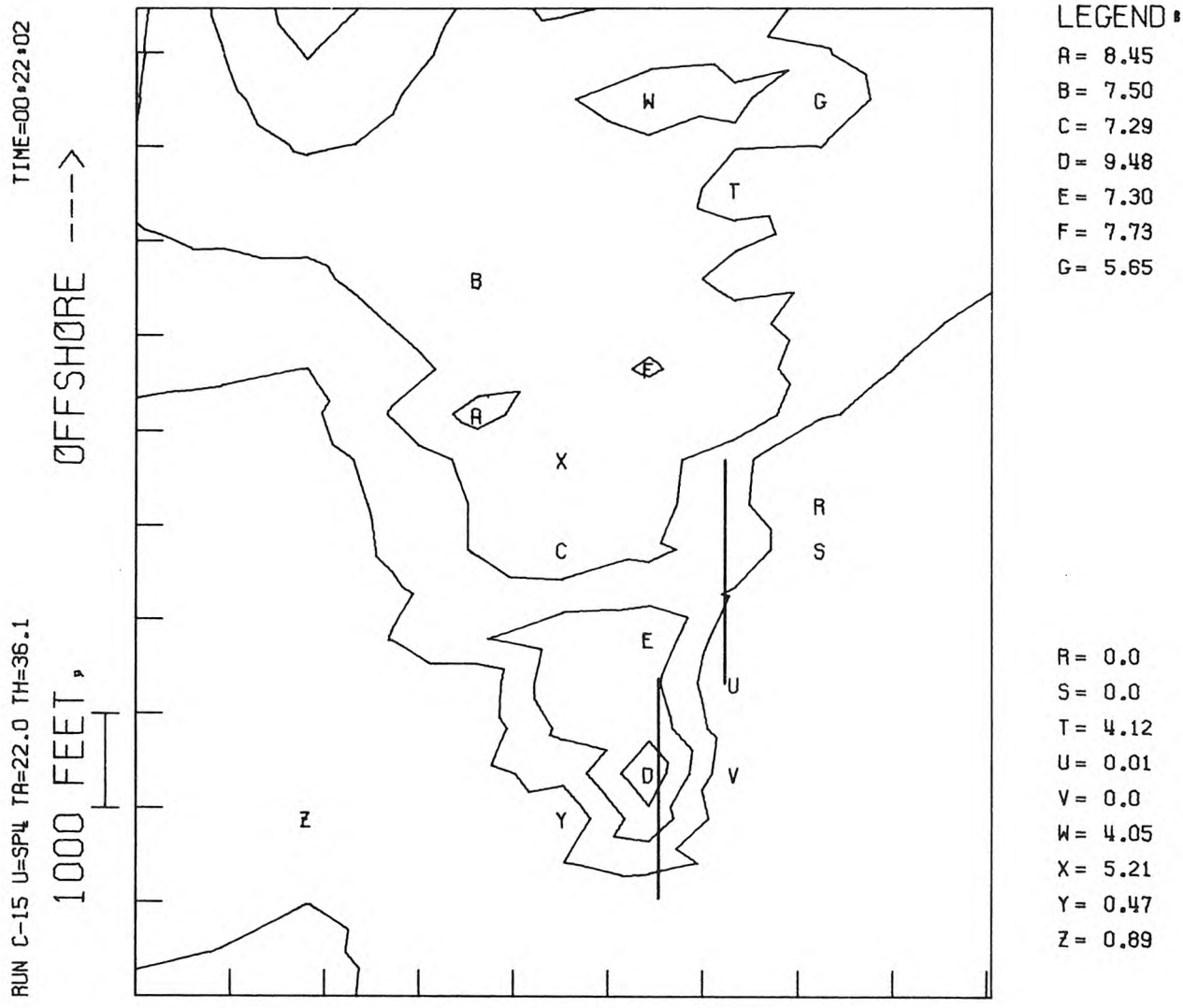

Figure 6.45 Surface isotherms (in increments of 2.5% of source ΔT_o) for special current sequence SP4 (Figure 6.40). (Diffusers shown as straight lines; instantaneous current speed = 0.13 knots.)

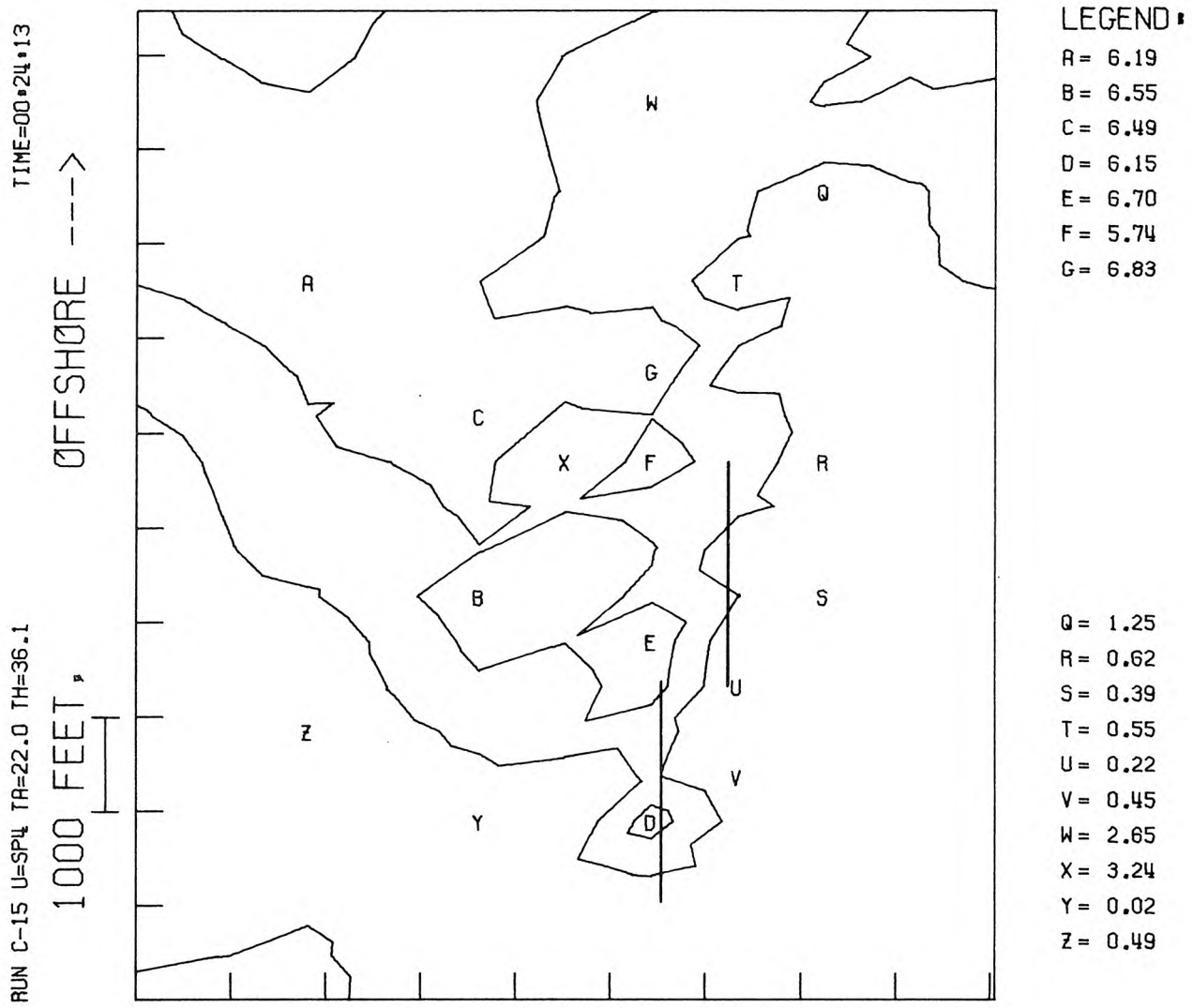

Figure 6.46 Surface isotherms (in increments of 2.5% of source ΔT_o) for special current sequence SP4 (Figure 6.40). (Diffusers shown as straight lines; instantaneous current speed = 0.3 knots.)

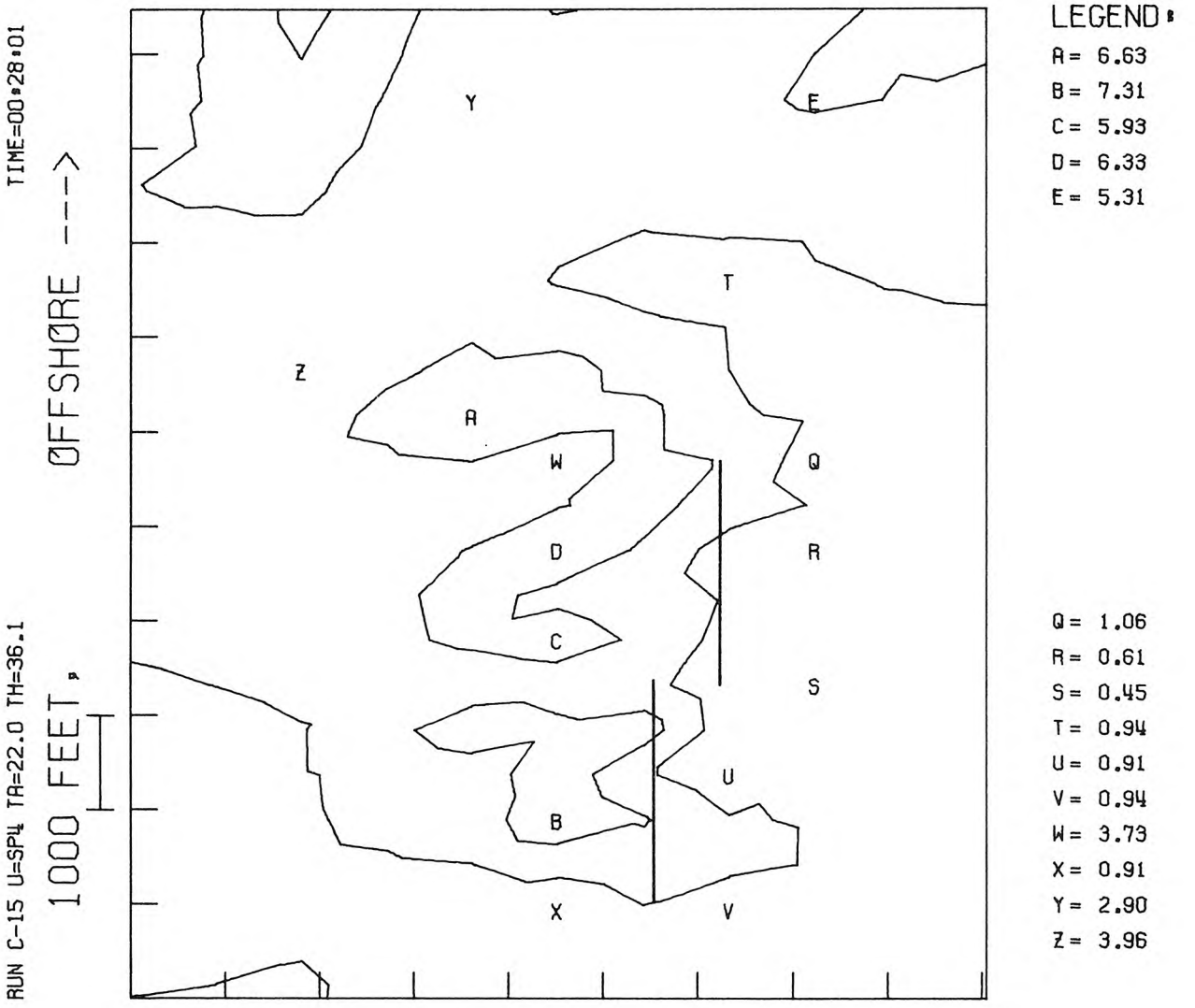

Figure 6.47 Surface isotherms (in increments of 2.5% of source ΔT_o) for special current sequence SP4 (Figure 6.40). (Diffusers shown as straight lines; instantaneous current speed = 0.23 knots.)

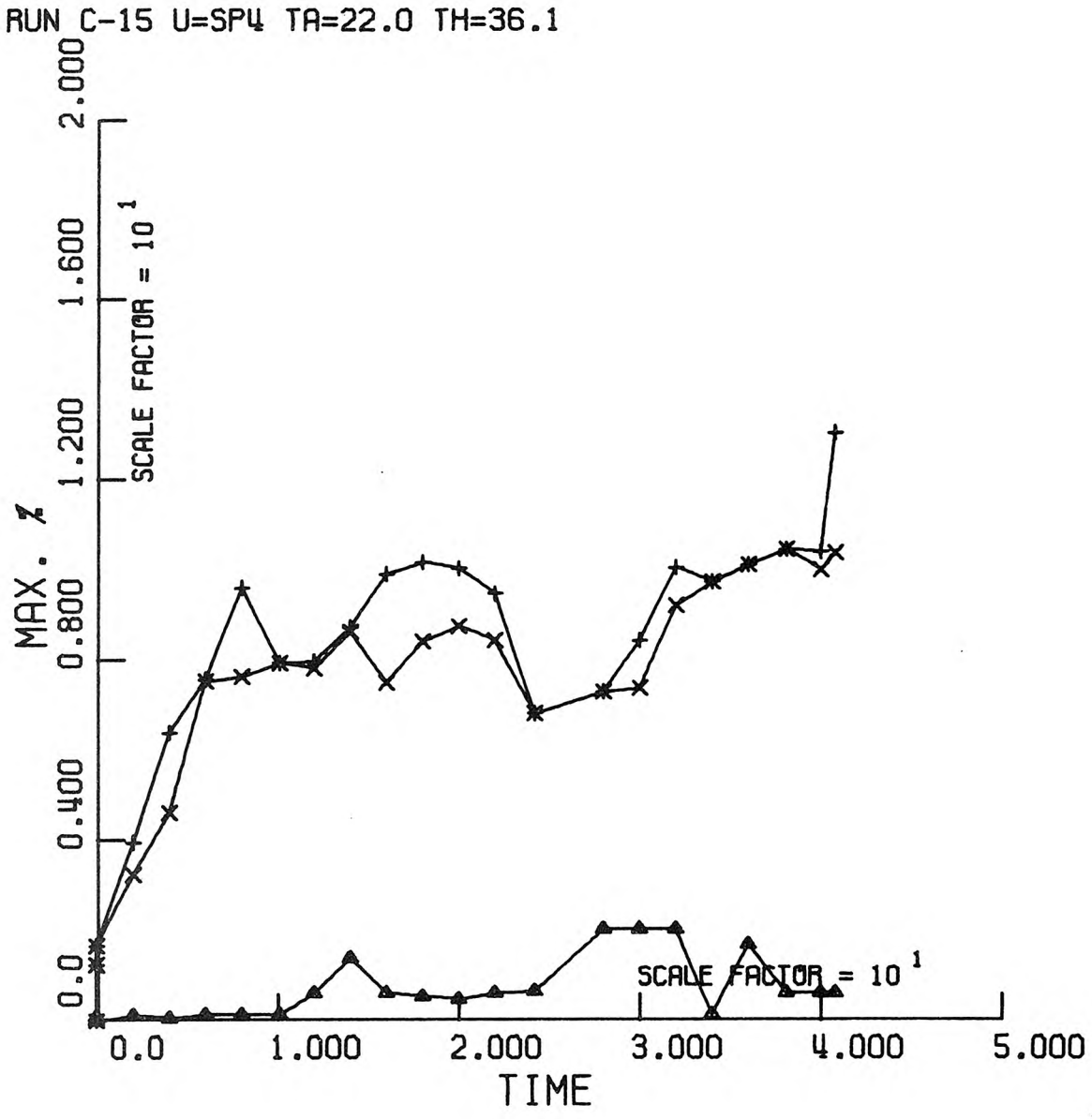

Figure 6.48 Summary of maximum temperature excesses (in % of source temperature excess) measured anywhere in basin (+), beyond 1000 ft of diffusers (x) and ambient temperature. (Run C-15, u = SP4, Figure 6.40)

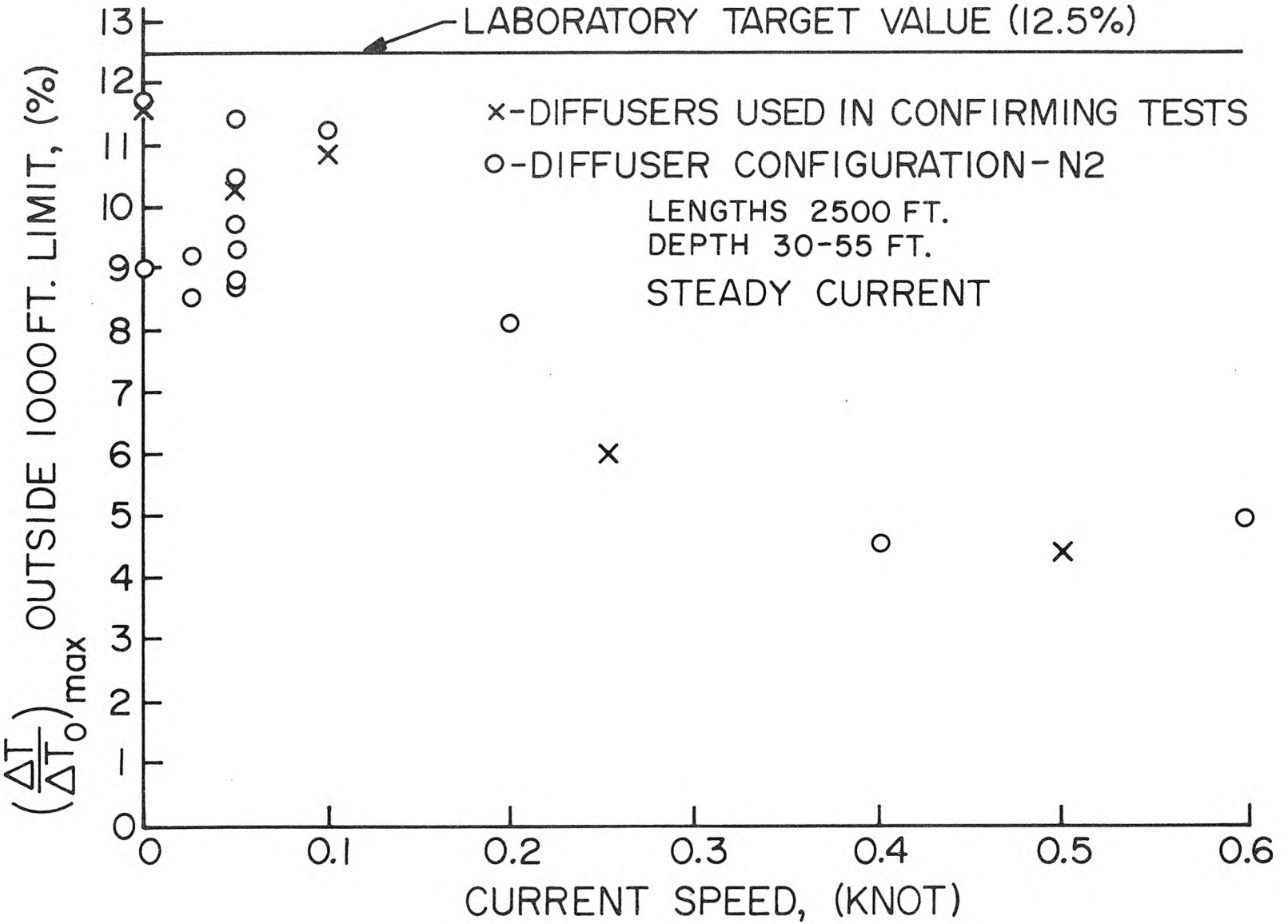

Figure 6.49 Summary of maximum surface temperature excess (beyond 1000 ft limit) as function of steady current speed.

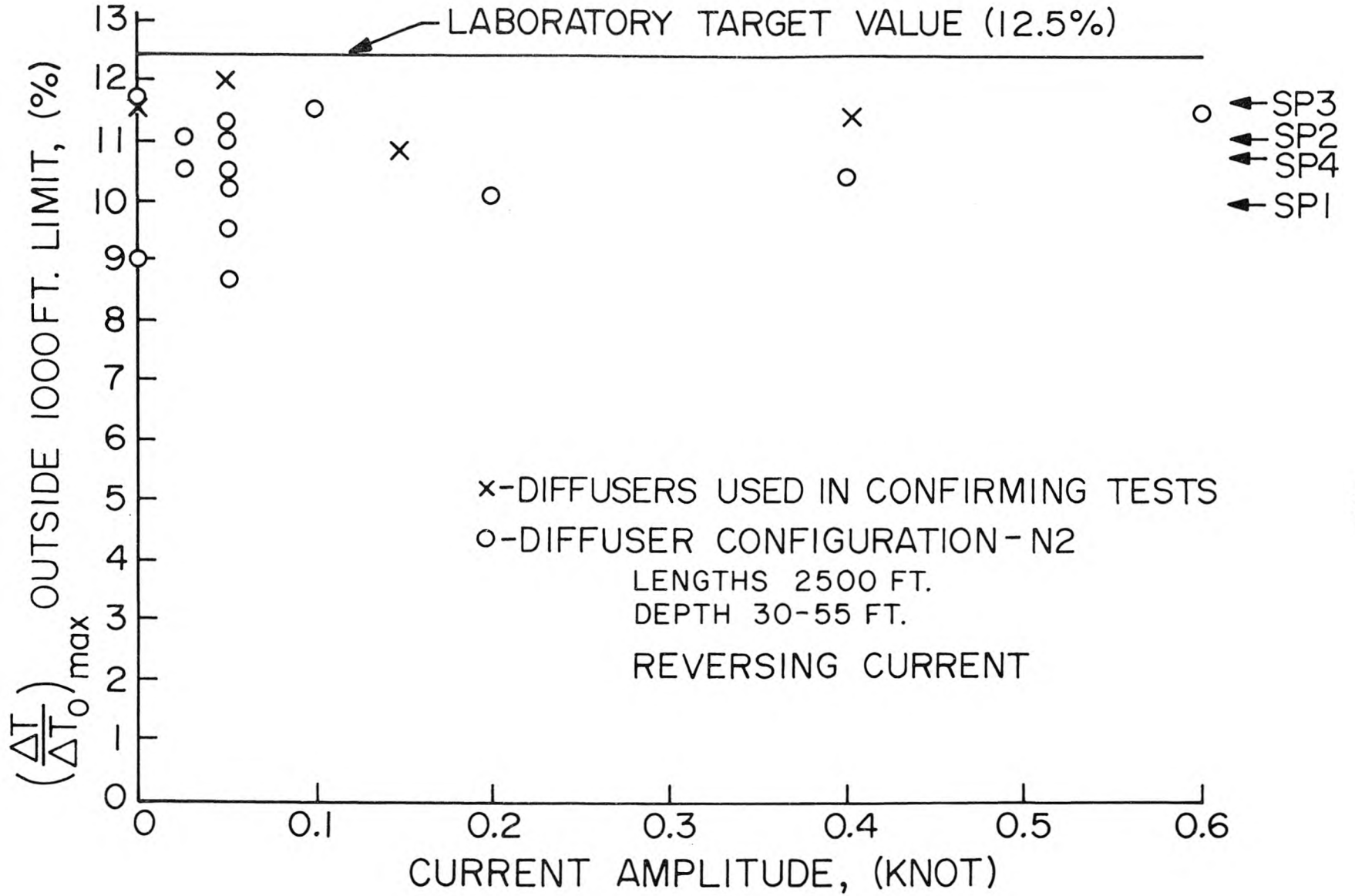

Figure 6.50 Summary of maximum surface temperature excess (beyond 1000 ft) as function of reversing current amplitude (special currents shown by arrows on right of figure since there is no clearly defined current amplitude).

6.5 Discussion of Results

The current sequences chosen for the confirming tests as listed in Table 6.1 were selected to give a representative sample of all the current patterns that appeared to occur at the San Onofre site. A substantial amount of field data was obtained at several locations at the site by Intersea Research Corporation* using various types of current meters and drogues. This field data, processed by Intersea to show frequency of occurrence of direction and magnitude of the ocean currents, was the basis on which the selection of the currents used in the tests was made. A cross-correlation of the current data was also made with wind data recorded at the meteorological station at San Onofre and it disclosed that on no occasion for the period of record (one year) was there any onshore current associated with onshore winds. In fact there were almost no onshore winds of significance.

In view of the excellent field data available for the site, it is therefore believed that the tests chosen form a valid and representative sequence of possible flow configurations that will occur at San Onofre. Further, selection of four actual current sequences (SP1 - SP4) that occurred at the site, coupled with the other representative samples, should provide an adequate indication of the results to be expected with prototype operation.

In effect the diffusers must be designed for practically zero current speed (or 0.05 knots) for substantial periods of time such as a day or two in order to satisfy the California thermal requirements which must be met on a daily basis. The performance of the recommended configuration of two 2500 foot diffusers, each with 63 jets which induce an offshore drift, meets the laboratory target value of 2.5°F. Thus, it is predicted that the prototype operation will easily conform to the 4°F limit.

---

* "Current Meter Observations and Statistics Off San Onofre Nuclear Generating Station, 5 Jan. - 22 Nov. 1972", Intersea Research Corporation, January, 1973.

CHAPTER 7

SUMMARY AND CONCLUSIONS

The major findings are summarized as follows:

1. Due to lack of previous model-to-prototype comparisons, the complex current structure at San Onofre, possible interference from Unit 1, and unknown scale effects, a laboratory target value of $\Delta T \leq 2.5°F$ was chosen instead of the 4°F in the California thermal standards (for surface temperature increase at 1000 feet from the diffusers). Results in this report are given as $\Delta T/\Delta T_o$, where ΔT_o is the condenser temperature rise, presumed to be 20°F; thus the target value of $\Delta T/\Delta T_o$ is 12.5%.

2. The diffusers tested represent the culmination of an interplay of previous test results and other design considerations. They are nominally 2500 feet long with 63 nozzles each (nozzles 20° up from horizontal and 25° off outfall axis on alternate sides pointing offshore). Nominal jet discharge velocity is 13 fps.

3. The offshore momentum generated by the discharge is important (particularly for low or reversing ocean current) in ensuring that a drift current carries the diluted effluent offshore away from the diffusers. This drift current is estimated to be 0.1 to 0.2 knots based on the thermal patterns observed.

4. For <u>steady</u> longshore currents, the peak value of ΔT beyond the 1000 ft limit decreases with increasing current magnitude.

5. For reversing longshore currents, the peak value of ΔT beyond the 1000 ft limit is essentially independent of current amplitude, and occurs approximately at the time of slack current.

6. The observed peak value of $\Delta T/\Delta T_o$ beyond the 1000 ft limit is approximately 12%, representing 2.4°F for a source ΔT_o of 20°F.

7. The results indicate that the diffusers will meet the laboratory target under all current conditions tested.

ACKNOWLEDGMENTS

The writers wish to acknowledge the valuable assistance of many members of the staff of the W. M. Keck Laboratory of Hydraulics and Water Resources. We make particular mention of Elton Daly, Joe Fontana, Carl Green and Bill Stone for their efforts in the erection and instrumentation of the basin and models: Max Irvine, Phil Roberts, and Nikos Kotsovinos, graduate research assistants; Robert Stecher, Manfred Chu and Bruce Bennett, undergraduate assistants; and Pat Rankin and Arvilla Stanton for their assistance in the typing and preparation of this report.

Particular thanks are also due to Martin Leonard for his assistance during the final confirming tests.

Mr. Ken Meddock of the Southern California Edison Company also participated part time and provided liaison with the Southern California Edison Company.

REFERENCES

The references listed below consist of two groups. The first contains the seven progress reports generated during the conduct of this project. The second is a selected bibliography containing references related to the various aspects of the overall dispersion phenomenon associated with buoyant discharges into the environment.

Progress Reports

1. N. H. Brooks, R. C. Y. Koh, and E. J. List, "Hydraulic Investigations of Thermal Outfalls for the San Onofre Nuclear Power Plant," W. M. Keck Laboratory of Hydraulics and Water Resources, Progress Report No. 1 to Southern California Edison Co. (Tech. Memo No. 72-2), Dec. 8, 1972, 47 pp.

2. N. H. Brooks, R. C. Y. Koh, E. J. List and Eric J. Wolanski, "Hydraulic Investigations of Thermal Outfalls for the San Onofre Nuclear Power Plant," W. M. Keck Laboratory of Hydraulics and Water Resources, Progress Report No. 2 to Southern California Edison Co. (Tech. Memo No. 73-2), January 26, 1973, 9 pp.

3. Robert C. Y. Koh, "Hydraulic Tests of Discharge Ports - Hydraulic Investigations of Thermal Outfalls for the San Onofre Nuclear Power Plant," W. M. Keck Laboratory of Hydraulics and Water Resources, Progress Report No. 3 to Southern California Edison Co. (Tech. Memo No. 73-4, March 30, 1973, 118 pp.

4. R. C. Y. Koh, N. H. Brooks, E. J. Wolanski, and E. J. List, "Basin Model Studies of Diffusers, Hydraulic Investigations of Thermal Outfalls for the San Onofre Nuclear Power Plant," W. M. Keck Laboratory of Hydraulics and Water Resources, Progress Report No. 4 to Southern California Edison Co. (Tech. Memo 73-5), May 1, 1973, 71 pp.

5. E. J. List, "Large Scale Sectional Model Tests of Diffuser Operation, Hydraulic Investigations of Thermal Outfalls for the San Onofre Nuclear Power Plant," W. M. Keck Laboratory of Hydraulics and Water Resources, Progress Report No. 5 to Southern California Edison Co. (Tech. Memo 73-6), July 16, 1973, 45 pp.

6. R. C. Y. Koh, "Hydraulic Tests of Thermal Dispersion for Unit 1 of the San Onofre Nuclear Power Plant," W. M. Keck Laboratory of Hydraulics and Water Resources, Progress Report No. 6 to Southern California Edison Co. (Tech.Memo 73-7), July 31, 1973, 50 pp.

7. R. C. Y. Koh, "Heat Treatment of Units 2 and 3 Intake for the San Onofre Nuclear Power Plant," W. M. Keck Laboratory of Hydraulics and Water Resources, Progress Report No. 7 to Southern California Edison Co. (Tech. Memo No. 73-8), September 1, 1973, 48 pp.

SELECTED BIBLIOGRAPHY

1. Abbott, M. B., "On the Spreading of One Fluid Over Another," La Houille Blanche, vol. 16, 1961, pp. 622-628 and 827-846.

2. Abraham, G., "Jet Diffusion in Stagnant Ambient Fluid," Delft Hydraulics Laboratory, Publ. No. 29, July 1963.

3. Abraham, G., "Horizontal Jets in Stagnant Fluid of Other Density," J. Hydraulics Division, ASCE, vol. 91, no. HY4, July 1965, pp. 139-154.

4. Abraham, G., "The Flow of Round Buoyant Jets Issuing Vertically into Ambient Fluid Flowing in a Horizontal Direction," Proceedings, 5th International Water Pollution Research Conference, San Francisco, July-August 1970, Paper III-15, 7 pp.

5. Abraham, G., "Jets and Plumes Issuing into Stratified Fluids," Proceedings, International Symposium on Stratified Flows, International Association for Hydraulic Research, Novosibirsk, 1972.

6. Abraham, G., and Koudstaal, R., "Wind Influence Upon Cooling Water Circulation," Proceedings, ASCE, vol. 95, no. PO1, 1969, pp. 63-75.

7. Abraham, G., and Eysink, W. D., "Jets Issuing into Fluid with a Density Gradient," J. Hydraulic Research, vol. 7, no. 2, 1969, pp. 145-175.

8. Ackers, P., "Modeling of Heated-Water Discharges," §6, Engineering Aspects of Thermal Pollution, Parker and Krenkel, Editors, Vanderbilt University Press, 1969.

9. Albertson, M. L., Dai, Y. B., Jensen, R. A., and Rouse, H., "Diffusion of Submerged Jets," Trans. ASCE, vol. 115, 1950, pp. 639-697.

10. Anwar, H. O., "Behavior of Buoyant Jet in Calm Fluid," J. Hydraulics Division, ASCE, vol. 95, no. HY4, July 1969, pp. 1289-1303.

11. Anwar, H. O., "Experiment on an Effluent Discharging from a Slot into Stationary or a Slow Moving Fluid of Greater Density," J. of Hydraulic Research, vol. 7, no. 4, 1969, pp. 411-431.

12. Anwar, H. O., "Measurements on Horizontal Buoyant Jet in Calm Ambient Fluid, with Theory Based on Variable Coefficient of Entrainment Determined Experimentally," La Houille Blanche, April 1972, pp. 311-319.

13. Anwar, H.O., "Appearance of Unstable Buoyant Jet," J. Hydraulics Div., ASCE, vol. 98, no. HY7, 1972, pp. 1143-1156.

14. Ayoub, G.M., "Buoyant Jets in a Co-flowing Current; and Experimental Investigation," Grenoble, Soc. Hydro-Techn. de France, 1972, Document R22.

15. Baines, W.D., and Turner, J.S., "Turbulent Buoyant Convection from a Source in a Confined Region," J. Fluid Mechanics, vol. 37, 1969, pp. 51-80.

16. Baldwin, R.C., "A Dispersion Model for Heated Effluent from an Ocean Outfall," M.Sc. Thesis, Naval Postgraduate School, April 1970.

17. Barr, D., "Densimetric Exchange Flow in Rectangular Channels - III Large Scale Experiments," LaHouille Blanche, vol. 6, 1967, pp. 619-632.

18. Barry, R.F., and Hoffman, D.P., "Computer Model for Thermal Pollution," Proceedings, ASCE, vol. 98, no. PO1, June 1972, pp. 117-132.

19. Baumgartner, D.J., and Trent, D.S., "Ocean Outfall Design Part I: Literature Review and Theoretical Development," U.S. Dept. of Interior, Federal Water Quality Administration, 1970, 127 pp.

20. Baumgartner, D.J., Trent, D.S., and Byram, K.V., "User's Guide and Documentation for Outfall Plume Model," Environmental Protection Agency, Pacific Northwest Water Laboratory, Working Paper #80, May 1971, 29 pp.

21. Becker, H.A., Hottel, H.C., and Williams, G.C., "The Nozzle-Fluid Concentration Field of the Round, Turbulent, Free Jet," J. Fluid Mechanics, vol. 30, no. 2, 1967, pp. 285-303.

22. Benedict, B.A., Polk, E.M., Jr., Yandell, E.L., Jr., and Parker, F.L., "Surface Jet and Diffusion Models for Discharge of Heated Water," Proc., 14th Congress IAHR, Paris, 1971, vol. 1, Paper A 22, pp. 183-190.

23. Bourodimos, E.L., "Turbulent Transfer and Mixing of Submerged Heated Water Jet," Water Resources Research, vol. 8, no. 4, August 1972, pp. 982-997.

24. Brady, D.K., Groves, W.L., and Geyer, J.C., "Surface Heat Exchange of Power Plant Cooling Lakes," Johns Hopkins University, Department of Environmental Engineering, Report No. 5, 1969.

25. Braun, W., and Goldstein, M.E., "Analysis of the Mixing Region for a Two-dimensional Jet Injected at an Angle into a Moving Stream," NASA Technical Note D-5531, Nov. 1969.

26. Briggs, G.A., "Plume Rise," USAEC Division of Technical Information, 1969, 81 pp.

27. Bringfelt, B., "A Study of Buoyant Chimney Plumes in Neutral and Stable Atmospheres," Atmospheric Environment, vol. 3, 1969, pp. 609-623.

28. Bringfelt, B., "Plume Rise Measurements at Industrial Chimneys," Atmospheric Environment, vol. 2, 1968, pp. 575-598.

29. Brock, R.R., "Power Law Solutions for Vertical Plumes," J. Hydraulics Division, ASCE, vol. 96, no. HY9, Sept. 1970, pp. 1803-1817.

30. Brooks, N.H., "Diffusion of Sewage Effluent in an Ocean Current," Proceedings, 1st International Conference on Waste Disposal in the Marine Environment, Pergamon Press, 1960.

31. Brooks, N.H., Discussion of paper, "The Mechanics of Thermally Stratified Flow," by D.R.F. Harleman, Proc., National Symposium on Thermal Pollution (1968), Vanderbilt University Press, Nashville, Tenn., 1969, pp. 165-172.

32. Brooks, N. H., "Lecture Notes on Conceptual Design of Submarine Outfalls," University of California, Berkeley, Water Resources Engineering Educational Series, Program VII, Pollution of Coastal and Estuarine Waters, Jan. 29-30, 1970 (Part I, 25 pp., Part II, 12 pp.). Available as Tech. Memos 70-1 and 70-2, W.M.Keck Laboratory of Hydraulics and Water Resources, California Institute of Technology, Pasadena, California.

33. Brooks, N.H., "Thermal Power-New Crisis for the Environment," Proc., Symposium on Water Environment and Human Needs, Ralph M. Parsons Laboratory, MIT, October 1970, pp. 146-177.

34. Brooks, N.H., "Dispersion in Hydrologic and Coastal Environments," W.M.Keck Laboratory of Hydraulics and Water Resources, California Institute of Technology, Pasadena, California, Report No. KH-R-29, December 1972.

35. Brooks, N.H., and Koh, R.C.Y., "Selective Withdrawal from Density-Stratified Reservoirs," J. Hydraulics Division, ASCE, vol. 95, no. HY4, July 1969, pp. 1369-1400. (Also in Proceedings, ASCE Specialty Research Conference on "Current Research into the Effects of Reservoirs on Water Quality," Portland, Oregon, Jan. 22-24, 1968, published by Vanderbilt University, Dept. of Environmental and Water Resources Engineering, Technical Report No. 17, pp. 169-214.)

36, Bryce, J.B., and Elliott, R.V., "Thermal Plume Measurements in Lake Ontario and Resulting Phenomenological Model," Proc., International Symposium on Stratified Flows, International Association for Hydraulic Research, Novosibirsk, 1972.

37. Carter, H.H., "Characteristics of a Heated Jet Discharged Horizontally into a Transverse Current," Johns Hopkins University, Chesapeake Bay Institute, Technical Report No. 61, 1969.

38. Cederwall, K., "Dispersion Phenomena in Coastal Waters," John Freeman Memorial Lecture, J. of Boston Society of Civil Engineers, vol. 57, no. 1, 1970, pp. 34-70.

39. Cederwall, K., Discussion of, "Horizontal Surface Discharge of Warm Water Jets," Proceedings, ASCE, vol. 97, no. PO1, 1971, pp. 229-234.

40. Cederwall, K., "A Buoyant Slot Jet into Stagnant or Flowing Environment," W.M. Keck Laboratory of Hydraulics and Water Resources, Report No. KH-R-25, March 1971, 86 pp.

41. Cederwall, K., "Float Diffusion Study," Water Research, vol. 5, Nov. 1971, pp. 889-907. (Also W.M. Keck Laboratory of Hydraulics and Water Resources, Tech. Memo 71-1, April 1971.)

42. Cederwall, K., "Dimensional Considerations Applied to Some Diffusion Problems," Sartryck ur Vatten, Feb. 1972, pp. 137-151. (Also Symposium on "The Physical Processes Responsible for the Dispersal of Pollutants in the Sea with Special Reference to the Nearshore Zone", Denmark, 1972.)

43. Colon, F., and Leavitt, J., "Lake Norman Hydrothermal Model Study," Alden Research Laboratory, Worcester Polytechnic Institute, Progress Report No. 1, 1973.

44. Coudert, Jean F., "A Numerical Solution of the Two-Dimensional Diffusion Equation in a Shear Flow," W.M. Keck Laboratory of Hydraulics and Water Resources, Tech. Memo 70-7, June, 1970, 38 pp.

45. Csanady, G.T., "Dispersal of Effluents in the Great Lakes," Water Research, vol. 4, 1970, pp. 79-114.

46. Csanady, G.T., "Bent-over Vapor Plumes," J. of Applied Meteorology, vol. 10, 1971, pp. 36-42.

47. Csanady, G.T., "Coastal Entrapment in Lake Huron," Proceedings, 5th International Water Pollution Research Conference, San Francisco, July-August 1970, Paper III, 7 pp.

48. Ditmars, J.D., "Computer Program for Round Buoyant Jets into Stratified Ambient Environments," W.M. Keck Laboratory of Hydraulics and Water Resources, California Institute of Technology, Pasadena, California, Tech. Memo 69-1, March 1969, 27 pp.

49. Ditmars, J.D., "Mixing of Density-Stratified Impoundments with Buoyant Jets," W.M. Keck Laboratory of Hydraulics and Water Resources, Report No. KH-R-22, Sept. 1970, 203 pp.

50. Dornhelm, R., Nouel, M., and Weigel, R.L., "Velocity and Temperature in Buoyant Surface Jet," Proceedings, ASCE, vol. 98, no. PO1, June 1972, pp. 29-47.

51. Edinger, J.E., and Polk, E.M., "Initial Mixing of Thermal Discharges into a Uniform Current," Vanderbilt University, Department of Environmental Engineering, Report No. 1, October 1969.

52. Ellison, T.H., and Turner, J.S., "Turbulent Entrainment in Stratified Flows," J. of Fluid Mechanics, vol. 6, 1959, pp. 423-448.

53. El Mahgary, Y.S., "Thermal Diffusion of the Warm Water of Power Plants into a Sea Basin," Proc., 14th Congress IAHR, Paris, 1971, vol. 1, Paper A 40, pp. 333-340.

54. Fan, L.N., "Turbulent Buoyant Jets into Stratified or Flowing Ambient Fluids," W.M. Keck Laboratory of Hydraulics and Water Resources, California Institute of Technology, Pasadena, California, Report No. KH-R-15, 1967.

55. Fan, L.N., and Brooks, N.H., "Numerical Solutions of Turbulent Buoyant Jet Problems," W.M. Keck Laboratory of Hydraulics and Water Resources, California Institute of Technology, Pasadena, California, Report No. KH-R-18, 1969.

56. Fay, J.A., Escudier, M., and Hoult, D.P., "A Correlation of Field Observations of Plume Rise," J. Air Pollution Control Association, vol. 20, no. 6, 1970, pp. 391-397.

57. Fay, J.A., "Buoyant Plumes and Wakes," Annual Review of Fluid Mechanics, vol. 5, 1973, pp. 151-160.

58. Fischer, H.B., and Brooks, N.H., "Technical Aspects of Waste Disposal in the Sea Through Submarine Outlets," FAO Technical Conference on Marine Pollution and Its Effects on Living Resources and Fishing, Rome, Paper FIR: MP/8-/R-4, 16 pp.

59. Fox, D.G., "Forced Plume in a Stratified Fluid," J. Geophysical Research, vol. 75, no. 33, 1970, pp. 6818-6835.

60. Geyer, J.C., Edinger, J.E., Brady, D.K., and Graves, W.L., "Field Sites and Survey Methods Used in the Study of Heat Dissipation from Steam Electric Condenser Discharges," Research Project RP-4, Report No. 3, 1968.

61. Giles, W., et al., "A Thermal Effluent Analysis for Electric Power Generating Plants," General Electric Company, Document No. 71SD257, 1971.

62. Gunwaldsen, R.W., Brodfield, B., and Hecker, G.E., "Cooling Water Structures for FitzPatrick Nuclear Plant," Proceedings, ASCE, vol. 97, no. PO4, Proc. Paper 8572, Dec. 1971, pp. 767-781.

63. Gustafson, B., and Larsen, I., "Jet Diffusion in Stagnant Stratified Waters," Water Research, vol. 4, no. 5, May 1970, pp. 353-361.

64. Hansen, J., and Schroeder, H., "Horizontal Jet Dilution Studies by Use of Radioactive Isotopes," Acta Polytechnical Scandinavica, Civil Engineering and Building Construction Series, no. 49, Copenhagen, 1968, 23 pp.

65. Harleman, D.R.F., "Submerged Diffusers in Shallow Coastal Waters," Presented at Coastal Zone Pollution Management Symposium, Charleston, S.C., February, 1972, 19 pp.

66. Harleman, D.R.F., "Thermal Stratification due to Heated Discharges," Proc., International Symposium on Stratified Flows, International Association of Hydraulic Research, Novosibirsk, 1972.

67. Harleman, D.R.F., Hall, L., and Curtis, T., "Thermal Diffusion of Condenser Water in a River During Steady and Unsteady Flows," Hydrodynamics Laboratory, Massachusetts Institute of Technology, Report No. 111, 1968.

68. Harleman, D.R.F., Jirka, G., and Stolzenbach, K.D., "A Study of Submerged Multi-port Diffusers for Condenser Water Discharge with Application to the Shoreham Nuclear Power Station," Ralph M. Parsons Laboratory, MIT, Report No. 139, July 1971, 121 pp.

69. Harleman, D.R.F., Jirka, G., Adams, E., and Watanabe, M., "Investigation of a Submerged, Slotted Pipe Diffuser for Condenser Water Discharge, from the Canal Plant, Cape Cod Canal," Ralph M. Parsons Laboratory, MIT, Report No. 141, October 1971, 58 pp.

70. Harleman, D.R.F., and Stolzenbach, K.D., "Fluid Mechanics of Heat Disposal from Power Generation," Annual Review of Fluid Mechanics, vol. 4, 1972, pp. 7-32.

71. Harleman, D.R.F., (ed.), "Engineering Aspects of Heat Disposal from Power Generation," Ralph M. Parsons Laboratory, MIT Summer Session, June 26-30, 1972, approx. 800 pp.

72. Harleman, D.R.F., Jirka, G., and Evans, D.H., "Experimental Investigations of Submerged Multi-port Diffusers for Condenser Water Discharge," Ralph M. Parsons Laboratory, MIT, Report No. 165, 1973.

73. Hayashi, T., "Dynamical Similitude on the Diffusion of Warm Water Jet Discharged Horizontally at Water Surface," Proc., U.S.-Japan Seminar on Similitude in Fluid Mechanics, Sept. 21-28, 1967, pp. 71-74.

74. Hayashi, T., "Turbulent Buoyant Jets of Effluent Discharged Vertically Upwards from an Orifice in a Cross-Current in the Ocean," Proc., 14th Congress IAHR, Paris, 1971, vol. 1, Paper A 19, pp. 137-166.

75. Hecker, G., Brodfeld, B., and Gunwaldsen, R., "Engineering and Ecological Studies for Design of Intake and Discharge Structures: James A. FitzPatrick Nuclear Power Plant," Stone & Webster Engineering Co., January 1970.

76. Hetsroni, G., and Sokolov, M., "Distribution of Mass, Velocity and Intensity of Turbulence in a Two-Phase Turbulent Jet," J. of Applied Mechanics, ASME, vol. 38E, no. 2, June 1971, pp. 315-327.

77. Hewett, T.A., Fay, J.A., and Hoult, D.P., "Laboratory Experiments of Smokestack Plumes in a Stable Atmosphere," Atmospheric Environment, vol. 5, Sept. 1971, pp. 767-789. (Also MIT, Fluid Mechanics Laboratory, Publ. 70-9, 1970.)

78. Hill, B.J., "Measurement of Local Entrainment Rate in the Initial Region of Axisymmetric Turbulent Air Jets," J. of Fluid Mechanics, vol. 51, part 4, 1972, pp. 773-779.

79. Hinze, J.O., Turbulence, McGraw-Hill, Series in Mechanical Engineering, 1959.

80. Hirst, E.A., "Analysis of Round, Turbulent, Buoyant Jets Discharged to Flowing Stratified Ambients," Oak Ridge National Laboratory, ORNL-4685, June 1971, 37 pp.

81. Hirst, E.A., "Analysis of Buoyant Jets Within the Zone of Flow Establishment," Oak Ridge National Laboratory, ORNL-TM-3470, August 1971, 41 pp.

82. Hirst, E.A., "Buoyant Jets Discharged to Quiescent Stratified Ambients," J. of Geophysical Research, vol. 76, no. 30, Oct. 20, 1971, pp. 7375-7383.

83. Hirst, E.A., "Zone of Flow Establishment for Round Buoyant Jets," Water Resources Research, vol. 8, no. 5, October 1972, pp. 1234-1246.

84. Hirst, E.A., "Buoyant Jets with Three-Dimensional Trajectories," J. Hydraulics Division, ASCE, vol. 98, no. HY11, Nov. 1972, pp. 1999-2014.

85. Holly, F.M., Jr., and Grace, J.L., Jr., "Model Study of Dense Jet in Flowing Fluid," J. Hydraulics Division, ASCE, vol. 98, no. HY11, Nov. 1972, pp. 1921-1933.

86. Hoult, D.P., Fay, J.A., and Forney, L.J., "A Theory of Plume Rise Compared with Field Observations," J. Air Pollution Control Association, vol. 19, 1969, pp. 585-590.

87. Hoult, D.P., and Weil, J.C., "Turbulent Plume in a Laminar Cross Flow," Atmospheric Environment, vol. 6, 1972, pp. 513-531. (Also MIT, Fluid Mechanics Laboratory, Publ. 70-8, 1970.)

88. Jain, S.C., Sayre, W.W., Akeyampong, Y.A., McDougall, D., and Kennedy, J.F., "Model Studies and Design of Thermal Outfall Structures, Quad-Cities Nuclear Plant," IIHR Report no. 135, University of Iowa, Sept. 1971, 101 pp.

89. Jen, Y., and Wiegel, R.L., "Surface Discharge of Horizontal Warm Jet," Proceedings, ASCE, vol. 92, no. PO2, April 1966, pp. 1-30.

90. Jirka, G., and Harleman, D.R.F., "The Mechanics of Submerged Multiport Diffusers for Buoyant Discharges in Shallow Water," Ralph M. Parsons Laboratory, MIT, Report No. 169, March 1973.

91. Keulegan, G.H., "Model Laws for Coastal Estuarine Models," Ch. 17 of Estuary and Coastline Hydrodynamics, McGraw-Hill, New York, 1966, pp. 691-710.

92. Koh, R.C.Y., and Fan, L.N., "Mathematical Models for the Prediction of Temperature Distributions Resulting from the Discharge of Heated Water into Large Bodies of Water," EPA, Water Quality Office, Report 16130 DWO 10/70, October 1970, 219 pp.

93. Koh, R.C.Y., "On Buoyant Jets," Proc., 14th Congress IAHR, Paris, 1971, vol. 1, Paper A 18, pp. 145-156.

94. Koh, R.C.Y., "Two-Dimensional Surface Warm Jets," J. Hydraulics Division, ASCE, vol. 97, no. HY6, June 1971, pp. 819-836.

95. Koh, R.C.Y., "Viscous Stratified Flow Towards a Sink," J. of Fluid Mechanics, vol. 24, part 3, 1966, pp. 555-575.

96. Krystantos, R., "The Turbulent Jet from a Series of Holes in Line," Aeronautical Quarterly, vol. 15, no. 1, 1964, pp. 1-28.

97. Larsen, J., and Hecker, G., "Design of Submerged Diffusers and Jet Interaction," ASCE National Water Resources Engineering Meeting, Jan. 24-28, 1972, Atlanta, Georgia, Meeting preprint 1614, 24 pp.

98. Larsen, J., and Hecker, G., "Hydrothermal Model Studies for Roseton Generating Station," Alden Research Laboratory, Worcester Polytechnic Institute, April, 1972.

99. Liseth, P., "Mixing of Merging Buoyant Jets from a Manifold in Stagnant Receiving Water of Uniform Density," Hydraulic Engineering Laboratory, University of California, Berkeley, Report HEL 23-1, Nov. 1970.

100. List, E.J., "Laminar Momentum Jets in a Stratified Fluid," J. of Fluid Mechanics, vol. 45, part 3, 1971, pp. 561-574.

101. List, E.J., and Imberger, J., "Turbulent Entrainment in Buoyant Jets and Plumes," J. Hydraulics Division, ASCE, vol. 99, no. HY9, 1973, pp. 1461-1474.

102. Ljatkher, V.M., "Hydrothermal Modeling and Design of Density Flows in Cooling Systems of Thermal and Nuclear Power Plants," Proceedings, International Symposium on Stratified Flows, International Association for Hydraulic Research, Novosibirsk, 1972.

103. Long, R.R., "Some Aspects of Turbulence in Stratified Fluids," Department of Mechanics and Earth and Planetary Sciences, The Johns Hopkins University, Technical Report No. 1, Series C, 1972.

104. Mahajan, B.M., and John, J.E.A., "Mixing of Shallow Submerged Heated Water Jet with an Ambient Reservoir," AIAA Journal, vol. 2, no. 11, 1971, pp. 2135-2140.

105. Marciano, J.J., and Harbeck, G.E., "Mass Transfer Studies," Water Loss Investigation: Lake Hefner Technical Report, U.S.G.S., Professional Paper 269, 1954.

106. Margason, R.J., "The Path of a Jet Directed at Large Angles to a Subsonic Free Stream," NASA Technical Note D-4919, 1968.

107. Maxwell, W.H.C., "Flux Development Region in Submerged Jets," J. Engineering Mechanics Division, ASCE, vol. 96, no. EM6, 1970, pp. 1061-1079.

108. Maxwell, W.H.C., and Pazwash, H., "Boundary Effects on Jet Flow Patterns Related to Water Quality and Pollution Problems," WRC Research Report no. 28, University of Illinois, Jan. 1970, 84 pp.

109. Maxworthy, T., "Experimental and Theoretical Studies of Horizontal Jets in a Stratified Fluid," Proc., International Symposium on Stratified Flows, International Association for Hydraulic Research, Novosibirsk, 1972.

110. Mih, W.C. and Hoopes, J.A., "Mean and Turbulent Velocities for Plane Jet," J. Hydraulics Division, ASCE, vol. 98, no. HY7, July, 1972, pp. 1275-1294.

111. Morton, B.R., "The Choice of Conservation Equations for Plume Models," J. of Geophysical Research, vol. 76, no. 30, 1971, pp. 7409-7416.

112. Morton, B.R., Taylor, G.I., and Turner, J.S., "Turbulent Gravitational Convection from Maintained and Instantaneous Sources," Proc. Roy. Soc. London, A234, 1956, pp. 1-23.

113. Motz, L.H., and Benedict, B.A., "Heated Surface Jet Discharged Into a Flowing Ambient Stream," U. S. Environmental Protection Agency, 16130 FDQ 03/71, March 1971, 207 pp.

114. Motz, L.H., and Benedict, B.A., "Surface Jet Model of Heated Discharges," J. Hydraulics Division, ASCE, vol. 98, no. HY1, Jan. 1972, pp. 181-199.

115. Muraoka, K., "Turbulent Diffusion of Free Jet by Tracer Test," Osaka University Technology Report No. 971, October 1970, pp. 809-822.

116. Murota, A., and Muraoka, K., "Turbulent Diffusion of a Vertically Upward Jet," Proceedings, 13th Congress, International Association for Hydraulic Research, Fort Collins, Colorado, 1964.

117. Neale, L.C., and Hecker, F.E., "Model Versus Field Data on Thermal Plumes from Power Stations," Proc., International Symposium on Stratified Flows, International Association for Hydraulic Research, Novosibirsk, 1972.

118. Parker, F.L., and Krenkel, P.A., "Thermal Pollution: Status of the Art," Department of Environmental and Water Resources Engineering, Vanderbilt University, 1969.

119. Pearce, A.F., "Critical Reynolds Number for Fully Developed Turbulence in Circular Submerged Water Jets," National Mechanical Engineering Research Institute, C.S.I.R. Report MET 475, Pretoria, South Africa, 1966.

120. Phillips, O.M., The Dynamics of the Upper Ocean, Cambridge University Press, Cambridge, England, 1968.

121. Platten, J.L., and Keffer, J.F., "Entrainment in Deflected Axisymmetric Jets at Various Angles to the Stream," University of Toronto Mechanical Engineering Department, UTME-TP-6808, 1968, 51 pp.

122. Platten, J.L., and Keffer, J.F., "Deflected Turbulent Jet Flows," J. Applied Mechanics, ASME, vol. 38E, no. 4, Dec. 1971, pp. 756-758.

123. Policastro, A.J., and Tokar, J.V., "Heated-Effluent Dispersion in Large Lakes: State of the Art of Analytical Modeling. Part I: Critique of Model Formulations," Argonne National Laboratory, ES-11, January 1972, 374 pp.

124. Pratte, B.D., and Baines, W.D., "Profiles of the Round Turbulent Jet in a Cross Flow," J. Hydraulics Division, ASCE, vol. 93, no. HY6, 1967, pp. 53-64.

125. Pritchard, D.W., "Modeling of Heated Discharges . . . A Lecture," Westinghouse School for Environmental Management, CSU, Fort Collins, Colorado, June 25, 1970.

126. Pritchard, D.W., and Carter, H.H., "Design and Siting Criteria for Once-through Cooling Systems Based on a First Order Thermal Plume Model," Johns Hopkins University, Chesapeake Bay Institute, Technical Report No. 75, 1972, 51 pp.

127. Prych, E.A., Discussion of "Numerical Studies of Unsteady Dispersion in Estuaries," by D.R.F. Harleman, Chok Hung Lee, and L.C. Hall, J. of Sanitary Engineering Division, ASCE, vol. 95, no. SA5, October 1969, pp. 959-964.

128. Prych, E.A., "Effects of Density Differences on Lateral Mixing in Open Channel Flows," W.M. Keck Laboratory of Hydraulics and Water Resources, California Institute of Technology, Pasadena California, Report No. KH-R-21, 1970.

129. Prych, E.A., "A Warm Water Effluent Analyzed as a Buoyant Surface Jet," Sveriges Meteorologiska Och Hydrologiska Institut, Serie Hydrologi, Nr. 21, Stockholm, 1972.

130. Quirk, Lawler and Matesby Engineers, New York Mohawk Power Co., "Nine Mile Point Nuclear Power Station," Vol. II, Appendix A, Hydraulic Model Study of Thermal Discharge - Acres American Incorporated, Buffalo, New York, February 1973.

131. Rao, K.V., "The Buoyant Plume Model Above a Heat Source," Atmospheric Environment, vol. 4, 1970, pp. 557-575.

132. Riesbol, H.S., and Wend, F.H., "Thermal-Hydraulic Study-Arkansas Cooling Reservoir," Proceedings, ASCE National Water Resources Engineering Conference, Memphis, Tennessee, January 1970.

133. Robideau, R.F., "The Discharge of Submerged Buoyant Jets Into Water of Finite Depth," General Dynamics, Electric Boat Division, Groton, Conn., Report No. U440-72-121, Nov. 1972, 57 pp.

134. Rouse, H., "Gravitational Diffusion From a Boundary Source in Two-Dimensional Flow," J. Applied Mechanics, ASME, Sept. 1947, pp. A225-A228.

135. Rouse, H., Yih, C.S., and Humphreys, H.W., "Gravitational Convection from a Boundary Source," Tellus, vol. 4, 1952, pp. 201-210.

136. Rumer, R.R., and Hoopes, J.A., "Modeling Great Lakes Circulation," Proc., Symposium on Water Environment and Human Needs, Parsons Water Resources and Hydrodynamics Laboratory, MIT, Oct. 1970, pp. 212-247.

137. Rumer, R.R., Jr., "Internal Seiches and Interfacial Mixing in Stratified Lakes," W.M. Keck Laboratory of Hydraulics and Water Resources, California Institute of Technology, Pasadena, California, Tech. Memo 71-3, July 1971, 39 pp.

138. Rumer, R.R., Jr., "Interfacial Wave Breaking in Stratified Liquids," J. Hydraulics Division, ASCE, vol. 99, no. HY3, March 1973, pp. 509-524.

139. Sami, S., Carmody, T., and Rouse, H., "Jet Diffusion in the Region of Flow Establishment," J. Fluid Mechanics, vol. 27, no. 2, 1967, pp. 231-252.

140. Sayre, W.W., and Parr, A.D., "Performance of the Diffuser Pipe System for Discharging Condenser Cooling Water at the Quad-Cities Nuclear Power Station, September 1972-January 1973," IIHR Report No. 15, University of Iowa, June 1973.

141. Schmidth, W., "Turbulente Ausbreitung eines Stromes erhitzter Luft," Zeitschr. Angew, Math. und Mech., vol. 21, 1941, pp. 265-278 and 351-363.

142. Schwartz, J., and Tulin, M.P., "Chimney Plumes in Neutral and Stable Surroundings," Atmospheric Environment, vol. 6, no. 1, Jan. 1972, pp. 19-36.

143. Senshu, S., and Wada, A., "Thermal Diffusion of Cooling Water Into the Stratified Sea Basin," Proc., 11th Congress IAHR, Leningrad, 1965.

144. Silberman, E., "Warm Water Discharges Into Lakes and Reservoirs," Proc., International Symposium on Stratified Flows, International Association for Hydraulic Research, Novosibirsk, 1972.

145. Sharp, J.J., "Physical Interpretation of Jet Dilution Parameters," J. Sanitary Engineering Division, ASCE, vol. 94, no. SA1, Feb. 1968, pp. 55-64.

146. Sharp, J.J., "Spread of Buoyant Jets at the Free Surface," J. Hydraulics Division, ASCE, vol. 95, no. HY3, May 1969, pp. 811-825.

147. Sharp, J.J., "Unsteady Spread of Buoyant Surface Discharge," J. Hydraulics Division, ASCE, vol. 97, no. HY9, September 1971, pp. 1471-1492.

148. Shirazi, M.A., and Davis, L.R., "Workbook of Thermal Plume Prediction, Vol. I, Submerged Discharge," U.S. Environmental Protection Agency, Report No. EPA-R2-72-005a, August 1972, 228 pp.

149. Shirazi, M.A., "A Critical Review of Laboratory and Some Field Discharge Data on Surface Jet Discharge of Heated Water," National Thermal Pollution Research Program, PNERL Working Paper, Environmental Protection Agency, 1973.

150. Shuto, N., "Buoyant Plume in a Cross Stream," Coastal Engineering in Japan, vol. XIV, December 1971, pp. 163-173.

151. Silberman, E., and Stefan, H., "Physical (Hydraulic) Modeling of Heat Dispersion in Large Lakes," St. Anthony Falls Hydraulic Laboratory, University of Minnesota, Project Report No. 115, 1970.

152. Slawson, P.R., and Csanady, G.T., "The Effect of Atmospheric Conditions on Plume Rise," J. of Fluid Mechanics, vol. 47, part 1, 1971, pp. 33-49.

153. Sonnichsen, J.C., "Lateral Spreading of Heated Discharge," Proceedings, ASCE, vol. 97, no. PO3, July 1971, pp. 623-630.

154. Sotil, C.A., "Computer Program for Slot Buoyant Jets Into Stratified Ambient Environments," W.M. Keck Laboratory of Hydraulics and Water Resources, California Institute of Technology, Pasadena, California, Tech. Memo 71-2, June 1971, 35 pp.

155. Stefan, H., "Modeling Spread of Heated Water Over Lake," Proceedings, ASCE, vol. 96, no. PO3, June 1970, pp. 469-482.

156. Stefan, H., "Stratification of Flow From Channel Into Deep Lakes," J. Hydraulics Division, ASCE, vol. 96, no. HY7, 1970, pp. 1417-1434.

157. Stefan, H., "Dilution of Buoyant Two-Dimensional Surface Discharges," J. Hydraulics Division, ASCE, vol. 98, no. HY1, 1972, pp. 71-86.

158. Stefan, H., "Spread and Dilution of Three-Dimensional Rectilinear Heated Water Surface Jets," Proc., International Symposium on Stratified Flows, International Association for Hydraulic Research, Novosibirsk, 1972.

159. Stefan, H., and Schiebe, F.R., "Heated Discharge from Flume Into Tank," J. Sanitary Engineering Division, ASCE, vol. 96 no. SA6, 1970, pp. 1415-1433.

160. Stefan, H., and Hayakawa, "Mixing Induced by an Internal Hydraulic Jump," Water Resources Bulletin, vol. 8, no. 3, 1972, pp. 531-545.

161. Stefan, H., and Vaidyaraman, P., "Jet Type Model for the Three-Dimensional Thermal Plume in a Crosscurrent and under Wind," Water Resources Research, vol. 8, no. 4, 1972, pp. 998-1014.

162. Stephens, N.T., and McCaldin, R.O., "Attenuation of Power Station Plumes as Determined by Instrumented Aircraft," Environmental Science and Technology, 1971, pp. 615-621.

163. Stolzenbach, K.D., and Harleman, D.R.F., "An Analytical and Experimental Investigation of Surface Discharges of Heated Water," Ralph M. Parsons Laboratory, MIT, Report No. 135, 1971, 212 pp.

164. Stolzenbach, K.D., Adams, E., and Harleman, D.R.F., "A User's Manual for Three-Dimensional Heated Surface Discharge Computations," Ralph M. Parsons Laboratory, MIT, Report No. 156, 1972.

165. Stolzenbach, K.D., and Harleman, D.R.F., "Physical Modeling of Heated Discharges," Chapter 10, Engineering Aspects of Heat Disposal From Power Generation, Ralph M. Parsons Laboratory, MIT Summer Session, June 26-30, 1972.

166. Sullivan, P.J., "Some Data on the Distance-Neighbour Function for Relative Diffusion," J. Fluid Mechanics, vol. 47, part 3, 1971, pp. 601-607.

167. Sullivan, P.J., "Longitudinal Dispersion Within a Two-Dimensional Turbulent Shear Flow," J. of Fluid Mechanics, vol. 49, part 3, 1971, pp. 551-576.

168. Sullivan, P.J., "The Penetration of a Density Interface by Heavy Vortex Rings," Water, Air, and Soil Pollution, vol. 1, no. 3, 1972, pp. 322-336.

169. Sundaram, T.R., Eastbrook, C.C., Piech, K.R., and Rudinger, G., "An Investigation of the Physical Effects of Thermal Discharges Into Cayaga Lake (Analytical Study)," Cornell Aeronautical Laboratory, Inc., CAL No. VT-2616-0-2, November 1969.

170. Sundaram, T.R., and Wu, J., "Wind Effects on Thermal Flumes in Water Bodies," Proceedings, Meeting of Applied Mechanics Division, ASCE, Atlanta, Georgia, June 1973.

171. Tamai, N., Wiegel, R.L., and Tormberg, G.I., "Horizontal Surface Discharge of Warm Water Jets," Proceedings, ASCE, vol. 95, no. PO2, 1969, pp. 253-276.

172. Telford, J.W., "Convective Plumes in a Convective Field," J. Atmospheric Sciences, vol. 27, no. 3, 1970, pp. 347-358.

173. Tennessee Valley Authority, "Full Scale Study of Plume Rise at Large Generating Stations," TVA, Division of Health and Safety, Muscle Shoals, 1968.

174. Thomas, F.W., Carpenter, S.F., and Colebaugh, W.C., "IV. Recent Results of Measurements, Plume Rise Estimates for Electric Generating Stations," Phil. Trans., Roy. Soc., London, Series A, 265, 1969, pp. 221-243.

175. Tokar, J.V., "Thermal Plumes in Lakes: Compilations of Field Experience," Argonne National Laboratory, Environmental Sciences, Argonne, Illinois, Report No. ES-3, August 1971, 170 pp.

176. Tollmien, W., "Strahlverbreiterung," Zeitschr. Angew, Math. and Mech., 1926, pp. 467-478.

177. Tomai, N., "Diffusion of Horizontal Buoyant Jet Discharged at Water Surface," Proc., 13th Congress IAHR, Kyoto, Japan, vol. 3, Paper C24, pp. 215-222.

178. Trent, D., "A Numerical Model for Predicting Energy Dispersion in Thermal Plumes Issuing from Large, Vertical Outfalls in Shallow Coastal Water," Ph.D. Thesis, Oregon State University, June 1973.

179. Tsang, G., and Wood, I.R., "Motion of Two-Dimensional Starting Plume," J. Engineering Mechanics Division, ASCE, vol. 94, no. EM6, 1968, pp. 1547-1561.

180. Tsang, G., "Laboratory Study of Line Thermals," Atmospheric Environment, vol. 5, 1971, pp. 445-471.

181. Tsang, G., "Entrainment of Ambient Fluid by Two-Dimensional Starting Plumes and Thermals," Atmospheric Environment, vol. 6, 1972, pp. 123-132.

182. Wada, A., "A Study on Phenomena of Flow and Thermal Diffusion Caused by Outfall of Cooling Water," Proceedings, 10th Conference on Coastal Engineering, Tokyo, Japan, Paper No. 5-14, 1966.

183. Wada, A., "A Study of Mixing Process in the Sea Caused by Outfall of Industrial Waste Water," Coastal Engineering in Japan, vol. 13, 1969, pp. 147-158.

184. Wada, A., "Studies of Prediction of Recirculation of Cooling Water in a Bay," Proceedings, 11th Conference on Coastal Engineering, London, England, vol. II, 1968, pp. 1453-1471.

185. Wada, A., "Study of Thermal Diffusion in a Two-Layer Sea Caused by Outfalls of Cooling Water," Proc., International Symposium on Stratified Flows, International Association for Hydraulic Research, Novosibirsk, 1972.

186. Weil, J., "Mixing of a Heated Surface Jet in Turbulent Channel Flow," Hydraulic Engineering Laboratory, University of California, Berkeley, Waste Heat Management Report WHM-1, June 1972.

187. Wnek, W.J., and Fochtman, F.G., "Mathematical Model for Fate of Pollutants in Near-Shore Waters," Environmental Science and Technology, vol. 6, no. 4, 1972, pp. 331-337.

188. Wolanski, E., "Turbulent Entrainment Across Stable Density-Stratified Liquids and Suspensions," Ph.D. Thesis, The Johns-Hopkins University, 1972.

189. Wygnanski, I., and Fiedler, H., "Some Measurements in the Self-Preserving Jet," J. of Fluid Mechanics, vol. 32, part 2, 1968, pp. 577-612.

190. Yudelson, J.M., "A Survey of Ocean Diffusion Studies and Data," W.M. Keck Laboratory of Hydraulics and Water Resources, California Institute of Technology, Pasadena, California, Tech. Memo 67-2, 1967.

191. Zeller, R.W., Hooper, J.A., and Rohlich, G.A., "Heated Surface Jets in Steady Cross-current," J. Hydraulics Division, ASCE, vol. 97, no. HY9, 1971, pp. 1403-1426.

APPENDIX

SUMMARY OF PROGRESS REPORTS

A1. Introduction

During the course of the project, a variety of experiments were performed in the test basin, and in a special setup for testing port configurations. The purpose of this appendix is to present, in summary form, the results and findings for these tests. The details may be found in the seven progress reports* issued to Southern California Edison Company.

The subjects covered are as follows:

Section A2. Preliminary Tests —to determine the operational characteristics of thermal diffuser configurations, and to bracket the design variables (Progress Reports No. 1 and 2).

Section A3. Systematic Determination of Preliminary Design —to perform tests of 12 alternative configurations resulting in the selection of two 2500-ft diffusers (Progress Report No. 4).

Section A4. Sectional Model Tests — tests of a section of the preliminary design diffuser at a larger scale (1:50 undistorted) to determine the near field jet mixing at larger Reynolds numbers (Progress Report No. 5).

Section A5. Thermal Dispersion for the Existing Unit 1 at San Onofre —to determine the dispersion characteristics of Unit 1 and the question of recirculation between Unit 1 and the new Units 2 and 3 intakes in an undistorted model at a scale of 100:1 (Progress Report No. 6).

---

* See pg. 102 for detailed reference.

Section A6. Heat Treatment of Intakes — to obtain the thermal field resulting from the discharge of warm water during heat treatment of the new Units 2 and 3 intakes (Progress Report No. 7).

Section A7. Hydraulic Tests of Discharge Ports — to perform hydraulic tests of various special discharge nozzle configurations for both normal and reverse flow modes (Progress Report No. 3).

A2. Preliminary Tests *

The purpose of the preliminary tests summarized here was to bracket the design variables such as location and length of the diffusers. At the time of these tests four possible new Units (Units 2, 3, 4, and 5)** were modeled, although only 2 new units are currently planned for construction; nonetheless the arrangement adopted for Units 2 and 3 should not preclude two additional units at the same site in the future.

Two sets of four diffusers were tested: a) a set of shorter diffusers (2000 ft long) located at a depth range of 30 to 50 ft, and b) a set of longer diffusers (2500 ft and 3000 ft long) located at a depth range of 40 to 67 ft. The layouts of these diffusers in the model basin are shown in Figures A-1 and A-2. The modeling ratios and diffuser characteristics are summarized in Tables A-1 and A-2. It should be noted that the existing Unit 1 was included in the model basin for these tests.

The results from the experiments are shown summarized in Figures A-3 and A-4 where the maximum observed ΔT on the surface beyond 1000 ft from the discharge structures (expressed as a percentage of the source ΔT_o) are shown plotted versus current speed. Figure A-3 shows the results obtained with the four 2000 ft long diffusers. In this series of tests, only steady longshore currents were used. It is readily observed that the peak temperature excesses (including or excluding the region bounded by the 1000 ft limit) decreases with increasing currents. Two special tests were performed where only Units 1 through 3 were operating (i.e.,

---

* Progress Report No. 1, December 8, 1972 and Progress Report No. 2, January 26, 1973.

** See Figures A-1 and A-2.

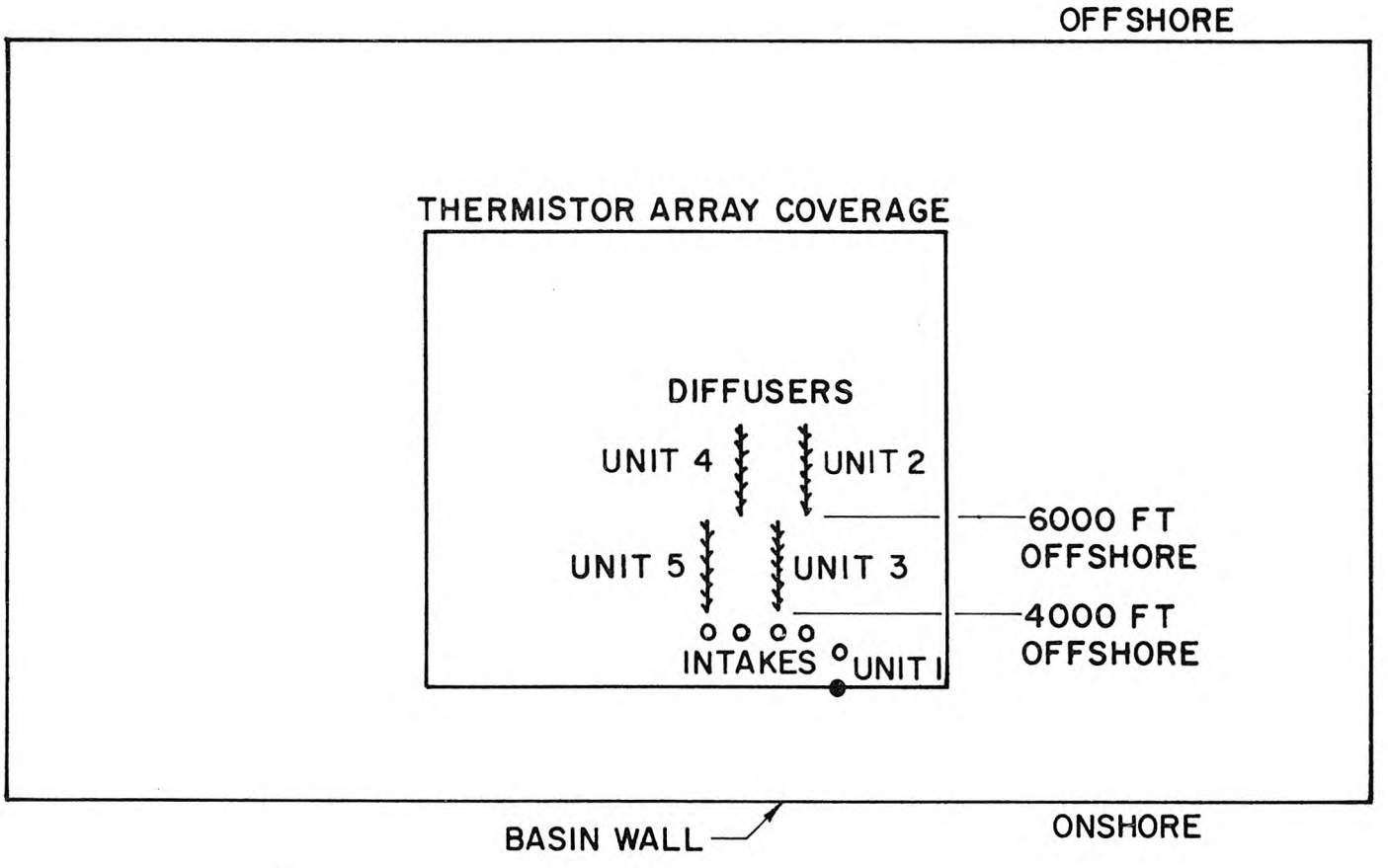

Figure A-1 Schematic of basin layout for first set of perpendicular-to-shore diffusers.

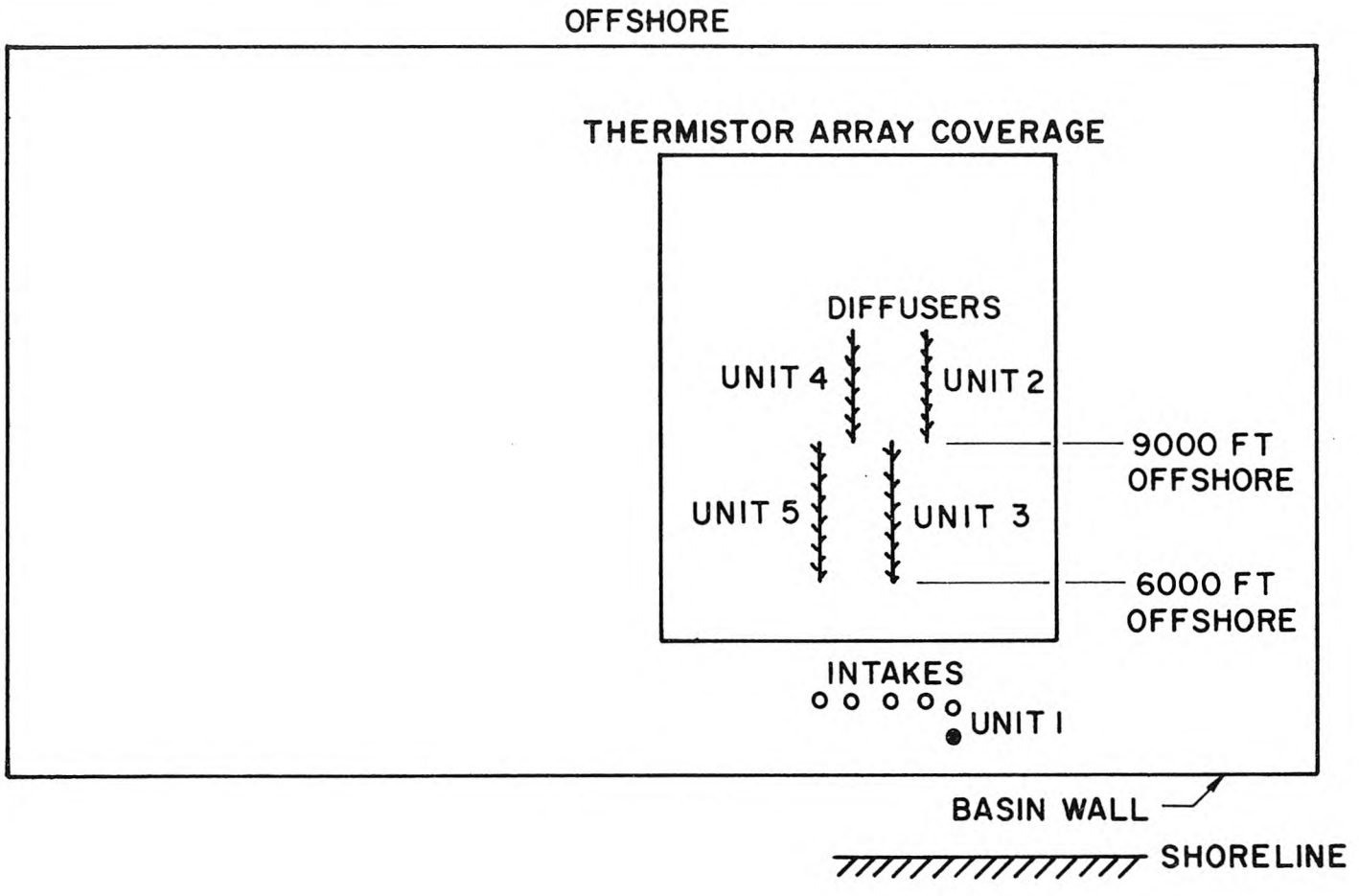

Figure A-2 Schematic of basin layout for second set of perpendicular-to-shore diffusers.

Table A-1

Model Ratios and Diffuser Characteristics for First Set of Perpendicular-to-Shore Diffusers

Model Ratios

	Prototype:Model
Length, horizontal	800:1
vertical	200:1
Density difference	0.68:1
Velocity	11.7:1
Time	68.6:1
Discharge	1.87×10^6:1

Diffuser Characteristics

	Model Diffusers	Prototype Diffusers
Length (nominal)	30 in.	2000 ft
Number of ports	15	60
Port spacing	2 in.	33.3 ft
Nozzle diameter	0.12 in.	24 in.
Jet velocity	0.84 fps	9.8 fps
Jet Reynolds number	1050	1.96×10^6
Nozzle angle up from horizontal	20°	20°
Nozzle angle with axis of diffuser pipe (in horizontal plane)	±20° (alternating)	±20° (alternating)
Elevation of the center of the nozzle above the sea floor	0.48 in.	8 ft

Table A-2

Model Ratios and Diffuser Characteristics for Second Set of Perpendicular-to-Shore Diffusers

Model Ratios

	Prototype:Model
Length, horizontal	800:1
vertical	200:1
Density difference	0.68:1
Velocity	11.7:1
Time	68.6:1
Discharge	1.87×10^6:1

Diffuser Characteristics

	Model Diffusers		Prototype Diffusers	
	Units 2 & 4	Units 3 & 5	Units 2 & 4	Units 3 & 5
Length	38 in.	46 in.	2533 ft	3067 ft
Number of ports	19	23	76	92
Port spacing	2 in.	2 in.	33.3 ft	33.3 ft
Nozzle diameter	0.093 in.	0.086 in.	18.6 in.	17.2 in.
Jet velocity	1.10 fps	1.07 fps	12.9 fps	12.5 fps
Jet Reynolds number	1066	959	2×10^6	1.8×10^6
Nozzle angle up from horizontal	20°	20°	20°	20°
Nozzle angle with axis of diffuser pipe (in horizontal plane)	±25° (alternating)	±25°	±25° (alternating)	±25°
Elevation of the center of the nozzle above the sea floor	0.36 in.	0.36 in.	6 ft	6 ft

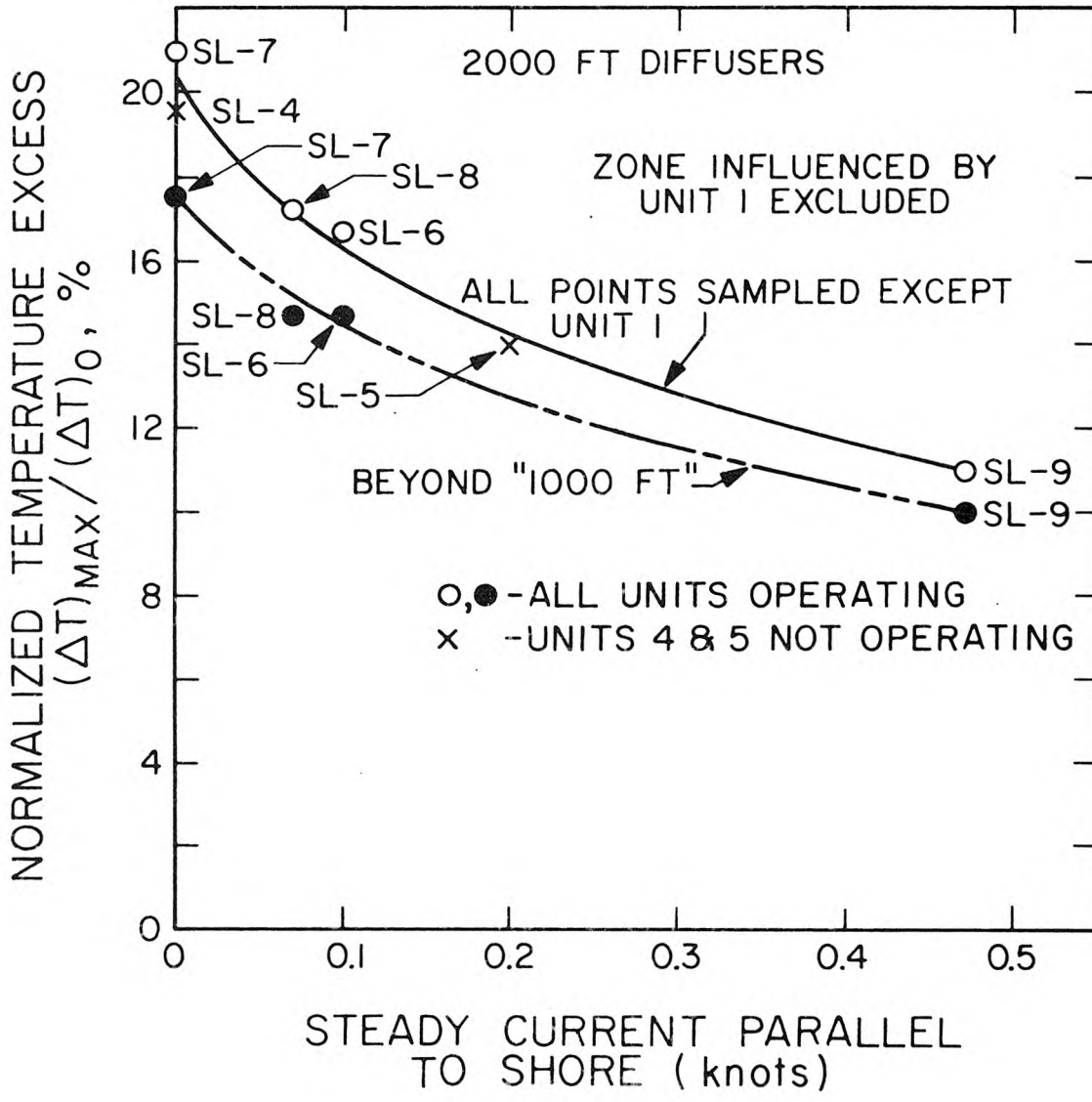

Figure A-3 Summary of experiments on 2000 ft long diffusers (all tests for five units except x which are for three units [1 through 3]).

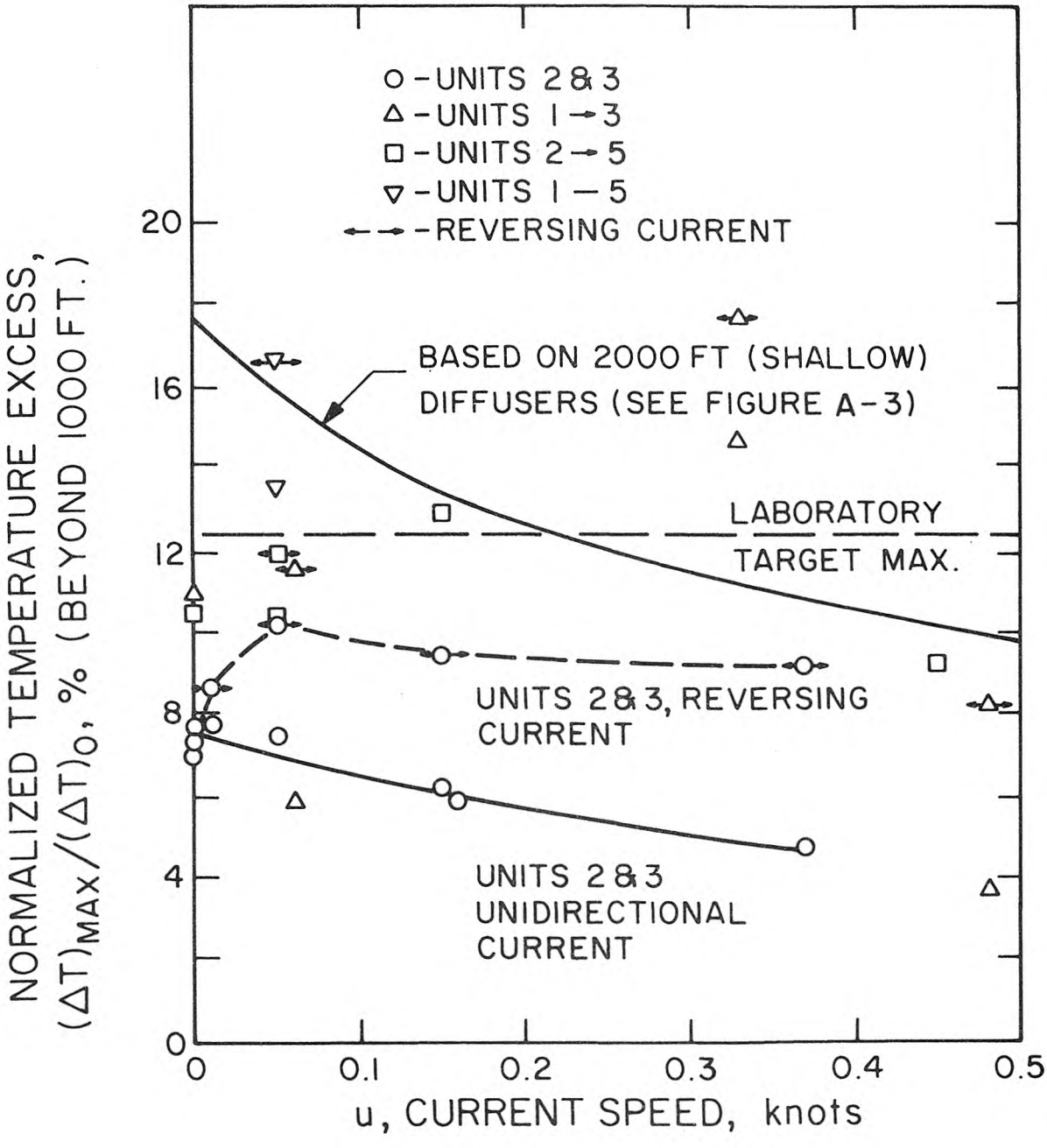

Figure A-4 Summary of experiments on 2500 ft/3000 ft long diffusers. (For reversing currents, speed plotted is the maximum during the cycle.)

Units 4 and 5 were turned off). These (shown as x in Figure A-3) did not exhibit any major difference from the case with 5 units (open circles). Figure A-4 shows the results obtained with the 2500 ft and 3000 ft diffusers (two each). In this figure only the maximum temperature excesses beyond 1000 ft from the discharge structures are shown. Both steady and reversing currents (prototype period = 18 hours) were tested and shown. Cases tested include those with two units (Units 2 and 3), three units (Units 1, 2, and 3), four units (Units 2, 3, 4, and 5) and five units (Units 1 through 5). The main conclusions drawn from these preliminary tests are that: 1) the shorter set of diffusers will not meet the laboratory target value of $\Delta T/\Delta T_o$= 12.5% (see Section 2.3), while the longer set will; and 2) the existing discharge (Unit 1) exerts a significant influence on the results.

A3. Systematic Determination of Preliminary Design *

Based on the results obtained in the preliminary tests discussed above, a systematic plan was devised to test the performance of Units 2 and 3 diffusers at various distances offshore and with several combinations of diffuser lengths. Unit 1 was excluded from these tests. Four of the model diffusers were chosen and installed in the model basin as shown in Figure A-5. The characteristics of the diffusers are detailed in Table A-3 where the model ratios used are also included. By activating only a neighboring pair of the four diffusers installed, it was possible to investigate three configurations of two diffusers as follows: **

1 2000 ft for Unit 2, 2500 ft for Unit 3

2 2500 ft for Unit 2, 2500 ft for Unit 3

3 2500 ft for Unit 2, 3000 ft for Unit 3

(It should be noted that in configuration 3 there is an overlap of 500 ft between the two diffusers.) Moreover by changing the water level in the basin, it was possible to simulate the operation of these diffusers at

---

* Progress Report No. 4, May 1, 1973.

** The lengths 2500 ft and 3000 ft are nominal inasmuch as the scaled lengths actually correspond to 2533 and 3067 ft respectively, because of the necessity to use an integral number of ports. We assume Unit 2 is always the offshore one, even though inverted in position in configuration 2.

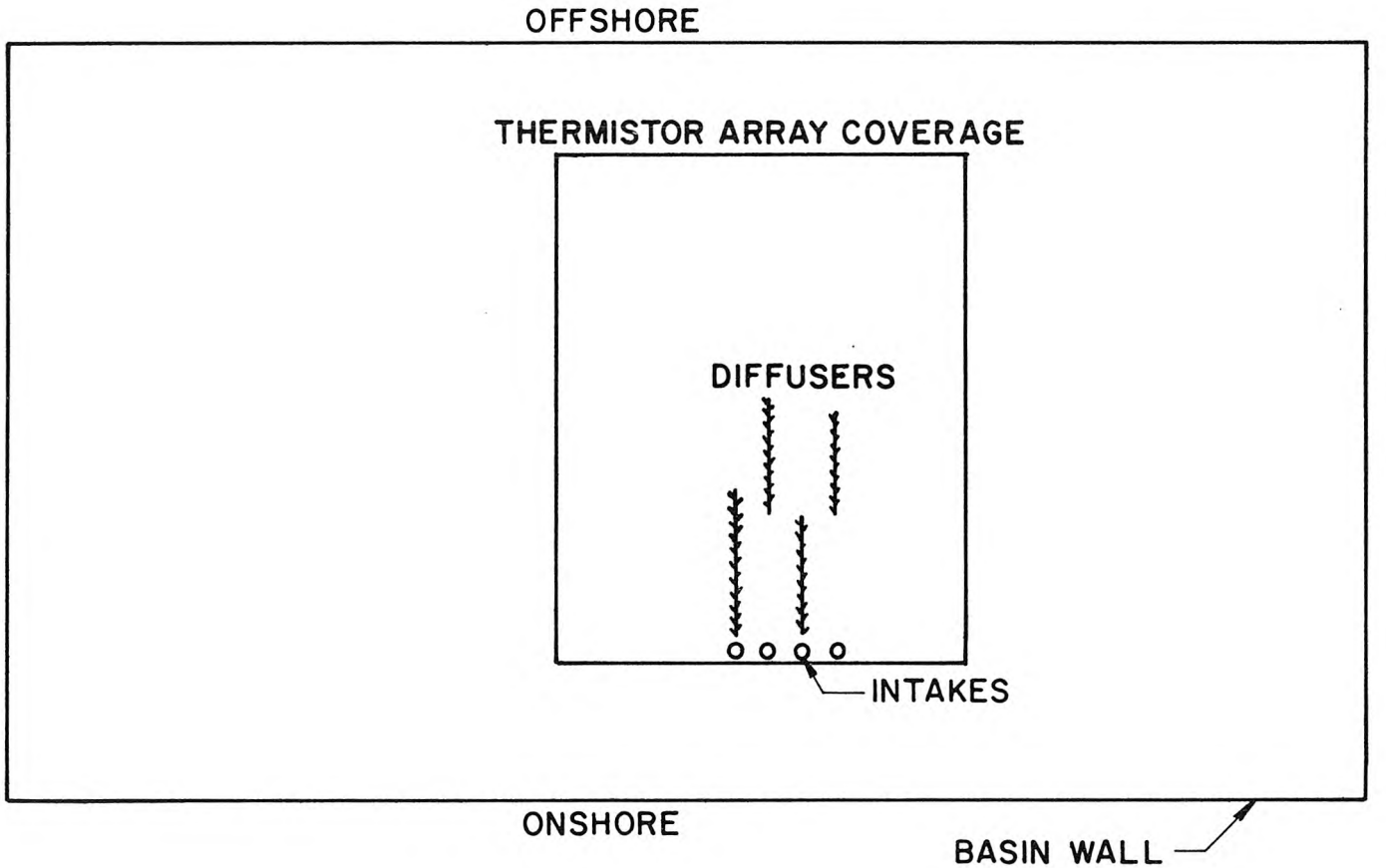

Figure A-5 Schematic of basin layout for systematic evaluation of diffuser performance described in detail in Progress Report No. 4.

Table A-3

Model Ratios and Diffuser Characteristics for

Systematic Evaluation of Perpendicular-to-Shore Diffusers

Model Ratios

	Prototype:Model
Length, horizontal	800:1
vertical	200:1
Density difference	0.68:1
Velocity	11.7:1
Time	68.6:1
Discharge	1.87×10^6:1

Diffuser Characteristics

	Model Diffusers			Prototype Diffusers		
Length (nominal)	30 in.	38 in.	46 in.	2000 ft	2533 ft	3067 ft
Number of ports	15	19	23	60	76	92
Port spacing	2 in.	2 in.	2 in.	33.3 ft	33.3 ft	33.3 ft
Nozzle diameter	0.12 in	0.093 in.	0.086 in.	24 in.	18.6 in.	17.2 in.
Jet velocity	0.84 fps	1.10 fps	1.07 fps	9.8 fps	12.9 fps	12.5 fps
Jet Reynolds Number	1050	1066	959	1.96×10^6	2.00×10^6	1.79×10^6
Nozzle angle up from horizontal	20°	20°	20°	20°	20°	20°
Nozzle angle with axis of diffuser pipe (in horizontal plane)	±20°	±25° (alternating)	±25°	±20°	±25° (alternating)	±25°
Elevation of the center of the nozzle above the sea floor	0.36 in.	0.36 in.	0.36 in.	6 ft	6 ft	6 ft

various distances offshore. Four cases were chosen as follows:

Designation	Prototype depth (ft) at first nozzle (nearest shore)	Approximate distance offshore (ft) to first nozzle (nearest shore)
N ("near")	30	3500
NM	35	4500
M ("medium")	40	5500
F ("far")	50	7500

In total, twelve combinations are possible — 4 distances offshore x 3 combinations of diffuser lengths. Experiments were performed on these various combinations under a variety of current conditions. In order to facilitate identification, a run number system was devised consisting of four to five characters. The first character(s) (N, NM, M, F) signifies the distance offshore. The first numeral (1, 2, 3) signifies the diffuser configuration and the remaining numerals serve to identify the sequential order of runs performed in the particular sequence.

The results of the forty-nine experiments (detailed in Progress Report No. 4) indicate that the N2 configuration (two 2500 ft long diffusers starting at approximately 3500 ft offshore) represents the most economical pair of diffusers which meets the laboratory target for the California thermal standards. Table A-4 shows the comparison of the performance among the various diffuser configurations under the conditions 0 and 0.05 knot ambient currents. Figures A-6 and A-7 show typical thermal distributions on the surface and in a vertical section for the N2 configuration.

The data obtained for the N2 configuration are shown summarized in Figures A-8 and A-9 where it may be seen that the peak temperature excesses measured beyond 1000 ft from the diffusers are below the 12.5% level set as the laboratory target. It may further be observed that for steady longshore current (Figure A-8), the peak value of ΔT beyond the 1000 ft limit decreases with increasing current magnitude, while for reversing current (Figure A-9), the peak value of ΔT beyond the 1000 ft limit is essentially independent of current amplitude, and occurs approximately at the time of slack current.

Table A-4

Comparison of Various Diffuser Configurations †

(Values shown are (F_{max}/R_{max}))

$F_{max} = (\Delta T/\Delta T_o)_{max}$ anywhere *

$R_{max} = (\Delta T/\Delta T_o)_{max}$ outside 1000 ft limit *

Diffuser Configuration \ Distance Offshore	N	NM	M	F
u = 0				
1	14.2/10.6	12.1/10.3	9.8/8.9	
2	14.2/11.7 12.4/ 9.0	10.6/10.3	8.3/7.5	
3	12.0/11.3	9.2/ 9.2	9.9/9.9	
u = 0.05 knot steady				
1	14.0/12.2	10.8/9.6	10.6/10.1	9.9/8.4
2	12.5/ 9.7	10.3/9.5	10.5/ 9.3	9.2/7.2
3	10.4/ 9.1	8.9/8.9	9.1/ 8.5	7.5/7.5
u = 0.05 knot reversing				
1	18.2/13.8	12.5/12.5	13.7/11.6	12.6/9.3
2	13.0/10.5	10.7/ 9.8	12.8/11.3	11.1/9.5
3	12.8/12.8	11.8/11.8	10.6/10.3	9.9/9.9

* Corrected for laboratory ambient temperature rise and difference in heat loss effect between model and prototype.

† Configurations defined on pages A-9 and A-12.

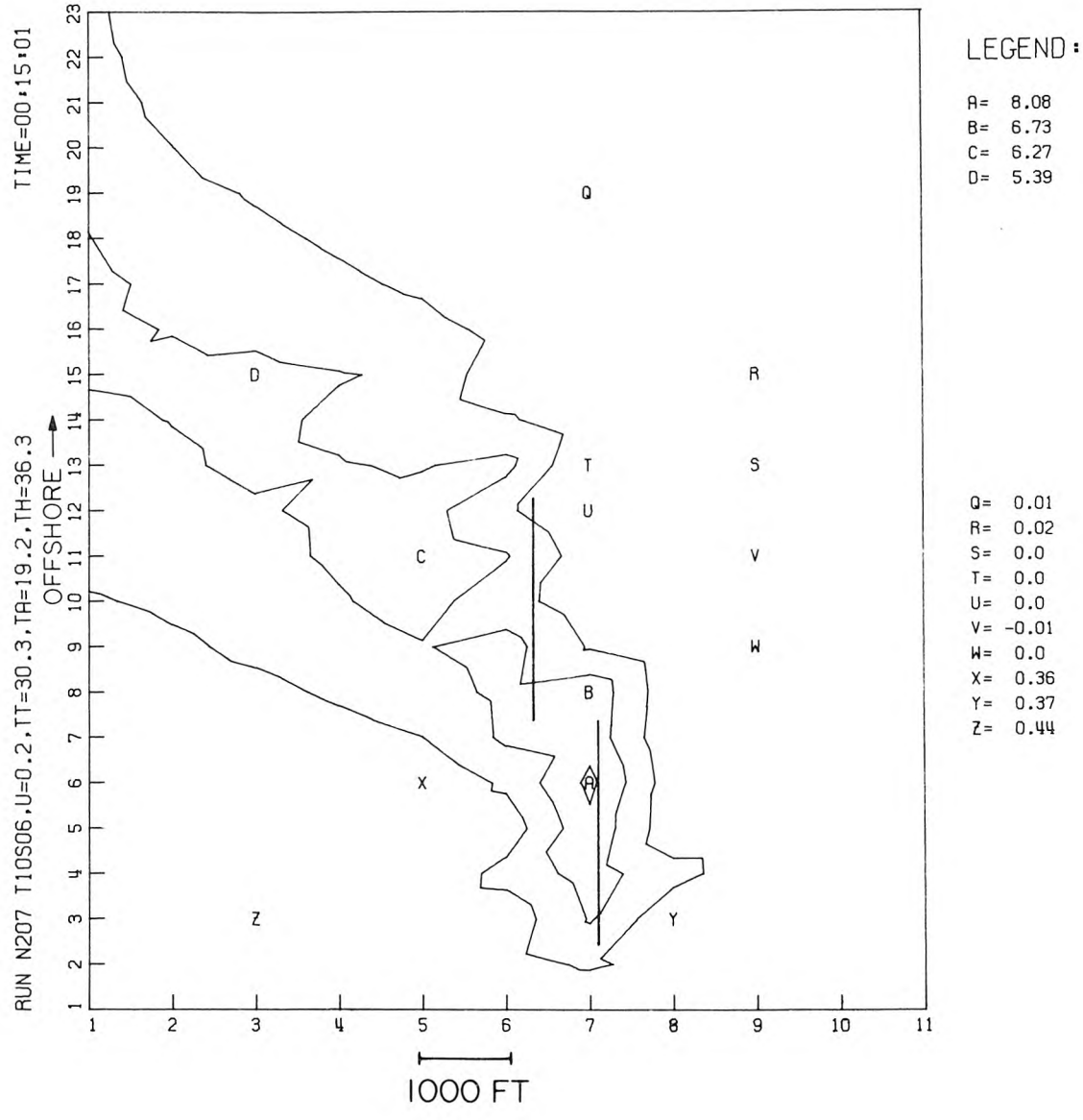

Figure A-6 Example surface thermal contour map obtained for configuration N2 in systematic evaluation tests (ambient current = 0.2 knots) [Progress Report No. 4].

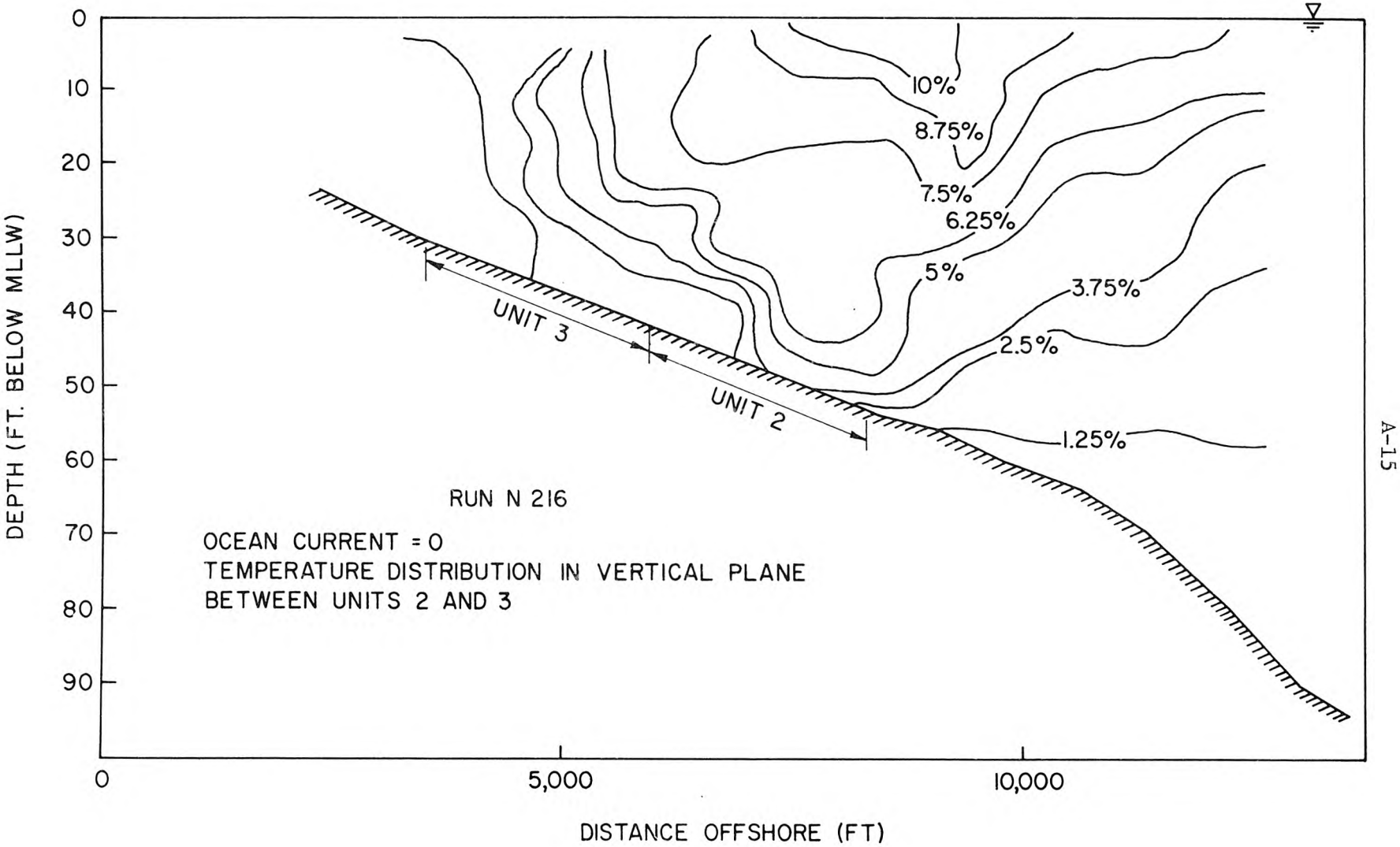

Figure A-7 Excess temperature distribution in vertical plane midway between and parallel to Units 2 and 3 (no ambient current) for N2 configuration.

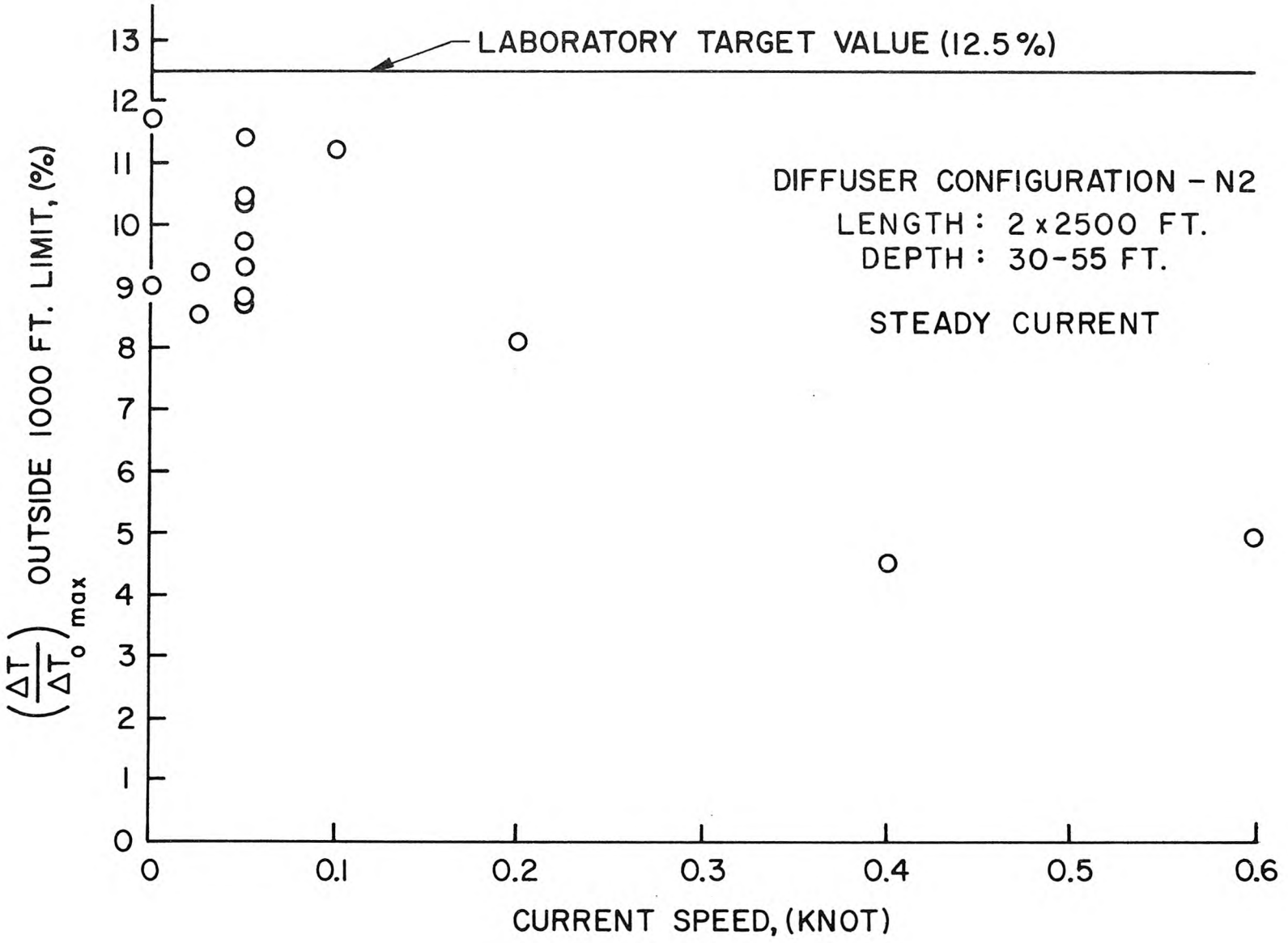

Figure A-8 Maximum surface excess temperature beyond 1000 ft limit under steady currents (from Progress Report No. 4).

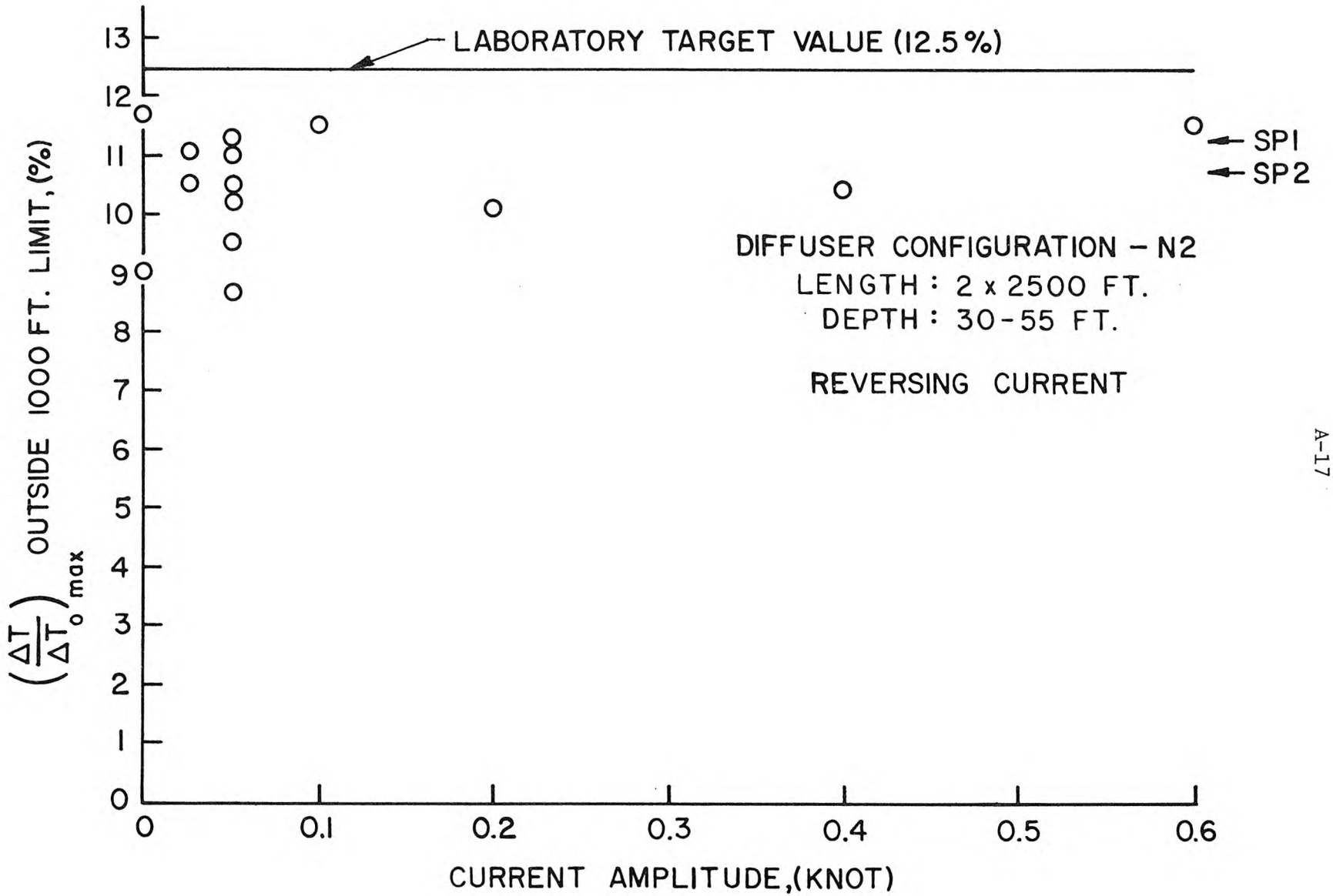

Figure A-9 Maximum surface excess temperature beyond 1000 ft limit under reversing currents (from Progress Report No. 4).

The offshore momentum generated by the discharge is found to be important (particularly for low or reversing ocean current) in ensuring that a drift current carries the diluted effluent offshore away from the diffusers. This drift current is estimated to be 0.1 to 0.2 knots based on the thermal patterns observed.

The main conclusion which was drawn from these experiments is that the N2 configuration diffusers were recommended for design. The diffusers finally adopted and tested in the confirming tests (reported in the main text of this report) are only slightly modified from the basic N2 configuration after due consideration had been given to other aspects of the design effort by the Southern California Edison Company. (See page 3.)

A4. Sectional Model Tests *

The hydraulic modeling of the diffusers, as described in Progress Report No. 4 was carried out in a 4:1 distorted model with a horizontal scale of 800:1 and a vertical scale of 200:1. In the confirming tests, reported in Chapter 5 of this report, the scales were practically the same (L_r = 787.5, y_r = 200, distortion 3.94:1). The tests were based on a condenser flow of 1850 cfs for each of the two units with a temperature rise of 20° F.

As a consequence of the relatively large scale ratios employed in those tests, the details of the diffusers were necessarily small, thus leading to diffuser jet Reynolds numbers barely into the turbulent regime of flow ($\sim$1000). Although the primary modeling parameter is the jet densimetric Froude number, it is important that the jet Reynolds number be sufficiently large if the jet dilutions are to be modeled correctly. In view of the rather marginal Reynolds number in the large scale ratio tests it was felt that confidence in the results of those tests could be reinforced if the dilution of the outfall diffuser jets was confirmed in a sectional model with a lower scale ratio, say, 50:1. At such a scale ratio the diffuser jets would be indisputably turbulent and, provided the modeling is according to Froude number similarity, the dilutions measured in the immediate neighborhood of the exit ports should be close to those actually occurring in the prototype. In order to accomplish

---

* Progress Report No. 5, July 16, 1973.

this purpose a 1/50th scale model (i.e., prototype to model scale ratio of 50:1) of a section of the diffuser incorporating six discharge ports was constructed. It was felt that with such a model the flow fields and dilutions in the neighborhood of any given discharge port could be investigated in some detail to a distance of approximately 100 jet diameters from the outfall. In this way a sufficiently accurate picture of the jet dilution would be obtained to enable confirmation of the dilutions obtained in the models of complete diffusers with much larger scale ratios.

However, the principal disadvantage of the sectional model is that it does not reproduce the overall circulation in the vicinity of the diffusers and intakes. Thus the results of these tests and the basin model tests of the full diffusers are not directly comparable. Since the overall flow of the warm water cloud tends to inhibit the inflow of cold diluting water along the bottom, the sectional model should show somewhat better mixing, apart from the scale effects discussed in the preceding paragraph.

A section of one of the 2500 ft long diffusers described in Section A3 (or in Progress Report No. 4) was constructed according to a scale ratio of 49.33:1 (nominally 50:1). This section of the diffuser contained six ports angled up from the horizontal at 20° and angled at 25° alternately to each side from the axis of the diffuser and was located in the test basin as shown in Figure A-10. The bottom configuration of the basin was rearranged to provide a section in which reasonable flow velocities could be maintained with the pumps available. The model and prototype details are summarized in Table A-5.

A series of eight experiments were performed for the case of steady currents varying from 0.0 to 0.2 knots. In these experiments, temperatures were measured along the vertical by means of a thermistor rake which was positioned sequentially at the nodes of a horizontal grid system around the location of the sectional diffuser. The overall measurements thus provide the assessment of the three-dimensional thermal field around the diffuser. The detailed results of this series of tests can be found in Progress Report No. 5.

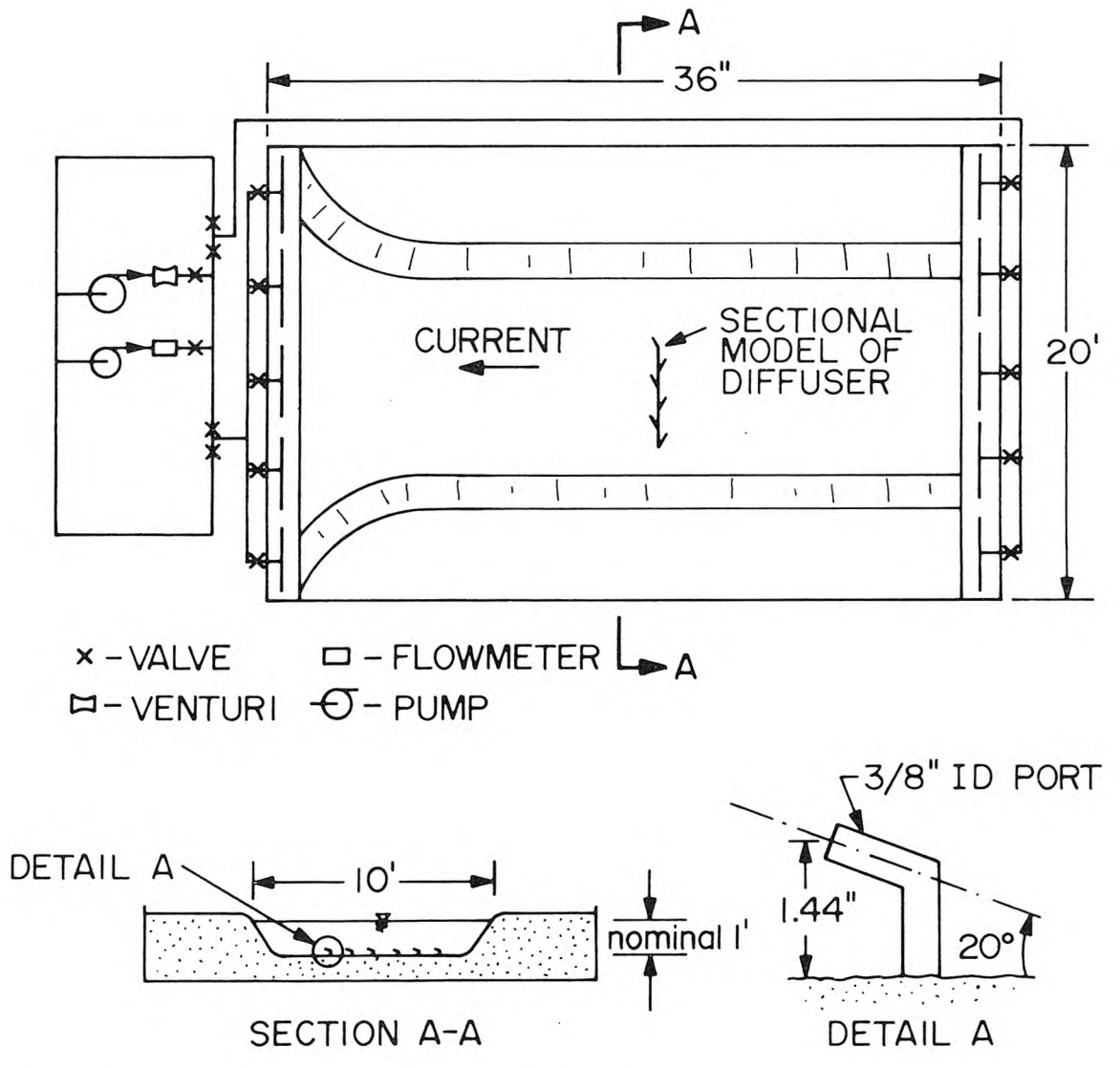

Figure A-10 Schematic of the laboratory test tank layout with sectional model of the diffuser used for cross-current flow tests.

Table A-5

Model and Prototype Variables Used in Sectional Tests

Variable	Prototype		Sectional Model
Nozzle diameter	18.5 in.		0.375 in.
Port spacing	33.33 ft		0.675 ft
Number of ports	76		6
Flow per port	24.34 cfs		0.00131 cfs *
Discharge velocity	13.04 ft/sec		1.71 ft/sec *
Ocean density (ρ)	1.025		0.9986
Density difference ($\Delta\rho$)	0.0028		0.00228 *
Density ratio ($\Delta\rho/\rho$)	0.0027		0.00228 *
Froude number	35.6		35.6
Reynolds number	2×10^6		6250
Length ratio		49.33	1
Velocity ratio		7.64	1
Time ratio		6.44	1
Discharge ratio		18640	1

* Nominal values; values varied for each test based on the precise density difference for that test.

Figure A-11 shows a summary of the experiments performed where it may be seen that the peak temperature increments at a distance of 120 ft from the diffuser ports will be in the range of 7.5 ±1.5% of ΔT_o, the temperature increment of the discharge, or 1.5 ±0.3°F for ΔT_o = 20°F. These results should be compared to the peak temperature range of 9.5 ±2% of ΔT_o (or 1.9° ±0.4°F) determined in the distorted model tests of the whole diffuser system.

The sectional model, therefore, clearly demonstrates that the jet mixing induced by the individual jets is fully capable of producing the dilutions implied by the basin model tests of the whole diffuser. The slightly larger ΔT's (smaller dilutions) observed in the full basin model probably result from the combined effects of 1) the overall flow pattern and interference, and 2) the lower jet Reynolds numbers.

No corrections in the basin model tests are believed to be necessary for the Reynolds number effect. Such an assumption is believed to be conservative. Therefore, a larger scale basin model is not considered necessary and would improve the accuracy by only about 1 or 2% of ΔT_o (or 0.2° to 0.4°F).

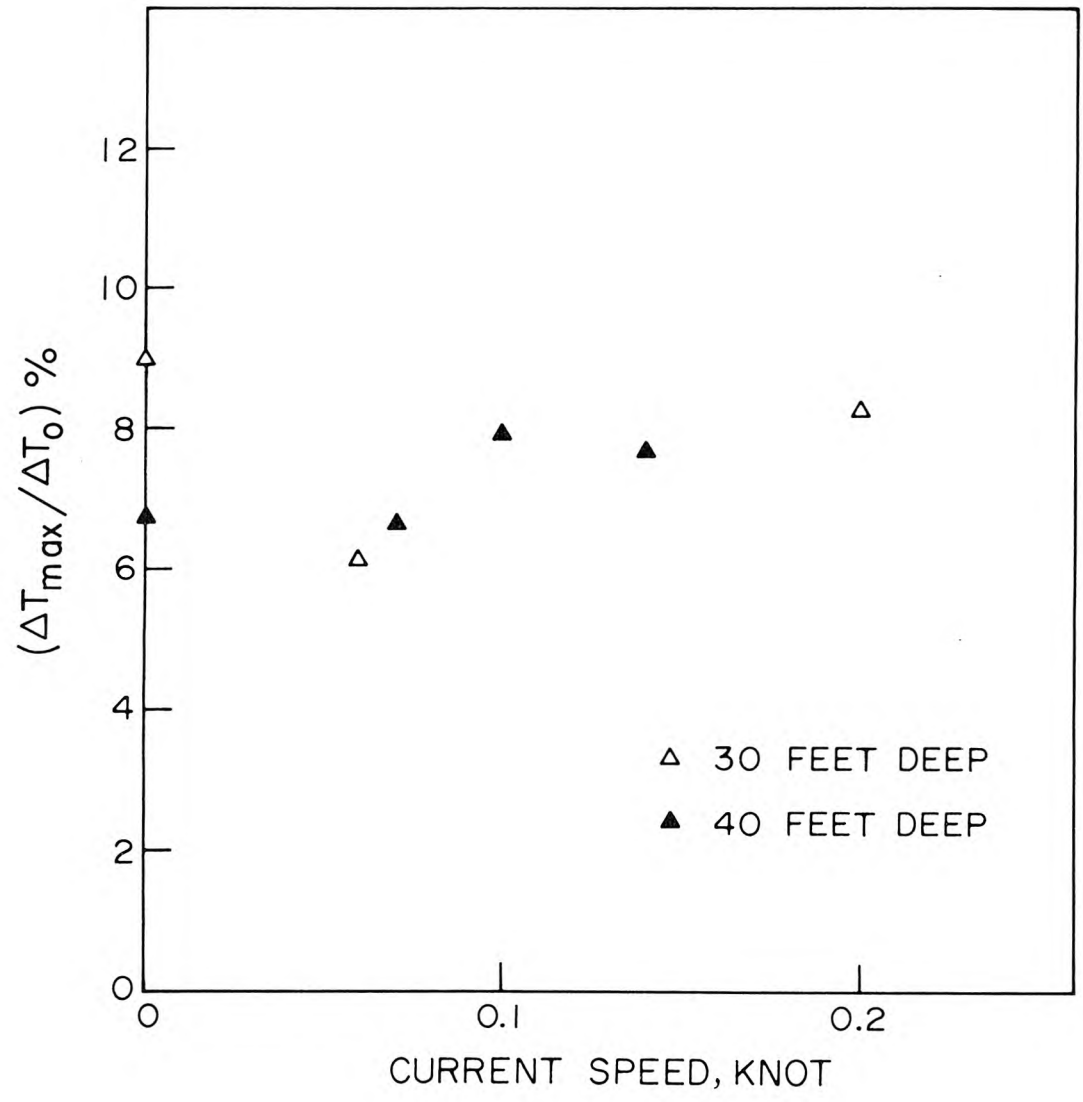

Figure A-11 Normalized maximum temperature, $\Delta T_{max}/\Delta T_o$, in percent recorded 120 feet perpendicular to the diffuser as a function of current speed. (ΔT_o is the temperature increment in the discharge.) [Sectional model tests.]

A5. Thermal Dispersion for the Existing Unit 1 at San Onofre *

A test program was also carried out to determine the heat dispersion due to the existing single point submerged discharge system of the existing Unit 1 at San Onofre (450 MW(e)). The purpose of this series of tests was two-fold. First it was desirable to simulate the operation of the existing Unit 1 discharge at an undistorted length scale of 100:1 in the 20 x 36 ft model basin in order to compare the results with field data and thus provide some verification data on the modeling techniques. Second, tests were performed to investigate the influence of Unit 1 on the performance of the new Units 2 and 3 when the latter are put into operation. In particular, the amount of recirculation between Unit 1 and the new Units 2 and 3 intakes was obtained.

Table A-6 summarizes the modeling ratios and pertinent data used in the tests. Figures A-12 through A-14 show the model details and the basin layout used.

Eleven experiments were conducted for the case when only the Unit 1 structures were operating at various steady currents with speeds from 0 to 0.5 knots. Further experiments were conducted where the Units 2 and 3 intakes were operated in their respective locations in the basin. The second series of tests were performed primarily to investigate the amount of recirculation to be expected between the Unit 1 discharge and the new intakes. To simulate the offshore drift current which would be generated by the Units 2 and 3 diffusers, special suction manifolds were installed at the offshore walls of the basin. The amount of offshore drift current was varied in an attempt to bracket the actual situation to be encountered.

Figure A-15 shows a photograph of the plume (made visible by dye) at $u = 0.27$ knot (prototype). Figure A-16 shows the surface thermal contours of the corresponding case while Figure A-17 shows vertical temperature profiles measured at several stations also for $u = 0.27$ knot.

---

* Progress Report No. 6, July 31, 1973.

Table A-6

Summary of Modeling Ratios and Parameters for Unit 1 Tests

Length ratio	100
Density difference ratio	1
Velocity ratio	10
Time ratio	10
Discharge ratio	10^5
Prototype discharge rate	315,000 gpm
Prototype density difference	0.0028 gm/ml
Prototype temperature difference	20°F

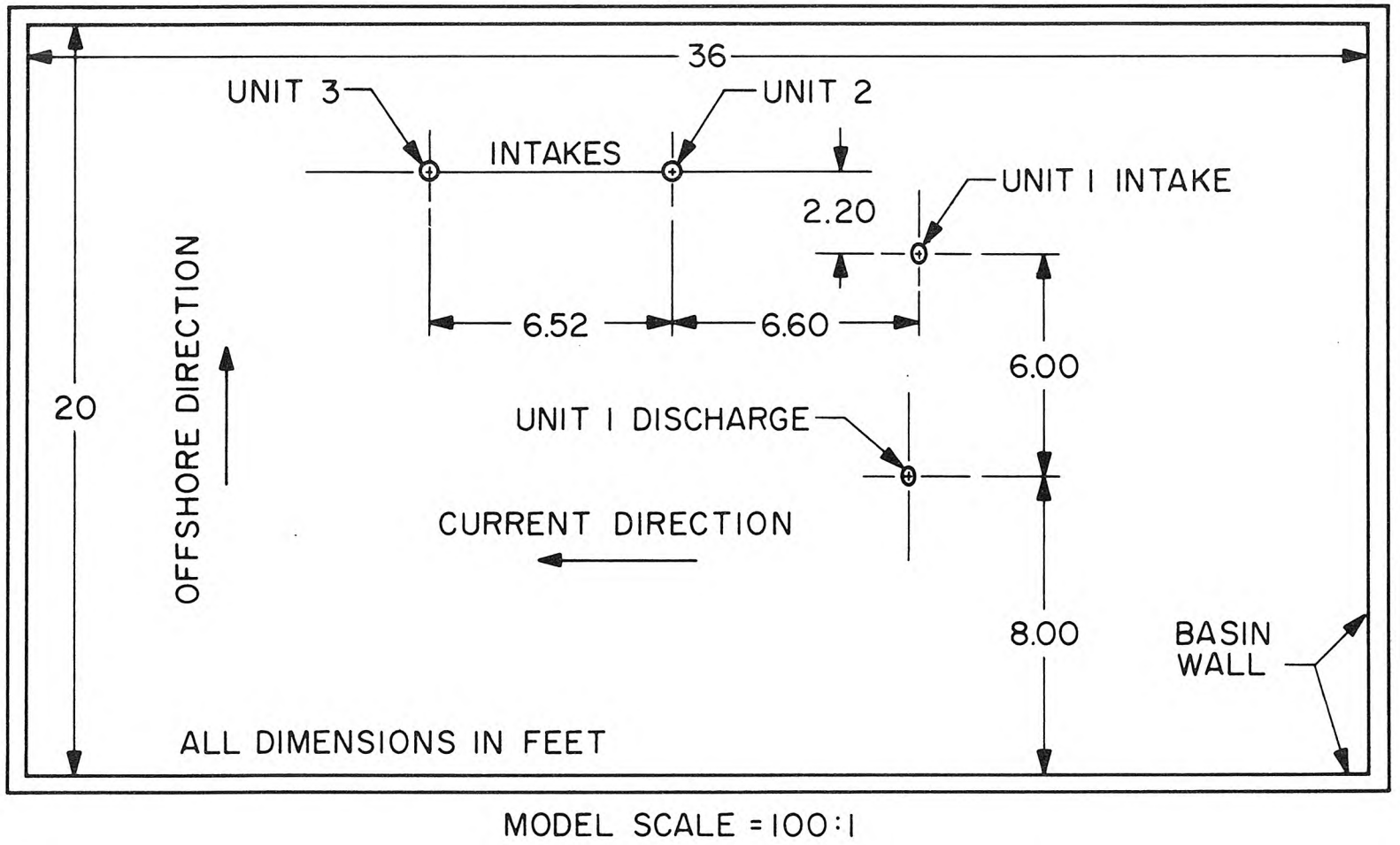

Figure A-12 Layout of test basin for modeling Unit 1 discharge.

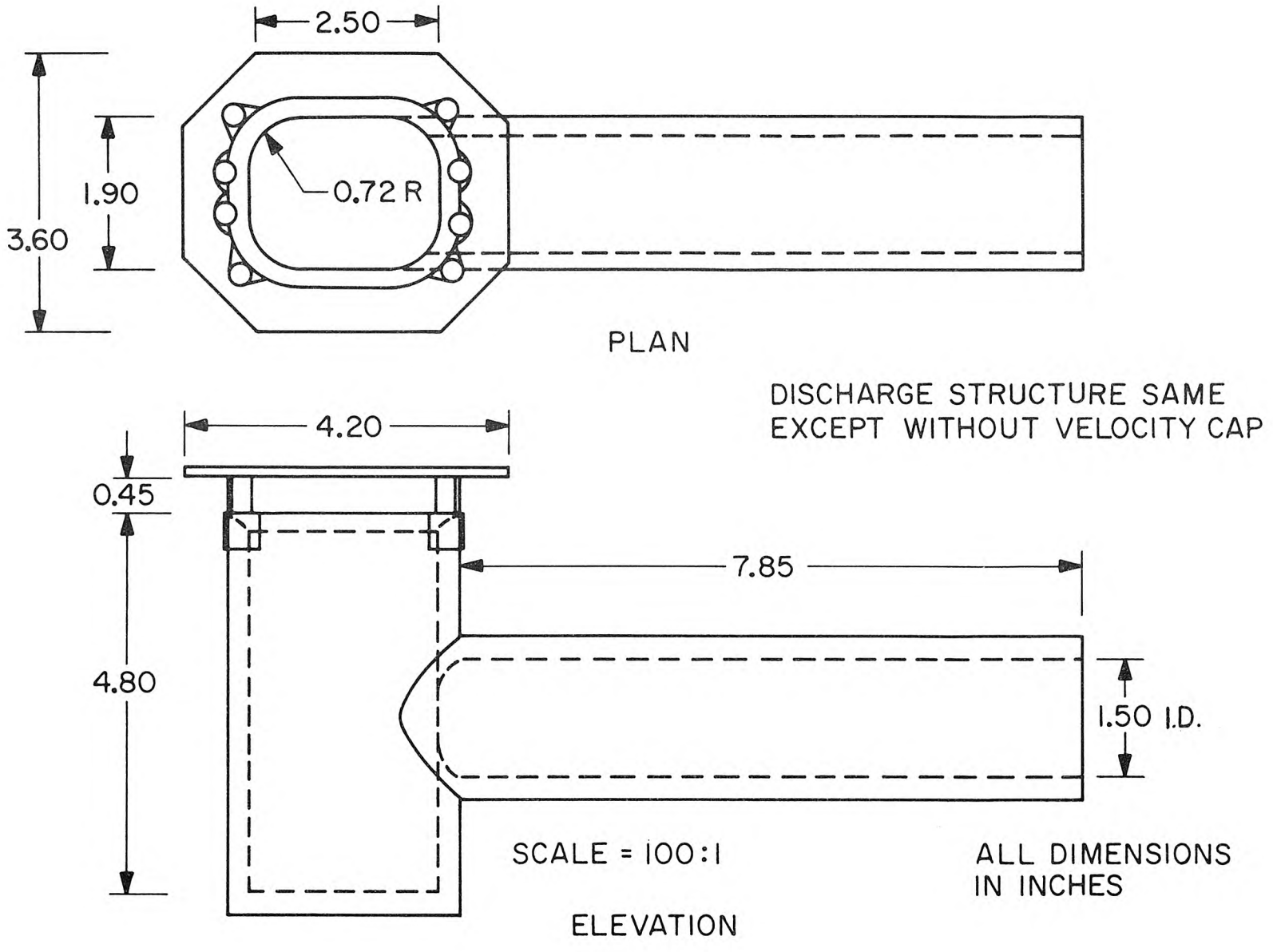

Figure A-13 Unit 1 discharge and intake models.

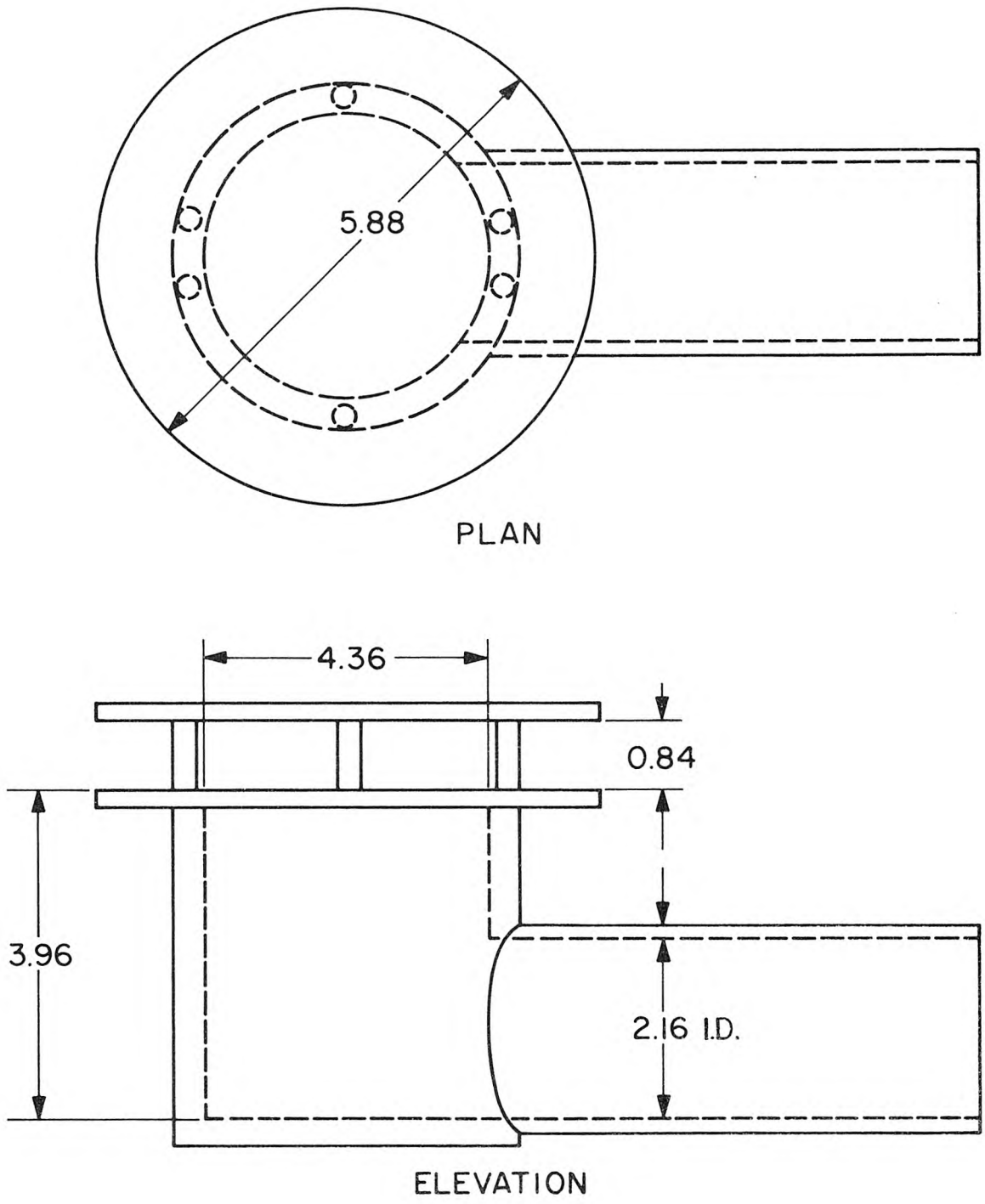

Figure A-14 Units 2 and 3 intake models.

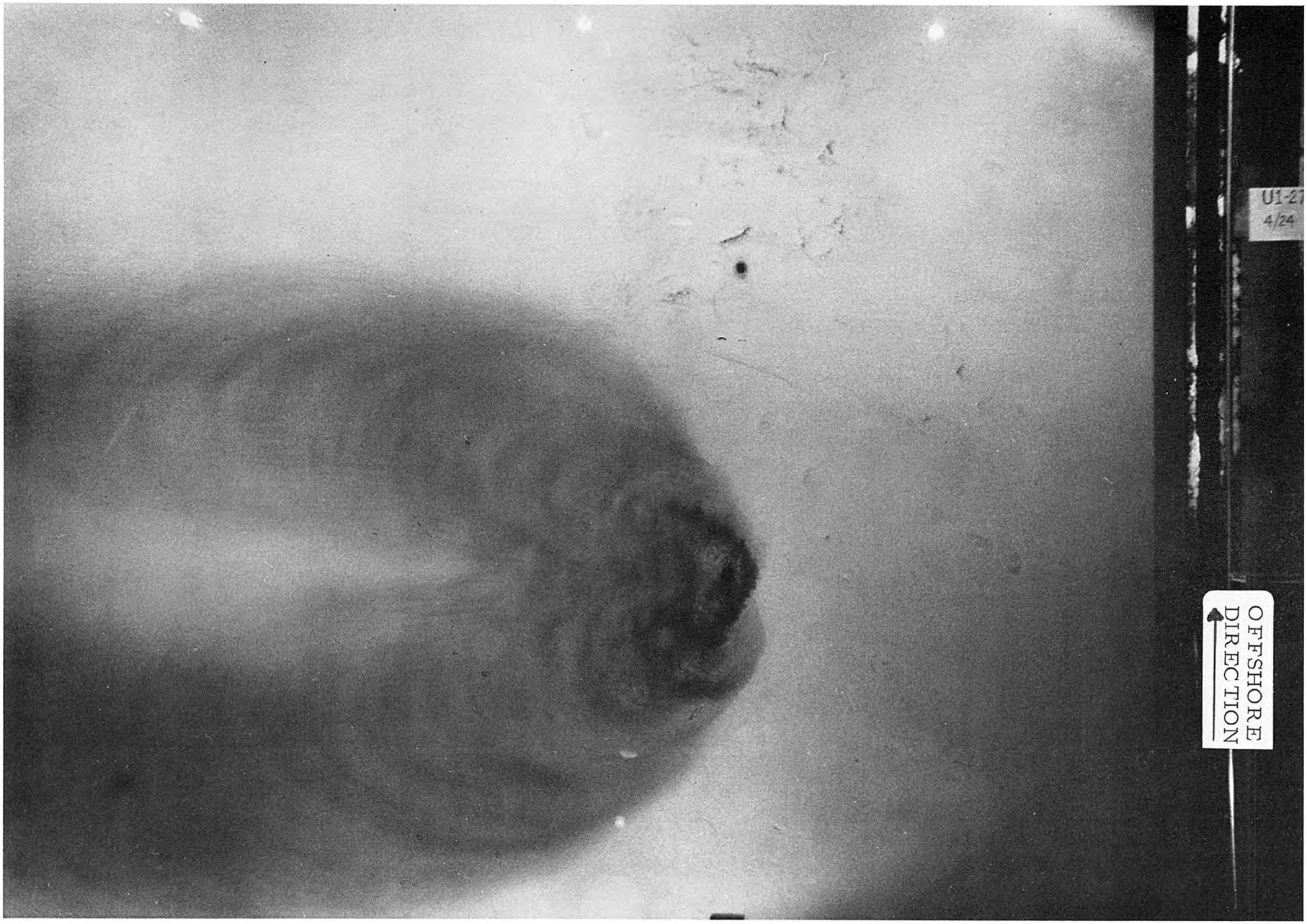

Figure A-15 Photograph showing dye pattern due to discharge of Unit 1 at ambient current = 0.27 knot prototype.

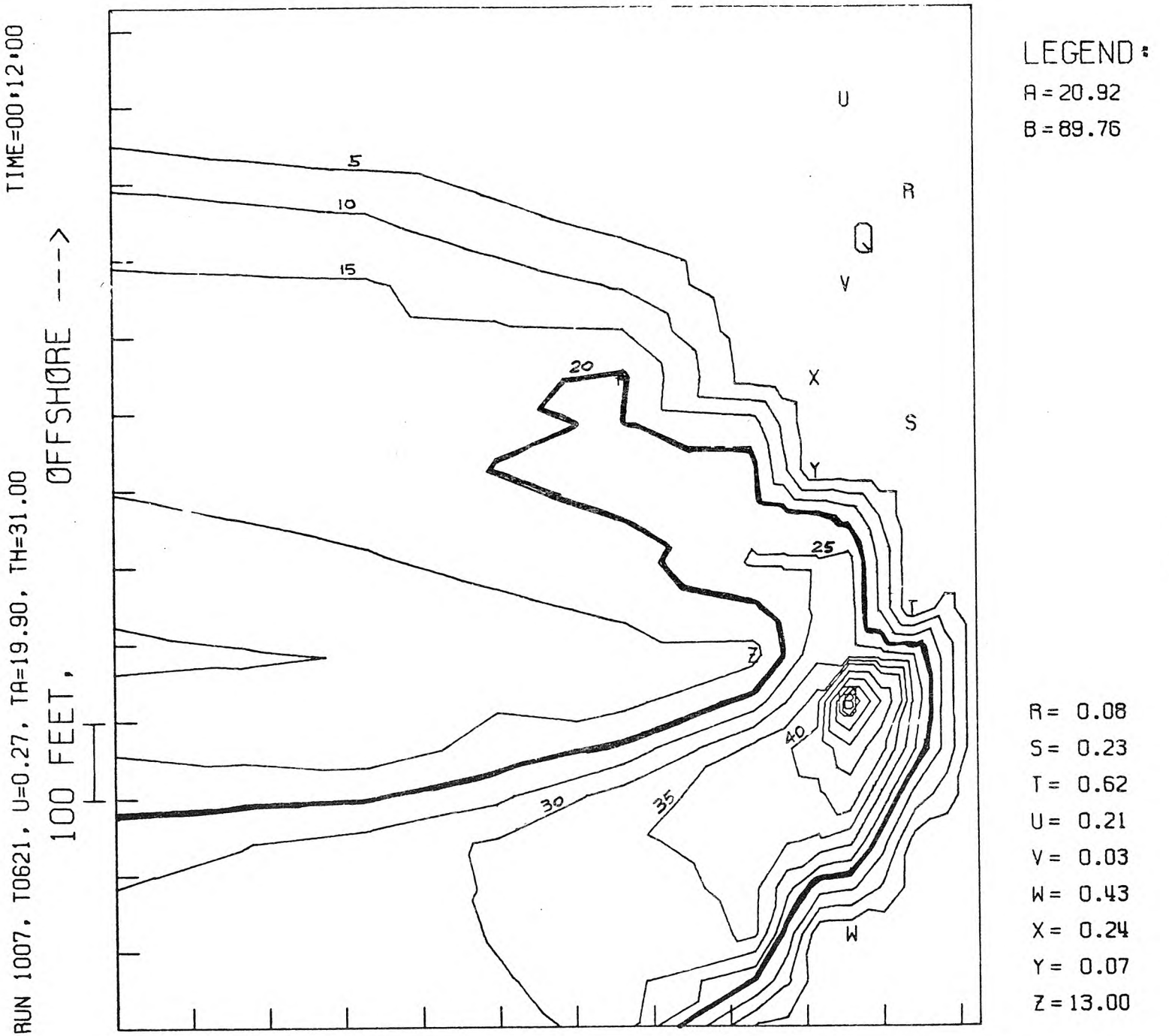

Figure A-16 Surface thermal contour map corresponding to case shown in Figure A-15

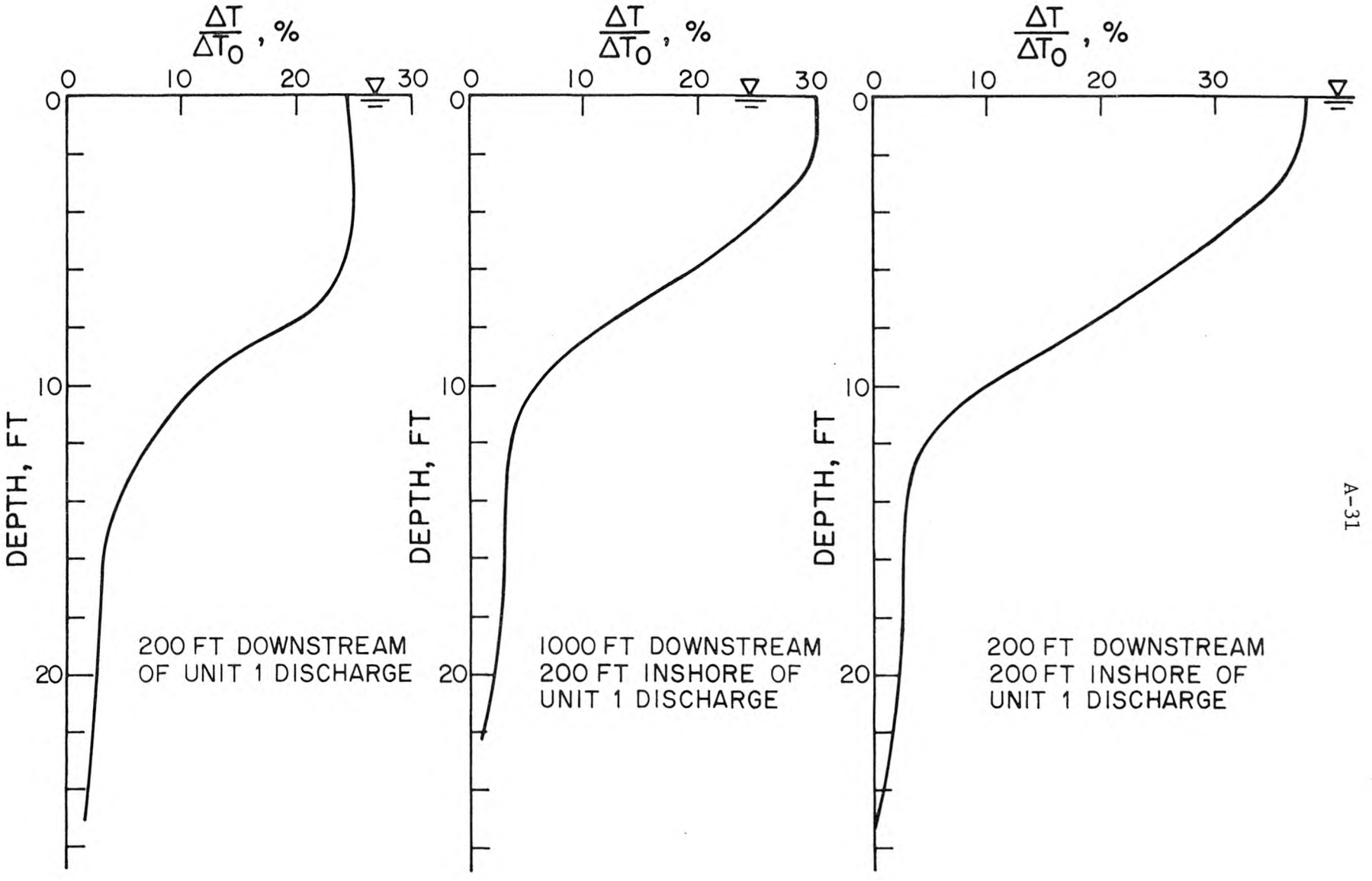

VERTICAL TEMPERATURE PROFILES (CURRENT = 0.27 KNOT)

Figure A-17 Vertical thermal distributions for the case shown in Figure A-15.

Based on these tests with Unit 1 operating alone, it may be summarized that:

1) The Unit 1 discharge has a tendency to direct the plume onshore, as is particularly noticeable for current speeds less than 0.2 knot. (This is believed to be the result of the internal hydraulics of the discharge structure.)

2) The thermal plume is warmer on the shoreward side than the offshore side even for high current speeds.

3) A colder "thermal wake" exists downstream of the discharge as shown by the contour maps.

4) The 20% contour (4°F for a discharge temperature excess of 20°F) extends beyond the 1000 ft limit for most current speeds tested. *

5) There is very little, if any, dilution immediately above the outfall.

6) Most of the dilution occurs within a small distance (of the order of 100 ft) from the discharge.

7) The surface warm layer is thin near the discharge (5 to 10 ft) and becomes thicker (10 to 15 ft) away from the discharge.

As a comparison with available field data, Figure A-18 shows the thermal pattern superimposed on contours obtained in the field by IR radiometry. There was no corresponding field measurement of the initial ΔT_o; it is estimated to have been 19°F, thereby making the 20% laboratory contour equivalent to 3.8°F in the field. The correspondence is very good, including the tendency of both model and prototype thermal fields to be directed toward shore.

---

* Since Unit 1 was already in operation at the time the new California thermal requirements were adopted, it does not have to comply with the new requirement of less than 4°F rise at 1000 ft.

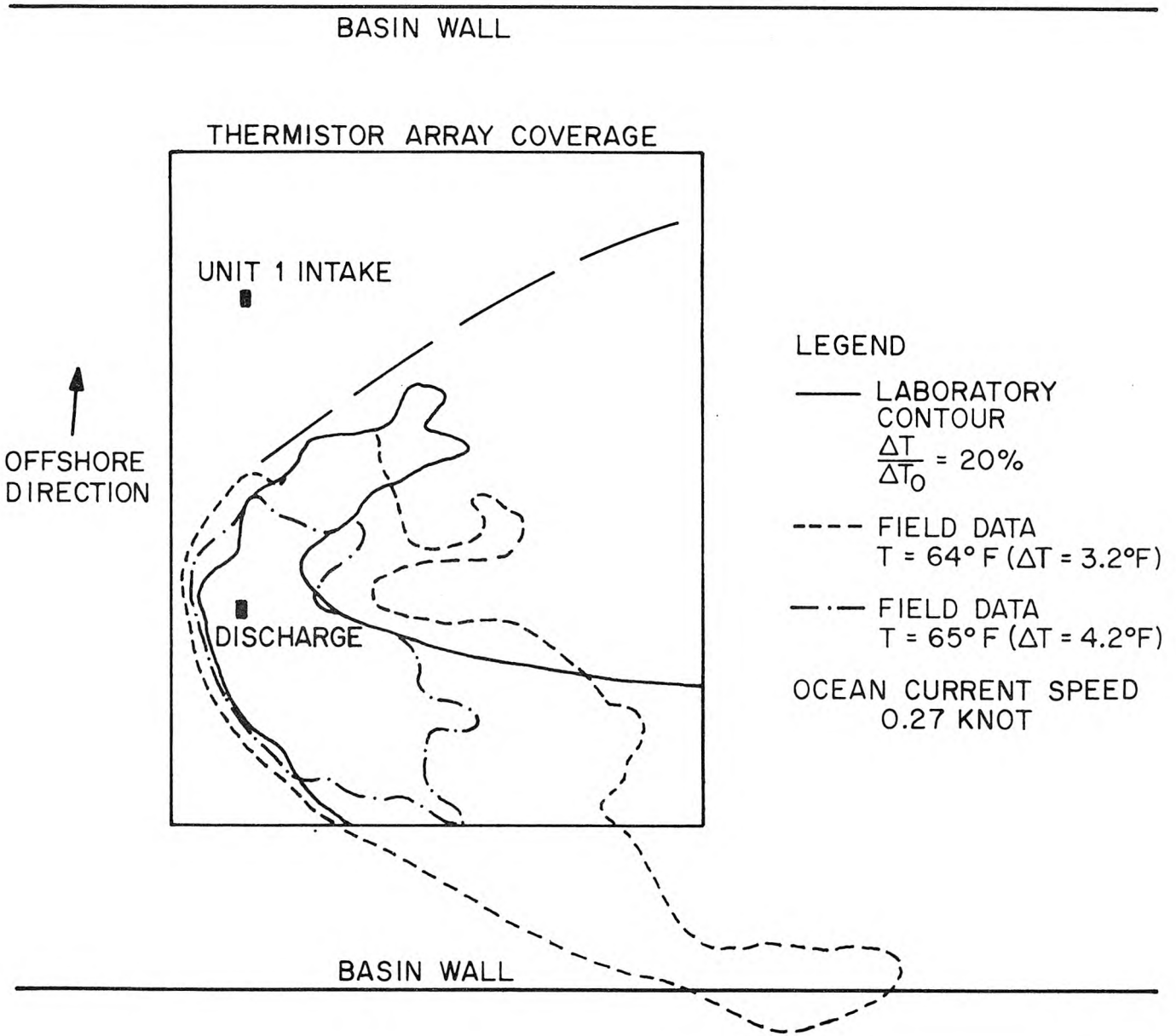

Figure A-18 Comparison of laboratory surface thermal contours with field data. (Field data at 1036 hrs, 11/15/72.)

The results of the recirculation tests are summarized in Table A-7 where it may be seen that

1. The phenomenon of recirculation can be expected to occur to some extent, the severity depending on current patterns.
2. Recirculation of warm water from the Unit 1 discharge to the Unit 1 intake was observed in the model for existing conditions. The temperature of the intake water may be as high as 0.5 to 1°F warmer than the ambient, depending on current conditions.
3. Recirculation of Unit 1 discharge into the proposed Units 2 and 3 intakes would probably lead to less than 0.5°F rise in the intake temperatures. The largest temperature increment due to recirculation from Unit 1 to Units 2 and 3 observed in this series of tests was approximately 3.5% (0.7°F for discharge ΔT_o = 20°F). (See Table A-7 for complete results.)

A6. Heat Treatment of Intakes *

This section summarizes the results of model tests simulating the dispersion of heated water discharged from the Units 2 and 3 intake structures of the San Onofre Nuclear Generating Station during heat treatment. Heat treatment is necessary due to the accumulation of marine growth on the interior walls of the conduits.

The models for the intakes are shown in Figure A-14 of Section A5 of this Appendix. They were inserted in the basin as shown schematically in Figure A-19. Table A-8 summarizes the modeling ratios used in this series of tests. The density ratio was selected to be 3 in order to avoid the use of excessively hot water (i.e., smaller ΔT_o in model than prototype).

The results of the experiments in this series of tests consist of temperature distributions both on the water surface and in vertical sections A-A, B-B, and C-C (Figure A-19). Example thermal map and

---

* Progress Report No. 7, September 1, 1973.

Table A-7

Temperature Rise in Intake Water (Recirculation Test), % of Discharge Temperature Excess

(Values given are for the test period equal to t_e, time it takes for a particle of water to travel the length of the basin and through the return circuit.)

Ocean Current Speed (knots)	Offshore Suction# → t_e(min) (elapsed time until basin water returns)	UNIT 1 INTAKE			UNIT 2 INTAKE			UNIT 3 INTAKE		
		NONE	HALF*	FULL**	NONE	HALF*	FULL**	NONE	HALF*	FULL**
		$\Delta T/\Delta T_o$ in percent								
0	>25	5.9			1.3			0.3		
0.05	>25	4.8	4.9	5.7	3.4	0.2	1.3	1.3	0.3	0.9
0.1	>25	3.0	5.1	4.9	3.6	2.3	3.2	1.0	0.3	1.0
0.27	13.	0.9	0.9	1.0	0.3	1.4	3.2	0.2	2.9	1.0
0.5	7.	0.3	0.3	0.2	0.3	0.3	2.9	0.3	0.3	2.2

To reproduce empirically the induced drift of the Units 2 and 3 diffusers.

* HALF = half the discharge of the current up to 20 gpm in model.

** FULL = entire discharge of the current is routed to offshore suction (up to 35 gpm in model).

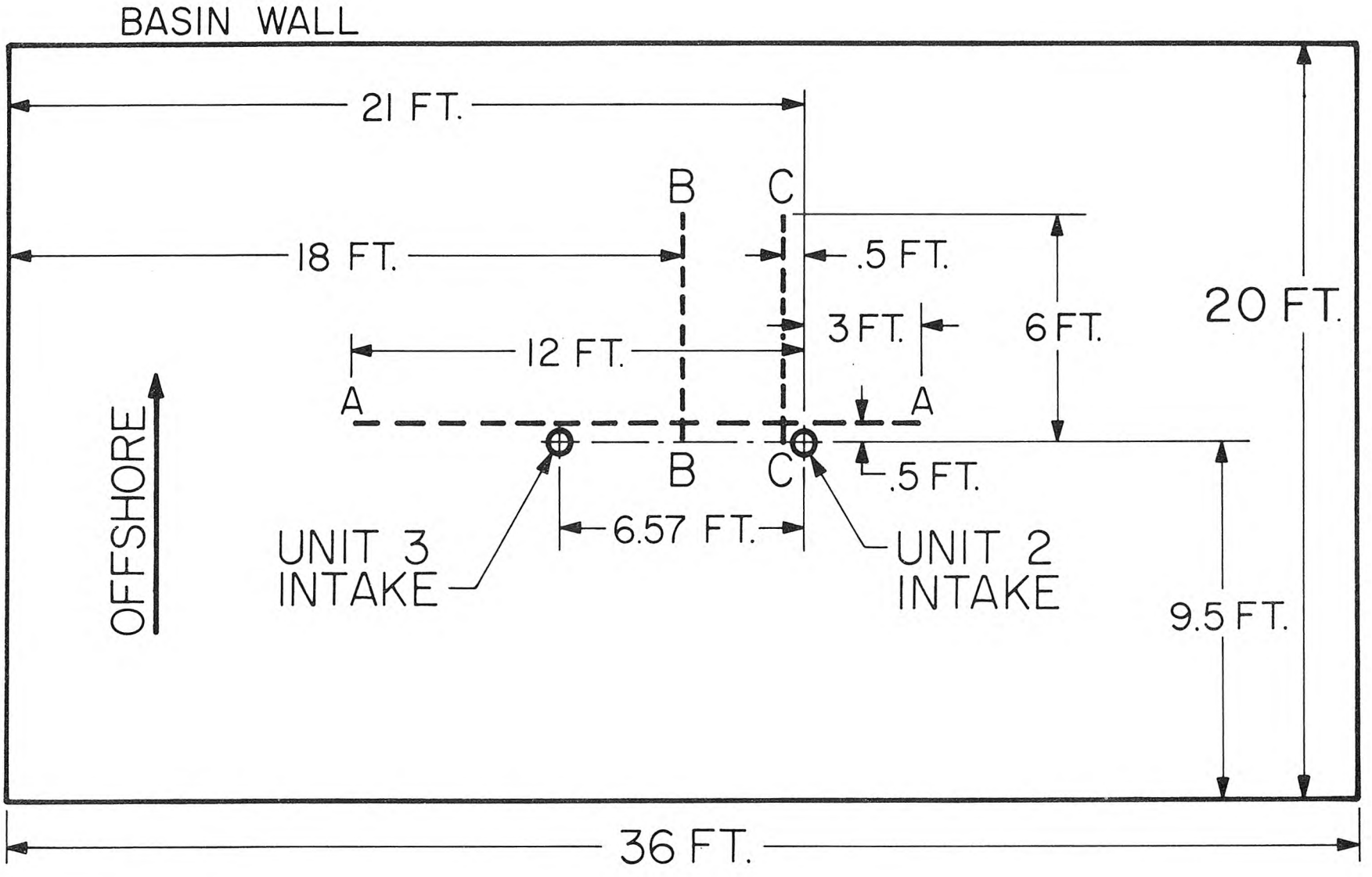

Figure A-19 Schematic plan view of basin layout for heat treatment tests.

Table A-8

Summary of Model Ratios (Prototype/Model)
For Heat Treatment Tests

Length	L_r	100
Density	$\left(\frac{\Delta\rho}{\rho}\right)_r$	3
Velocity	u_r	17.3
Time	t_r	5.8
Discharge	Q_r	1.73×10^5

vertical distribution are shown in Figures A-20 and A-21. The results are summarized as follows:

1. The distribution of surface temperature excess is similar in nature to that from the Unit 1 discharge in normal operation. However, the pattern tends to be more symmetric.
2. A "thermal wake" is present downstream of the structure for the larger current speeds tested.
3. The 4°F (ΔT) contour can be expected to extend beyond 1000 ft before the end of the two-hour heat treatment cycle.
4. The surface layer of warm water is relatively thin (5 to 10 ft thick), being thickest for the smallest currents.
5. There is little, if any, recirculation of the discharge from the intake structure being heat treated to the nearby intake structure of the other unit in normal operation.

A7. Hydraulic Tests of Discharge Ports *

The thermal outfall diffuser systems for the San Onofre Nuclear Generating Station Units 2 and 3 will consist of multiple port diffusers with a total of 63 risers along each of the two diffusers (each approximately 2500 feet long) for the purpose of dispersing the heated effluent over a large area in the ocean so that the California thermal standards can be met.

To accomplish this goal, the discharge nozzles must be designed so that the distributions of port flow and discharge velocity (or momentum flux) be as desired, e.g., uniform along the pipe. Hydraulic evaluation of candidate diffuser designs requires accurate predictions of these distributions which in turn requires an accurate knowledge of the discharge coefficients of the ports and their dependence on the velocity in the diffuser pipe.

---

* Progress Report No. 3, March 30, 1973.

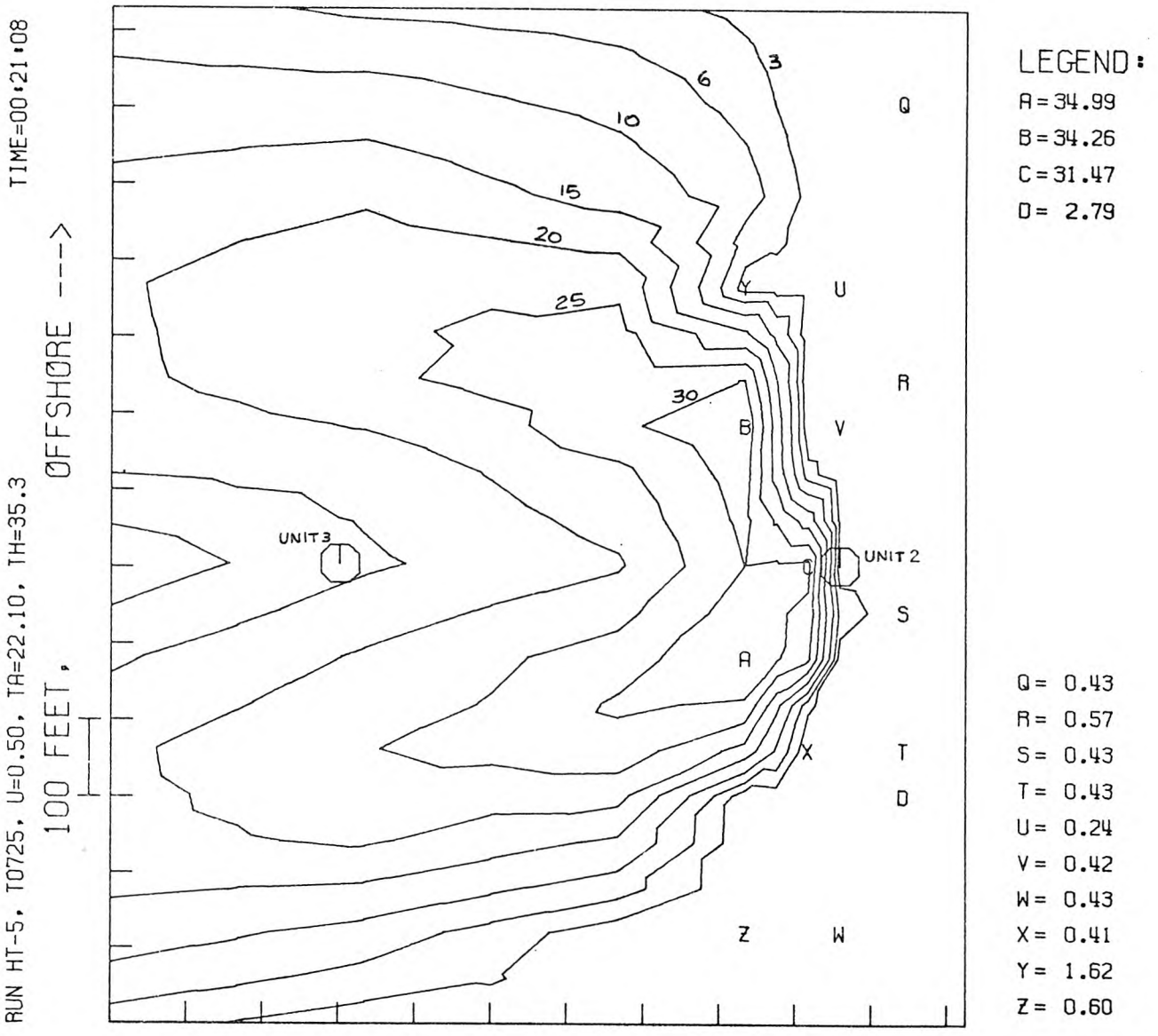

Figure A-20 Surface thermal contour maps for heat treatment tests (contour lines at 3, 6, 10, 15, 20, 25, 30, 35, 40, 50, 60, ... 100% $\Delta T/\Delta T_o$).

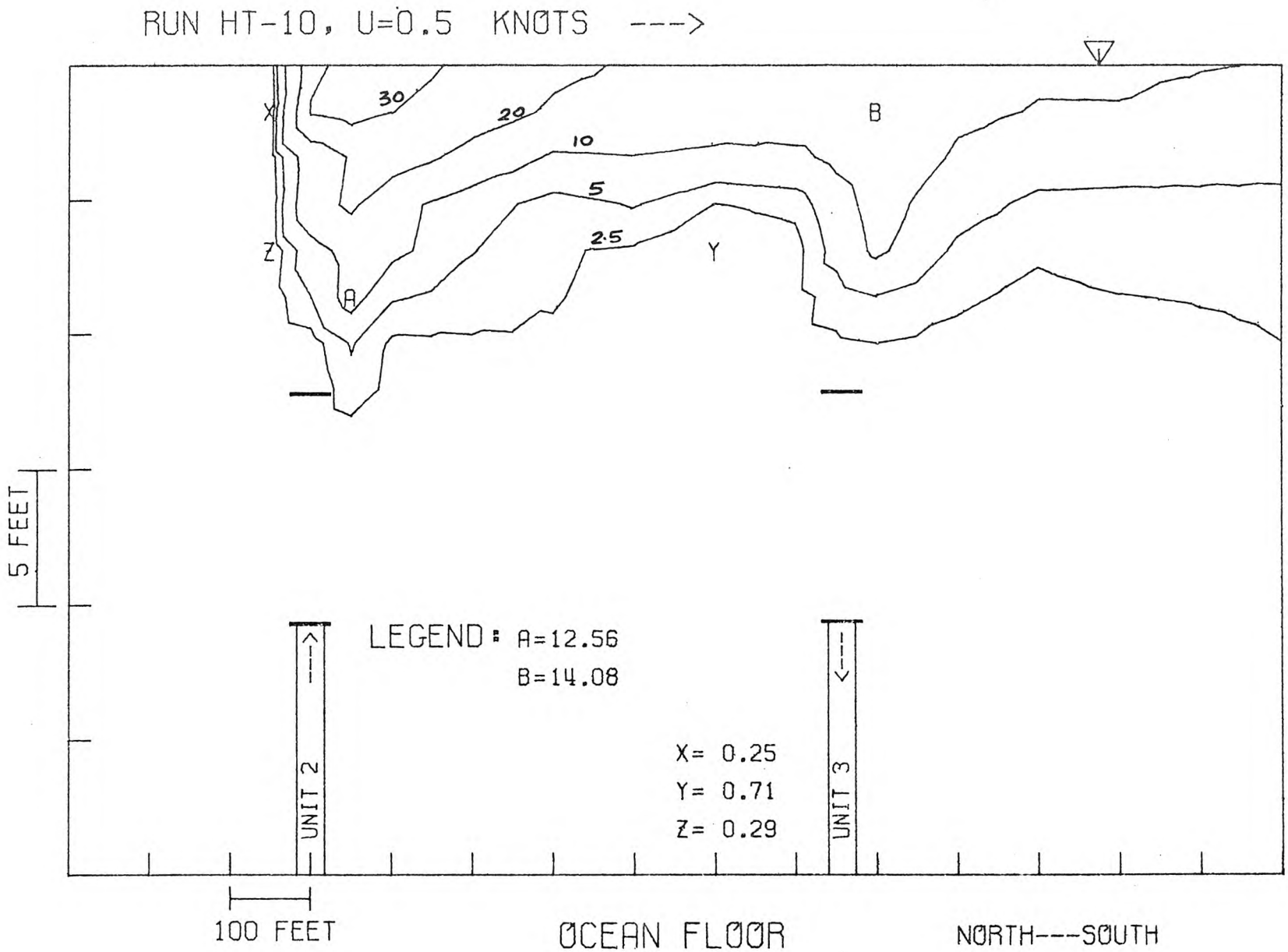

Figure A-21 Thermal contours in vertical plane A-A (contour lines at 2.5, 5, 10, 20, 30, ... 100% $\Delta T/\Delta T_o$) for heat treatment test.

In the case of the thermal outfall diffuser system to be used in the San Onofre Nuclear Generating Stations Units 2 and 3, an added requirement is placed on the discharge structure. This arises from the need for occasional heat treatment of the intake pipeline, requiring the diffuser systems to be operated in reverse so that the discharge nozzles are operated as intake ports. Proper operation of the pumps used for the circulating water system requires that the water level in the wet well be above a certain datum to assure adequate submergence of the pumps' impellers.

From the above discussion, it is seen that the nozzles must be designed such that

a) the discharge velocity be predictable within a few percent; and
b) the head loss, particularly during reverse flow, be kept at a minimum.

Tests were conducted on nozzle-riser assemblies specifically designed to achieve the goals. Figure A-22 shows a schematic drawing of the riser nozzle assembly and Table A-9 summarizes the dimensions of the sixteen nozzles tested.

An attempt was also made to predict the discharge and intake coefficients as functions of nozzle-riser parameters based on assumed head loss characteristics. The discharge coefficients C_D (based on total head) and C_{DH} (based on piezometric head) are defined by:

$$Q_p = C_D A_p \sqrt{2gE} = C_{DH} A_p \sqrt{2gH}$$

The results of the analysis are given by

$$C_D = \frac{-r^2 \frac{V}{\sqrt{2gE}} + \sqrt{X\left(1 - \frac{V^2}{2gE}\right) + r^4}}{X + r^4}$$

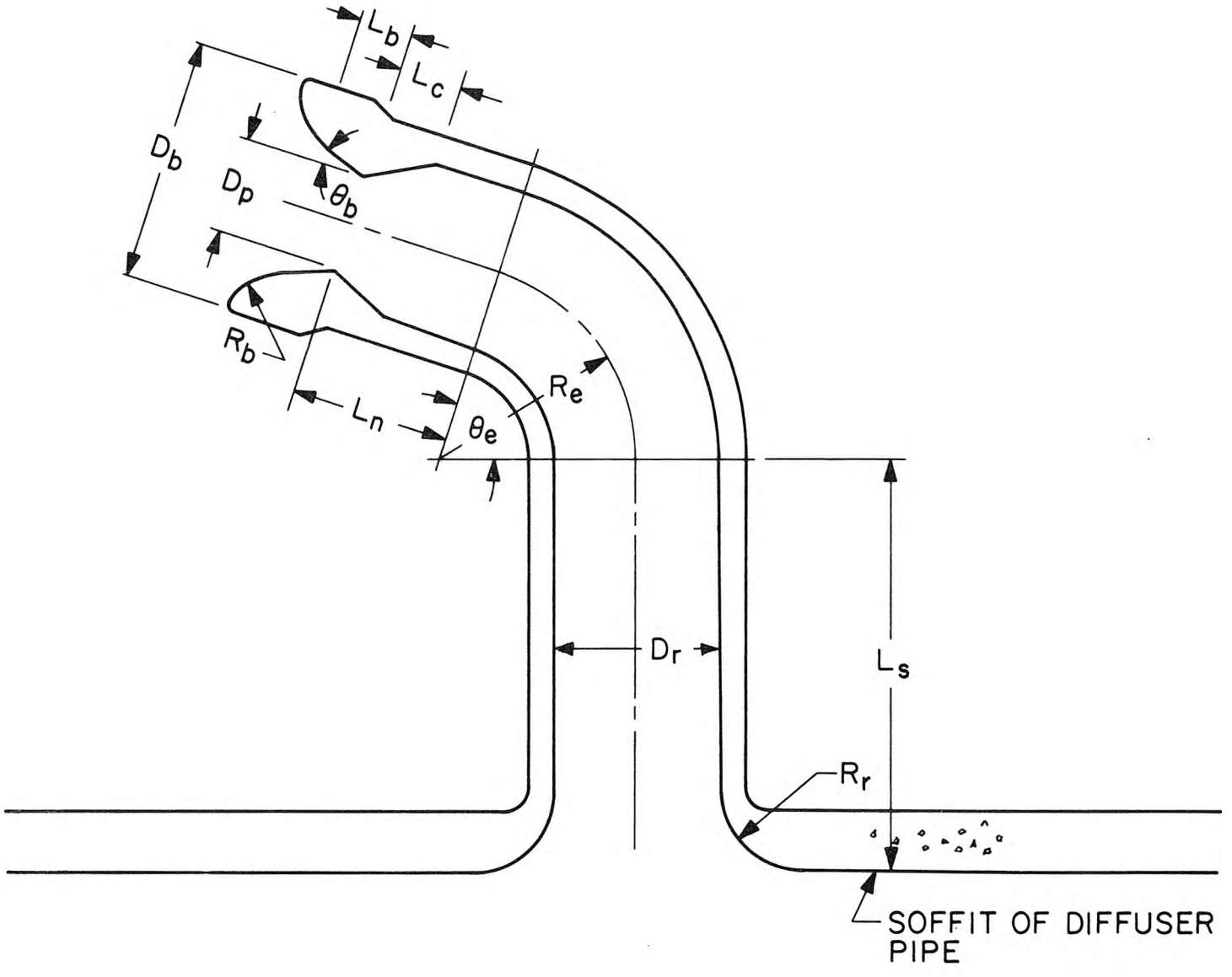

Figure A-22 Schematic of nozzle-riser assemblies tested.

Table A-9

Dimensions of Model Nozzles Tested
(see Figure A-22 for definitions)

Port	D_p	D_b	L_c	L_b	θ_b
	(in.)	(in.)	(in.)	(in.)	(Deg.)
1	1.270	2.56	0.79	0	0
2	1.267	2.58	1.32	0.30	10
3	1.266	*	0.80	*	*
4	1.269	1.54	0.81	0	90
5	1.605	2.97	0.80	0.38	15
6	1.268	2.32	0.71	0.26	20
7	1.265	2.80	1.32	0.43	15
8	1.268	2.75	0.79	0.43	15
9	1.265	2.82	1.30	0.36	20
B	2.002	*	0	*	*
C	1.268	2.79	0.51	0.33	20
D	1.267	2.75	0.51	0.36	15
E	1.601	2.42	0.81	0	90
F	2.003	2.89	0	0.34	25
G	1.264	2.79	0	0.38	20
H	1.269	2.82	0	0.35	15

* no bell mouth for ports 3 and B.

Following dimensions same for all riser-nozzle assemblies:

$R_r = R_b = 0.899$ in. $\quad R_e = 2.4$ in.

$D_r = 2$ in. $\quad L_n = 1.5$ in.

$D_d = 8$ in. $\quad L_s = 6.8$ in.

$\theta_e = 70°$

Scale ratio ∿18 to 1 (prototype to model)

Note: In Progress Report No. 3, this was reported as 15 to 1; however, subsequently the riser and port sizes have been increased and their number decreased in the final design. Thus, the approximate scale ratio should now be considered as 18:1.

$$C_{DH} = \frac{-r^2 \frac{V}{\sqrt{2gH}} + \sqrt{X + r^4 \left(1 + \frac{V^2}{2gH}\right)}}{X + r^4}$$

where $$X = (x_e + f_r \frac{L_r}{D_r} + x_1 + x_c)\left(\frac{D_p}{D_r}\right)^4 + \frac{1}{C_c^2}$$

$r = D_p/D_d$

x_e, x_1, x_c are the head loss coefficients for the entrance from the diffuser pipe to the riser; for the elbow; and for the contraction at the nozzle respectively.

f_r = the Darcy-Weisbach friction coefficient for the riser

A_p = the port throat area = $\pi D_p^2/4$

D_p = the port throat diameter

D_r = the riser diameter

D_d = the diffuser pipe diameter

C_c = the contraction coefficient for the nozzle

V = the velocity in the diffuser (downstream of the nozzle)

Q_p = port discharge

g = gravitational acceleration

E = the difference in total head between the diffuser and the ocean

H = the difference in piezometric head between the diffuser and the ocean (downstream of the nozzle).

Similarly, the intake coefficients C_I and C_{IH} (same definition as C_D and C_{DH}) are given by *

---

* The formulas are slightly different from those given in Progress Report No. 3 due to a change in the assumption regarding the head loss in the main pipe at the point where the riser flow enters. The formulas given here assume no head loss occurs at the junction.

$$C_I = \frac{r^2 \frac{V}{\sqrt{2gE}} + \sqrt{X_I \left(1 + \frac{V^2}{2gE}\right) - r^4}}{X_I - r^4}$$

$$C_{IH} = \frac{r^2 \frac{V}{\sqrt{2gH}} + \sqrt{X_I - r^4 \left(1 - \frac{V^2}{2gH}\right)}}{X_I - r^4}$$

where

$$X_I = \frac{x_b}{C_{c_r}^2} + x_k \left(\frac{1}{C_{c_r}} - \left(\frac{D_p}{D_r}\right)^2\right)^2 + \left(1 + x_1 + f_r \frac{L_r}{D_r}\right)\left(\frac{D_p}{D_r}\right)^4$$

C_{c_r} = contraction coefficient for the entrance bell

x_b = head loss coefficient for the entrance bell

x_k = head loss coefficient for the expansion, and

H = the piezometric head difference between the diffuser and the ocean upstream of the nozzle.

Two example ports (8 and C) are selected and the result included here as Figures A-23 and A-24 respectively. A summary of all the port coefficients (for V = 0) both tested and predicted is shown in Table A-10.

The principal conclusions based on these tests may be summarized as follows:

1. It is possible to design ports such that the intake coefficient is significantly larger than the discharge coefficient.
2. The addition of an intake bellmouth entrance increases the intake coefficient (by about 50% in the configurations tested).
3. To achieve the goal normally required of these ports, (i.e., given jet discharge velocity and minimum intake losses), the ratio of the intake to the discharge coefficient should be as large as possible.

Table A-10

Summary of Port Discharge Test Results (at $V \cong 0$)

(V = Velocity in diffuser pipe)

	Measured		Predicted ***			Port Description **		
Port	C_D	C_I	C'_D	C'_I	$\beta = \frac{C_I}{C_D}$	$\frac{D_p}{}$ (in.)	θ_b (Deg.)	Taper (L_c)
1	1.17	1.265	--	1.34	1.08	22.8	0	short
2	0.95	1.30	0.894	1.25	1.37	22.8	10	long
3	(0.84)*	0.79	0.845	--	(0.94)	22.8	none	(flat) short
4	0.84	0.77	0.845	--	0.92	22.8	none	(thin) short
5	0.90	1.265	0.880	1.17	1.41	28.8	15	short
6	0.84	1.17	0.845	1.17	1.39	22.8	20	short
7	0.89	1.23	0.894	1.21	1.38	22.8	15	long
8	0.85	1.22	0.845	1.21	1.44	22.8	15	short
9	0.89	1.175	0.894	1.17	1.32	22.8	20	long
B	0.85	0.865	0.864	--	1.02	36	none	(thin)
C	0.79	1.165	0.789	1.17	1.48	22.8	20	short short
D	0.79	1.19	0.789	1.21	1.51	22.8	15	short short
E	0.86	0.82	0.880	--	0.95	28.8	none	(flat) short
F	0.87	0.99	0.864	0.89	1.14	36	25	
G	0.67	1.16	0.660	1.17	1.73	22.8	20	sudden contraction
H	0.67	1.21	0.660	1.21	1.81	22.8	15	sudden contraction

* estimated (same as Port 4)

** See Table A-9 and Figure A-22 for detailed dimensions (assuming 18:1 scale)

*** based on formulas derived with following values for loss coefficients and prototype dimensions:

L_s = 10 ft

f_r = 0.017 (laboratory value based on smooth lucite)

x_e = 0.08

x_l = 0.15 for discharge; 0 for intake

D_r = 3.0 ft

x_c = 0.02

x_k = 0.8

x_b = 0.1

Note: Since all values are for the case $V \doteq 0$, $C_D \simeq C_{DH}$ and $C_I \simeq C_{IH}$.

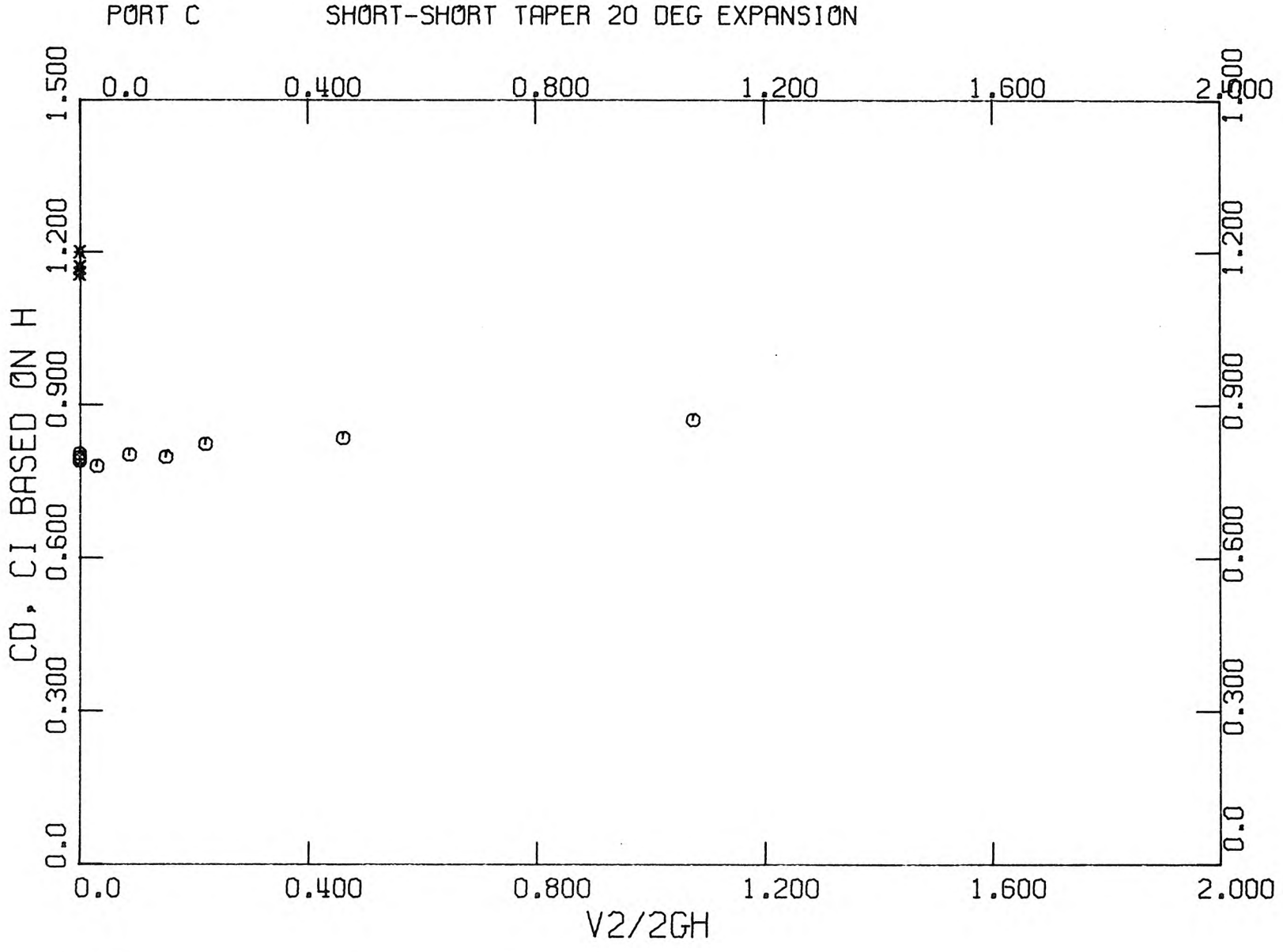

Figure A-23 Measured port discharge (0) and intake (*) coefficient as function of $V^2/2gH$.

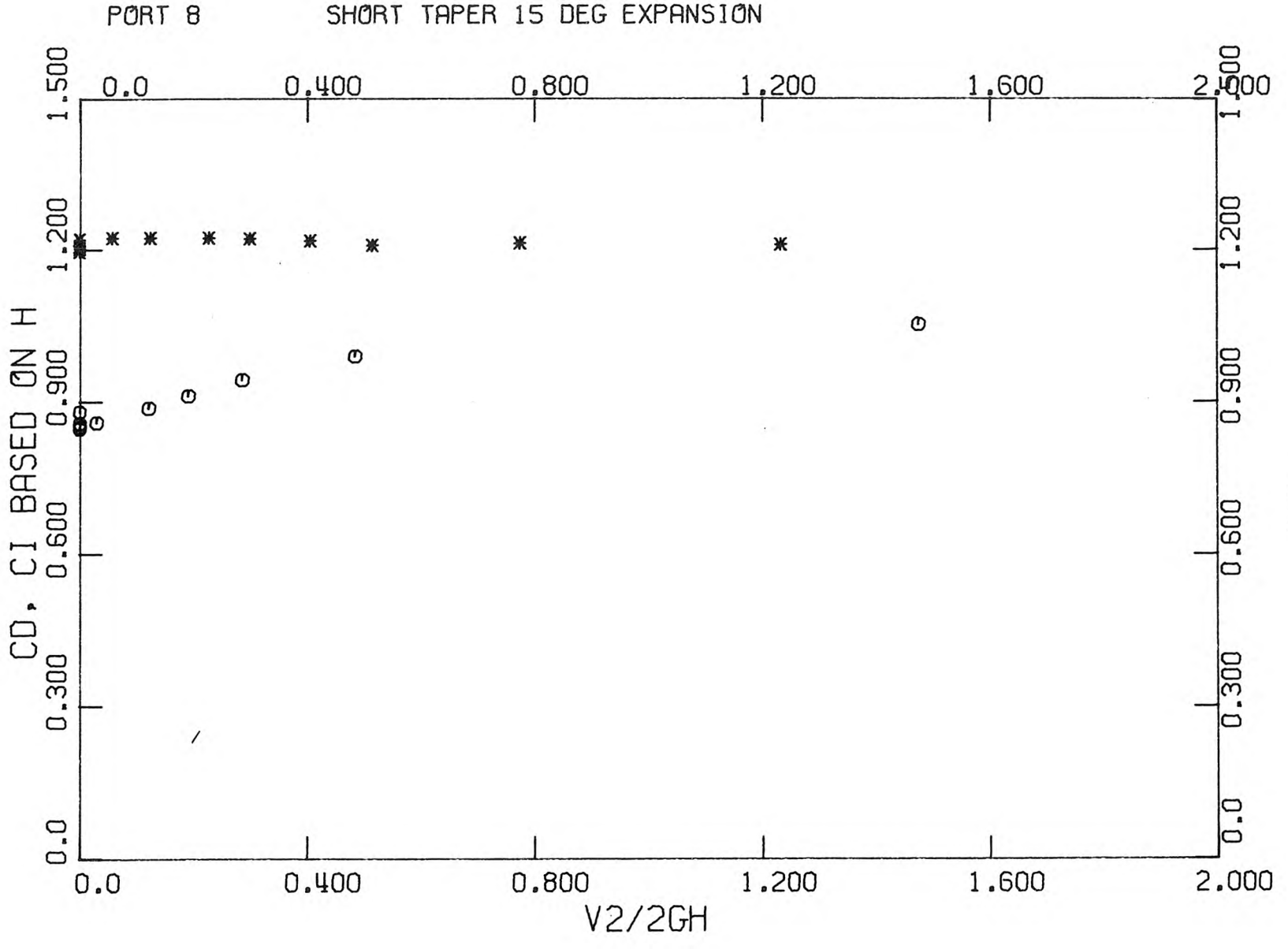

Figure A-24 Measured port discharge (0) and intake (*) coefficient as function of $V^2/2gH$.

4. The values of the intake and discharge coefficients can be reasonably predicted by semi-empirical formulas derived in this section.

5. Based on the results of this investigation, the configurations of Ports 6, C, and H were recommended, the choice being dependent on system hydraulics and structural design. The choice of port diameter also depends on the overall system hydraulics and thus is not exactly the 22.8 inch nominal value used in these tests, based on 18:1 scale. (Final design values selected are 21.85 in., 22.8 in., and 23.9 in.)

In the final design of the San Onofre Units 2 and 3 diffusers, the port configuration chosen is based on Port C. The nozzle-riser assemblies are actually concrete blocks with special metal inserts used to define the port inner geometry. The throat diameters used are as follows:

Port Number (from inshore)	Throat Diameter (inches)	No. of Ports
1-25	21.85	25
26-44	22.8	19
45-63	23.9	19

Figure A-25 shows a schematic of the port used. To vary the throat diameter, the angles of contraction and expansion (θ_c and θ_e in Figure A-25) are held constant at 35° and 20° while the length of the port is varied. The choice of throat diameters were based on analyses of manifold hydraulics of the diffusers with the objectives of achieving a uniform port discharge distribution and a mean jet velocity of 13 fps (at the vena contracta).

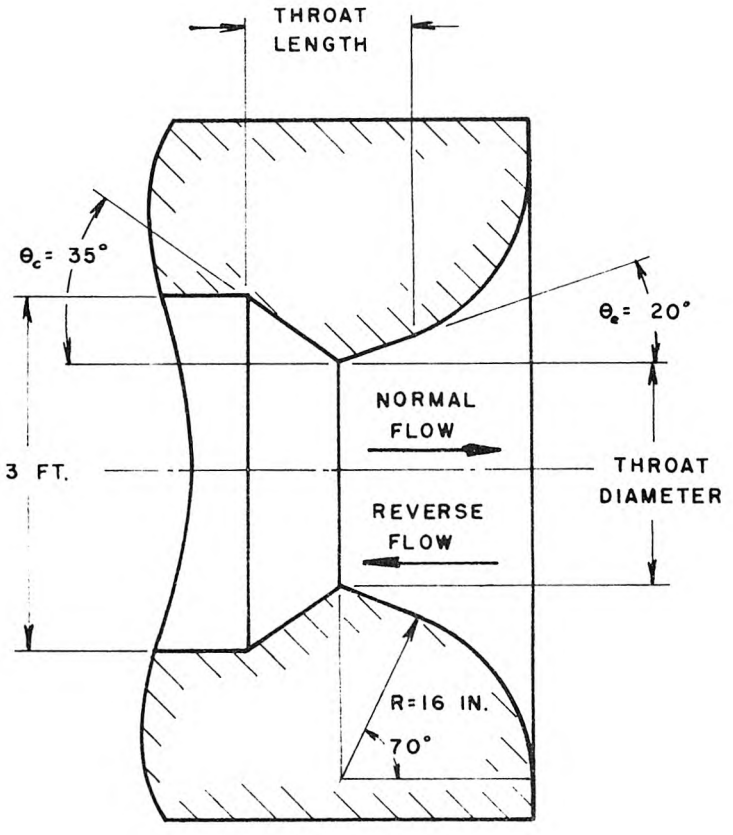

THROAT DIAMETER = 21.85, 22.80, OR 23.90 IN.

NOMINAL THROAT LENGTH ~ 17 IN.
(DEPENDS ON THROAT DIAMETER)

Figure A-25 Schematic of port configuration used in final design.

#26008